Université de Montréal

Bcl-xL (S49) and (S62) sequential phosphorylation/dephosphorylation during mitosis prevents chromosome instability and aneuploidy

Par
Prasamit Saurav Baruah

Programme de biologie moléculaire
Faculté de Médecine

Thèse présentée à la Faculté de Médecine
En vue de l'obtention du grade de doctorat en
Biologie Moléculaire

Juin 2016

Université de Montréal
Faculté de Médecine

Cette thèse intitulée :

Bcl-xL (S49) and (S62) sequential phosphorylation/dephosphorylation during mitosis prevents chromosome instability and aneuploidy

Présentée par :
Prasamit Saurav Baruah

A été évaluée par un jury composé des personnes suivantes :

Président-rapporteur
Directeur de recherche
Membre du jury
Examinateur externe
Représentant de la doyenne

Abstract

An interesting feature of Bcl-xL protein is the presence of an unstructured loop domain between its α1 and α2 helices, a domain not essential for its anti-apoptotic function and absent in CED-9, ortholog protein in *Caenorhabditis elegans*. Within this domain, Bcl-xL undergoes dynamic phosphorylation and dephosphorylation at Ser49 and Ser62 during G2 and mitosis in human cancer cells. When these residues are mutated and proteins expressed in cancer cells, cells harbor mitotic defects, including chromosome mis-attachment, lagging, bridging and mis-segregation, events associated with chromosome instability and aneuploidy. To further analyze the effects of Bcl-xL Ser49 and Ser62 in normal cells, the present studies were performed in normal human diploid cells, and *in vivo* in *Caenorhabditis elegans*.

First, we studied normal human diploid BJ foreskin fibroblast cells expressing Bcl-xL(wild type), (S49A), (S49D), (S62A), (S62D) and the dual (S49/62A) and (S49/62D) mutants. Cells expressing S49 and/or S62 phosphorylation mutants showed reduced kinetics of cell population doubling. These effects on cell population doubling kinetics correlated with early outbreak of senescence with no impact on the cell death rate. Senescent cells displayed typical senescence-associated phenotypes including high-level of senescence-associated β-galactosidase activity, interleukin-6 secretion, tumor suppressor p53 and cyclin-dependent kinase inhibitor p21Waf1/Cip1 activation as well as γH2A.X-associated nuclear chromatin foci. Fluorescence in situ hybridization analysis and Giemsa-banded karyotypes revealed that the expression of Bcl-xL phosphorylation mutants in normal diploid BJ cells provoked chromosome instability and aneuploidy. These findings suggest that dynamic Bcl-xL Ser49 and Ser62 phosphorylation/ dephosphorylation cycles are important in the maintenance of chromosome integrity during mitosis in normal cells.

Second, we undertook experiments in *Caenorhabditis elegans* to understand the importance of Bcl-xL Ser49 and Ser62 *in vivo*. Transgenic worms carrying single-site S49A, S62A, S49D, S62D and dual-site S49/62A mutants were generated and their effects were analyzed in germlines of young adult worms. Worms expressing Bcl-xL variants showed decreased egg-laying and hatching, variations in the length of their mitotic regions and transition zones, chromosomal abnormalities at their diplotene stages,

and increased germline apoptosis. Some of these transgenic strains, particularly the Ser to Ala variants, also showed slight modulations of lifespan compared to their controls. The *in vivo* observations confirmed the importance of Ser49 and Ser62 within the loop domain of Bcl-xL in maintaining chromosome stability.

These studies could impact future strategies aiming to develop and identify compounds that could target not only the anti-apoptotic domain of Bcl-xL protein, but also its mitotic domain for cancer therapy.

Key Words: Bcl-xL, mitosis, chromosome instability, aneuploidy, senescence, apoptosis.

Résumé

Une caractéristique intéressante de la protéine Bcl-xL est la présence d'un domaine en boucle non-structurée entre les hélices α1 and α2 de la protéine. Ce domaine protéique n'est pas essentiel pour sa fonction anti-apoptotique et absent chez CED-9, la protéine orthologue chez *Caenorhabditis elegans*. A l'intérieur de ce domaine, Bcl-xL subit une phosphorylation et déphosphorylation dynamique sur les résidus Ser49 et Ser62 en phase G2 du cycle cellulaire et lors de la mitose. Lorsque ces résidus sont mutés et les protéines exprimées dans des cellules cancéreuses, les cellules démontrent plusieurs défauts mitotiques liés à l'instabilité chromosomique. Pour analyser les effets de Bcl-xL Ser49 et Ser62 dans les cellules normales, les présentes études ont été réalisées dans des cellules diploïdes humaines normales, et *in vivo* chez *Caenorhabditis elegans*.

Dans une première étude, nous avons utilisé la lignée cellulaire de cellules fibroblastiques diploïdes humaines normales BJ, exprimant Bcl-xL (type sauvage), (S49A), (S49D), (S62A), (S62D) et les double (S49/62A) et (S49/62D) mutants. Les cellules exprimant les mutants de phosphorylation ont montré des cinétiques de doublement de la population cellulaire réduites. Ces effets sur la cinétique de doublement de la population cellulaire corrèle avec l'apparition de la sénescence cellulaire, sans impact sur les taux de mort cellulaire. Ces cellules sénescentes affichent des phénotypes typiques de sénescence associés notamment à haut niveau de l'activité β-galactosidase associée à la sénescence, la sécrétion d' interleukine-6, l'activation de p53 et de p21WAF1/ Cip1, un inhibiteur des complexes kinase cycline-dépendant, ainsi que la formation de foyers de chromatine nucléaire associés à γH2A.X. Les analyses de fluorescence par hybridation *in situ* et des caryotypes par coloration au Giemsa ont révélé que l'expression des mutants de phosphorylation de Bcl-xL provoquent de l'instabilité chromosomique et l'aneuploïdie. Ces résultats suggèrent que les cycles de phosphorylation et déphosphorylation dynamiques de Bcl-xL Ser49 et Ser62 sont importants dans le maintien de l'intégrité des chromosomes lors de la mitose dans les cellules normales.

Dans une deuxième étude, nous avons entrepris des expériences chez *Caenorhabditis elegans* pour comprendre l'importance des résidus Ser49 et Ser62 de Bcl-xL *in vivo*. Les vers transgéniques portant les mutations de Bcl-xL (S49A, S62A, S49D, S62D et

S49/62A) ont été générés et leurs effets ont été analysés sur les cellules germinales des jeunes vers adultes. Les vers portant les mutations de Bcl-xL ont montré une diminution de ponte et d'éclosion des oeufs, des variations de la longueur de leurs régions mitotiques et des zones de transition, des anomalies chromosomiques à leur stade de diplotène, et une augmentation de l'apoptose des cellules germinales. Certaines de ces souches transgéniques, en particulier les variants Ser/Ala, ont également montré des variations de durée de vie par rapport aux vers témoins. Ces observations *in vivo* ont confirmé l'importance de Ser49 et Ser62 à l'intérieur du domaine à boucle de Bcl-xL pour le maintien de la stabilité chromosomique.

Ces études auront une incidence sur les futures stratégies visant à développer et à identifier des composés qui pourraient cibler non seulement le domaine anti-apoptotique de la protéine Bcl-xL, mais aussi son domaine mitotique pour la thérapie du cancer.

Mots clé: Bcl-xL, mitose, instabilité chromosomique, aneuploïdie, sénescence, apoptose

Contents

List of figures and tables

1. Introduction

3. Bcl-xL (S49) and (S62) dynamic phosphorylation/dephosphorylation during mitosis prevents chromosome instability and aneuploidy in human normal diploid fibroblasts

4. Expression of human Bcl-xL Ser49 and Ser62 mutants in *Caenorhabditis elegans* causes germline defects and aneuploidy

6. Summary of major findings

Abbreviations:

Apaf-1	Apoptotic peptidase activating factor 1
APC/C	Anaphase promoting complex/cyclosome
AKT	commonly known as Protein kinase B (PKB)
Arf	Alternate reading frame
Atm	Ataxia telangiectasia mutated
Atr	Ataxia telangiectasia and Rad-3 related protein
B56-PP2A	B56 regulatory subunit of PP2A
Bad	Bcl-2 associated death promoter protein
Bak	Bcl-2 homologous antagonist killer
Bax	Bcl-2 associated X protein
Bcl-2	B-cell lymphoma 2 protein
Bcl-b	B-cell lymphoma B protein
Bcl-g	B-cell lymphoma G protein
Bcl-rambo	B-cell lymphoma Rambo
Bcl-xL	B-cell lymphoma extra long
Bcl-xES	B-cell lymphoma extra short
Bcl-x	B-cell lymphoma X
Bcl-w	B-cell lymphoma W
Bfl-1/A1	Synonym for Bcl-2 related protein A1
BH	Bcl-2 homology domain
BHRF-1	BamH1 restricted fragment 1
Bid	BH-3 interacting domain death agonist
Bik	Bcl-2 interacting killer protein
Bim	Commonly called for protein Bcl-2 like protein 11
BMP	Bone morphogenic protein
Bmf	Bcl-2 modifying factor
Boo/Diva	Bcl-2 homologue of ovary/ Death inducer binding to vBcl-2
53BP-1	p53 binding protein 1
Bok/Mtd	Bcl-2 related ovarian killer/ Matador
Brca1/2	Breast cancer protein 1/2
BubR1	Budding uninhibited by benzimidazoles related protein 1
Bub3	Budding uninhibited by benzimidazoles 3 homolog
C	Celsius
CARD	Caspase recruitment domain
Ccl	Chemokine ligand
Cdc20	Cell division cycle protein 20
Cdc42	Cell division cycle protein 42
Cdk	Cyclin dependent kinase
CED-9	*C. elegans* cell death protein 9
CEP-1	*C. elegans* p53 like-1
Cenp-E	Centromere protein E
Chmp3	Charged multivesicular protein 3
Chk1/2	Checkpoint kinase1/2
CIN	Chromosomal instability

Cki	Cyclin-dependent kinase inhibitor protein
CPC	Chromosome passenger complex
CRISPR/Cas9	Clustered regulatory interspaced short palindromic repeats/ CRISPR associated protein 9
Cxcl8	Chemokine (C-X-C motif) ligand-1
Dad-1	Defender against apoptotic death-1
DAPI	4',6'-diamidino-2-phénylindole
DDR	DNA damage response
DNA	Dexyribonucleic acid
DNA –SCAR	DNA segments with chromatin alterations reinforcing senescence
DNMT	DNA methyl transferases
Drp	Dynamin related protein
DSB	Double-strand break
DTC	Distal tip cell
Ect2	Epithelial cell transforming sequence 2
ECM	Extracellular matrix
EGL-1	Egg laying defective -1
Ercc	Excision repair cross-complementing
ERK	Extracellular signal-regulated kinases
ESCRT	Endosomal sorting complex required for transport machinery
FBF	Fem-3 binding factor
FISH	Flourescent *in-situ* hybridization
FRAP	Fluorescence recovery after photobleaching
GAP	GTPase activating protein
GEF	Guanine exchange factor
GFP	Green fluorescent protein
GIN	Genomic instability
GLD	Germ line defective
GLP-1	Glucagon like peptide-1
GLD-2 PAP	GLD-2 poly (A)-polymerase
GM-Csf	Granulocyte macrophage colony-stimulating factor
GSC	Germline stem cell
GTP	Guanine nucleotide phosphate
h	hour
HAT	Histone acetyltranferase
HDAC	Histone deacetylase
Ha-Ras	Harvey rat sarcoma
γ-H2A.X	H2A histone family member X phospho-serine 139
H3K9-me3	histone-3- lysine 9 trimethyl
HmgA	High-mobility group A
Hp-1	Heterchromatin protein 1
HR	Homologous recombination
Hrk	Harakiri Bcl-2 interacting protein
HUS-1	Hydroxyurea sensitive-1
ICD-1	Inhibitor of cell death-1
Igf	Insulin-like growth factor

IgfBPs	Igf-binding proteins
Il	Interleukin
Il-6R	Il-6 receptor
IF	Immunofluorescence
InsR	Insulin receptor
IP	Immunoprecipitation
IR	Ionizing radiation
Jnk	c-Jun N-terminal kinase
Kif14	Kinesin-like protein 14
KMN	Knl-1/Mis12/Ndc80 complex
KSHV	Kaposi sarcoma associated herpes virus
LAG-1	Longevity assurance gene 1
Mad2	Mitotic arrest deficient 2
Mapk	Mitogen-activated protein kinase
Mcak	Mitotic centromere-associated kinesin
MCC	Mitotic checkpoint complex
Mcl-1	Myeloid leukemia cell differentiation protein 1
Mdm2	Mouse double minute 2 homolog
MEF	Mouse embryonic fibroblast
MES	Maternal-effect sterile
MgcRacGAP	RACGAP1 gene encoding Rac GTPase-activating protein
min	minute
Mip-3α	Macrophage inflammatory protein 3α
Mklp2	Mitotic kinesin like protein 2 phosphatase
Mlcp	Myosin light chain phosphatase
Mlck	Myosin light chain kinase
Mmp	Metalloproteinase
MOF	Males absent on the first protein (*D. melanogaster*)
MosSCI	Mos1-mediated Single Copy Insertion
MPS-1	Monopolar spindle
Mre-11	Meiotic recombination 11
MRN	MRE11, RAD50, NBS1 complex
mRNA	messenger ribonucleic acid
MRT	Mortal germline-2
MT	Microtubule
mTor	Mammalian target of rapamycin
NF-κβ	Nuclear factor kappa B
NGM	Nematode growth medium
NMR	Nuclear magnetic resonance
NOEs	Nuclear Overhauser effects
Nos-3	Nitric oxide synthase protein 3
Noxa	*Latin word* for Damage/ Phorbol-12-myristate-13-acetate-induced protein 1
NWGR	Asp-Trp-Gly-Arg motif
OIS	Oncogene-induced senescence
PAI-1	Plaminogen activator inhibitor-1

PCAF	P300/CBP-associated factor
PCD	Programmed cell death
PDK-1	3-Phosphoinositide dependent protein kinase
PIE-1	Pharynx and intestine in excess protein 1
Plk1	Polo like kinase 1
PML	Promyelocytic leukaemia
Pmp-3	Plasma membrane proteolipid protein 3
PP1	Protein phosphatase 1
PP2A	Protein phosphatase 2A
pRb	Retinoblastoma
PRC1	Protein regulator of cytokinesis 1
PS	Premature senescence
PSR	Phosphatidylserine receptor
Pten	Phosphatase and tensin homolog
Puma	p53 upregulated modulator of apoptosis
Ras	Rat sarcoma
RE	Recycling endosomes
RhoA	Ras homolog gene family, member A
RNAseq	RNA sequencing
ROCK	Rho-associated *protein* kinase
ROS	Reactive oxygen species
RT-PCR	Reverse transcriptase polymerase chain reaction
RS	Replicative senescence
SA-β-Gal	Senescence-associated β-galactosidase
SAC	Spindle assembly checkpoint
SAHF	Senescence-associated heterochromatin foci
SAPK	Stress-activated protein kinases
SASP	Senescence-associated secretory phenotype
SMAD	Small body size Mothers Against Decapentaplegic (*D. melanogaster*)
s	second
SEC	Securin
SKY	Spectral karyotype
SOG	Short gastrulation
SSB	Single-strand break
TIF	Telomere dysfunction-induced foci
TGF- β	Transforming growth factor-β
TGF- βR1	Transforming growth factor-β receptor 1
TM	Transmembrane domain
TUNEL	Terminal deoxynucleotidyl transferase dUTP nick end labeling
VEGF	Vascular endothelial growth factor
VP16	Synonym for etoposide
wt	wild-type
XPF	Xeroderma Pigmentosum Group F-Complementing Protein
YFP	Yellow fluorescent protein
Zwint1	ZW10 interacting protein

Nomenclature convention

Human genes and mRNAs are with *ITALIC* scripts (example *BCLX*)
Human proteins are with Normal scripts (example Bcl-xL)

C. elegans genes and mRNAs are with *italic* scripts *(*example *ced-9)*
C. elegans proteins are with NORMAL scripts (example CED-9)

Mouse genes and mRNAs are with *Italic* scripts (example *Bclx*)
Mouse proteins are with Normal scripts (example Bcl-xL)

Genes from other species (yeast, virus) are with *Italic* scripts (example *Cdc8*)
Proteins from other species (yeast, virus) are with NORMAL scripts (example BHRF1)

Protein domains are with NORMAL scripts (example BH1)
Protein complexes are with NORMAL scripts (example APC/C)

Acknowledgements

First and foremost I will like to thank God for his continuous blessings and guidance throughout this project. I'm very much grateful beyond words towards my supervisor, Dr. Richard Bertrand without whom I would never have either got this opportunity or this research program. He has been always there relentlessly and guiding me throughout in every ups and downs of my doctorate career. I forward my heartful gratitude to Myriam Beauchemin who has been with me in every step of this journey and has given me so much love and affection making my working environment a stress less ambience. I have learnt and gathered much experience after entering this laboratory.

My family has been a big support in the completion of this project and without them I can hardly see myself here. Special thanks my friends Redwane Boukharfane, Ahmed Mohammed Abdel Latiff, Macha Samba Mondonga, Abdel Hamid Bekri, Anne Calvé, Julie and Yasmin who have always helped and motivated me in this adventure.

I would like to thank studentship support from Faculté des études supérieures de l'Université de Montréal, the Fondation de l'institut de Cancer de Montréal and Centre de Recherche du Centre hospitalier de l'Université de Montréal for their financial aid and support.

1. Introduction

1.1 Cell cycle, senescence and cell death : A brief overview

The term cell cycle refers to the orderly biological process where one cell will generate 2 daughter cells through the duplication of their genetic material and cell division. In eukaryotes the cell cycle is divided into specific phases, gap phase 0 (G0), gap phase 1 (G1), DNA synthesis phase (S), gap phase 2 (G2), and mitosis (M)[1-4]. To ensure that the cells pass accurate copies of their genomes on to the next generation, evolution has overlaid the core cell cycle machinery with a series of surveillance pathways termed cell cycle checkpoints[5,6,7]. DNA damage including single nucleotide damage, base pair mismatch, DNA single-strand breaks (SSB) and double-strand breaks (DSB), chromosome misattachment and missegregation during mitosis represent global and serious threats to genomic and chromosome stability which will rapidly induce complex pleiotropic cell responses paired to cell cycle checkpoints and repair mechanisms[1,8-10]. The overall function of these checkpoints in response to damaged or abnormally structured DNA is to slow down and halt cell cycle progression, thereby allowing time for appropriate repair mechanisms to correct the genetic lesions and/or structural aberrations before they are passed on to the next generation of daughter cells. At their most proximal signaling elements, these complex machineries contain, sensor proteins or protein complexes that scan chromatin for partially replicated DNA, DNA errors, DNA strand breaks, or chromosome misattachment and missegregation, and translate these derived stimuli into biochemical signals that will modulate the functions of specific target proteins[11]. These mechanisms first promote cell cycle arrest, DNA repair and proper chromosome alignment and segregation, but can also promote irreversible cellular senescence or cell death[12]. The repair mechanisms correct minor irregularities during a temporary cell cycle halt, whereas more deleterious defects are believed to result in the induction of cellular senescence or cell death. Defects in those signalling cascades and/or repair mechanisms combined with errors initiating cellular senescence or cell death could yield to mutations and/or aneuploidy leading to genomic and/or chromosome instability [13,14].

Cells can enter into an irreversible cell cycle arrest termed cellular senescence. The process of cellular senescence was first described more than 50 years ago by Hayflick and Moorehead as an irreversible cell cycle arrest of human fibroblasts that lost their proliferative capacity[5,15,16]. It was later found that telomeres, necessary for chromosome integrity and proper cell division, were gradually depleted to a threshold level within 40–45 generations, which triggered the induction of senescence. This threshold was termed as the Hayflick limit[17]. This natural process was named replicative senescence (RS), which differs from premature senescence (PS), an accelerated mechanism that occurs in response to extrinsic or intrinsic stress stimuli. These include DNA damage, disrupted chromatin organization, increased oncogenic signalling, increased replicative stress, treatment with chemotherapeutic drugs or irradiation[18] and oxidative stress[19,20]. Cellular senescence is a safeguard limiting the proliferative competence of cells in living organisms and can act as a potent tumor suppressor mechanism for normal cells [21].

Cell death is often associated with apoptosis[22], a morphologically distinct form of physiological and programmed cell death, explicitly described through many years of research[22,23]. An understanding of apoptosis in mammalian cells was first achieved by research in the nematode *Caenorhabditis elegans* (*C. elegans*)[24]. Apoptosis has since been widely accepted as the primary mode of programmed cell death (PCD), which genetically eliminates predetermined cells from an organism during development. The process is also active in adult organisms as a homeostatic mechanism to maintain cell populations in tissues. Apoptosis also occurs as a defense mechanism such as in immune reactions or when cells are damaged in association with diseases, noxious agents or deregulation of cellular processes[25]. Programmed necrosis or necroptosis and, in some contexts, autophagy are often considered as two others forms of PCD, easily distinguished by their morphological differences[26]. Apoptosis, or type I PCD, described by Kerr et al.[22] is characterized by cell shrinkage, nuclear disassembly associated with chromatin condensation and fragmentation, dynamic membrane blebbing and loss of adhesion to neighbors or to extracellular matrix. Biochemical changes include chromosomal DNA cleavage into internucleosomal fragments, phosphatidylserine externalization and a number of intracellular substrate cleavages by specific proteolysis[27,28]. Autophagy, or type II PCD, is a catabolic process beginning with

formation of autophagosomes, which plays a crucial pro-survival role in cell homeostasis. It is required during periods of starvation or stress due to growth factor deprivation but in some contexts also leads to a form of cell death[29, 30-33]. Type III PCD termed programmed necrosis or necroptosis, involves cell swelling, organelle dysfunction and cell lysis[34-36]. Thus, PCD may play an important role during preservation of tissue homoeostasis and elimination of damaged cells; this has profound effects on malignant tissues[37].

The intimate link between the cell cycle, cellular senescence and cell death with diseases including cancer initiation and development and tumor responses to cancer treatment is getting clearer as research progresses, but it is very far from being completely understood[38-42]. A schematic view of these concepts is shown in Figure 1.

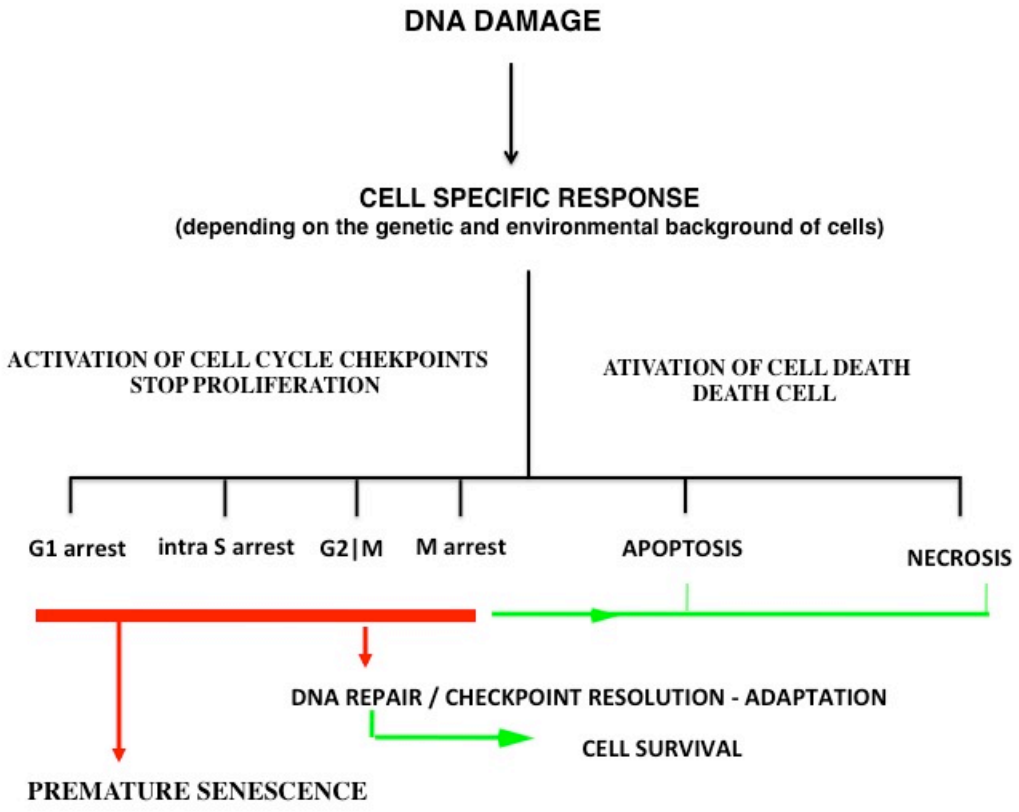

Figure 1: Schematic view of cellular response and fate after DNA damage (adapted from Wang et al., 2011 [43]).

The first sections of the Introduction (1.2 to 1.6) focus on mechanisms in mammalian cells, whereas the last section (1.7) is devoted to *C. elegans*, the second model used for these studies.

1.2 Bcl-2 family of proteins

BCL2 was the first anti-death gene discovered in mammals[44], a milestone with far reaching implications for tumor biology. *BCL2* was discovered because of its involvement in t(14;18) chromosomal translocations observed in non-Hodgkin's lymphomas[44,45]. Multiple members of Bcl-2 family of apoptosis regulating proteins have been identified since, including mammalian anti-apoptotic proteins (Bcl-2, Bcl-xL, Mcl-1, Bcl-xES, Bcl-B, Bcl-w, Bfl-1/A1, Boo/Diva), structurally similar pro-apoptotic proteins (Bax, Bak, Bok/Mtd, Bcl-xS, Bcl-rambo, Bcl-gL) and several structurally diverse pro-apoptotic interacting proteins that operate as upstream agonists or antagonists, called the BH3-only proteins (Bad, Bik, Bid, Bim, Noxa, Puma, Hrk, Bnip1 - 3, Bmf, Mcl-1s, Bcl-gS, Spike)[46]. Proteins of the Bcl-2 family play central roles in cell death regulation and are capable of regulating diverse cell death mechanisms that encompass apoptosis, necrosis and autophagy[47,48], and thus are found undoubtedly altered in many cancers and leukemia[49-52]. Apart from their well-studied roles in controlling apoptosis, members of the Bcl-2 family of proteins also interface with the cell cycle[53-69], DNA repair pathways[70-73] and membrane remodelling mechanisms[74,75], pathways which are well separated from their roles in apoptosis[53-55,75-77].

1.2.1 Structure of anti-apoptotic Bcl-xL protein

The pro-survival family of Bcl-2 proteins has been divided into two sub-classes based on the presence of one or more of Bcl-2 homology (BH) regions (Fig. 2). Four of these regions (BH1-4) of sequence homology have been identified, and each Bcl-2 family members contains at least one of them[78,79]. Several members of the pro-survival subclass, such as Bcl-2, Bcl-xL, Bbl.-w, and the CED-9 protein from *C. elegans*, possess all four BH regions. Others, such as Mcl-1, the BHRF1 protein from Epstein–Barr virus, and KSHV- Bcl-2 from Kaposi sarcoma virus, only possess strong sequence homology in the BH1, BH2, and BH3 regions.

The first published structure of a Bcl-2 family member was that of human Bcl-xL determined by X-ray crystallography and nuclear magnetic resonance (NMR) spectroscopy. It showed that the overall structure of Bcl-xL consists of nine α–helices connected by loops of varying lengths. Bcl-xL adopts a globular structure; it consists of two central, primarily hydrophobic α-helices (α5 and α6), which are surrounded by amphipathic helices: α3 and α4 and by α1, α2 and α7. A 60-residue loop connecting helices α1 and α2 are flexible and non-essential for anti-apoptotic activity[80]. The signature "NWGR" sequence directly precedes α5. In Bcl-xL, this region appears to play both an important structural and functional role. Structurally, the tryptophan residue makes extensive hydrophobic contacts with residues in α7 and α8. The arginine residue also plays a key functional role in the binding of Bcl-xL to pro-apoptotic proteins and peptides such as Bax and Bak. The Bcl-2 family of proteins share homology domains BH1 and BH2 and mutations in these regions in either Bcl-2 or Bcl-xL abrogates the anti-apoptotic activity and block the heterodimerization with other members of the Bcl-2 family (e.g., Bax and Bak) that promote apoptosis[81,82,83]. BH1, BH2 and BH3 are in close proximity and form an elongated hydrophobic cleft in Bcl-xL, the site for interaction with death-promoting BH3-only proteins. The BH3 region is involved in activity of the death promoting proteins[84-86]. The BH3 amphipathic helix of BH3-only proteins binds the hydrophobic groove of pro-survival proteins predominantly by the insertion of four hydrophobic residues (h1–h4) along one face into hydrophobic pockets in the groove, and by the formation of a salt bridge between a conserved BH3 Asp residue and a conserved Arg residue in the BH1 domain of the pro-survival proteins[87-89]. Structural studies have shown that the BH3 binding groove of the pro-survival Bcl-2 family members has considerable plasticity[90,91], which probably contributes to their ability to associate with multiple distinct BH3 domains. Besides the BH regions, many of the Bcl-2 family members possess a carboxy-terminal hydrophobic domain, which is predicted to be responsible for membrane localization[92,93].

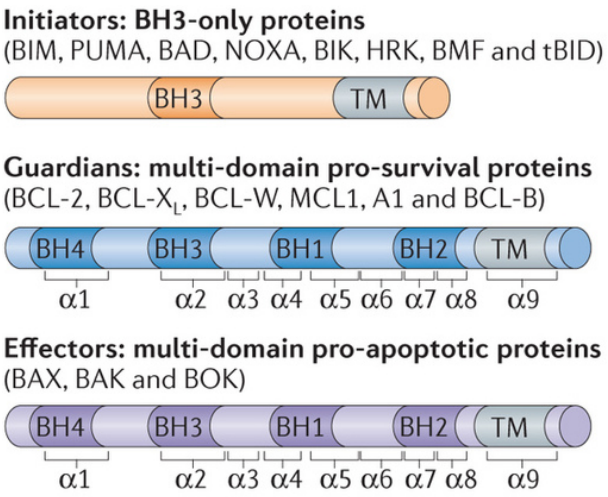

Figure 2: Comparison of domain structures of Bcl-2 family members. All Bcl-2 family of proteins contains at least one of the Bcl-2 homology (BH) domains; BH1, BH2, BH3 and BH4. They also possesses a Transmembrane (TM) domain. The BH3 only proteins contain only one, BH3 domain for their pro-apoptotic functions. (diagram adapted from Peter E. Czabotar et. al 2014[79]).

The sequence homology between Bcl-xL and other Bcl-2 members suggests similar structural folds. The arrangement of α-helices in Bcl-xL is reminiscent of the membrane translocation domain of bacterial toxins, in particular diphtheria toxin and the colicins[94].

1.2.2 Structure and importance of the loop domain of Bcl-xL

An interesting feature of the Bcl-xL protein is the presence of a long loop between α1 and α2[95] (Fig. 3). This loop is largely unstructured as evidenced by the lack of electron density for residues 28-80 and the lack of medium and long range nuclear Overhauser effects (NOEs) for these residues[78]. In addition, this region has highly variable amino acid sequence among Bcl-2 family members. This loop domain has been shown to be the site of some post-translational modifications affecting the activity of both Bcl-xL and Bcl-2[96]. For example, interleukin-3 (Il-3) or erythropoietin treatment of NSF/N1.H7 cells induced the phosphorylation of Ser70, resulting in the inactivation of Bcl-2[97]. Mutant proteins with Ser to Ala mutation[80] or deletion of the loop domain together[98] was able to inhibit PCD better than the wild type protein. In contrast, proteolytic cleavage of the Bcl-2 loop at Asp34 by caspase-3 converts it from an anti-apoptotic to a pro-apoptotic protein[99,100].

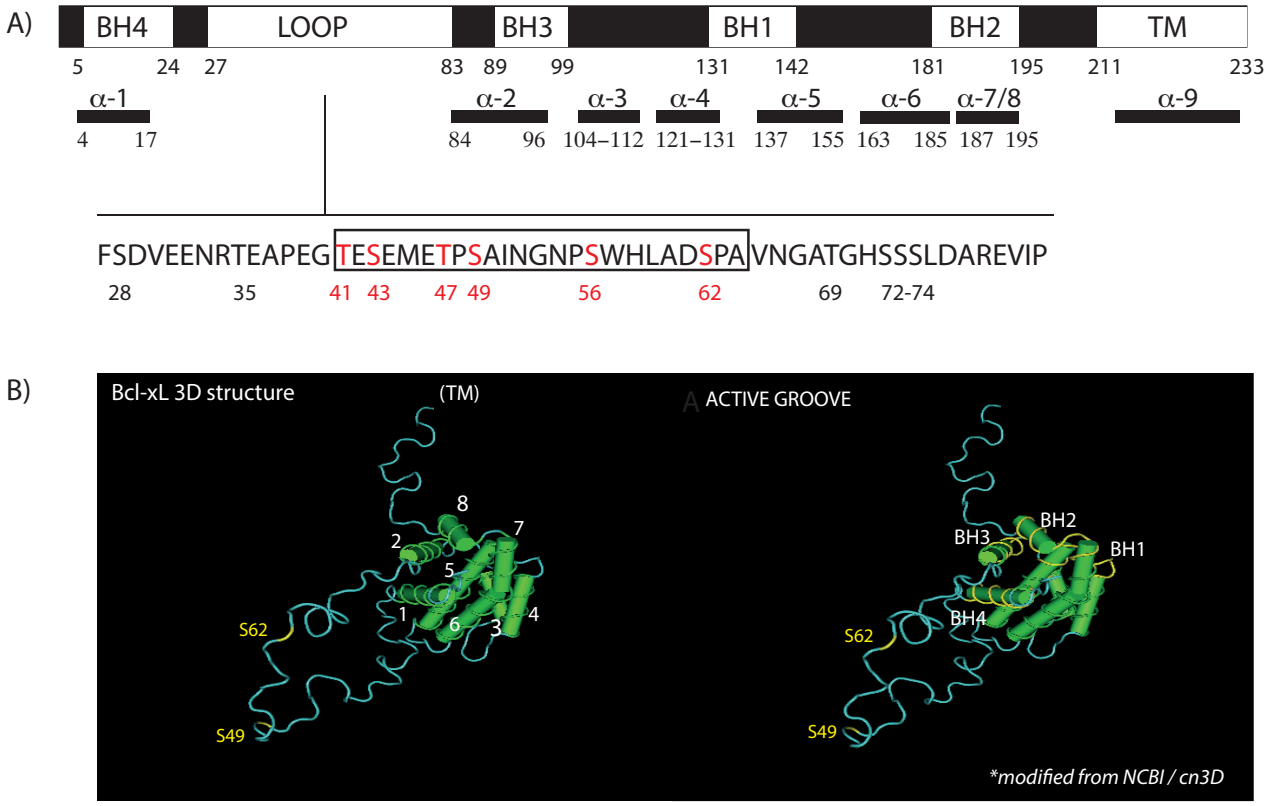

Figure 3: Bcl-xL structure. A) Bcl-xL contains BH1, BH2, BH3 and BH4 domains, a COOH-terminus hydrophobic transmembrane domain (TM) and an unstructured loop domain (LOOP), between BH4 and BH3. The amino acid sequence of the flexible loop domain is indicated. A region of the loop domain previously identified as important for Bcl-xL cell cycle functions is highlighted in the boxed region[53]. Amino acids that have been mutated (Thr/Ala, Ser/Ala) and studied in a series of functional assays are highlighted in red[101-103] (adapted from Wang et al 2011[43]). **B)** Visualization of the 3D structure of Bcl-xL, with the annotated α-helices, BH domains, S49 and S62 (modified from the National Center of Biotechnology Information (NCBI)/ cn3D Web site.)

However, compared to the full-length protein, Bcl-xL loop deletion mutants tend to display a similar ability to inhibit apoptosis and do not show significant alterations in their ability to bind pro-apoptotic proteins[53,95,98]. There is growing evidence indicating that Ser62 of Bcl-xL is highly phosphorylated in cells exposed to microtubule inhibitors, and a few protein kinases have been proposed to phosphorylate Bcl-xL(Ser62) in microtubule inhibitor-exposed cells[104-109]. Previous work in our laboratory has revealed that two serine residues within the unstructured loop domain of Bcl-xL, Ser49 and Ser62, undergo

dynamic phosphorylation/dephosphorylation events during cell cycle progression[101-103]. The function of the unstructured loop domain within Bcl-xL remains elusive, and is the subject of this work.

1.2.3 Bcl-2 family proteins interface with cell cycle

Numerous studies have revealed links between some Bcl-2-like family members, cell cycle progression and cell cycle checkpoint regulation. First, Bcl-2 has been shown to slow entry from the quiescent G0 into the G1 phase of the cell cycle in multiple cell lineages from transgenic mice. In contrast, *Bcl2*$^{-/-}$ knockout cells enter S-phase more quickly[108,110]. More recently, phosphorylated forms of Bcl-2 also have been found to co-localize in nuclear structures and on mitotic chromosomes, revealing the importance of phosphorylation events for Bcl-2 protein localization during cell cycle progression[111]. Mcl-1, another Bcl-2 homologue known to function as an anti-apoptotic protein[112], inhibits cell cycle progression through the S phase of the cell cycle. The cell cycle regulatory function of Mcl-1 is partially mediated through its interaction with proliferating cell nuclear antigen, a cell cycle regulator that is crucial in DNA replication[53,113]. Others have reported that a proteolytic fragment of Mcl-1 regulates cell proliferation via its interaction with cyclin-dependent kinase 1 (Cdk1/Cdc20)[114] and that Mcl-1 is essential in Atr-mediated Chk1 phosphorylation[106]. Others have discerned the involvement of Bid, a BH3-only protein with pro-apoptotic activity, at the intra-S phase checkpoint under replicative stress and in response to DNA-damaging agents. This function of Bid is mediated through its phosphorylation at Ser78 and Ser61/64 by the DNA-damage signaling kinase Atm [115,116].

Previous studies from our laboratory reported that Bcl-xL, an anti-apoptotic Bcl-2 family member, not only counteracts BH3-only protein-mediated cell death signals after DNA-damaging treatment, it also stabilizes the G2 cell cycle checkpoint and favours the establishment of premature senescence in surviving cells after DNA topoisomerase I (camptothecin) and II (VP16) inhibitor exposition[53]. Bcl-xL co-localizes with Cdk1/Cdc2 in nucleolar structures and binds to Cdk1/Cdc2 during the G2 checkpoint, whereas its overexpression stabilizes G2 arrest and premature senescence in surviving cells after DNA damage. Interestingly, Bcl-xL potently inhibits Cdk1/Cdc2 kinase activities *in*

vitro. In *in vitro* kinase assays using recombinant Bcl-xL protein, this effect was reversed by the addition of a synthetic peptide corresponding to the 41st to 60th amino acids, a region rich in Ser- and Thr- putative phosphorylation residues within the flexible loop domain of Bcl-xL. Furthermore, a deletion mutant of this region (Bcl-xLΔP3) did not alter the anti-apoptotic function of Bcl-xL, but impeded its effect on Cdk1/Cdc2 activities and on the G2 checkpoint after DNA damage[53]. Bcl-xL is phosphorylated on Ser62 at the loop domain during normal cell cycle progression and DNA-damage induced G2 arrest by Plk1 and Mapk9/Jnk2[102]. Phosphorylated Bcl-xL(Ser62) accumulates in nucleolar structures including nucleoli and Cajal bodies during the stabilization of DNA damage-induced G2 arrest and co-localizes with Cdk1/Cdc2 avoiding unwanted mitosis during DNA damage[102].

During mitosis, Bcl-xL(Ser62) is strongly phosphorylated by Plk1 and Mapk14/Sapkp38α at prometaphase, metaphase and the anaphase boundary, while it is dephosphorylated at telophase and cytokinesis[103]. Phospho-Bcl-xL (Ser62) localizes in centrosomes with γ-tubulin, and in the mitotic cytosol with some spindle-assembly checkpoint (SAC) signaling components, including Plk1, BubR1 and Mad2. In taxol- and nocodazole-exposed cells, phospho-Bcl-xL(S62) also binds to Cdc20- Mad2- BubR1- and Bub3-bound complexes, while the phosphorylation mutant Bcl-xL(S62A) does not[103] (Fig. 4).

In parallel, Bcl-xL undergoes cell cycle-dependent phosphorylation on Ser49, which accumulates in centrosomes during the G2 cell cycle checkpoint, particularly during DNA damage-induced G2 arrest [101]. Bcl-xL(Ser49) is rapidly dephosphorylated at early mitotic phases (prometaphase, metaphase, anaphase) and is rephosphorylated during telophase/cytokinesis by Plk3. Phospho-Bcl-xL(S49) is found in association with microtubule-associated dynein motor proteins and at the mid-zone body during telophase/cytokinesis[101] (Fig. 4).

In tumor cells, expression of the phosphorylation mutants Bcl-xL(S62A), Bcl-xL(S49A) or dual Bcl-xL(S49/62A) has no effect on apoptosis, but leads to an increased number of cells harbouring mitotic defects[103]. These defects include multipolar spindles, chromosome lagging and bridging, and cells with micro-, bi- or multi-nucleated cells, and

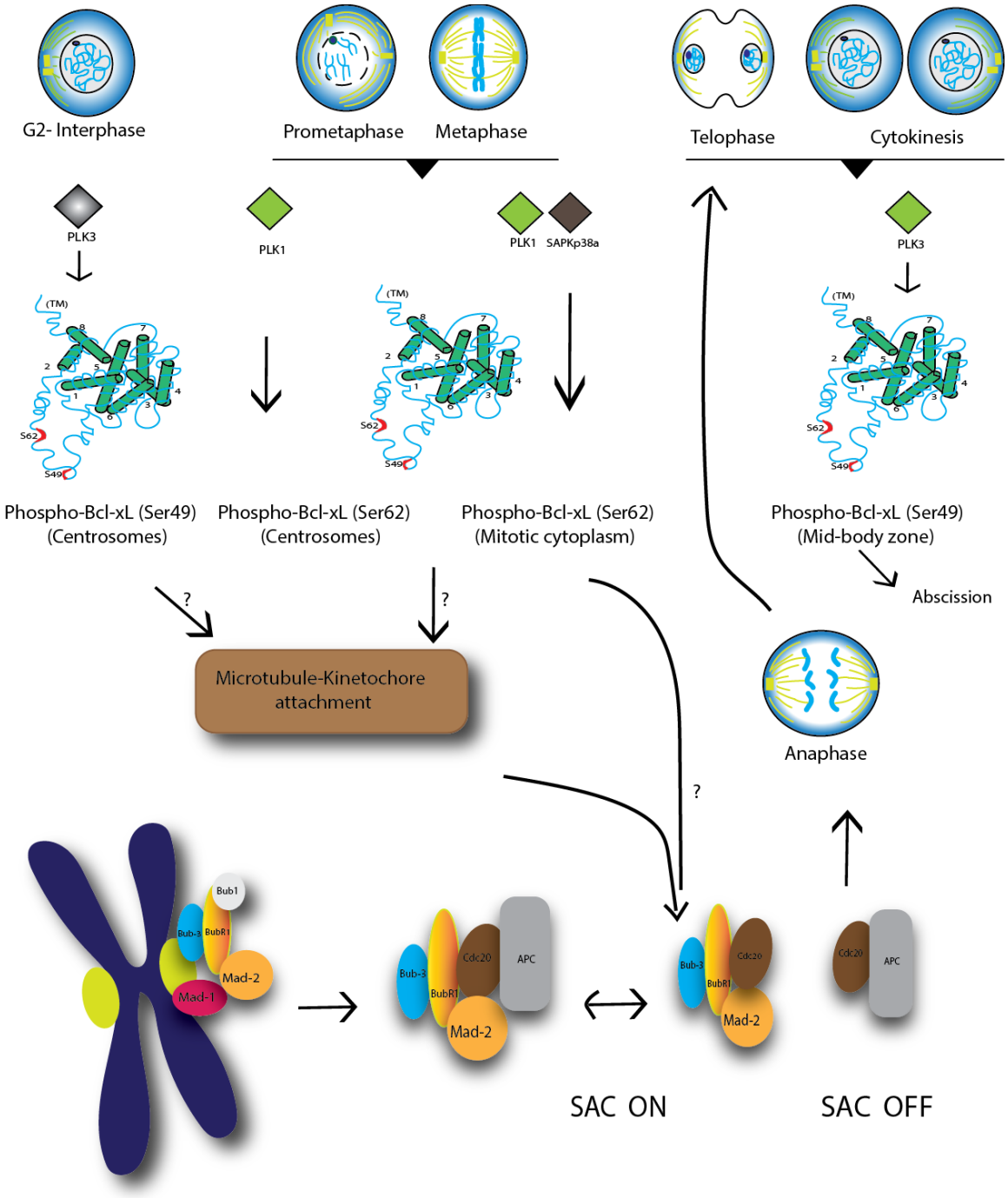

Figure 4: Schematic representation of Bcl-xL phosphorylation during the progression of mitosis. Question marks (?) indicate that the exact mechanisms are still unknown (modified from Wang et al 2014[103]).

cells that fail to resolve and complete mitosis[103]. Together, these observations indicated that during mitosis, Bcl-xL(S49) and (S62) phosphorylation/dephosphorylation dynamics impact on chromosome stability, mitosis resolution and cytokinesis completion, at least in tumour cells[101-103].

1.3 The cell cycle : regulation at interphase

1.3.1 Cyclin-dependent kinases and cyclin-dependent kinase inhibitors

Proper progression through the cell cycle is monitored by checkpoints that sense possible defects during DNA synthesis and chromosome segregation. During interphase, activation of these checkpoints induces cell cycle arrest, which is controlled by interplay modulation of cyclin dependent kinases (Cdks) and their associated cyclins. Cell cycle arrest at these checkpoints allows the cell to repair defects, thus preventing transmission of damage to the daughter cells[117]. Cdks are the catalytic subunits of a family of mammalian heterodimeric serine/threonine kinases, best characterized in the control of cell cycle progression. Cdks were first implicated in cell cycle control based on pioneering work in yeast, in which *Cdc* genes were identified including *Cdc8* in the budding yeast *S. cerevisiae* and *Cdc2* in the fission yeast *S. pombe*, and were found to promote transitions between different cell cycle phases through its interactions with various regulatory cyclin subunits[118-121]. Cyclins are synthesized and destroyed at specific times during the cell cycle, regulating kinase activity of Cdks in a timely manner. Soon, homologs of *CDC2* were identified in human cells [122] by their ability to complement yeast mutants[123]. Subsequently, *CDK2* was discovered because of its ability to complement *Cdc8 S. cerevisiae* mutants[124-127]. Currently more than 20 members of the Cdk family each characterized by a conserved catalytic core made of an ATP binding pocket, a PSTAIRE-like cyclin binding domain and an activating T-loop motif. Cyclins belong to a remarkably diverse group of proteins classified solely on the existence of a cyclin box that mediates binding to Cdk[128]. Cdk activities are restrained by another class of proteins, the cyclin-dependent kinase inhibitors (Cki). Cki are subdivided into two families based on their structure and Cdk specificity. Ink4 proteins, including Ink4A, Ink4B, Ink4C and Ink4D[129]; primarily target Cdk4 and Cdk6. The Cip/Kip family composed of p21, p27 and p57[129] are more promiscuous and broadly interfere with the activities of cyclin D, E, A and B dependent kinase complexes[130]. Cki have been shown to block the proliferation of adult stem cells in multiple tissue types. Loss of Cki may expand the stem cell population, possibly contributing to the development of specific tumours.

1.3.2 G1-S phase transition

After cytokinesis is completed, the newly generated cells can either continue cell division or stop proliferating. If cells are deprived of growth factors prior to the G1 checkpoint, they exit into a state of quiescence known as G0. Those cells that continue proliferating advance to the G1 phase of the new cycle (Fig. 5). According to the classical model for the mammalian cell cycle, specific Cdk-cyclin complexes are responsible for driving the various events known to take place during interphase in a sequential and orderly fashion. Progression through G1 is mainly regulated by Cdk4, Cdk6 and Cdk2 and their regulatory cyclins[130,131]. At the beginning of G1, the mitogenic signaling induces synthesis of the D-type cyclins (D1, D2 and D3) and possibly the proper folding and transport of Cdk4 and/or Cdk6 to the nucleus and the activation of the latter. These Cdk-cyclin complexes phosphorylate members of the retinoblastoma (Rb) protein family; pRb, p107 (RbL1) and p130 (RbL2) at their unique phoshorylation sites. The retinoblastoma protein (pRb) and the pRb-related p107 and p130 comprise the 'pocket protein' family of cell cycle regulators. These proteins are best known for their roles in restraining the G1-S transition through the regulation of E2f-responsive genes. pRb and the p107/p130 pair are required for the repression of distinct sets of genes, potentially due to their selective interactions with E2fs that are engaged at specific promoter elements[132]. Inactivation of pocket proteins allow for the expression of the E-type cyclins (E1 and E2) which bind and activate Cdk2[133,134]. Cyclin E- cdk2 complexes further phosphorylate these pocket proteins, leading to their complete inactivation[134,135]. Another kinase, Cdk3 might also participate in inactivation of pRb.

Cyclin E-Cdk2 activity is thought to be essential for initiating DNA replication by facilitating loading of the Mcm chromosome maintenance proteins onto origins of replication. Once cells enter S-phase, cyclin E-cdk2 complexes need to be silenced to avoid the re-replication of DNA[136]. Rapid degradation of cyclin E is carried about by Scf-Fbxw7 ubiquitin ligase followed by its subsequent cleavage by the proteasome. In addition, cyclin E-cdk2 phosphorylates its own inhibitor p27 , thereby facilitating the degradation of this inhibitor by the proteasome[136]. Inactivation of pRb also activates transcription of A-type and B-type cyclins. Cyclin A-cdk2 is required for proper completion and exit from S phase. S phase proteins also include upstream regulators of

cyclin A (pRb), transcription factors (E2f1, B-Myb), protein involved in DNA replication (Cdc6, Hssb, Mcm4), DNA repair (Brca1, Ku70), histone deposition and nucleosome assembly (Hira)[137], ubiquitin mediated proteolysis (hHR6A and Cdc20) and cell cycle checkpoints (p53, $p21^{Cip1}$, Mdm2)[130].

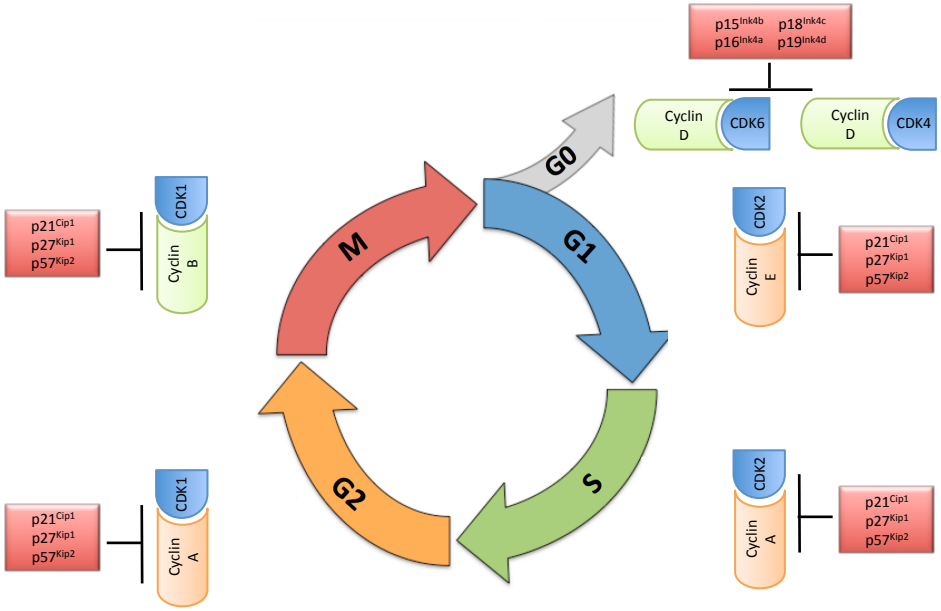

Figure 5: Eukaryotic cell cycle phases with respective cyclin-Cdk complexes and inhibitors. The Cdk-cyclin complexes regulate the cell cycle in terms of its entry from one phase to another apart from the checkpoint proteins. Cyclin D-Cdk4/6 complex stimulates the initiation of G1 phase and the start of the cell cycle. Increasing levels of cyclin E-Cdk2 triggers the onset of S phase towards the end of G1 phase. Then, Cyclin A- Cdk2 regulates the completion of S phase and entry into G2, where cyclin B-Cdk1 is involved. The level of cyclin B increases initially and decreases at the end of M phase, followed by a decrease in Cdk1. (Diagram modified from Moghadam et al., 2011[138])

1.3.3 G2-M phase transition

At the end of the G2 phase, B-type cyclins associate with Cdk1(cdc2), the master regulatory kinase that controls the entry into mitosis. Cdk1 is only active at the G2/M border and becomes inactive as cells enter the anaphase stage of mitosis[139,140]. During G2, mammalian cyclin B1/Cdk1 complexes are held in an inactive state by phosphorylation of Cdk1 at two negative regulatory sites; Thr14 and Thr15, catalyzed by Myt1 and Wee1

kinases respectively, when it is bound to cyclin B1[141-146]. Cdc25 phosphatases dephosphorylate these sites for the activation of Cdk1. Mammalian cells have three Cdc25 phosphatases, Cdc25A, B and C, which appear to have some level of specificity for different cyclin/Cdk complexes along the cell cycle. Studies indicate that Cdc25A regulates G1/S and G2/M transitions, whereas Cdc25B and Cdc5C are involved in intra-S and G2/M regulation[140,147-153]. Entry into mitosis absolutely requires progressive accumulation of active cyclin B1/Cdk1(cdc2) complexes in the nucleus. Cyclin B1/Cdk1(cdc2) kinase activity is therefore highly organized to coordinate and trigger different mitotic events. The initial activation of cyclin B1/Cdk1(cdc2) complexes occurs about 20 to 25 minutes before nucleolar disassembly and nuclear breakdown[154,155]. After these events, cyclin B1/Cdk1(cdc2) rapidly reaches its maximum activity to promote mitosis.

1.4 The cell cycle : mitosis regulation

Mitosis can be divided into five distinct phases: prophase, prometaphase, metaphase, anaphase and telophase (Fig. 6). During prophase, chromosomes condense into highly compacted rigid bodies for physical segregation of sister chromatids into the daughter cells[156]. Centrosomes increase the assembly rate of dynamic microtubules and move apart to form a bipolar spindle. During prometaphase chromosomes successively attach to the mitotic spindle microtubules via their kinetochores, multi protein structures that assemble on centromeric chromatin[157]. Chromosomes align at the metaphase plate along the spindle equator with sister chromatids, the two identical copies of a chromosome, facing opposite poles[158]. Once all sister kinetochores are attached to microtubules originating from opposite spindle poles, mitotic exit initiates by cleavage of the cohesion rings that hold sister chromatids together[159]. In anaphase sister chromatids are then segregated towards opposite spindle poles.

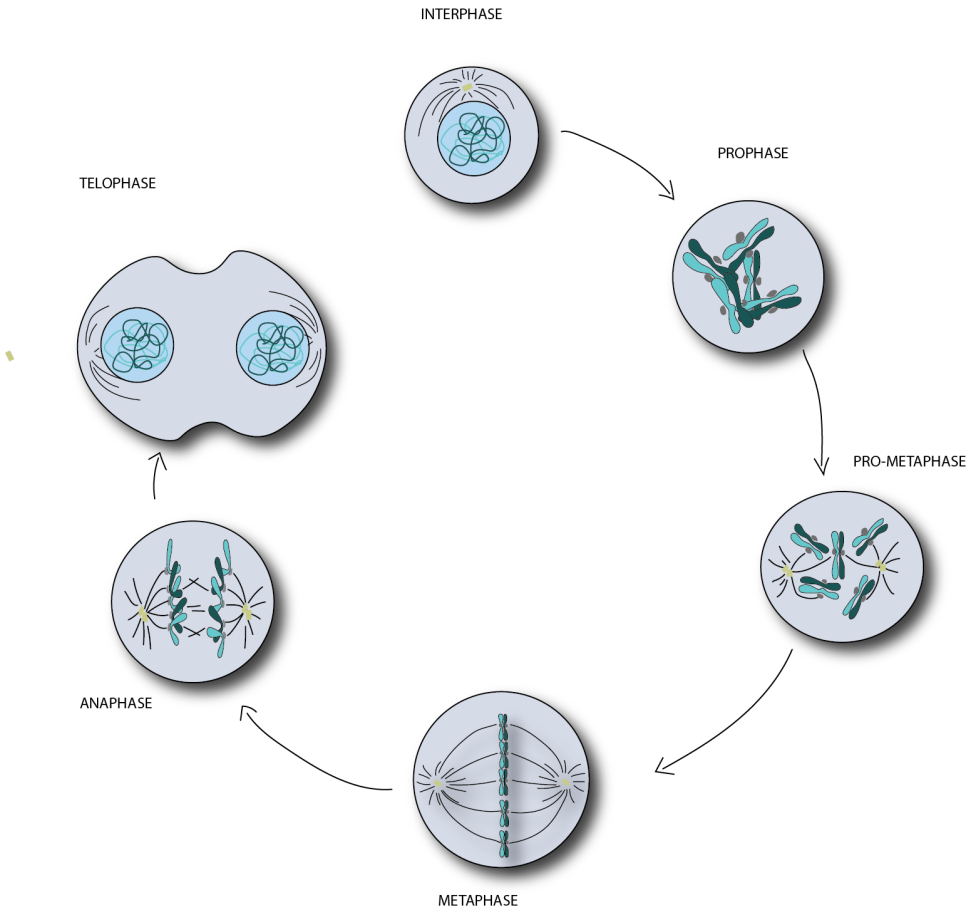

Figure 6: Progression through mitosis. Mitosis proper in general involves four major stages- Prophase, metaphase, anaphase and telophase. The stages are shown by schematic of the mitotic spindle and chromosomes. Sister chromatids, the two identical copies of a chromosome, are separated at the end of the mitosis into two equal daughter cells. (diagram inspired from Cheeseman and Desai, 2008[157])

In telophase, many mitotic changes revert back to the interphase state; chromosomes decondense and the nuclear envelope reassembles around two individual nuclei. Finally, cytokinesis physically splits the cytoplasm to form the two new daughter cells. To ensure smooth progression of the cell cycle, cell cycle checkpoints constantly monitor the molecular mechanistics of cell division.

Monitoring the order and fidelity of chromosome alignment and segregation through mitosis and meiosis is largely achieved by the actions of two checkpoints during mitosis: the spindle assembly checkpoint (SAC) and the mitosis exit network (MEN). The SAC functions in metaphase to prevent premature separation of sister chromatids at anaphase

[160-162]. The MEN acts at the end of telophase and control cytokinesis and cell division itself [163]. Accurate chromosome segregation is essential for genome inheritance and cellular fitness. Lethality or aneuploidy results when chromosomes fail to segregate during mitosis. Aneuploidy leads to aberrant gene dosage and exposes detrimental recessive mutations, potentially causing birth defects and promoting cancer cell proliferation[164,165]. Accurate segregation is achieved by linking sister chromatids after replication, which is mediated by spindle microtubules that attach to chromosomes at the kinetochores.

1.4.1 Chromosome - microtubule attachment

1.4.1.1 The kinetochores

The kinetochore is a hierarchical protein assembly composed of nearly 100 proteins that links centromeric DNA to spindle microtubules and thereby couples forces generated by microtubule dynamics to power chromosome movement. Core components of the kinetochore is established by the constitutive centromere associated network (CCAN)[166] and the Knl1-Mis12-Ncd80 (KMN) protein complex[167], which bind centromeric DNA and microtubules, respectively. These networks are conserved across eukaryotes, with additional contributions from species-specific auxiliary DNA and microtubule binding proteins. Regulatory proteins at the kinetochore safeguard against erroneous segregation and thereby increase the fidelity of mitosis in two ways. First, attachments on bi-oriented kinetochore pairs are selectively stabilized, whereas erroneous attachments are destabilized and eliminated. This allows for another opportunity for bi-orientation. Second, unattached kinetochores are the primary signal to activate the SAC. The competing need for speed and fidelity in chromosome segregation are integrated mainly at the kinetochore. The KMN network is an essential and conserved complex of proteins that constitutes the core microtubule binding activity at the kinetochore and is a platform for SAC signaling. In addition to mediating chromosome spindle attachment, the kinetochore also plays an essential role in relaying microtubule binding status to the SAC to delay exit from metaphase and chromosome segregation.

1.4.1.2 The KMN network

The kinetochore localized KMN network is composed of Knl1 (Kinetochore null protein 1), four subunits of Mis12 (Mis-segregation 12) and four subunits of Ndc80/Hec1 (Nuclear division cycle 80) (Fig. 7). The Ndc80 complex is a heterotetramer comprising Ndc80/Hec1, nuclear filamentous 2 (Nuf2), spindle pole component 24 (Spc24) and Spc25. The site where kinetochores are assembled is determined by the presence of a modified histone H3 or Cenp-A in humans, within nucleosomes at the periphery of each sister centromere. The KMN network associates with kinetochores in prophase and disappears from kinetochores in telophase[168]. Heterodimers of Spc24-Spc25 and Ndc80/Hec1-Nuf2 interact via coiled coil domains and assemble into a coiled like structure with distinct functional domains at each end[169-172]. The globular domains of the Ndc80/Hec1-Nuf2 heterodimer fold into a calponin homology domain, which mediates microtubule binding[167,173,174]. The Spc24-Spc25 heterodimer globular domains are essential for kinetochore targeting of the Ndc80/Hec1 complex, as they directly bind to the Mis12 complex[175] and CCAN components[176]. To couple chromosome movement to microtubule dynamics, an electrostatic interaction between the basic amino terminal tail of the Ndc80/Hec1 protein and the acidic E-hook of tubulin confers affinity[172,173,177]. The complex then binds to microtubules by recognizing both α-tubulin and β-tubulin at the inter- and intra-tubulin interfaces[177]. The Ndc80/Hec1 complex binds to the microtubule every 4 nm space, acting as a sensor allowing it to detach near depolymerizing microtubule ends.

Knl1 has a microtubule binding activity, which enhances the binding of the KMN network with microtubules in vitro[167]. The Mis12 complex function as an inter-complex scaffold that links the KMN network to the centromeric DNA via direct association with the CCAN protein CenpC[178,179]. The Mis12 complex also bridges Knl1 and Ndc80 complex at the kinetochores[175].

A number of other proteins within and at the periphery of the kinetochore outer domain depend on the presence of members of the KMN network for their kinetochore localization. These include MT-associated proteins in the proximity of kinetochore MT plus ends and members of the SAC[160,180]. Current understanding of how KMN networks promote kinetochore function is limited and requires further work.

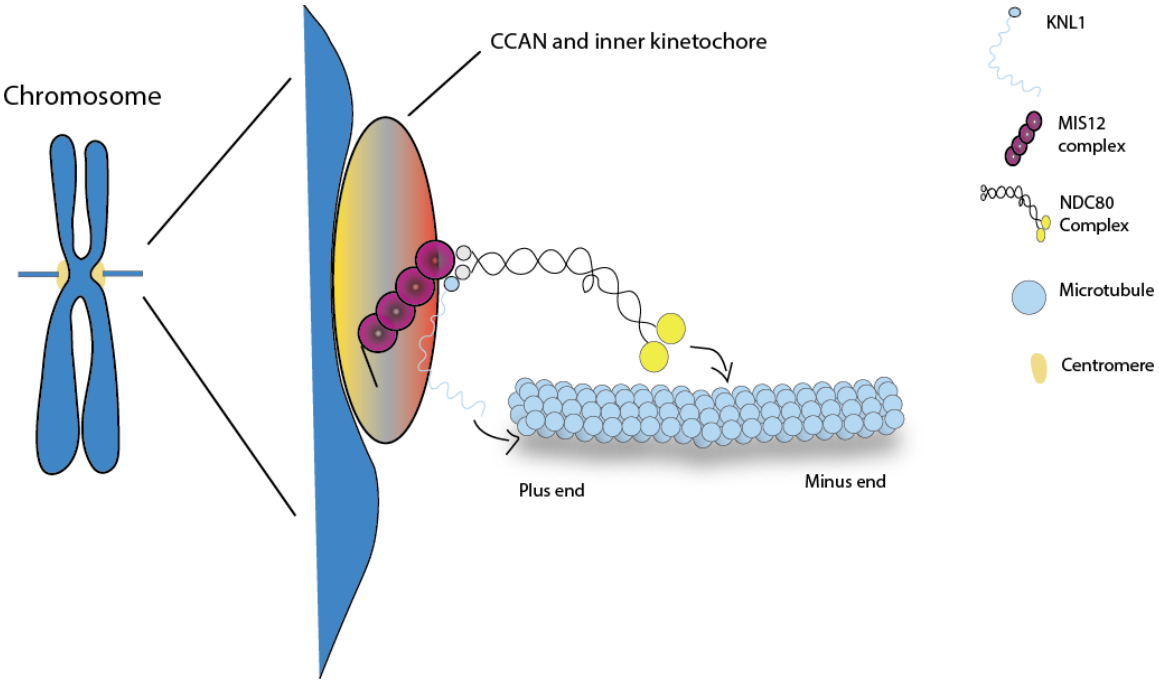

Figure 7: Organization of the KMN network. The KMN network consists of KNL1, NDC80 and MSL12. The four subunits of the MSL12 complex bridges KNL1 and the NDC80 complex to the constitutive centromere associated network (CCAN) and centromeric DNA. (diagram inspired from Emily A. Foley 2013[181])

1.4.2 Activation of the spindle assemble checkpoint

In 1991, two independent screens identified various genes, mutation of which bypassed the ability of wild type *S. cerevisiae* cells to arrest in mitosis in the presence of spindle poisons[182,183]. The genes which are conserved across eukaryotes, include the human Ser/Thr kinases multipolar spindle protein 1 (Mps1) and budding uninhibited by benomyl 1 (Bub1), as well as the non-kinase components including mitotic arrest deficient 1 (Mad1), Mad2, Bub3 and the likely pseudo-kinase Bub1 related (BubR1)[182-184]. These genes are collectively involved in a pathway that is active in prometaphase and which prevents the premature separation of sister chromatids[185,186]. This pathway constitutes the spindle assembly checkpoint (SAC). These proteins delay the activation of Cdc20, a cofactor of the E3 ubiquitin ligase known as anaphase promoting complex/cyclosome (APC/C)[187,188]. The APC/C is a master regulator of anaphase entry[189]. A mitotic checkpoint complex (MCC) that contains three SAC proteins, Mad2, BubR1/Mad3 and Bub3, as well as Cdc20 acts as a SAC effector. The MCC binds the

APC/C and seems to render it unable to exercise its ubiquitin-ligase activity on securin and cyclin B[190-196]. Besides MCC, other core SAC components include Mad1, Bub1, Mps1 and Aurora-B. These proteins are required to amplify the SAC signal and the rate of MCC formation[197]. The SAC inhibits the APC/C functions by inactivation of Cdc20 through the MCC complex[198].

The key step in MCC formation is conformational activation of Mad2 from the free 'open' form (O-Mad2) to the Cdc20-bound 'closed' form (C-Mad2)[198,199]. This conversion is a catalytic process, occurring through the association of soluble O-Mad2 with kinetochore bound C-Mad2. Mad1 is the receptor for C-Mad2 at the kinetochore, distinct from Cdc20-bound C-Mad2, which facilitates Mad2 conformational conversion. The kinetochore at this point promotes Mad2 conversion through hierarchical recruitment of SAC proteins. This cascade seems to consist of kinases Aurora-B and Mps1 at top, followed by recruitment of the Bub1-Bub3 complex, then by the recruitment of BubR1-Bub3, and finally by recruitment of a heterotetramer composed of Mad1 and Mad2[200-204].

1.4.2.1 Bub-related protein kinetochore recruitment

Recently it has been established that core kinetochore protein Knl1 recruits Bub1, BubR1 and Bub3[205-208], although complex recruitment isn't clearly understood. Bub1, a protein kinase, and BubR1, a pseudokinase in vertebrates, contain catalytic domains that are universally required for the checkpoint and are important for kinetochore bi-orientation[209,210]. Bub1 and BubR1 bind to Bub3 through a Bub3-binding domain also known as GLEBS domain. Bub1 interacts via its TPR motif with the KI motif on Knl1 of the kinetochore[204,205]. Mps1 kinase activity stimulates Bub1 localization and checkpoint activation and Mps1 mediated phosphorylation of Thr residues on the MELT-like motifs of Knl1, which is required for Bub1 kinetochore localization[206-208]. Crystallography and biochemical studies have shown that Bub3 binding to Knl1 is the key step in localizing Bub1-Bub3 to kinetochores[211]. In contrast, BubR1 localization depends on Bub1 but not through Bub3-KNL1 binding. It is suggested that Bub1 directly recruits BubR1 through dimerization[212-214].

1.4.2.2 Mad1 and Mad2 kinetochore localization

Although Bub1-Bub3 localization is required for the checkpoint, its localization does not always correlate with checkpoint activation. For instance, some Bub1 is retained on early anaphase kinetochores[203,215,216] and Bub1 but not Mad1 is present on kinetochores bound to the sides of microtubules, which do not signal the checkpoint[217]. Bub1 is a key component in localizing Mad1 to the kinetochore via its RLK motif[218]. Another Mad1 co-receptor Rod-Zwilch-Zw10 (RZZ) is thought to play role in Mad1 localization[219].

Knl1 and its constituent binding partner Zwint are required to localize RZZ[220,221] and RZZ localization may be regulated through Aurora-B dependent phosphorylation of Zwint[222]. RZZ is required for stable Mad1 localization in human cells. The kinetochore dynamics of Mad1 consists of two roughly equal sized pools: a more stably bound pool and a mobile, high turn-over pool[223]. Mad2 when bound to Mad1 adopts the C-Mad2 conformation and doesn't seem to dissociate from Mad1 during checkpoint activation.

Mad1-C-Mad2 accounts for the more stable kinetochore pool of Mad2. C-Mad2 bound to Mad1 is the kinetochore receptor for O-Mad2[224-226]. Therefore, the mobile and immobile fractions of kinetochore Mad2 consist, respectively, of rapidly cycling C- and O-Mad2 and the Mad1-Mad2 receptor.

1.4.2.3 The Mad2 template model

How kinetochores promote MCC formation is not entirely clear. Fluorescence recovery after photobleaching (FRAP) experiments revealed that some of the checkpoint proteins are stably bound to unattached kinetochores (Bub1, Mad1 and a pool of Mad2), whereas other checkpoint components turnover more rapidly (BubR1, Mps1, Bub3, a pool of Mad2 and Cdc20) supporting the idea that unattached kinetochores catalyze the formation of a diffusible checkpoint inhibitor[201,223]. The existence of C-Mad2 and O-Mad2 lead to the Mad2 template model[227] (Fig. 8). The fundamental principle is that O-Mad2 can dimerize with C-Mad2, which induces a conformational change from O-Mad2 to C-Mad2, thereby binding to Cdc20. Unattached kinetochores stably bind a tetrameric Mad1:C-Mad2 complex[226,228] and thus, unattached kinetochores can serve as template for continuous conversion of cytosolic O-Mad2 molecules. This model explains how a single unattached kinetochore can generate an efficient checkpoint response. However, it also

predicts that the checkpoint signal spreads in the cytoplasm: C-Mad2:Cdc20 could then serve as template and hence uncouple checkpoint signaling from unattached kinetochores. Amplification of C-Mad2 away from kinetochores might be prevented by several mechanisms. First recruitment of O-Mad2 to Mad1:C-Mad2 depends on Mps1 activity[229], a process that might be restricted to the kinetochore environment. Second, in the cytosol the dimerization interface of C-Mad2 is blocked when bound to p13/comet, a protein with structural similarity to Mad2[230]. Third, to form functional inhibitory MCC, C-Mad2:Cdc20 forms a complex with the Bub3:BubR1 where binding to Mad3 has been shown to block the dimerization interface of Mad2[231].

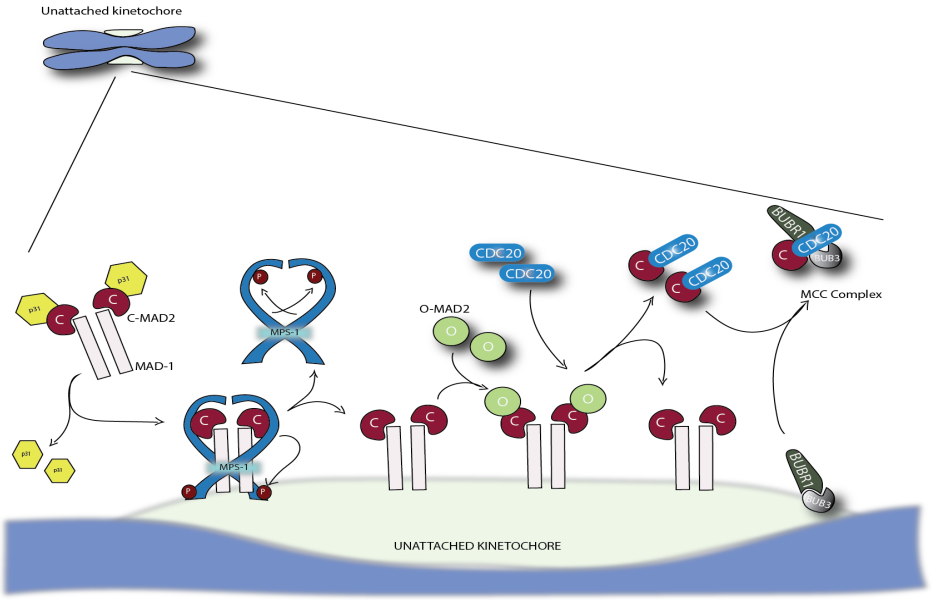

Figure 8: Mad2-template model of MCC production at unattached kinetochores. In the cytoplasm C-Mad2 forms a tetrameric complex with Mad1, but dimerization with O-Mad2 is blocked by p31/comet. Upon Mps1 phosphorylation Mad1:C-Mad2 binds to unattached kinetochores. This releases p31/comet, and together with Mps1 activity allows cytosolic O-Mad2 to dimerize with C-Mad2. This initiates a conformational change and enables the formation of C-Mad2:Cdc20, which subsequently assembles with the Bub3:BubR1 complex to form the MCC (diagram inspired from Lara-Gonzales et al., 2012[232]).

1.4.2.4 Phosphorylation control

In order to prevent chromosome missegregation, the SAC delays anaphase until all kinetochores are correctly attached to the mitotic spindle[160]. Phosphoregulation plays a part in this checkpoint, with contributions from the Mps1 kinase, which is required for the recruitment of essentially all other SAC components to the kinetochore. Phosphorylation of Knl1 by Mps1 creates a docking site for the SAC kinase Bub1 and its binding partner Bub3[206,207]. Kinetochore-localized Bub1 is necessary and sufficient for recruiting the SAC proteins Bub3 and BubR1/Mad3. Much like Bub1, Zwint1 (ZW10 interacting protein 1) which associates with both Knl1 and RZZ complex, localizes Mad1 to the kinetochore. Mps1 kinase also localizes RZZ complexes to the kinetochore.

At the start of mitosis, all chromosomes lack spindle attachments. Initial interactions between chromosomes and spindle microtubules occur predominantly along the microtubule (MT) lattice, rather than at the MT plus ends[233], later replaced by stable end-on attachments, which depends on the KMN network. Error-free chromosome segregation requires that MT binding be dynamic such that erroneous attachment can be eliminated while proper attachments on bi-oriented chromosomes persist through anaphase. These two competing needs are balanced through reversible phosphorylation events at the kinetochore, with essential contributions from Aurora-B kinase and phosphatase PP2A containing a B56 regulatory subunit (B56-PP2A). Aurora-B targets centromeric DNA and has a conserved role in destabilizing and eliminating erroneous kinetochore-MT attachments[234,235].

A large body of work suggests that phosphorylation of Aurora-B substrates at the kinetochore reduces MT-binding affinity[236]. Current models suggest that differential levels of phosphorylation of Aurora-B substrates arise because Aurora-B is located closer to kinetochore substrates on erroneously attached kinetochores, where tension is low, compared with bi-oriented kinetochores, where tension is high and the distance between the kinetochore and centromere is increased[237].

A model was suggested to describe how stable kinetochore-MT interactions are formed during prometaphase[181] (Fig. 9). The model suggests that at unattached kinetochores, Aurora-B is close to its outer kinetochore substrates (e.g., KMN network) and phosphorylation is maximal[238]. During prometaphase, many kinetochores begin

establishing lateral interactions along MT walls, which do not require the KMN network[233,239]. Crucially, these later interactions produce tension, which increase the distance between centromeric Aurora-B and the KMN network, decreasing the phosphorylation of KMN network proteins in comparison to unattached kinetochores.

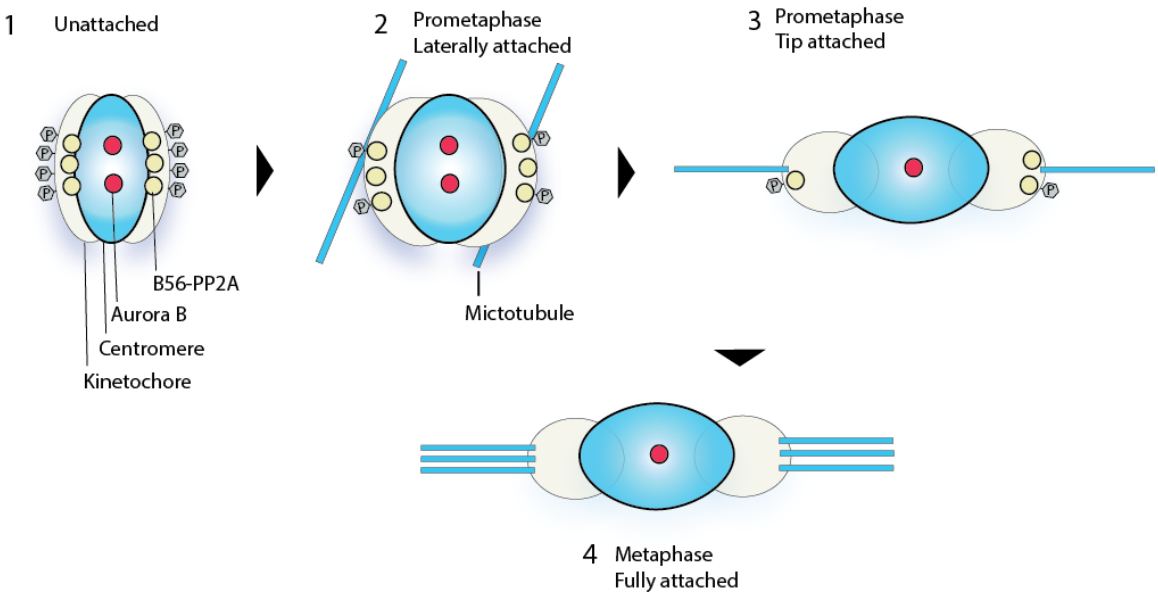

Figure 9: Speculative model of the regulation of kinetochore–MT binding through outer kinetochore phospho-regulation by Aurora-B and B56-PP2A. On unattached kinetochores lacking tension, centromeric Aurora-B kinase is in close proximity to its outer kinetochore substrate allowing for high levels of phosphorylation, despite the presence of B56-PP2A phosphatase, also at the kinetochore (1). During prometaphase, lateral interactions produce intermediate tension, which results in both inter- and intra-kinetochore stretching. This increases the distance between Aurora-B and its outer kinetochore substrates, while B56-PP2A localization relative to the outer kinetochore is unchanged (2). The net result is a decrease in substrate phosphorylation and stabilization of initial microtubule tip interactions (3). At metaphase, full MT occupancy results in the loss of B56-PP2A from the kinetochore, and limited access of Aurora-B to its substrates on stretched centromeres allows for stable attachments (4) (diagram inspired from Foley and Kapoor 2013[181])

Finally, as MT occupancy increases, inter- and intra-kinetochore tension is established and the accessibility of Aurora-B kinase to the kinetochore is reduced, and B56-PP2A is removed from kinetochore[240]. These two events ensure phosphorylation remains low on bi-oriented kinetochore pairs. The regulation of kinetochore-MT attachments also depends on Plk1[241]. Recruitment of B56-PP2A to the kinetochore depends on Plk1-

mediated phosphorylation of BubR1. B56-PP2A in turn, regulates the phosphorylation of BubR1 and Plk1 kinetochore targeting[242]. Such inter- dependencies of kinase and phosphatase recruitment, combined with MT attachment-sensitive targeting, allow for feedback mechanisms capable of rapidly responding to MT binding.

1.4.2.5 Cdc20 under control

During prometaphase, Cdc20 concentrates at the kinetochores[243,244] (Fig. 10). Kinetochores provide the catalytic platform to accelerate the production of the MCC. The SAC targets Cdc20, the co-factor of APC/C. Specifically, the SAC negatively regulates the ability of Cdc20 to activate the APC/C mediated polyubiquitylation of two key substrates, cyclin B and securin, thereby preventing their destruction by the 26S proteasome[245,246]. Securin is a stoichiometric inhibitor of a protease known as separase. Separase is required to cleave the cohesion complex that holds the sister chromatids together and cohesion cleavage is required to execute anaphase[189]. The proteolysis of cyclin B inactivates the master mitotic kinase Cdk1, which promotes exit from mitosis. By keeping Cdc20 in check, the SAC prevents this chain of events, prolonging prometaphase until all chromosomes have become bi-oriented between separated spindle poles on the metaphase plate. Chromosome bi-orientation finally extinguishes the checkpoint, relieving the mitotic arrest and allowing anaphase to proceed.

1.4.3 Silencing of the spindle assemble checkpoint

Once the spindle assembly checkpoint is cleared, inhibition of the APC/C needs to be released to promote anaphase entry and chromosome segregation. This requires halting MCC production as well as disassembly of existing MCCs.

1.4.3.1 Correct kinetochore-microtubule attachment stops mitotic checkpoint complex production

Production of new MCC ceases when kinetochores stably attach to spindle MTs[180]. Upon MT attachment checkpoint components diminish, such as Bub1, BubR1 and Mps1, or nearly disappear, such as Mad1 and Mad2[201,215,247,248]. Removal of checkpoint components may be accomplished by several mechanisms.

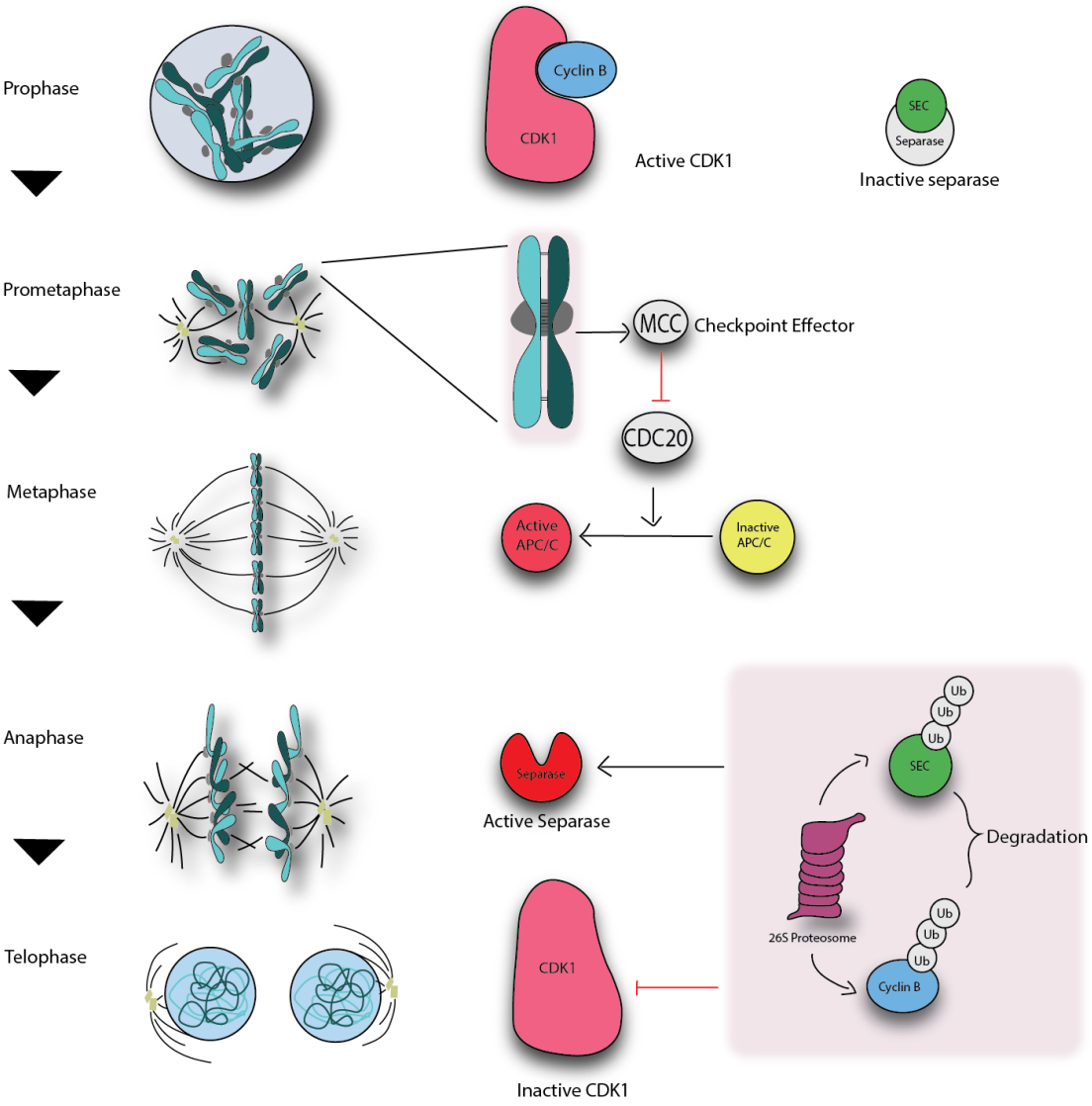

Figure 10: The spindle assembly checkpoint delays mitotic progression. Mitotic entry is driven by Cdk1-cyclin B phosphorylation. In the beginning of mitosis securin (SEC) binds to the protease separase, thereby preventing cleavage of the cohesin rings (yellow dots) that hold the sister chromatids together. Unattached kinetochores (red ovals) catalyze MCC production, which inhibits activity of APC/C-Cdc20. The SAC is only satisfied when all kinetochores are attached (green ovals), and MCC production stops. APC/C-Cdc20 can then polyubiquitylate (UbUbUb) cyclin B and securin, which targets them for degradation by the 26S proteasome. Degradation of securin frees separase to cleave cohesin, which enables chromosome segregation. Degradation of cyclin B inactivates CDK1-cyclin B, which induces cytokinesis and further drives mitotic exit (diagram modified from Musacchio and Salmon, 2007[160]).

The depletion of the Mad1:C-Mad2 complex from kinetochores is important for spindle assembly checkpoint silencing. This is mainly achieved by dynein-mediated "stripping"

of Mad1 and Mad2 along kinetochore fibres towards the poles[249]. Mad1 and Mad2 have actually been visualized to move along kinetochore fibres, but other checkpoint proteins such as BubR1 and Mps1, may also be reduced in this way[250].

However, this might not be the only mechanism by which checkpoint proteins are removed from kinetochores, as fungi and higher plants do not have kinetochore dynein and in human cells dynein-independent pathways also exist[251]. While Mad1 and Mad2 are removed from kinetochores already upon MT attachment, other checkpoint components, such as Mps1, BubR1 and Bub1, require correct bi-orientation for an efficient depletion[201,252]. Upon bi-orientation outer kinetochore components are removed from centromeric Aurora-B and subsequent localization and phosphatase activity of PP1 might not only stabilize MT attachments, but may also contribute to checkpoint silencing[253].

According to the role of Aurora-B in establishing and maintaining spindle checkpoint signalling, removal of Aurora-B-mediated phosphorylation might initiate spindle checkpoint silencing at kinetochores[254]. In addition, MT binding could directly compete with checkpoint protein binding sites at kinetochores or induce structural changes within the kinetochore that abolish spindle assembly checkpoint signalling[180]. The MCC exists either in a free form or bound to the APC/C. Disassembly of free MCC can be mediated by p31/comet, which is structurally similar to Mad2 and binds the dimerization interface of C-Mad2[255]. Binding to p31/comet could disrupt BubR1 interactions with C-Mad2:Cdc20[256]. Alternatively, p31/comet could extract Mad2 from the MCC and leave Bub3:BubR1:Cdc20 in complex thereby providing a rationale how Mad2 can be a sub-stoichiometric component of the MCC[257,258]. When the MCC is bound to the APC/C it is always disassembled. This depends on ubiquitylation and possibly proteolysis of Cdc20[259-261]. At the same time, continuous re-synthesis of Cdc20 sustains nearly steady-state levels in mitotically arrested cells[257]. Ubiquitylation of Cdc20 within the MCC requires the recently identified APC/C subunit APC15, which is not required for ubiquitylation of canonical APC/C substrates[262,263].

The continuous turnover of MCCs may explain why even in the presence of a fully active checkpoint, APC/C inhibition is never complete. Cyclin B is slowly but continuously degraded and eventually cells may prematurely exit mitosis despite the presence of an active checkpoint, a phenomenon termed “mitotic slippage”[264]. This has

been proposed as one possibility of how cancer cells escape chemotherapeutics that target the mitotic spindle[265].

1.4.3.2 Inactivation of spindle assembly checkpoint re-engagement

During prometaphase, error correction and the SAC are constantly engaged to ensure that all chromosomes become correctly attached to the mitotic spindle. During metaphase the checkpoint is satisfied, but acute addition of spindle poisons re-engages the checkpoint, demonstrated by a halt of Cyclin B1 degradation[266]. Presumably, cohesin cleavage results in a drop of tension on sister kinetochores, which re-engages Aurora-B-mediated error correction and spindle assembly checkpoint signalling[267]. However, when cohesin is cleaved to initiate anaphase kinetochores remain attached and the spindle checkpoint is not re-engaged (Fig. 11), suggesting that mechanisms exist that prevent untimely checkpoint re-engagement at anaphase onset[268,269]. This is essential as splitting of sister chromatids during anaphase is irreversible and thereafter the spindle checkpoint must not be re-activated to allow unidirectional exit from mitosis.

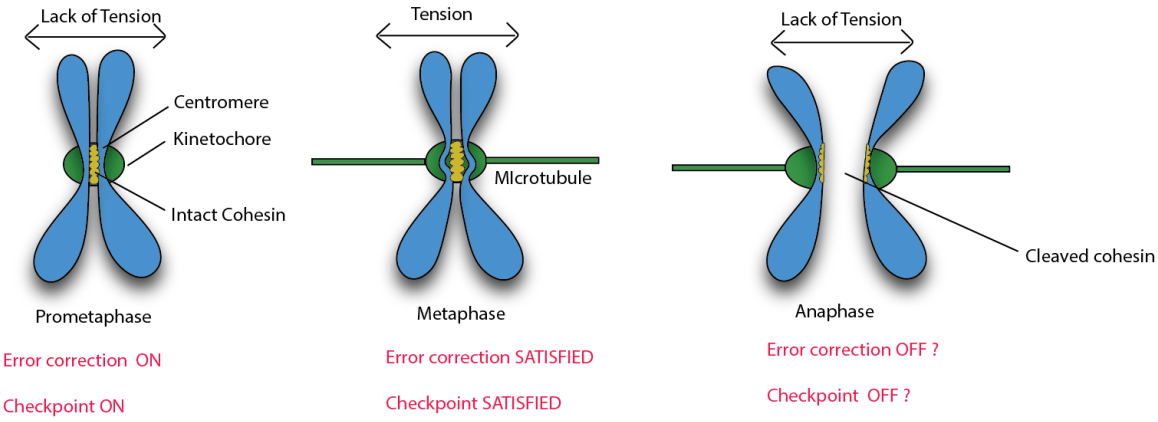

Figure 11: Error correction and the spindle assembly checkpoint at different stages during mitosis. In Prometaphase unattached kinetochores are not under tension and Aurora-B (red ellipse) can phosphorylate substrates on the outer kinetochore. Error correction and the spindle checkpoint are on. In metaphase sister kinetochores are attached as well as under tension. Thus, outer-kinetochore components are removed from the zone of Aurora-B phosphorylation. Error correction and the spindle checkpoint are satisfied. In anaphase cleavage of cohesin presumably relieves kinetochore tension, but error correction and the spindle checkpoint are not re-engaged (diagram modified from Musacchio, 2010[268]).

Studies in budding yeast suggested that APC/C-mediated proteolysis of essential checkpoint components like Mps1 may irreversibly inactivate the checkpoint during anaphase[270]. However, Mps1 levels decrease only gradually during late anaphase[271] which is inconsistent with the expected inactivation prior to cohesin cleavage[271]. Some have proposed that Mps1 levels only decrease gradually during late anaphase, which is inconsistent with the expected inactivation prior to cohesion cleavage[270]. Some posit that re-localization of Aurora-B to the spindle mid-zone at anaphase onset prevents ultimately reengagement of the checkpoint following cohesion cleavage[269,271]. Artificially retaining Aurora-B at anaphase kinetochores induced re-accumulation of the checkpoint proteins Mps1, Bub1 and BubR1. However, Aurora-B retention at anaphase kinetochores did not destabilize kinetochore-MT attachments, localize Mad1 and Mad2 to kinetochores, or inhibit APC/C[269]. This suggests that additional mechanisms may contribute to irreversibly abrogating SAC in anaphase. Cdk1(cdc2) activity has been suggested to be a pre-requisite for SAC signalling as well as several checkpoint components (Cdk1(cdc2) substrates, whose phosphorylation has been proposed to be required for checkpoint function)[272,273]. Cdk1(cdc2) inactivation by APC/C-mediated degradation of cyclin B1 at the metaphase-to-anaphase transition makes Cdk1(cdc2) a prime candidate to globally inactivate SAC signalling.

1.4.4 Mitotic exit and cytokinesis

Cytokinesis is the final stage of the cell cycle in which a single cell is physically separated into individual daughter cells. In eukaryotes, this process leads to the division and partitioning of chromatin, organelles and cytoplasmic components as well as the construction of new membrane between the daughter cells. The process begins during chromosome segregation, when the ingressing cleavage furrow begins to partition the cytoplasm between the nascent daughter cells. The process is not completed until much later, however, when the final cytoplasmic bridge connecting the two daughter cells is severed[274].

Cytokinesis is a highly ordered process, requiring an intricate interplay between cytoskeletal, chromosomal, and cell cycle regulatory pathways. Classical manipulation experiments have shown that the mitotic spindle dictates the position of the cleavage

furrow[275]. However, it's a not pre-requisite process as MTs themselves play an essential role in initiating cleavage[276,277]. First, equatorial astral MTs are stabilized at the equatorial cortical region and deliver stimulatory signals for the formation and contraction of the cleavage furrow[276]. The polar astral MTs may help position the cleavage furrow by inhibiting cortical contractility, perhaps by spatially biasing the pattern of myosin recruitment[278-282]. Finally, central spindle MTs sends positive signals that become specially important during the later steps of cytokinesis.

1.4.4.1 RhoGTPase and Myosin II

Localized activation of the small GTPase RhoA at the site of the future furrow is a central event to cytokinesis. RhoA is essential for furrow formation in animal cells and activated RhoA localizes to a specific zone within the furrow[283-287]. A narrow zone of activation is established by tethering RhoA activators to the central spindle, delivering a strong yet spatially restricted signal for cytokinesis initiation. An essential activator of RhoA is the guanine nucleotide exchange factor Ect2, which localizes in late anaphase to the central spindle and associates with the centralspindlin complex, composed of the kinesin protein Mklp1 and the GTPase activating protein (GAP) MgcRacGAP[284,288-290].

The tethering of MgcRacGAP and Ect2 to the central spindle is not essential for RhoA activation, but is important for efficient furrowing by restricting the zone of RhoA to a narrow zone at the equator of the cell. Other regulators of the Rho GEF family such as GEF-H1[291] and MyoGEF[292] may regulate Rho activity during cytokinesis. Additional proteins such as armadillo protein p0071 and Rho effector mDia1, may sustain RhoA activation in a positive feedback loop[293,294]. Activated RhoA leads to recruitment and activation of effector proteins that organize the furrow and stimulate ingression. RhoA stimulates actin polymerization through activation of formins and stimulates myosin activity by activating kinases such as Rho kinase (Rock) and citron kinase. Scaffolding proteins such as anillin and septins also play roles in organizing the cleavage furrow and promoting cytokinesis[274]. Myosin II is the principle motor protein required for cytokinesis. It is recruited to the cleavage furrow during the early stages of cytokinesis in a RhoA-dependent fashion. At anaphase, inactivation of Cdk1, controlled by the

degradation of mitotic cyclins by the APC/C is important for myosin II activation and phosphorylation during cytokinesis[295,296].

The central spindle midzone plays an important role in keeping separated chromosomes apart prior to cytokinesis completion, because when MTs are depolymerized in late anaphase, the nuclei collapse back together[297]. As cytokinesis progresses, the constricting furrow compacts the midzone MT array. The furrow ingresses until a cytoplasmic bridge is formed that is 1–1.5 microns in diameter. Several kinesin-like motor proteins and chromosomal passenger proteins move along the midzone spindle towards the plus ends and accumulate in the overlapping region, forming a phase-dense structure referred to as the Flemming body, stembody, telophase disc, or midbody[298]. Prc1 is a MT bundling protein that is critical for midzone formation in mammalian cells[299]. Prc1 accumulates on the central spindle in anaphase and suppression of Prc1 expression causes failure of MT interdigitation. Prc1 is targeted to the midzone by the kinesin protein Kif4, which transports Prc1 to the ends of the MT. Prc1 in turn recruits the centralspindlin complex, and additional mitotic kinesins including Cenp-E, Mcak and Kif14[300]. It also serves as a docking site for Plk1 in the central spindle[301]. Plk1 is an essential positive regulator of cytokinesis. Plk1 activity is required for recruitment of itself and Ect2 to the central spindle and its inhibition abolishes the RhoA GTPase localization to the equatorial cortex, suppressing cleavage furrow formation[302-304]. Plk1 activity may be required for later steps in cytokinesis as well, as Plk1 is targeted to the central spindle by the motor protein Mklp2, and phosphorylation of Mklp2 by Plk1 is required for cytokinesis[305]. Proteomic screens have shown that the Rho kinase Rock binds to the polo box domain of Plk1[306].

1.4.4.2 Chromosome passenger complex

Another important complex during cytokinesis is the chromosome passenger complex (CPC), which consists of the proteins Aurora-B, IncepP, survivin and borealin. This complex plays an important role throughout mitosis, and has been implicated in the regulation of cytokinesis. At the metaphase-anaphase transition, the CPC relocalizes from centrosomes to the spindle midzone and equatorial cortex and ultimately concentrates near the midbody, adjacent to centriolin ring[307-310]. Aurora-B activity is required for

proper localization of Mklp1. Another substrate of Aurora-B is MgcRacGAP, whose phosphorylation appears important to completion of cytokinesis[311,312]. Phosphorylation of MgcRacGAP has been proposed to stimulate its activity as a GAP for RhoA[313], terminating RhoA activity later during cytokinesis[311]. Other important substrates of Aurora-B include vimentin, an abundant intermediate filament protein. Intermediate filaments must be disassembled during mitosis to allow cell division, and mitotic phosphorylation is important for filament dissociation[314,315]. Aurora-B may also promote cytokinesis by inhibiting Mlc phosphatase[316]. Aurora-B also phosphorylates CenpA, which appears to play an important role in cytokinesis[317].

1.4.4.3 Membrane trafficking and remodelling during cytokinesis

Membrane trafficking plays a critical role in the process of cytokinesis. Three pathways, which involve membrane trafficking, have been implicated in the process of cytokinesis. First, the secretory pathway, including Golgi-derived components, may contribute new membranes and proteins to the ingressing furrow. The role of Golgi-derived vesicles in cytokinesis completion emerged from studies of the protein centrolin, which may help the recruitment of secretory vesicles to the site of abscission at the midbody[318]. Centrolin localizes to a ring like structure within the midbody that also contains gamma globulin, GAP-CenpA, and the centralspindlin complex[317]. Second, the endocytic pathway and endosome recycling may remodel membranes in the cleavage furrow and also contribute vesicles that may participate in the final steps of cytokinesis. Endocytosis within the furrow may be important for remodeling the plasma membrane during ingression. In addition, endocytosis from other regions of the cell for example, endocytic vesicles internalized from polar regions are also shown to be trafficked to the midbody during the later stages of cytokinesis[319]. Small GTPases that regulate membrane trafficking have been directly implicated in cytokinesis completion. Arf GTPases initiate the budding of coated carrier vesicles by recruiting coat protein complexes onto donor membranes. RabGTPases on the other hand regulate the targeting and docking/fusion of vesicles with acceptor membranes[320]. RabGTPase localizes to recycling endosomes (RE) and is required for proper RE organization and the recycling of vesicles to the plasma membrane[321,322]. Both GTPases interact with a common set of effector proteins that assist

in delivery of endosomal vesicles to the cleavage furrow, termed Fip3 (Arfophilin-1) and Fip4 (Arfophilin-2)[319,321]. Dynamin is a GTPase responsible for clathrin-mediated endocytosis in the eukaryotic cell[323-325]. Dynamin was first identified to be the mammalian homolog of the Shibire protein in Drosophila[326]. The dynamin superfamily is composed of conventional dynamin and dynamin related protein (DRPs), and is conserved throughout eukaryotes. Dynamin interacts directly with two scaffolding proteins Intersectin-I and Tuba that have been proposed to link dynamin with the actin cytoskeleton[327,328]. Recently it was shown that Bcl-xL regulates vesicle endocytosis in hippocampal neurons. Bcl-xL interacts in a complex with clathrin and Drp-1 to alter the kinetics of vesicle pool recovery. Bcl-xL and Drp-1 acts downstream of calcium influx/calmodulin[75]. Perhaps a similar mechanism might exist during cytokinesis for membrane vesicle trafficking.

Finally, recent evidence suggests that components of the endosomal sorting complex required for transport machinery (ESCRT), best characterized for its role in multi-vesicular body formation, are normally involved in late endosome to lysosome trafficking but have also been implicated in abscission during cytokinesis. These proteins are important for membrane invagination. Chmp3, a subunit of the ESCRT-III complex localizes to the midbody and deletion of an auto-inhibitory domain in Chmp3 can inhibit cytokinesis. ESCRT-1 complex subunit tumor susceptibility gene 101 (Tsg-101) and Alix, an ESCRT associated protein, may interact with actin and MTs[329,330], establishing a link between the ESCRT machinery and cytoskeletal components present at the midbody.

Cytokinesis failure can arise through defects in any of the stages of cytokinesis, or as a consequence of inactivation or hyperactivation of any number of different components. Cytokinesis failure leads to both centrosome amplification and production of tetraploid cells, which may set the stage for the development of either tumor cells or let the cells enter into cellular senescence or apoptosis.

1.5 Cellular senescence

First described in normal human fibroblasts[15] as the finite proliferative capacity of normal cells in culture, cellular senescence is a part of various physiological and pathological processes. Various morphological and biochemical changes differentiate

senescent cells from normal cells. A decade of research has shown that senescence has both beneficial and detrimental roles. It has been shown that cellular senescence contributes to ageing, and senescence-associated phenotypes can contribute to tumor progression and normal tissue repair[331]. In general, transient induction of senescence followed by tissue remodelling is beneficial, because it contributes to the elimination of damaged cells. In contrast, persistent senescence or the inability to eliminate senescent cells could be detrimental. Conceptually similar to apoptosis for eliminating unwanted cells, senescence is relevant in cancer and ageing[332]. It's a crucial barrier against cancer progression. Senescence can be induced by multiple stimuli. These can include telomeric uncapping resulting from repeated cell division, oxidative stress, severe or irreparable DNA damage and chromatin disruption and expression of oncogenes associated with replicative stress[333].

1.5.1 Replicative senescence

First, it was found that finite proliferation of culture cells is due in part to telomere erosion, the gradual loss of DNA at telomere of chromosomes during each S-phase of the cell cycle. This is termed as replicative senescence[334]. The loss of telomeres is sensed by cells as DNA damage and therefore triggers a DNA damage response (DDR), which is similar to that produced by external DNA double-strand break damaging agents, such as ionizing radiation and some chemotherapeutic drugs. These stimuli are signalled through various pathways, many of which could activate p53. The exact threshold of telomere length or the number of dysfunctional telomeres within a cell that triggers senescence is still unclear[335]. The main mediators of the DDR are the DNA damage sensing upstream kinases Atm and Atr, the signal transduction downstream kinases Chk1 and Chk2, and effector proteins such as p53 and Cdc25. In senescent cells, persistent DDR is visualized by telomere dysfunction-induced foci (TIF) or DNA segments with chromatin alterations reinforcing senescence (DNA-SCAR)[331,336]. One of the activated proteins that mediate a cell cycle arrest downstream of p53 is the Cdk inhibitor p21, which could be upregulated in replicative senescence[337,338]. However the activation of p53 and p21 in senescent cells is only transient, and protein levels of p53 and p21 can decrease after the establishment of sustained proliferation arrest.

Replicative senescence is also linked to the *CDKN2A* locus (also known as *INK4A* and *ARF*), which encodes two crucial tumour suppressors, p16 and Arf. P16 is an inhibitor of Cdk4/6 and Arf regulates p53 stability through inactivation of Mdm2[339,340]. P16 often becomes constitutively upregulated suggesting that p16 may be responsible for maintenance of proliferation arrest in senescent cells[338,341]. Both p21 and p16 upregulation results into inhibition of pRb protein phosphorylation, which controls the S phase entry [130].

1.5.2 Premature senescence

Non-telomeric DNA damage (genomic and replicative stress) also generates persistent DDR signalling associated to outbreak of senescence. This is often termed as premature senescence. Premature senescence (PS) is an accelerated mechanism that occurs in response to extrinsic or intrinsic stress stimuli. These stimuli include DNA damage, disrupted chromatin organization, increased oncogenic signalling, increased replicative stress, treatment with DNA damaging drugs or irradiation[18] and oxidative stress[19,20].

Oncogene- induced senescence (OIS) was originally observed when an oncogenic form of Ras was expressed in human fibroblasts with accumulation of p53 and p16/Ink4a[342]. Also, loss of tumor suppressors *PTEN* and *NF1* can trigger PS. OIS generally is seen *in vivo* and associated with derepression of *CDKN2A* locus[339]. OIS may also induce a robust DDR owing to the DNA damage that is caused by aberrant DNA replication and reactive oxygen species (ROS)[343-345].

In normal unstressed cells, p53 is maintained at low levels by continuous ubiquitylation by E3 ligases such as Mdm2, Cop1, and Pirh2 that promote p53 degradation by the 26S proteasome pathway[346]. In response to genotoxic stress, p53 is rapidly stabilized via the inhibition of its interaction with Mdm2. Subsequently, p53 activity can be supported by post-translational modifications mediated by several protein kinases and acetylases[347,348].

The tumor suppressor PML (promyelocytic leukaemia) is involved in the pathogenesis of acute promyelocytic leukaemia and is found to regulate the p53 response to oncogenic signals[349]. PML regulates p53 activity by physically associating with CBP/p300, acetyltransferase that modifies p53 at K382 and thus activates p53. Ras

regulates PML expression and induces re-localization of p53 and CBP acetyltransferase within the PML nuclear bodies and induces the formation of a trimeric p53-PML-CBP complex that induces senescence[349].

Plaminogen activator inhibitor-1 (PAI-1) is also a critical downstream target of p53 in senescence. p53 upregulates PAI-1, leading to the down-regulation of PI(3)K/PKB signaling and nuclear exclusion of cyclin D1. Significantly high level of cyclin D1 is observed in senescent human BJ fibroblasts. Interestingly, simultaneous knockdown of PAI-1 and p21 results in a more efficient bypass of senescence arrest than knockdown of p53 itself thus making them both relevant downstream targets of p53 in the induction of senescence in human fibroblasts[350].

1.5.3 Senescence-associated phenotypes and markers

Under the microscope, most senescent cells acquire characteristic morphological changes. They become flat, increase their volume and display a vacoule-rich cytoplasm. The nucleus-to-cytoplasm ratio and mitochondrial mass increases. Currently there are many commonly used biomarkers for the detection of senescence both *in vitro* and *in vivo*. Nevertheless, use of a single senescence marker is not always specific and can vary depending on the cell type and senescence trigger. For this reason, most investigators used multiple markers when tested for senescence.

1.5.3.1 Senescence-associated Beta galactosidase activity

The increase of lysosomal biogenesis is characteristic of senescent cells leading to higher activity levels of the lysosomal enzyme β-galactosidase (SA-β-Gal). Cytochemical detection of SA-β-Gal at pH 6.0 allows for detection of senescent cells[351]. This marker is expressed during senescence, but not pre-senescence. SA-β-Gal is believed to be absent in quiescent fibroblasts and terminally differentiated keratinocytes, although this has been challenged recently. This marker also provides *in-situ* evidence that senescent cells may exist and accumulate with age *in vivo*.

1.5.3.2 Senescence-associated secretory phenotype

Senescent cells implement a complex pro-inflammatory response termed as senescence-associated secretory phenotype (SASP)[352,353]. SASP reflects a non-cell autonomous functionality of senescent cells and underpins their *in vivo* role in the pathos-physiology of ageing and age related disorders. This phenotype is also termed as senescence messaging secretome[354]. SASP involves both autocrine and paracrine signalling, pro-tumorigenic and tumor suppressive effects and pro- and anti-inflammatory signalling[355]. Senescence-associated changes in gene expression are mostly conserved within individual cell types. SASP factors can be globally divided into soluble signalling factors (interleukins, chemokines and growth factors), secreted proteases, and secreted insoluble extracellular matrix (ECM) components[353].

Senescent cells secrete interleukins, inflammatory cytokines and growth factors that can affect surrounding cells. Interleukin-6 (Il-6), a pro-inflammatory cytokine, is one of the most prominent cytokines of the SASP. During DNA damage and oncogenic stress, Il-6 has been shown to be associated with senescence in mouse and human fibroblasts and epithelial cells among others[356]. Persistent DNA damage signalling directly controls the secretion of Il-6, independent of the p53 pathway[357]. Surface receptors such as Il-6R (gp80) and gp130 signalling complex can interact directly with Il-6 secreted from neighbouring senescent cells. Il-1 (both Il-1α and Il-1β) are overexpressed and secreted by senescent endothelial cells, fibroblasts and chemotherapy-induced senescent epithelial cells[358,359]. These cytokines may act via their respective receptors, primarily to trigger nuclear factor kappa B (NF-κβ)[360]. Most senescent cells also express and secrete Il-8 (Cxcl-8) along with Groα and Groβ (Cxcl-1 and Cxcl-2). Ccl family members that are generally upregulated in senescent cells include Mcp-2, Mcp-4 and Mcp-1 (Ccl-8, -13 and -2); Hcc-4 (Ccl-16); eotaxin (Ccl-26); and macrophage inflammatory protein (Mip)-3α and -1α (Ccl-20, -3)[361].

The insulin-like growth factor (Igf)/Igf receptor network may also contribute to the effect senescent cells exert on their microenvironment. Senescent endothelial, epithelial, and fibroblast cells express high levels of almost all the Igf-binding proteins (IgfBPs), including IgfBP-2, -3, -4, -5 and -6 and their regulators, IgfBP-rP1 and –rP2[353,362-364].

Inflammatory cytokines such as the colony-stimulating factors Csf, Gm-Csf and G-Csf, are secreted at high levels by senescent fibroblasts[353].

An intracellular Il-1α/ miR-146a/b / Il-6 / C/Ebp-β loop as well as related p38/NK-κβ and mTor-mediated pathways appear to contribute to the changes in gene expression that result in the SASP[365,366] (Fig. 12). The composition of the SASP may vary as time progresses and might partly depend on the mechanism through which senescence is induced. Little is known about the contribution of non-protein factors such as nucleotides, bradykines, prostenoids and ceramides on the SASP.

The SASP is primarily a DDR[357]. It can alter its microenvironment (Fig. 12), attract immune cells, and, ironically, support malignant phenotypes in nearby cells. There are diverse downstream effects of the SASP that are dependent on the context and cell stimulation. These effects can include paracrine stimulation such as pro-tumorigenesis and modulation of micro-environment and autocrine stimulation such as senescence reinforcement[367]. It has been shown that secreted proteins from senescent human fibroblasts promote proliferation and malignant transformation of pre-malignant epithelial cells[368]. These paracrine effects include promotion of epithelial-mesenchyme transition and invasion, tumor vascularization and abnormal tissue morphology, which are mediated by the pro-inflammatory cytokines Il-6 and Il-8, Vegf, and the metalloprotease Mmp-3[353,356,361].

Il-6 and Il-8 reinforce senescence rather than spreading senescent phenotypes to the healthy neighbouring cells. Recent studies show Il-1β can induce senescence in normal cells, as a paracrine SASP[369]. Pro-Il-1β needs to be cleaved and modified by inflammasome activated caspase-1 and therefore the inflammasome is involved in local progression of not only inflammation but also senescence in the tissue microenvironment. This was also observed in murine HSC senescence[370].

Paracrine effects of senescence also can provoke anti-tumor immunity. In a Ha-Raps driven mouse liver cancer model, the reactivation of p53 during senescence results in the raps-driven tumor regression. The SASP triggers the infiltration by NK cells and other innate effector cells to eliminate tumor cells[371]. In non-malignant cells, including

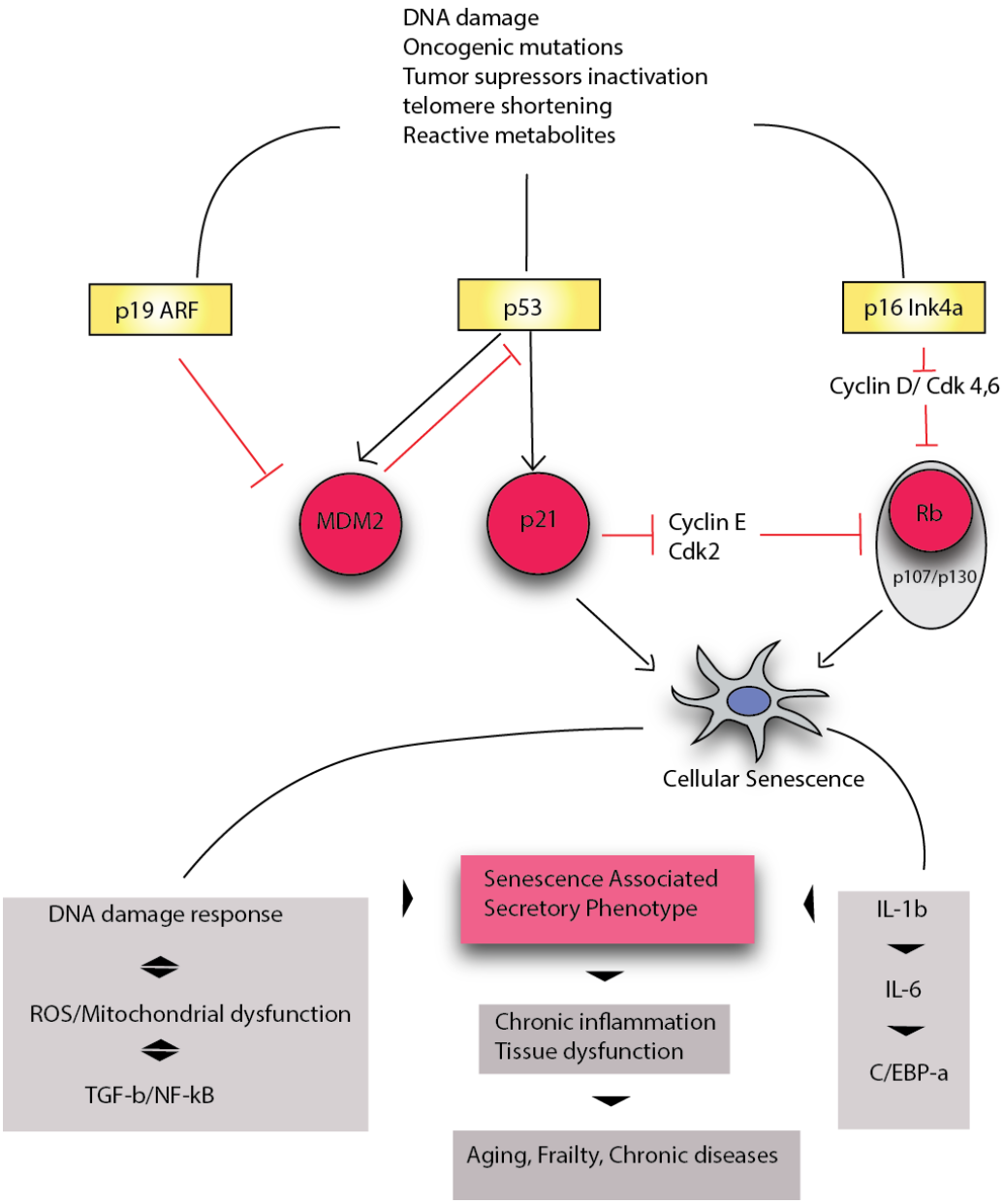

Figure 12: Pathways inducing senescence. Various inducers can act alone or in combination to push cells into senescence through pathways involving p16/Ink4a-Rb, p53-p21, and likely other pathways. p19/Arf inhibits p53 via Mdm2. Triggers activate downstream pathways in terms of gene expression and chromatin remodelling (heterochromatin formation) that underlies senescence-associated growth arrest, the SASP.

infiltrating immune cells, surrounding early neoplastic lesions exhibit focal p16 activation. Multiple factors secreted by senescent cells mediate paracrine senescence.

Most Tgf-β-dependent genes were shown to be upregulated during paracrine senescence. Tgf-β1 and other ligands of the Tgf-β and BMP branches, including Bmp6, Bmp2, inhibin-A and Gdf15 were shown to be upregulated during senescence. BMP-like ligands and Tgf-β-like ligands signal through the Smad family members, and indeed phosphorylation of Smad2/3 and Smad1/5 is upregulated in cells undergoing paracrine senescence. Many components of SASP execute paracrine senescence, of which Il-1α is identified as one of the most robust inducers of multiple SASP components. Cells expressing inhibin-A or Tgf-β induced some SASP components such as Il-8 or Ccl2, but they do not mimic the SASP. Inhibiting Tgf-β R1 do not affect the secretome induced by Il-1α. Il-1 has a more prominent role than Tgf-β signaling in controlling the SASP. Il-1 signaling has been shown to be associated with both paracrine senescence and OIS in culture and *in vivo*. Secretion of mature forms of Il-1α and Il-1β suggests the activation of inflammasome. Paracrine senescence arrest depends on the activation of p16, p21 and p53, the same genetic network as in OIS. Inhibition of Vegf-R2/Flt3, Tgf-β R1 and Ccr2 receptors inhibits paracrine senescence in a dose-dependent manner[372].

A localized time-limited SASP may be important in resolving tissue damage, at least in younger individuals, in cases such as antagonistic pleiotropy[373-375]. In addition to secreting soluble signalling cytokines and growth factors, senescent cells also secrete proteases such as matrix metalloproteases (MMPs). SASP MMPs limit fibrosis following liver injury or during skin wound healing. Il-6 and Il-8 reinforce the senescence growth arrest, at least in some senescent cells which is beneficial against cancer[356]. In contrast, these cytokines can also cause epithelial to mesenchymal transitions, which promote cancer[376].

Human and mouse fibroblasts undergoing replicative or stress-induced senescence secrete stromelysin-1 and -2 (Mmp-3 and Mmp-10, respectively) and collagenase-1 (Mmp-1)[377]. Mmp-1 and Mmp-3 produced by senescent cells can also regulate the activity of the soluble factors present in the SASP[378].

1.5.3.3 Senescence-associated heterochromatin foci

Senescence is accompanied by extensive changes in the chromatin structure and organization. Many senescent cells accumulate specific domains of heterochromatin as a

result of modification of transcriptionally silent heterochromatin foci mediated by lysine 9-trimethylated histone-3 (H3K9-me3)[379]. These chromatin foci are called the senescence-associated heterochromatin foci (SAHF). Their presumed function is the repression of genes that promote proliferation, contributing to growth arrest associated with cellular senescence. Primary human fibroblasts undergoing OIS or replicative senescence are known to form SAHF, which can be visualized as compacted foci of DNA enriched with H3K9-me3. The SAHF are formed by nuclease-resistant compaction of chromatin where each focus represents the condensed chromatin of one chromosome[380]. While cellular senescence also occurs in premalignant human lesions, it is unclear how conserved SAHF formation is among various cell types, under diverse stresses, and *in vivo*. Unlike the widely present DDR marker γ-H2A.X, SAHF are cell type restricted under genotoxic-induced and replicative senescence[381]. A number of additional proteins are known to contribute to formation and/or maintenance of the SAHF, including histone chaperons Hira and Asf1[382], heterchromatin protein 1 (Hp1)[379] and high-mobility group A (HmgA) proteins[383], histone variant macroH2A[384], and pRb[379]. The p16/Ink4a-pRb pathway appears to be required for SAHF formation[379].

1.5.3.4 γ-H2AX as a marker of DNA damage foci

After an episode of DNA damage, histone H2As present in the chromatin at the DNA break site are rapidly phosphorylated. The phosphorylated derivative γ-H2A.X forms a focus at the damage site. This focal point increases after formation, and remains present until the break or damage is repaired[385]. In DDR implicated senescence, a number of foci have been demonstrated in culture and ageing in mice[336,386]. Telomere shortening can cause telomere uncapping and activates p53 in a variety of human and mouse cell types[387,388]. Since the signalling pathway activated by DNA damage has to be maintained to keep cells in a senescent state, cellular senescence can be regarded as a permanently maintained DNA damage response state. Therefore, γ-H2A.X foci can be a marker for replicative and premature senescence. Uncapped telomeres are also associated with DNA damage factors such as 53BP1, Mre11 and phosphorylated forms of Rad51, and Atm at the foci[389].

1.5.3.5 p16/ Ink4-pRB and p53-p21/Cip pathways

Two major pathways, p16/Ink4a-pRb and p53-p21/Cip are mainly associated for the execution of the proliferative arrest that characterises senescence in human cells[355]. These powerful tumor suppressor pathways are highly mutated in many tumors. In response to DDR, p53 levels rises within cell. Enhanced expression of p16, Arf and p53 are seen in murine tissues undergoing OIS and in pre-malignant neoplastic lesions[390-392]. One of the activated proteins that mediate the cell cycle arrest downstream of p53 is the Cdk inhibitor p21, which is upregulated in replicative senescence[337,338]. However, the activation of p53 and p21 in senescent cells is often transient, and protein levels of p53 and p21 will decrease over time after the establishment of senescence. These proteins are frequently monitored by immunofluorescence and protein blotting in senescent cells .

1.6 Aneuploidy

Aneuploidy refers to the state in which the number of chromosomes in a cell is not an exact multiple of the haploid set. Chromosomal instability (CIN) defines a condition in which cells are unable to accurately segregate whole chromosomes (whole-CIN [W-CIN]) or are prone to structural chromosome rearrangements (structural-CIN [S-CIN]) including translocations, deletions, and duplications of large parts of chromosomes[393]. In the early 1900s, Theodor Boveri hypothesized that aneuploidy was a causal feature of human cancers. Most forms of genomic instability (GIN) are driven by DNA damage, which can result in genetic or epigenetic mutations after erroneous DNA repair or replication. A wide range of technical approaches are available to study aneuploidy. The gold standard for cytogenetic analysis is the study of metaphase chromosomes, in particular spectral karyotypic (SKY), the most sophisticated molecular cytogenetic application. These techniques are restricted to the analysis of mitotically active cell populations. Flourescent *in-situ* hybridization (FISH), with both chromosome painting probes and locus specific subcentromeric enumerization probes, is also used for the analysis of aneuploidy. In contrast to SKY this method is applicable to interphase cells. Using interphase FISH methods it is possible to detect chromosomal aneuploidy, which has been linked to tumorigenesis and has detrimental effects on cell and organism physiology[161]. Aneuploidy has been also associated with aging and cellular senescence[394].

Chromosomal aneuploidy can be regarded as an indicator of genomic instability and may be one of the hallmarks of cancer and aging (Fig. 13).

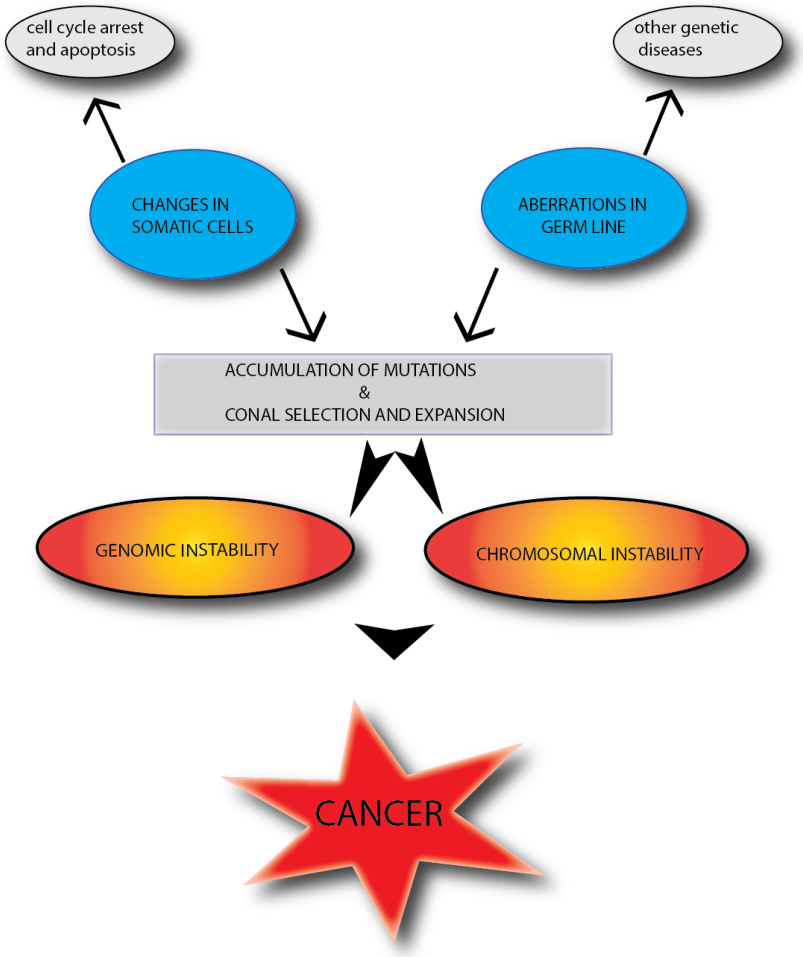

Figure 13: Genomic and chromosome instability. Schematic pathways showing link between genotoxic stress, genomic instability, chromosome instability and cancer.

The mechanisms leading to aneuploidic cells are commonly described as functional defects of MT-kinetochore attachment, SAC, cytokinesis or DDR. However, chromosomal aneuploidy has now been detected even in fully differentiated tissues that lost their ability to self-renew through mitotic regeneration, such as the brain. This suggests that aneuploidy could be a widespread phenomenon occurring at different ages and perhaps through different mechanisms[395].

1.6.1 Failure of spindle assembly checkpoint and aneuploidy

One of the mechanisms leading to aneuploidy involves abnormalities in the mitotic checkpoints[396], the major cell cycle control machineries that ensure high fidelity of chromosome segregation. The SAC is responsible for the delay of anaphase until all chromosomes are properly oriented on the MT spindle and the checkpoint is released when all chromosomes are correctly attached to the kinetochore. Any perturbation of the checkpoint leads to initiation of anaphase before the spindle has established proper orientation and proper attachment to its chromosomes (Fig. 14). This can result in chromosome mis-segregation and consequently aneuploidy[395]. Accuracy of chromosome segregation is greatly affected when BubR1, a SAC component, drops below a certain level. Mice with constitutively low BubR1 level develop progressive aneuploidy along with variety of progeroid features, including short lifespan, cachectic dwarfism and impaired wound healing. Graded reduction of BubR1 expression in mouse embryonic fibroblasts causes increased aneuploidy and senescence[394]. In mice it has been shown that BubR1 variations can have a dual effect. It induces p16/Ink4a as an effector of cellular proliferation arrest and senescence, and p19/Arf as a suppressor, which acts to suppress cellular senescence and aging[397]. Bidirectional deviation of BubR1 results in divergent effects on aneuploidy, with BubR1 overexpression providing protection against aneuploidy and BubR1 insufficiency perturbing accurate chromosome segregation[394,398]. Yeasts lacking core SAC components grow normally under unperturbed conditions yet display increased rates of chromosome mis-segregation and are unable to grow in the presence of spindle poisons, such as nocodazole[399-401]. In contrast, murine models lacking core SAC components (*Bub3*, *Mad1*, *Mad2* or *BubR1*), display very early embryonic lethality[401-404]. However, mouse embryonic fibroblasts (MEF) heterozygous for *Mad2*, *Bub3*, and *BubR1* displayed haploinsufficiency, resulting in higher levels of mitotic abnormalities[394,405]. Conditional knockout for *Bub1* demonstrated that premature centromeric separation is a consequence of mitotic checkpoint weakening. Meanwhile, complete ablation of Bub1 kinase activity unveiled how Bub1-mediated histone H2A phosphorylation promotes Aurora-B inner centromeric localization. Whereas, Bub1 overexpression uncovered that Bub1 carefully controls that level of Aurora-B activity to

prevent chromosome mis-segregation and aneuploidy[393]. In MEFs, Bub1 mutation causes high rates of chromosome mis-segregation and aneuploidy, accompanied by growth defects and premature senescence[406].

P31/comet protein acts as a silencer of SAC via its communication with the Mad2 complex. Overexpression of p31/comet can lead a cell towards cellular senescence. P31/comet was initially discovered as a Mad2-interacting protein[407]. P31/comet counteracts Mad2 function and is required for silencing the SAC. Studies have shown that p31/comet-mediated senescence is closely associated with p53 and p21 accumulation[407] but does not cause any changes in p16 expression. Depletion of p21 completely blocked p31/comet-induced senescence, revealed by dramatic reversion in the percentage of SA-β-gal-positive cells. Evidently, induction of p21 is a critical step in p31/comet -mediated senescence. p31/comet-induced senescence is also accompanied by mitotic catastrophe with massive nuclear and chromosomal abnormality[407].

The mitotic checkpoint proteins Bub3 and Rae1 along with other mitotic checkpoint proteins bind to kinetochores that lack attachment or tension and generate a 'stop anaphase' signal that diffuses into the cytosol[408]. Bub3 has substantial sequence similarity with the mRNA export factor protein Rae1[409]. Mice with homozygous null for *Bub3* or *Rae1* die during embryogenesis, whereas mice with $Bub3^{-/+}$ or $Rae1^{-/+}$ show similar mitotic defects, including spindle assembly checkpoint impairment and chromosome missegregation. Both Bub3 and Rae1 interacts with Bub1. It is suggested that Bub3-Bub1 and Rae1-Bub1 complexes might fulfill redundant functions at unattached kinetochores[403]. This indicates that Rae1 cooperates with Bub3 and that the combination of the 2 mitotic checkpoint activities is critical for the prevention of chromosomal mis-segregation. Haplo-insufficient *Rae1*/*Bub3* mice are viable but show greater rates of premature sister chromatid separation and chromosome missegregation, aneuploidy than single haplo-insufficient cells[403] and reduced life-span[410]. $Bub3^{-/+}$/$Rae1^{-/+}$ mice do not increase the rate of cell death but showed early onset of cellular senescence, indicated by increased expression of p53, p21, p16 and p19[410].

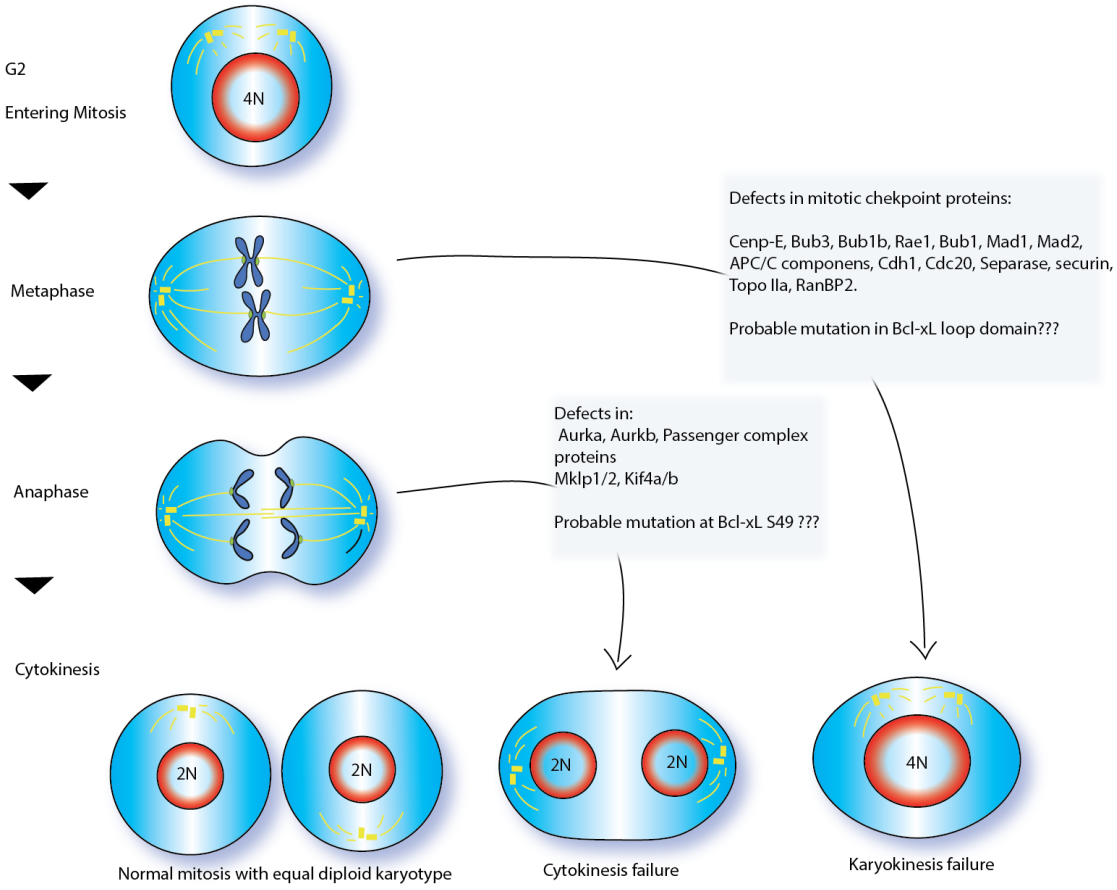

Figure 14: Aneuploidy due to SAC failure during mitosis. Normally a 4N cell in G2 enters mitosis, aligns its chromosomes in the metaphase plate and equally distributes the DNA over two nuclei (karyokinesis) and subsequently two daughter cells (cytokinesis). During SAC failure due to mutation in SAC regulatory genes, chromosomes mis-segregate leading to aneuploidy. When cytokinesis fails, the DNA is divided into two nuclei that remain within one cell (diagram modified from Ricke et al., 2008[393]).

When mutated, Mad2, a major component of SAC, causes aneuploidy in human tumor cells. Haplo-insufficient Mad2 cells showed genomic instability and aneuploidy with typical features of cellular senescence, including increased SA β-galactosidase expression and upregulation of p53, p21 and p14 proteins. Partial depletion of *Mad2* weakened the SAC causing premature chromatid separation, and induced aneuploidy[411]. Moreover, it was shown that Mad2 overexpression is associated with aneuploidy induced by inactivation of pRb and p53 tumor suppressors in tumor cells[412]. In partially Mad2-

depleted IMR90 cells, p14Arf caused an initial G1/S arrest and mediated increase in p53 protein level by targeting Mdm2. Mad2 depletion is sensed as a stress signal in normal cells, that triggers the p53-p21 pathway that arrest cells in G1/S boundary and subsequently a pathway controlled by p14Arf is activated that drives premature cellular senescence acting as a barrier to the proliferation of cells with unbalanced karyotypes[411].

Hypomorphic expression of *Espl* (gene that encodes separase) in a *p53*$^{-/-}$ null background mouse model display significantly higher levels of GIN and aneuploidy than normal cells[413]. Optimum levels of separase acts as a tumor suppressor in the absence of *p53*, but the loss of separase and *p53* effectively synergize to cause lymphoma and leukemia formation[413]. *In vivo* studies in the mouse mammary epithelium have shown that over expression of separase results in the development of gross aneuploidy[414,415].

Finally, overexpression of UbcH10, the E2 ubiquitin enzyme that works in tandem with APC/C during metaphase-to-anaphase transition, leads to precocious securin and cyclin B degradation, and provokes supernumerary centrioles, chromosome laggings and aneuploidy[416].

1.6.2 Failure of cytokinesis and aneuploidy

Cytokinesis is the final step in cell division. It is a highly ordered process, requiring an intricate interplay between cytoskeletal, chromosomal, and cell cycle regulatory pathways. Cytokinesis failure leads to both centrosome amplification and tetraploid cells, which may set the stage for the development of tumor cells. In animal cells, RhoA is the central player in cytokinesis, regulating the assembly of actin filaments in the cortex during cytokinesis and proper constriction of contractile furrows. Cells depleted of RhoA by RNAi or cells injected with a Clostridial enzyme, C3 transferase, show no cortical contractility or furrow formation[417,418]. These cells do not undergo anaphase spindle elongation, perhaps because reorganization of the actin cytoskeleton is impaired. Furthermore, in cells that fails to undergo cytokinesis, astral MTs fail to contact the equatorial cortex, suggesting that the delivery of RhoA activators to the cortex is impaired[419]. Apart from RhoA, inhibition of regulators of cytokinesis such as MlckII[420] and Rock[421] also leads to cytokinesis failure. Plk1 is overexpressed in a broad range of human tumors. Overexpression of Plk1 in HeLa cells leads to an increase of cells with

large, often fragmented nuclei or multiple nuclei[422] as well as centrosome amplification[423], suggesting Plk1 overexpression has an effect on chromosome segregation and cytokinesis completion. Inhibition of Aurora-B during later stages of mitosis inhibits phosphorylation of Mklp1 which perturbs cytokinesis[424].

1.6.3 DNA damage, aneuploidy and senescence

The purpose of the later phases of mitosis occurring after APC/C activation is to distribute sister chromatids to the daughter cells correctly, so that single nuclei with identical genetic information are formed in each daughter cell. Failure of this process is evident when segregating chromosomes lag at the anaphase spindle midzone. Such lagging chromosomes eventually cause aneuploidy. Furthermore, even if lagging chromosomes are eventually separated correctly, they can form a micronucleus apart from the main nucleus[425]. When cells encounter insults during the G1, S or G2 phase of the cell cycle, the canonical DDR pathway delays cell cycle progression, which are known as DNA damage G1/S , intra-S and G2/M checkpoints. In consequence of DNA damage on the lagging chromosomes, Atm and Chk2 become activated in the following G1 phase, resulting in p53-dependent cell cycle arrest[426], which can either activate the cell death machinery or cause cellular senescence. Although cell fate regulation by p53 is coming to light, the mechanism of onset of cellular senescence due to aneuploidy still requires further research. Once cells are committed to entering mitosis, they do not activate a full DDR pathway upon DNA damage[427]. The point of the commitment has been proposed to be in late prophase, since irradiation-induced DNA damage in early prophase but not late prophase causes a reversion of cell cycle to interphase[428,429]. Beyond this point, irradiation of prometaphase and metaphase cells still generates γ–H2A.X foci on condensed chromosomes. However, downstream accumulation of DDR regulators, Rnf8, Rnf168, Brca1 and 53Bp1 are attenuated[430,431]. It has been described that prolonged arrest in prometaphase causes accumulation of γ–H2A.X during and after the arrest[432], which is accompanied by the activation of Atm[433]. Recent findings have demonstrated that lagging chromosomes induced by the Mps1 inhibitor Mps1-IN-1 cause *de novo* DNA damage foci formation after the onset of anaphase[426]. In the absence of p53, these cells keep dividing and exhibit not only an abnormal number of whole chromosomes, but also

chromosome translocation, one of the structural chromosomal aberrations associated with tumorigenesis, underscoring the significance of DNA damage-induced cell cycle arrest after the generation of lagging chromosomes. Usually this results in the formation of a single tetraploid nucleus, or multiple nuclei and micronuclei carrying a 4N genomic content in the following G1 phase leading to aneuploidy. These cells then enter either the apoptotic pathway or cellular senescence.

Aneuploidy induces complex cellular responses impacting cell fate. Compelling evidence from cultured cells suggests that aneuploidization is associated with engagement of certain cellular stress pathways, including those responding to genotoxic, proteotoxic, metabolic, or proliferative stress.

1.7 The *C. elegans* experimental model

Roughly five decades ago, Sydney Brenner famously proposed *C. elegans* as an outstanding experimental system, because of its small size, rapid life-cycle, transparency, and well-annotated genome. *C. elegans* is a tiny, free-living soil nematode found worldwide which survives by feeding on microbes, primarily bacteria. It has a rapid life-cycle and exists as a self-fertilizing hermaphrodite, although males arise at a lower frequency (< 0.2%). Self-fertilizing hermaphrodites provide several advantages for genetic analysis such as the ability to maintain stocks from a single animal, easy production of isogenic mutants and finally simple Mendelian genetics of segregation. They are easy to maintain in the laboratory, and are normally grown on agar plates containing a lawn of *Escherichia coli* (OP50) bacterium. Due to their small size, they can be grown in small petri dishes. Without food, the development of young larval stage animals is arrested, although they can survive for at least one month.

1.7.1 The anatomy and development of *C. elegans*

An anatomical description of the whole animal has been completed at an electron microscopy level as well as its complete invariant cell lineage[434-436]. The adult body plan is rather simple with 1000 somatic cells. Like all nematodes, the *C. elegans* body is made up to two concentric tubes separated by a fluid filled space, the pseudocoelom (Fig.14). The animal's shape is maintained by internal hydrostatic fluid. The outer tube is covered

by the collagenous extracellular cuticle, which is secreted by the hypodermis. The body musculature is arranged in four longitudinal strips that are attached to the cuticle through a thin layer of hypodermis. The inner tube is composed of the muscular pharynx with its nearly autonomous nervous system and the intestine. The bi-lobed pharynx pumps food into the intestine, grinding it as it passes through the second bulb. The intestinal cells surround a central lumen, which connects to the anus near the tail. The excretory cell with excretory canals runs the length of the body connected to the excretory pore on the ventral side of the head. The total digestion time is 330-350 minutes at 22^0C.

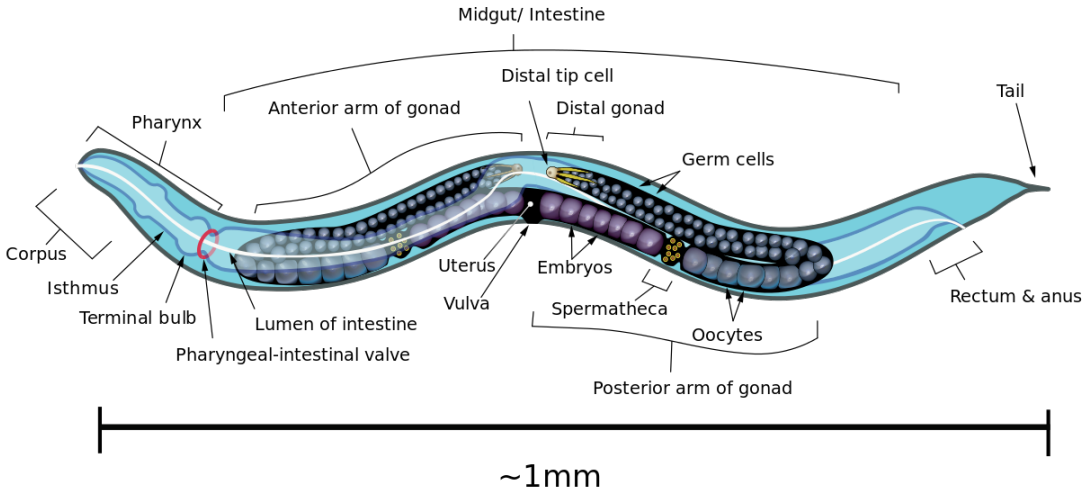

Figure 15: Anatomy of *C. elegans* adult hermaphrodite (diagram adapted from Wikipedia.com).

Embryogenesis in *C. elegans* starts with zygote proliferation and continues until the embryo has reached 558 cells. The hermaphrodite reproductive system consists of functionally independent anterior and posterior arms (Fig. 16). Each arm contains an ovary that is distal to the vulva, a more proximal oviduct, and a spermatheca connected to a common uterus centered around the vulva. The adult uterus contains fertilized eggs and embryos in the early stages of development. Vulval contractions, mediated by the hermaphrodite-specific neuron, are required for egg laying. The germ nuclei are mitotic near the distal end. As the mitotic germ cells progress in the gonad, they enter meiosis.

Meiotic cells in progressively later stages of spermatogenesis are distributed along the gonad to the spermatheca, in which spermatids are stored.

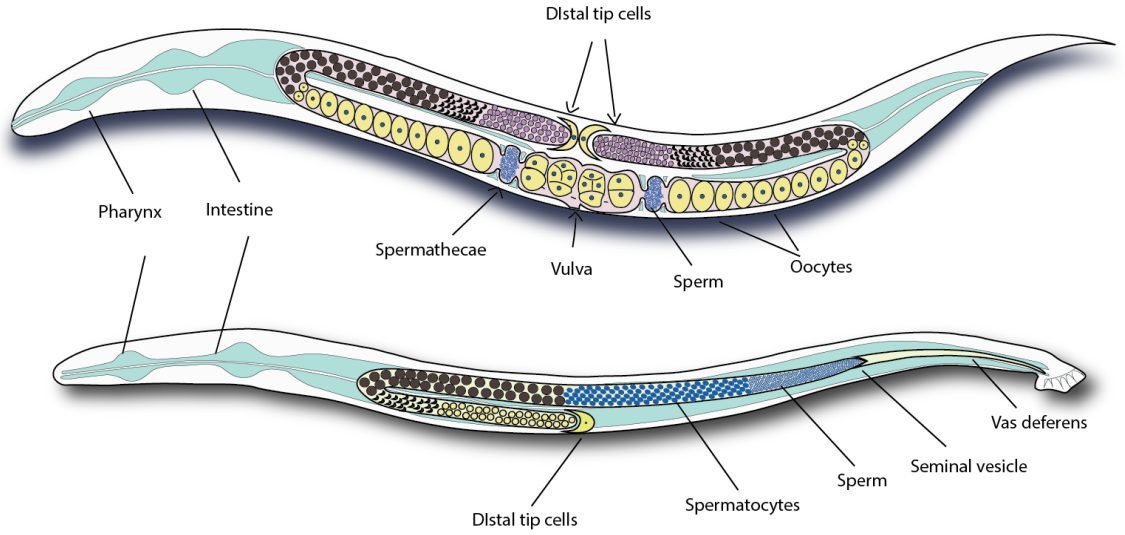

Figure 16: Anatomy of the germ line in adult hermaphrodite and male. The hermaphrodite contains two bilaterally symmetric, U-shaped gonad arms that are connected to a central uterus through spermatheca. The germline within the distal gonad arms (ovaries) is syncytial with germline nuclei surrounding a central cytoplasmic core. The male gonad is a single organ extending anteriorly from its distal tip, then posteriorly to connect via the vas deferens to the cloaca near the anus. (diagram inspired from Altun, Z. F. and Hall, D. H. 2005. Handbook of *C. elegans* Anatomy, In *WormAtlas at* (http://www.wormatlas.org/ver1/handbook/contents.htm).

The germ line is a specialized cell lineage that gives rise to eggs and sperm. Following the formation of zygote (P0) (also considered the first germline blastomere), a series of asymmetric cell divisions results in the production of the primordial P4 cell. Germ cells are exclusively derived from the P4 cell. The cell enters the interior of the embryo during gastrulation and divides symmetrically to form the two germ-line precursor cells, Z2 and Z3[436,437]. The daughter cells Z2 and Z3 can all be referred to as primordial germ cells (PGCs). At hatching, the gonad is comprised of four Z1, Z2, Z3 and Z4. Z1 and Z4 divide in the middle of the L1 larval stage. By the end of the L2 stage, the hermaphrodite somatic gonad consists of 12 Z1/Z4 descendants, but the germ line has proliferated to about 30 cells[438]. In the L3 stage, proximal germ cells enter meiotic

prophase. Several important reproductive structures made of 140 cells are generated from the L3 and L4 stage. An approximately four-fold amplification in total gem cell numbers occurs during the L4 and young adult stages. All somatic structures of the mature adult gonad are derived from Z1 and Z4, which includes the distal tip cell (DTC), sheath cells and spermathecae in the hermaphrodite. In adults, germ cell proliferation continues in the distal mitotic zone and later enters the meiotic pathway. In *C. elegans*, the DTC acts as a niche that maintains germ line proliferation[438]. The germ-line nuclei exist as a continuous syncytium but are referred as germ cells.

The gonadal sheath cells appear to play important roles for the structure, integrity, and reproductive functions of the gonad[439,440]. There are ten thin sheath cells, subdivided into five pairs (1-5) with each pair having a distinct position along the proximal-distal axis of each gonad arm. These elongated myoepithelial cells lay between germ cells and the gonadal basal lamina[441]. Pair 1 has cellular structures some of which are pressed into the gonad such that the cytoplasm is concentrated into a series of wedges that insert between the germ cells. Pair 2 ensheathes the loop region of the gonadal arm.

The spermatheca is a flexible accordion-like structure connected to the gonad arm distally and to the uterus proximally. It expands when needed to accommodate oocytes. The walls of the spermatheca are highly involuted, enabling expansion and providing an adherent surface for the spermatozoa awaiting an ovulated oocyte.

The uterus connects to the spermathecae and the vulva, functioning as a holding area for developing embryos prior to their expulsion through the vulva, a specialization of the external epidermis[442].

1.7.2 Germ cell specification

In *C. elegans*, the germline separates from the soma during the first four embryonic cleavages[436] (Fig. 17). Differences exist in the transcriptional activity of somatic *versus* germline blastomeres in early embroys[443,444]. *pie-1* is a maternal-effect gene that prevents mRNA transcription in early germ cells. *pie-1* is required for germ line generation and for proper specification of blastomere identity. PIE-1 prevents SKN-1, another maternal factor, from functioning in P2 by generally preventing mRNA transcription in the germ lineage[445]. PIE-1 disappears from the germ lineage shortly after the division of P4 into Z2

and Z3. After PIE-1 disappears, the germ line pattern of expression is established by the MES group (MES-2, MES-3, MES-4 and MES-6) of polycomb proteins[446]. They are needed for the normal proliferation and viability of the germ line[447]. MES-2 and MES-6 appear to constitute the polycomb group in *C. elegans*. The MES proteins are enriched in, but not restricted to, the germ line. By the time of hatching, first-stage larvae contain detectable MES protein only in the two primordial germ cells, Z2 and Z3. It is suggested that MES proteins serve a general role in modulating chromatin structure and repressing gene expression from autosomal sites as well as sites on the X-chromosome[448].

During early embryonic divisions, germ line-specific ribonucleoprotein granules (P-granules) are asymmetrically partitioned into germ line blastomeres[449-451]. P-granules contain a heterogenous mix of RNAs and proteins. PIE-1 proteins are found to associate with P-granules[452] but it is not clear whether PIE-1 must be associated with P-granules to control blastomere identity. Two related CCCH-type zinc finger proteins, POS-1 and MEX-1, are also required for specification of germline blastomeres and are components of P granules[453,454]. P granules remain associated with the nuclear envelope throughout germ line proliferation, and detach only during the maturation of male and female gametes. Some P granule components have been placed into a P granule assembly pathway: DEPS-1→GLH-1→PGL-1→IFE-1. Analysis of *deps-1*, *glh-1*, *pgl-1*, and *ife-1* mutants has revealed the germ line regulatory processes that those P granule components participate in regulating. *deps-1*, *glh-1*, and *pgl-1* mutants have underproliferated germ lines, and the majority of mutants fail to make oocytes and sperm at restrictive temperatures[455]. Further research is required to establish the significance of P-granules. Another gene, *patched-1* (*ptc-1*), which is a member of multiclass membrane protein, was shown to be required for cytokinesis in the germ line syncytium but is not essential for zygotic development[456].

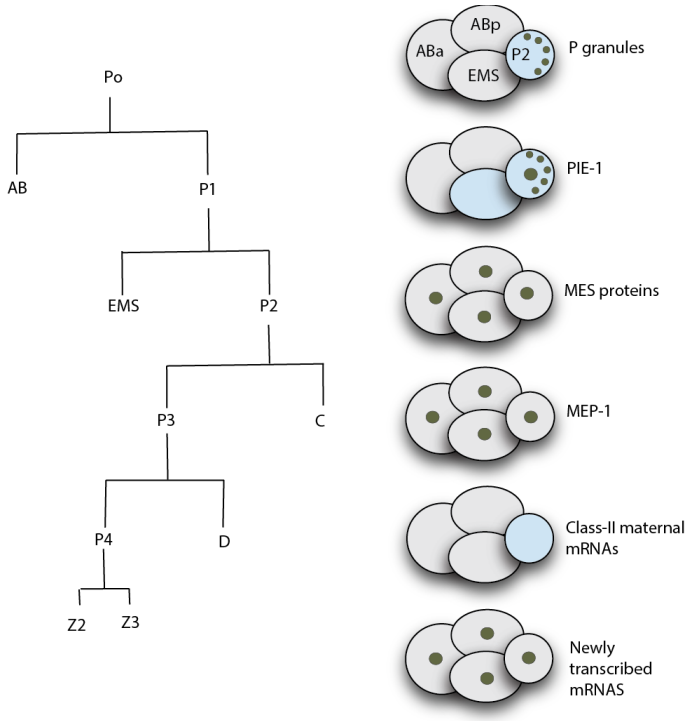

Figure 17: Germ line specification during the embryogeneis in *C. elegans*. At the beginning, the blastomeres, P_0, P_1, P_2 and P_3 in *C. elegans* embryos undergoes unequal divisions to generate somatic blastomeres, AB, EMS, C and D and the primordial germ cell P_4. Z_2 and Z_3 are generated equally from P_4 at 100 cell stage. The P-granules are well partitioned in the blastomeres at even 4-cell stage. PIE-1 resides in the germline cytoplasm and nucleus. The MES proteins and MEP-1 reside in the nuclei. Germline blastomeres also contains class II maternal mRNAs but are degraded in the somatic blastomeres and replaced by the newly transcribed mRNAs. (diagram modified from wormbook.org).

The germ line stem cells (GSC) are maintained by their proximity to the DTC. The DTC forms a niche, which is central to stem cell regulation in *C. elegans*. The DTC is born in the invariant cell lineage of the somatic gonad[437] and its fate is controlled through the Wnt/β-catenin asymmetric pathway[457,458]. In daughter cells destined to become the DTC, the WNT/β-CATENIN asymmetric pathway activates transcription of *ceh-22*, which encodes the single *C. elegans* NKX2.5 homeodomain transcription factor[459]. The CEH-22/Nkx2.5 homeodomain transcription factor is a key regulator of DTC specification.

1.7.3 Germ line proliferation and maintenance

The GSCs are responsible for the proliferation and maintenance of the germ line. The niche for GSC consists of a single mesenchymal cell, the DTC. Each hermaphrodite has two DTCs, one located at the distal end of each gonadal arm. The large cell body of the DTC encapsulates the tip of the gonad, and an elaborate network of DTC processes extends along the gonad proximally, ending at the boundary of early meiotic entry. The DTC is responsible for maintaining GSCs throughout the life of the animal. Ablation of the DTC at any stage of development causes all GSCs to enter the meiotic cell cycle and differentiate[438]. The DTC niche is maintained through GLP-1/Notch signaling (Fig.17).

The canonical Notch signalling pathway employs a DSL transmembrane ligand (LAG-2), a transmembrane Notch receptor LIN-12 and GLP-1, and a pathway-specific transcription factor complex to activate transcription[460]. The DTC expresses DSL ligands (LAG-2 and APX-1) and GSCs express the Notch receptor GLP-1[461-463]. GLP-1/Notch receptors works with a CSL DNA-binding protein, LAG-1, and a transcriptional co-activator, LAG-3/SEL-8, to activate transcription[464,465].

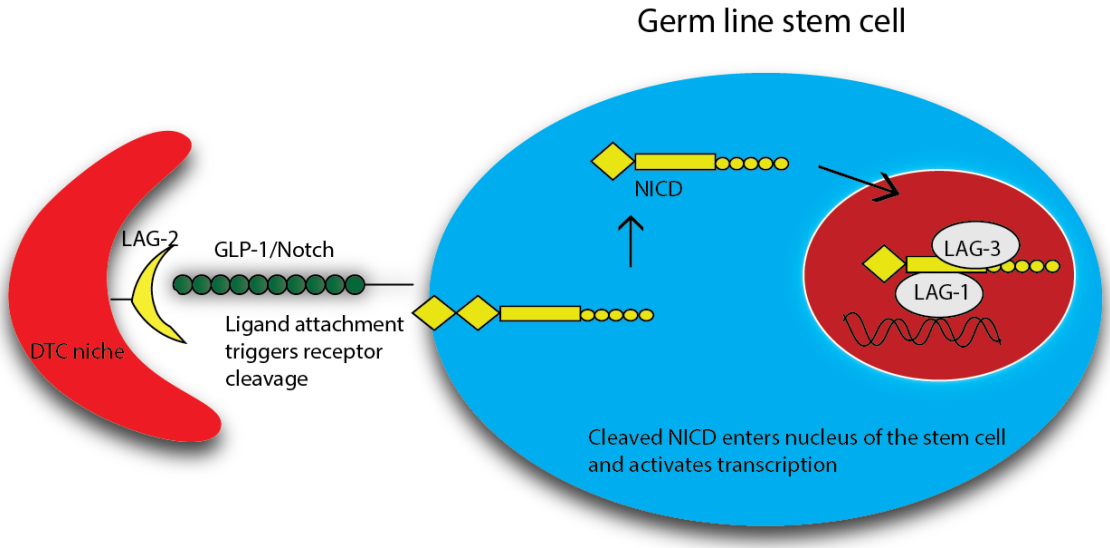

Figure 18: DTC niche maintains GSCs through Notch signalling. The DSL ligand of DTC, LAG-2 activates the GLP-1 receptor generating NCID which then enters the nucleus to form a ternary complex with the LAG-1 and transcriptional co-activator LAG-3. LAG-1 is a CSL DNA binding protein.

The LAG-2 ligand from the DTC niche activates GLP-1 receptor through its proteolytic cleavage, which generates the Notch intracellular domain (NICD). The NICD enters the nucleus to form a ternary complex with LAG-1, a CSL DNA-binding protein, and LAG-3/SEL-8, a transcriptional co-activator [466].

Removal of the GLP-1/Notch receptor mimics DTC ablation; all GSCs enter meiotic cell cycle and differentiate[467]. Conversely, for GLP-1 gain-of-function mutants, where the GLP-1 receptor signals independently of the ligand, meiotic entry doesn't occur and the germ line becomes tumorous and filled with mitotic cells[468]. Thus GLP-1 signaling is required continuously for GSC maintenance throughout post-embryonic development.

Downstream of GLP-1 signaling there exists an intrinsically acting regulator of GSCs, FBF (sequence specific RNA binding proteins). FBF-1 and FBF-2 belong to the Puf protein family and are collectively called FBF [469]. Removal of either FBF-1 or FBF-2 has little effect on the GSCs but removal of both causes a complete failure of adult GSCs maintenance.

1.7.4 Regulation of mitotic and meiotic progression in the germ line

The adult germ line possesses a mitotic region at its proximal end near the DTC and a transition zone more distally. Mitotic germ cells serve as stem cells that can self-renew and differentiate into gametes. In young adults, the mitotic region is composed of about 225-250 germ cells. FBF1 and FBF2 are required for continued mitotic division in late larval and adult animals and the maintenance of GSCs[470]. FBF targets *gld-1* and *gld-3* mRNAs, both of which promote commitment to meiosis[471]. FBF also targets itself in order to maintain relatively low FBF levels in the wild type germ line. FBF-1 and FBF-2 have distinct effects on the size of the mitotic region. Germ lines lacking *fbf-1* activity have smaller mitotic regions with around 200 cells, whereas *fbf-2* mutants have larger mitotic regions with ~400 cells.

Three GLD proteins (germ line differentiation) GLD-1, GLD-2, GLD-3 and NOS-3 (nanos-3) promote entry into the meiotic cell cycle[472]. They are all RNA regulators that control germ line development (Fig. 19). GLD-1, a member of the STAR/KH family of RND binding proteins, likely represses *glp-1* translation, which encodes glp-1/Notch

receptor[473]. NOS-3, a member of Nanos family of zinc finger protein was shown to activate GLD-1, in turn balancing the activity of *glp-1* through GLD-1[474]. GLD-2 and GLD-3 function together to promote entry into meiosis[475]. GLD-2 is the catalytic subunit of cytoplasmic poly-(A)-polymerase. GLD-2 promotes general mRNA-polyadenylation in germ cells. Large amount of GLD-1 and FBF-1 mRNAs are putatively stabilized by GLD-2[476]. GLD-3 promotes GLD-2 PAP (GLD-2 poly (A)-polymerase) activity. Genetic anaylsis suggests that GLD-3 may act as a negative feedback system for FBF activity[475].

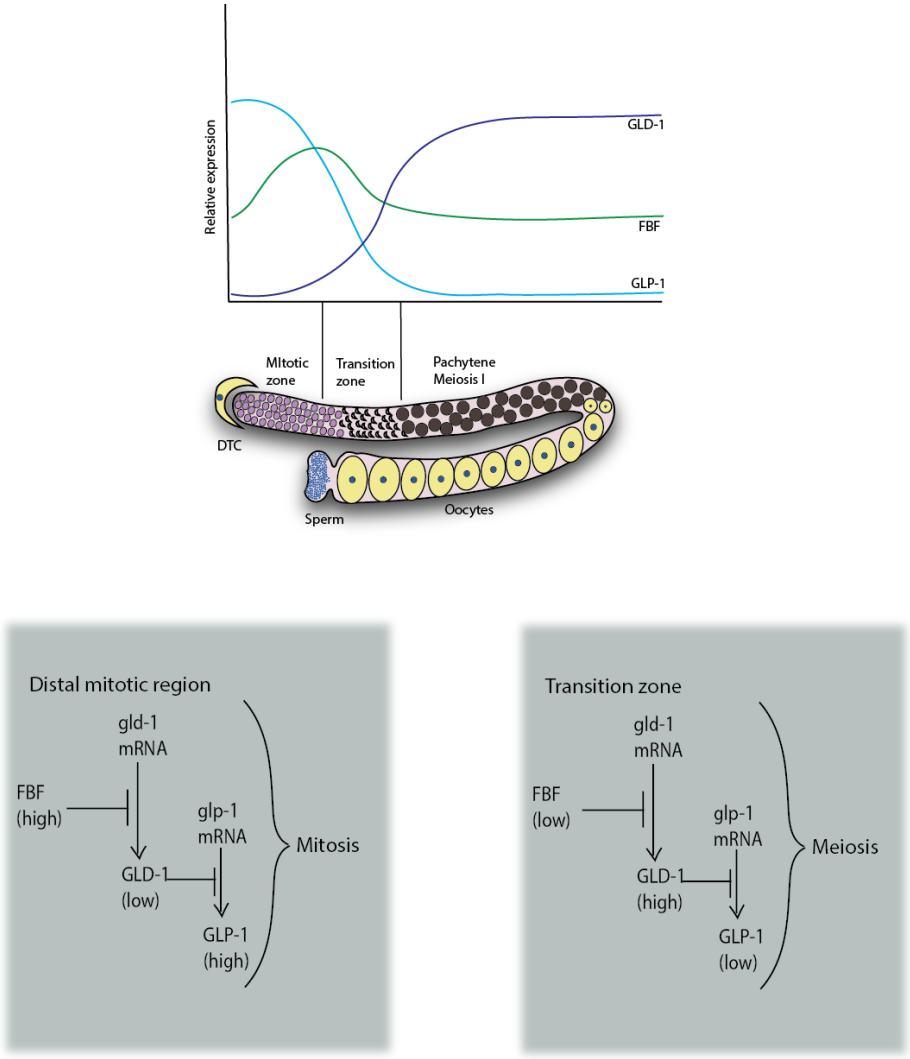

Figure 19: Interplay between FBF1/2 and GLD-1 determines the fate of germ line cells. (diagram inspired from Kuersten and Goodwin, 2003[477])

The *glp-1/Notch* was shown to be controlled by different regulators. Five ego genes (*ego-1*, *ego-2, ego-3*, *ego-4* and *ego-5*) and *epn-1* were shown to act as enhancers of *glp-1*[478]. Whereas, six sog genes (*sog-1*, *sog-2*, *sog-3*, *sog-4* and *sog-5*) acts as suppressors of *glp-1*[479].

1.7.5 Physiological germ line apoptosis in *C. elegans*

The *C. elegans* adult hermaphrodite generates 1090 somatic cells during development, of which 131 cells undergo PCD[436,480]. 113 cells die during embryogenesis between 250-450 minutes after fertilization[436]. A second wave of PCD occurs in the L2 stage, following the divisions of several neuroblasts, and marks the end of PCD in the soma. Ectodermal cells, comprised mainly of neurons and neuron-associated cells and hypodermal cells, make up the bulk of dying cells. A small number of mesodermal cells, such as muscle cells and pharyngeal gland cells also die during PCD. PCD is characterized by an early nuclear chromatin condensation and reduction in cell volume. The dying cells are quickly engulfed and degraded by neighboring cells, and their corpses remain visible for only a few minutes. The process of engulfment can begin even before a cell that will die has been completely separated from its sister by cell division. As engulfment proceeds, the dying cells splits into membrane bound fragments, and the nuclear membrane degenerates. The last recognizable features of the dead cell are whorls of membrane contained in vacuoles within the engulfing cell[481]. In contrast, PCD continues in the adult hermaphrodite germ line[482]. Physiological germ cell apoptosis occurs in the region where the developing oocytes enlarge, suggesting that apoptotic germ cell nuclei serve as 'nurse cells'. The doomed nuclei become rapidly cellularized, and are subsequently engulfed to provide most of their surrounding cytoplasm to the central gonad rachis[482].

1.7.6 DNA damage and apoptotic pathway in *C. elegans*

Multiple mechanisms have evolved to ensure the fidelity of genome duplication and to guarantee faithful partitioning of chromosomes at cell division in *C. elegans*. The effect of genotoxic stress shows that little or no checkpoint exists during embryonic

development, except for a transient intra-S checkpoint during early embryo development[483]. However, in the germ line, DNA damage induces cell cycle arrest and apoptosis, both of which are spatially separated. Ionizing radiation (IR) causes a transient halt in cell cycle progression in the mitotic zone, but in the meiotic compartment, after the exit from the pachytene region causes apoptotic cell death 2-3 hours after the genotoxic insult. Other DNA damaging agents such as alkylating agents induce germ cell death[484]. In the worm, DDR and repair pathways dealing with DNA double strand breaks (DSBs) are well characterized. Two major pathways of DSB repair are non-homologous end joining (NHEJ) restricted to G1 cell cycle stage and homologous recombination (HR) predominant at the germ line. In *C. elegans*, DDR is mediated largely by ATL-1, the worm Atr ortholog.

Three prominent genes were revealed by genetic screens to cause cell cycle arrest and apoptosis after DNA damage; mortal germline-2 (mrt-2), hus-1 and rad-5[483,485,486]. HUS-1 is a nuclear protein that interacts physically with MRT-2, and localizes to distinct nuclear foci of unrepaired damage, thus acting as a sensor of DDR. CtIP, a protein related to yeast Sae2, acts in conjunction with the MRN (MRE11, RAD50, NBS1) complex to resect the DBSs yielding 3' overhangs that can initiate homologous recombination. The SPO-11 gene product is responsible for enzymatic DNA cleavage to create DSBs and MRE-11 subsequently processes these though its intrinsic exonuclease activity. The MRE-11 nuclease is required for ATL-1 loading[487]. RAD-51, a member of the RecA-strand exchange proteins catalyzes the invasion of the single stranded DNA overhangs generated by MRE-11, initiating the formation of D-loops for meiotic recombination. In the worm *chk-1*, like *atl-1* is required for all checkpoint responses in unchallenged germ lines and mediating IR induced cell cycle arrest and apoptosis[488]. It also activates the secondary wave of phosphorylation waves. *chk-2* doesn't affect IR-dependent checkpoint responses but is rather required for UV-induced DDR[489] and meiotic recombination[490].

Another gene *gen-1* likely acts a Holliday junction resolvase for Holliday junctions generated during HR[491]. Furthermore, GEN-1 acts redundantly with the 9-1-1 complex to ensure genome stability. The heterotrimeric 9-1-1 complex (RAD-9, RAD-1 and HUS-1) is phosphorylated by ATL-1 and needed for full ATL-1 activation. Mutants of this complex fail to trigger the DDR upon IR treatment [484,492,493] (Fig. 20).

The tumor suppressor protein p53 homolog, CEP-1 (*C. elegans* p53 like-1) plays a key role in the integration of cellular responses to genotoxic stimuli[494,495]. CEP-1 is required for DNA damage-induced germ cell apoptosis. It is a direct transcriptional activator of *egl-1* (egg laying defective) and a second BH3-only protein, CED-13 (cell death abnormal-13)[496].

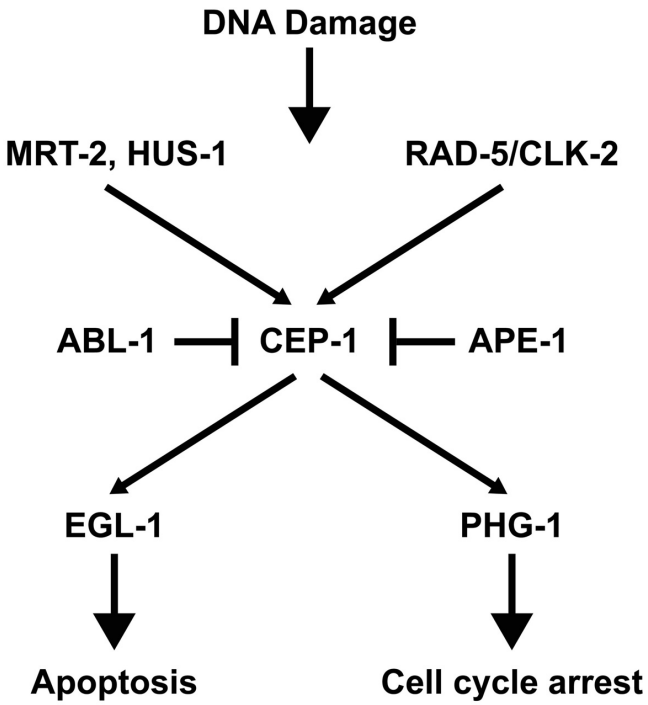

Figure 20: DNA damage responses at the germ line (diagram adapted from wormbook.org).

Three *C. elegans* death promoting genes, *egl-1*, *ced-4* and *ced-3* seem to be required for all somatic PCD to occur[497,498] (Fig. 21). These three genes act within the dying cell to promote apoptosis suggesting an intrinsic suicide mechanism. *egl-1*, coding for a BH3-only protein, acts upstream of *ced-9*, the only anti-apoptotic Bcl-2 homolog in *C. elegans*, which protect cells from PCD[499]. EGL-1 is expressed in cells destined to die[497] and appears to be regulated at the level of transcription. The *egl-1* gene encodes a small protein of 91 amino acids with BH3 motif. After activation by upstream signals, the EGL-1 interacts with CED-9 at the mitochondrial outer membrane. CED-9 like other Bcl-2 family members has a hydrophobic C-terminus that causes it to be membrane

associated. CED-9 localizes to the outer mitochondrial membrane, and it is through the physical interaction between CED-9 and an asymmetric dimer of CED-4 that the ability to CED-4 to form an active apoptosome and to mediate procaspase-3 activation is blocked[500,501]. Notably, CED-9 is the only *C. elegans* anti-apoptotic member of the core Bcl-2 family. There is no evidence of pro-apoptotic Bax-like molecule in *C. elegans*. Once EGL-1 acts to induce apoptosis, CED-9 undergoes a conformational change releasing CED-4[502]. EGL-1 binds to CED-9 and adopts an extended α-helical conformation that induces substantial structural rearrangements in CED-9. Once CED-4 is released from the CED-9-mediated inhibition, it is freed to translocate to the perinuclear membranes, and undergoes oligomerization. Endogenous CED-9 and CED-4 protein co-localize at the surface of mitochondria in *C. elegans* embryos and the mitochondrial localization of CED-4 is dependent on CED-9[503]. *ced-4* encodes a protein similar to human Apaf-1 (apoptotic protease activating factor), an activator of human caspase-9[504]. Like Apaf-1, CED-4 contains a CARD (caspase recruitment domain) domain and nucleotide binding motifs that are critical for their function. Active oligomerized CED-4 interacts with and facilitates the processing of inactive pro-CED-3 to active proteases p13 and p17. *ced-3* encodes a caspase (member of family of aspartate-specific cysteine proteases) synthesized as proenzyme and must be proteolytically activated to generate active proteases containing p13 and p17 subunit[505,506]. The active caspases acts as the mediators of downstream events in cell death, eventually leading to the destruction of the cell by cleaving and, thereby activating additional killing proteins.

Recently it was shown that EGL-1 induced mitochondrial fragmentation, is dependent on the functions of *ced-9* gene and is mediated by dynamin-related GTPase DRP-1, which is required for mitochondrial fission[507,508]. Other genes are also shown to be implicated in supressing apoptotic programs during *C. elegans* development: *dad-1* (defender against apoptotic death-1) and *icd-1* (inhibitor of cell death-1). How these genes interact with the core apoptotic program is currently unclear. CED-13, another BH3-only protein, also directly interacts with CED-9. *ced-13* mRNA accumulates after DNA damage, and this accumulation is dependent on the *cep-1* gene[509].

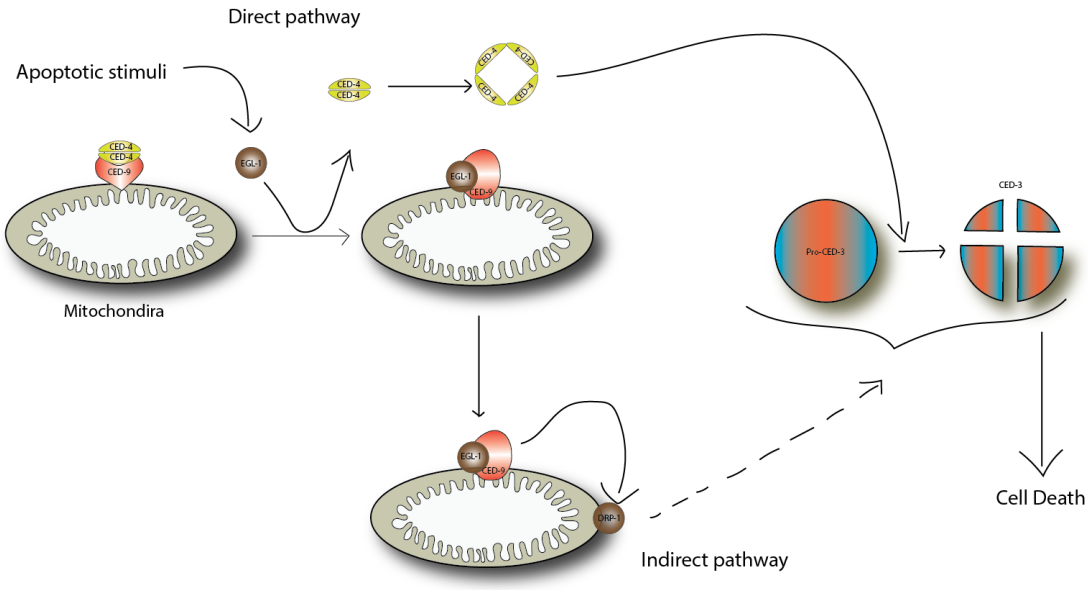

Figure 21. Direct and indirect pathway of apoptosis in *C. elegans* (diagram inspired from Nehme and Conradt 2008[510]).

Apoptotic cells signal at their surface for the neighbouring engulfing cells to engulf them. The engulfment signal is transduced to the cellular machinery in the phagocyte to trigger the phagocytic process. Eight genes have been identified in this process: *ced-1*, *ced-2*, *ced-3*, *ced-5*, *ced-7*, *ced-10*, *ced-12* and *psr-1* (phosphatidylserine receptor homologue)[511]. Most of these genes act in engulfing cells to promote corpse removal, with the exception of *ced-7* whose activity is required in both dying cells and the engulfing cells[512].

2. Rationale of the thesis and contribution of authors

Previous work in the laboratory using a series of mutants with functional assays, in addition to molecular analysis and live-cell imaging, revealed that Bcl-xL functions in mitosis are governed by 2 major sequential phosphorylation and dephosphorylation events that occur on Bcl-xL at Ser49 and Ser62, residues located within the unstructured loop domain of the protein[101,103]. Phosphorylation at Ser62 is mediated by Plk1 and Mapk14/Sapk p38✔ during prophase, metaphase and the anaphase boundary. Phosphorylation at Ser49 is mediated by Plk3 during G2 and at telophase and cytokinesis [101, 103]. Phospho-Bcl-xL (Ser62) localizes to centrosomes with γ-tubulin, and the mitotic cytosol with some SAC signaling components, including Plk1, BubR1 and Mad2. In taxol- and nocodazole-exposed cells, phospho-Bcl-xL(S62) also binds to Cdc20- Mad2- BubR1- and Bub3-bound complexes, while the phosphorylation mutant Bcl-xL(S62A) does not[103]. Phospho-Bcl-xL(S49) is found in in centrosomes with γ-tubulin at G2 and in association with MT-associated dynein motor protein and at the mid-zone body during telophase/cytokinesis[101]. Silencing Bcl-xL expression, or expressing the Bcl-xL (S62A) and (S49A) mutants in cancer cells, leads to important defects in mitosis associated with chromosome mis-segregation and cytokinesis failure[103]. Because the above observations were made in tumor cells which already display genomic instability, chromosome instability and aneuploidy, the present studies were performed in normal human diploid cells, and *in vivo* in *C. elegans,* to monitor the importance of Bcl-xL mitotic function to maintain chromosome stability in normal cells.

Section 3 described the studies conducted in BJ normal foreskin diploid fibroblast cells, where Bcl-xL(wt), Bcl-xL(S49A), (S49D), (S62A), (S62D) and the dual (S49/62A) and (S49/62D) mutants were expressed using a Lentivirus system. The BJ cells have a very stable normal diploid karyotype at population doubling up to 62, but display an abnormal karyotype at the outbreak of senescence at population doubling 80[513]. We hypothesized that although BJ cells contain a very stable and normal genetic background, the expression of Bcl-xL (S49) and/or (S62) phosphorylation mutants alone will provoke chromosome instability and aneuploidy. Indeed, normal diploid human BJ foreskin fibroblasts expressing exogenous Bcl-xL phospho-mutants showed a decrease in the kinetics of cell population doubling, which is associated with appearance of chromosome

instability and aneuploidy, coupled to the occurrence of cellular senescence with no striking effects on cell death. Experimental design, data collection and data analysis were conducted by PS Baruah (55%), M. Beauchemin (40%) and J. Hébert (5%). R. Bertrand supervised all aspects of the project.

Section 4 described the *in vivo* studies conducted in the nematode *C. elegans*. Although the Ced-9 protein, which correspond to Bcl-2 and Bcl-xL orthologs in *C. elegans*, lacks the functional loop domain, we hypothesised that expression of the mutants will have dominant effects on mitotic behaviours and on development of the worms. A series of transgenic worms expressing Bcl-xL(wt) and the phosphorylation mutants Bcl-xL(S49A), (S49D), (S62A), (S62D) and (S49/62A) have been generated with the Mos1-mediated Single Copy Insertion technique (MosSCI)[514] and provided to us by Knudra transgenics. The transgenic worms expressing the phosphorylation mutants showed a decrease in egg laying capacity, decreased hatching, aberrant mitotic and meiotic germ cells, and increased number of apoptotic bodies in the gonads of adult hermaphrodites. The mutant worms displayed an increased or decreased length of the mitotic regions and transition zones suggesting delay in mitotic exit, with some cells exhibiting an abnormal number of chromosomes, or increased apoptosis, respectively. In addition, variable life spans of the adult transgenic hermaphrodites were monitored compared to the wild type worms N2 in animal expressing the Ser to Ala phosphorylation mutants. Experimental design, data collection and data analysis were conducted by PS Baruah (90%) and M. Beauchemin (10%). JA Parker and R. Bertrand co-supervised all aspects of the project.

3. Dynamic Bcl-xL (S49) and (S62) phosphorylation/dephosphorylation during mitosis prevents chromosome instability and aneuploidy in normal human diploid fibroblasts

Baruah PS[1,2], Beauchemin M[1,2], Hébert J[3,4], Bertrand R[1,2,4].

[1]Centre de recherche, Centre hospitalier de l'Université de Montréal (CRCHUM) and [2]Institut du Cancer de Montréal, [3] Quebec Leukemia Cell Bank, Centre de recherche, Hôpital Maisonneuve-Rosemont, and [4]Département de médecine, Université de Montréal, Montréal (Québec) Canada

Corresponding author: Richard Bertrand, CRCHUM, 900 rue St-Denis (Room R10.424), Montréal (Québec) Canada H2X 0A9.
Telephone: +1-514-890-8000 Extension 26615
Fax: +1-514-412-7938

Running title: Bcl-xL and chromosome instability

3.1 Summary

Bcl-xL proteins undergo dynamic phosphorylation/dephosphorylation on Ser49 and Ser62 residues during mitosis. The expression of Bcl-xL(S49A), (S62A) and dual (S49/62A) phosphorylation mutants in tumor cells lead to severe mitotic defects associated with multipolar spindle, chromosome lagging and bridging, and micro-, bi- and multi-nucleated cells (Wang J. et al,., *Cell Cycle 2014; 13:1313-1326)*. As the above observations were made in tumor cells, which display genomic instability, we now address the questions: will similar outcome occur in normal human diploid cells? and what will be the fate of normal cells? We studied normal human diploid BJ foreskin fibroblast cells expressing Bcl-xL(wt), (S49A), (S49D), (S62A), (S62D) and the dual (S49/62A) and (S49/62D) mutants. Cells expressing S49 and/or S62 phosphorylation mutants showed reduced kinetics of cell population doubling. These effects on cell population doubling kinetics correlated with early outbreak of senescence with no impact on the cell death rate. Senescent cells displayed typical senescence-associated phenotypes including high-level of senescence-associated β-galactosidase activity, interleukin-6 (IL-6) secretion, tumor suppressor p53 and cyclin-dependent kinase inhibitor p21Waf1/Cip1 activation as well as γH2A.X-associated nuclear chromatin foci. Fluorescence *in situ* hybridization analysis and Giemsa-banded karyotypes revealed that the expression of Bcl-xL phosphorylation mutants in normal diploid BJ cells provoked chromosome instability and aneuploidy. These findings suggest that dynamic Bcl-xL(S49) and (S62) phosphorylation/dephosphorylation cycles are important in the maintenance of chromosome integrity during mitosis in normal cells. They could impact future strategies aiming to develop and identify compounds that could target not only the anti-apoptotic domain of Bcl-xL protein, but also its mitotic domain for cancer therapy.

3.2 Introduction

The Bcl-2 family of proteins, including Bcl-xL (1), stands out among key regulators of apoptosis, executing crucial functions and controlling whether cells will live or die during development and cellular stress (2). Studies have revealed that members of the Bcl-2 family, in addition to their central role in apoptosis, are also involved in membrane dynamics and remodelling (3, 4), cell cycle regulation (5-12), DNA damage responses, repair and recombination (13-17), effects that are generally distinct from their purpose in apoptosis.

The pleiotropic functions of Bcl-xL depend at least on post-translational modifications and its sub-cellular location. Bcl-xL phosphorylation on Ser62 residues was first detected in various cancer cell lines treated with microtubule inhibitors (18-20), and later found in synchronized cells (11). A subset of the Bcl-xL protein pool undergoes dynamic phosphorylation at Ser62 during the S and G2 phases of the cell cycle, followed by a high phosphorylation peak during the early step of mitosis (11, 12). During cell cycle progression, Polo kinase 1 (PLK1) and mitogen-activated protein kinase 9 / c-jun N-terminal kinase 2 (MAPK9/JNK2) are major protein kinases associated with progressive phosphorylation of Bcl-xL(S62) during G2, where it accumulates in nuclear structures, including nucleoli and Cajal bodies (11).

During mitosis, Bcl-xL(S62) is strongly phosphorylated by PLK1 and MAPK14/ stress-activated protein kinase p38α (SAPKp38α) at the prometaphase, metaphase and anaphase boundaries, with its rapid dephosphorylation at telophase and cytokinesis (12). At mitosis, phospho-Bcl-xL(S62) localizes in centrosomes with γ-tubulin and in mitotic cytosol with some spindle-assembly checkpoint (SAC) signaling components including PLK1, BubR1 and Mad2. In taxol- and nocodazole-exposed cells, phospho-Bcl-xL(S62) also binds to Cdc20-, Mad2-, BubR1-, and Bub3-complexes, while the phosphorylation mutant Bcl-xL(S62A) does not (12).

Dynamic cell cycle-dependent Bcl-xL phosphorylation at Ser49 also has been reported. In synchronized cells, phospho-Bcl-xL(S49) appears during the S and G2 phases, whereas it disappears rapidly in early mitosis during prometaphase and metaphase, re-appearing during ongoing anaphase, telophase and cytokinesis (10). During G2, a significant phospho-Bcl-xL(S49) protein pool accumulates in centrosomes,

particularly after DNA damage-induced G2 arrest, while during telophase and cytokinesis, it is found with microtubule-associated dynein motor protein and in the mid-zone body. PLK3 is the key protein kinase involved in Bcl-xL(S49) phosphorylation (10).

Ser49 and Ser62 residues are located within the unstructured loop domain of Bcl-xL, a region generally not essential for its anti-apoptotic function (9-12, 21, 22). Indeed, Bcl-xL's anti-apoptotic function is inherent to the BH1, BH2 and BH3 domains of the protein that create a hydrophobic pocket where the amphipathic α-helix of another BH3-containing protein can bind (23-25). Bcl-xL proteins exert their anti-apoptotic activity by binding to and inactivating pro-apoptotic members of the family, including Bax and Bak. In contrast, a subset of Bcl-2 pro-apoptotic members (BH3-only proteins), mediate interaction with Bcl-xL and inhibit the anti-apoptotic function, thereby promoting apoptosis (26-28).

In tumor cells, expression of the phosphorylation mutants Bcl-xL(S62A), Bcl-xL(S49A) and dual Bcl-xL(S49/62A) shows anti-apoptotic properties similar to Bcl-xL wild-type (wt) protein. However, expression of the phosphorylation mutants Bcl-xL(S62A), Bcl-xL(S49A) and dual Bcl-xL(S49/62A) leads to an increased number of cells harboring mitotic defects, as visualized by time-lapse live-cell imaging microscopy (12). These defects include multipolar spindle, chromosome lagging and bridging, micro-, bi- and multi-nucleated cells, and cells that fail to complete mitosis (12). Together, these observations indicate that during mitosis, Bcl-xL(S49) and (S62) phosphorylation/dephosphorylation dynamics impact on chromosome stability, mitosis resolution and cytokinesis completion. In these studies, exogenous Bcl-xL phospho-mutants showed dominant effects even in the presence of endogenous Bcl-xL. In addition, when endogenous Bcl-xL expression was silenced, expression of the mutants showed stronger effects indicating competition between the wild-type and mutant forms (12).

Because the above findings occurred in tumor cells, which already display genomic instability with chromosome aberrations and aneuploidy, the present studies were performed in normal human diploid BJ fibroblast cells. BJ cells have a normal very stable diploid karyotype at population doubling up to 62, but begin to display karyotype abnormalities at population doubling of 80 at the outbreak of replicative senescence (29).

We hypothesized that although BJ cells have a normal and very stable genetics until the outbreak of replicative senescence, the expression of Bcl-xL (S49) and/or (S62) phosphorylation mutants will provoke their early chromosomal instabilty and aneuploidy.

3.3 Results

Expression of Bcl-xL phosphorylation mutants in BJ cells and effects on cell population doubling and cell fate

First, we confirmed that Bcl-xL proteins undergo dynamic phosphorylation and dephosphorylation cycles on Ser49 and Ser62 at different steps of mitosis in normal human diploid foreskin fibroblast BJ cells (Fig. 1A). Indeed, in highly-enriched cell populations synchronized either at G2 or at specific steps of mitosis, Western immunoblotting disclosed that Bcl-xL proteins were highly phosphorylated at Ser62 at the prophase, prometaphase, metaphase and anaphase boundaries, but dephosphorylated at telophase/cytokinesis. In contrast, Bcl-xL proteins were phosphorylated at Ser49 during G2, but not at Ser49 at prophase, prometaphase and metaphase, while they were re-phosphorylated later at telophase and cytokinesis (Fig. 1A). To obtain highly-enriched sub-populations of cells at specific steps of mitosis, BJ cells were synchronized by double-thymidine block (2 mM) and released upon progression to G2. They were then treated with nocodazole (0.35 μM, 5 h), and prophase/prometaphase cells were collected by mitotic shake-off. A portion of these cells was released from nocodazole and grown in the presence of MG-132 (25 μM, 3 h), a proteasome inhibitor that prevents cyclin B1 and securin destruction, to obtain cell populations at the metaphase/anaphase boundary by mitotic shake-off. A second set was released from nocodazole and grown in the presence of blebbistatin (10 μM, 3 h), a selective non-muscle contractile motor myosin II inhibitor that prevents furrow ingression, to attain cell populations at telophase/cytokinesis (10, 12). Bcl-xL expression levels remained stable along G2 and mitosis, with cyclinB1 and phospho-H3(Ser10) expression shown as specific mitotic phase markers (Fig. 1A). Identical Bcl-xL phosphorylation patterns were observed previously in cancer cells (10, 12). Studies were therefore conducted in BJ cells expressing human influenza hemagglutinin (HA)-tagged Bcl-xL(wt), (S49A), (S49D), (S62A), (S62D) or dual (S49/62A) and (S49/62D) phosphorylation mutants. The cells were infected with

lentiviruses expressing various cDNAs at early cell population doubling, and the kinetics of cell population doubling were monitored over a period of 4 months post-infection.

Figure 1B represents a typical experiment and Figure 1C illustrates the expression of endogenous Bcl-xL, HA-Bcl-xL(wt) and various phosphorylation mutants, by Western immunoblotting, at different cell population doublings. Two similar additional experiments are reported in expanded view (Fig. S-1). The kinetics of cell population doubling were similar in control BJ cells and BJ cells infected by control lentivirus vector or HA-Bcl-xL(wt) (Fig. 1B). In contrast, cells expressing Ser49 and/or Ser62 phosphorylation mutants showed reduced kinetics of cell population doubling (Fig. 1B). The observed decrease in the kinetics of cell population doubling was associated with increased senescence, as measured by senescence-associated β-galactosidase assays (30) (Fig. 2A and 2B) and senescence-associated secretory phenotypes, with Il-6 secretion as biomarker (31) (Fig. 2C).

No significant effects on apoptotic or necrotic cell death were seen in cells expressing the HA-Bcl-xL phosphorylation mutants, with cell death rates less than 2-3% over the time-course of the experiments. The morphology of more than 25,000 Hoechst 33342- and propidium iodide (PI)-stained cells was analyzed for each phosphorylation mutant at different population doublings (data not shown).

Expression of HA-Bcl-xL phosphorylation mutants in BJ cells and chromosome instability and aneuploidy

Striking effects were noted by time-lapse live-cell imaging microscopy of human cancer HeLa cells expressing HA-Bcl-xL(S49A), (S62A) and dual (S49/62A) phosphorylation mutants with an increased number of cells harboring multiple mitotic defects, including multipolar spindle, chromosome lagging and bridging, micro-, bi- or multi-nucleated cells, and cells that fail to complete mitosis (12). To establish if the expression of Bcl-xL phosphorylation mutants in normal diploid BJ cells provokes chromosome instability and aneuploidy, fluorescence *in situ* hybridization (FISH) analysis of interphasic cells was performed at various cell population doublings, with a fluorophobe-labeled 6p11.1-q11 alpha satellite DNA probe (Fig. 3A). These analyses provided simple determination by looking at chromosome 6.

Figure 3A shows a significant increase of aneuploidy in all Bcl-xL phosphorylation mutants compared to control BJ cells or BJ cells infected by control lentivirus vector or HA-Bcl-xL(wt). Typical FISH micrographs are represented in Figure 3B. To validate these observations, standard cytogenetic analysis was also performed on mitotic cells at various cell population doublings. Table 1 list the various chromosomal aberrations detected and monitored by G-banded karyotyping. It is noteworthy that, typically, FISH analysis was performed on interphasic cells (either proliferative and non-proliferative or senescent cells), while G-banded karyotyping was done on metaphasic cells, which implies that these cells are proliferative, at least through 1 mitotic cycle.

In cells expressing Bcl-xL phosphorylation mutants S62A, S49D and S62D, chromosomal abnormalities were detected, indicating that even in the presence of chromosome abnormalities, these cells were able to undergo at least through 1 mitotic cycle (Table 1). Control BJ cells or BJ cells infected by control lentivirus vector or HA-Bcl-xL(wt) presented very low-level aneuploidy, based on FISH analysis (Fig. 3A, 3B), and have normal karyotypes, based on cytogenetic analysis (Table 1).

Expression of senescence-associated phenotypes and biomarkers in BJ cells expressing HA-Bcl-xL phosphorylation mutants

Senescent cells can display a series of phenotypes: senescence-associated β-galactosidase activity (30) (Fig. 2A, 2B), senescence-associated secretory phenotypes (31) (Fig. 2C), as well as nuclear foci linked to chromatin alterations and activation/recruitment of DNA damage response proteins, such as phospho-histone γH2A.X (32). Senescence is also often associated with sustained expression of the cell cycle-dependent kinase inhibitors p16INK4A and/or p21Waf1/Cip1 (33). Figures 4A, 4B and 4C (left panels) illustrate, at the single cell level, the expression of key biomarkers revealed by immunofluorescence (IF) imaging and analysis. Both p21Waf1/Cip1 (Fig. 4A) and γH2A.X (Fig. 4B) expression increased significantly in late population doubling BJ cell compared to corresponding early population doubling cells. p21Waf1/Cip1 and γH2A.X expression was increased much more significantly in late population doubling BJ cells expressing Bcl-xL phosphorylation mutants compared to late population doubling control BJ cells or BJ cells infected by control lentivirus vector or HA-Bcl-xL(wt) ($p < 0.01$; not indicated on graphs). In contrast, Ki67 expression (Fig. 4C), a

marker of proliferative cells, decreased significantly in late population doubling BJ cells expressing Bcl-xL phosphorylation mutants compared to corresponding early population doubling cells, and population doubling control BJ cells or BJ cells infected by control lentivirus vector or HA-Bcl-xL(wt) ($p < 0.01$; not indicated on graphs). These observations are consistent with the kinetics of population doubling (Fig. 1B) and the outbreak of senescence in late population doubling BJ cells expressing Bcl-xL phosphorylation mutants (Fig. 2A).

Typical IF micrographs are presented in Figures 4A, 4B and 4C (right panels). Involvement of the p53 and p21Waf1/Cip1 DNA damage response pathway was confirmed by Western blottings (Fig. 4D). p16INK4A expression was barely detectable in BJ cells, even in late population doubling cells exhibiting a high senescence rate (data not shown), suggesting that p16INK4A is not part of the process.

We attempted to correlate the expression of these biomarkers with aneuploidy at the single cell level in a limited number of samples. To do so, we implemented a FISH labeling experimental protocol, followed by IF labeling. Most, but not all cells, harbouring aneuploidy, detected by FISH, displayed high-level p21Waf1/Cip1 expression (Fig. S-2A) and low-level Ki67 expression (Fig. S-2B). These observations correlated at the single cell level, with aneuploidy, p21Waf1/Cip1 and Ki67 expression, consistent with non-proliferative and/or senescent cells. Interestingly, correlation did not fit all aneuploid cells, indicating a mosaic or progressive response, where some aneuploid cells still had proliferative potency at least for 1 or a few cell cycle divisions, finding consistent with our ability to perform G-banding analysis at metaphase (Table 1). Attempts to detect aneuploidy and γH2A.X-associated nuclear foci or senescence-associated β-galactosidase activity by similar experimental approaches were unsuccessful; the FISH experimental protocol involved an alkaline DNA denaturation step that most likely released nuclear foci-associated proteins from chromatin and destroyed acidic β-galactosidase activity (data not shown).

3.4 Conclusion and discussion

Together, our experiments revealed that the expression of Bcl-xL(S49) and (S62) phosphorylation mutants in normal human diploid BJ cells provoked chromosome

instability and aneuploidy. These effects correlated with reduced cell population doubling and the outbreak of senescence with typical senescence-associated phenotypes, including high-level senescence-associated β-galactosidase activity, IL-6 secretion, p53 and p21Waf1/Cip1 expression and γH2A.X-associated nuclear foci. Our observations suggest that dynamic Bcl-xL(S49) and (S62) phosphorylation and dephosphorylation cycles are key determinants of Bcl-xL functions in maintaining chromosome integrity. These effects, by Bcl-xL(S49) and (S62) phosphorylation mutants during mitosis, are consistent with previous findings in cancer cells (10, 12). They are also consistent with Ser49 and Ser62 which are located within the protein's unstructured loop domain (21, 22), are non-essential for Bcl-xL anti-apoptotic function (9-12), but indeed play roles in chromosome stability.

Our study revealed that, concomitant with chromosome abnormalities mediated by the expression of Bcl-xL(S49) and (S62) phosphorylation mutants, BJ cells underwent senescence. This observation further reinforced the concept that senescence can act as a potent tumor suppressing mechanism in normal cells (34). Interestingly, Bcl-xL is very rarely mutated in human tumors, suggesting that putative key mutations within Bcl-xL would be unsuitable for cell proliferation and survival (see mutations and polymorphisms in Figure S-3A and -3B). Bcl-xL overexpression rather than mutation is associated with tumor development and poor treatment response in various cancers (35-41). Indeed, tumor cells are believed to depend on, or are addicted to, anti-apoptotic Bcl-2 family members, including Bcl-xL (42), providing a selective advantage to cancer cells by allowing them to survive various stressful environments, cell stress phenotypes and/or cell death signals that directly ensue from oncogenic signaling, tumor suppressor deficiency or anticancer treatments (42). Although Bcl-xL(S49) and (S62) are not found yet mutated in cancer cells, the two major protein kinases involved in Bcl-xL phosphorylation during mitosis, PLK-1 and PLK-3 are often linked to aneuploidy and cancer development. Indeed, human PLK-1 is essential during mitosis, DNA damage responses and for maintenance of genomic stability (43). The spatio-temporal regulation of PLK-1 direct its activity at various locations, including cytoplasm, centrosomes, along microtubules, at spindle midzones, kinetochore/centromere regions and in post-mitotic bridges of the dividing cells (43). Many studies showed the various roles of PLK-1

during mitosis, more importantly, its role in ensuring SAC fidelity, kinetochore-microtubule attachment and sister chromatid separation. Misexpression of PLK-1 causes mitotic abnormalities including aneuploidy leading to tumorigenesis, and its often found overexpressed in a variety of tumors (43). PLK-3 is also involved in regulating a variety of molecular and cellular events, including DNA replication, DNA damage responses, cell cycle control and tumor angiogenesis (44). Aberrant expression of PLK-3 is also found in different types of tumors (44). Small-molecule inhibitors of PLK are under clinical trials and provided a survival benefit for patients with leukemia (45-47).

Our data indicate that if a putative mutation occurs randomly within Bcl-xL(S49) or (S62) in normal cells, they will undergo aneuploidy with senescence, rather than outbreak into a tumorigenesis path. However, the possibility that mutations within oncogenes or tumor suppressor genes, in combination with Bcl-xL mutations, could lead to a tumorigenesis path cannot be ruled out completely. Nevertheless, the fact that Bcl-xL mutations are very rarely found in human tumors, and yet, to the best of our knowledge, have never been detected on Ser49 and Ser62, strongly suggests that putative random mutations within Bcl-xL(S49) or (S62) in normal cells will lead to senescence outbreak. Perturbation of the SAC is well-known to result in chromosome mis-segregation and aneuploidy. Only few studies have ascertained correlations between aneuploidy and the outbreak of senescence. Reduced BubR1 expression in mouse embryonic fibroblasts causes increased aneuploidy and senescence, an effect associated with opposing roles of p16INK4A and p19Arf controlling senescence and aging (48, 49). Furthermore, in mouse embryonic fibroblasts, Bub1 mutation which causes high rates of chromosome mis-segregation and aneuploidy, has been reported to be accompanied by growth defects, premature senescence, as well as tumorigenesis (50).

One of the main questions raised by this study is: how do phospho-Bcl-xL(S62) and (S49) act at the molecular level during mitosis? In a previous study, we demonstrated that phospho-Bcl-xL(S62) localizes in mitotic cytosol with some SAC signalling components, including Plk1, BubR1 and Mad2. In addition, a series of co-immunoprecipitation experiments, on taxol- and nocodazole-exposed cells, revealed that phospho-Bcl-xL(S62) binds with Mad2-, BubR1-, Bub3- and Cdc20-complexes, but not Bub1 and Cdc27, a subunit of anaphase-promoting complex/cyclosome (APC/C) itself

(12). These interactions were confirmed by series of reciprocal co-immunoprecipitations in 2 cancer cell lines (12). Intriguingly, when Bcl-xL is phosphorylated on Ser62, mitosis occurs normally, while expression of the non-phosphorylation mutant S62A, leads to many defects, including, delayed anaphase and chromosome mis-segregation (12). Moreover, only the phospho-Bcl-xL(S62) form, and not the S62A form, binds to Cdc20-, Mad2-, BubR1-, Bub3-bound complexes, suggesting that it has a salutary effect on SAC resolution and proper mitosis progression (12). Further work is ongoing to understand these protein:protein interactions and their impact on APC/C-cdc20 ubiquitin ligase activity and anaphase entry.

The molecular mechanisms of phospho-Bcl-xL(S49) action is more mysterious. Our previous observations indicate that phospho-Bcl-xL(S49) localizes at centrosomes in the G2 phase of the cell cycle and in the mid-zone body during telophase/cytokinesis (10), a region where membrane vesicule fusion occurs, to provide the necessary membrane addition that will surround 2 daughters cells during full ingression of the contractile ring and abscission (51). Considering that Bcl-xL has been reported to play role in membrane remodeling (4), it is tempting to speculate on phospho-Bcl-xL(S49) in the mid-zone body, promoting membrane vesicle recruitment to provide the necessary membrane addition for complete abscission of mother cells into daughters cells. This hypothesis will need to be evaluated in the near future. Similarly, the involvement of centrosome-associated phospho-Bcl-xL(S49) (late G2) and phospho-Bcl-xL(S62) (prometaphase and metaphase) in microtubule elongation and chromosome capture remains to be elucidated.

Many efforts, including new clinical trials, are currently being pursued to develop new drugs targeting the anti-apoptotic domain of Bcl-2 protein members, including Bcl-xL (52-56, 57). In addition, recent findings, including our observations suggest that other protein activities could be of interest as targets for cancer therapy. Understanding how Bcl-xL proteins governs their mitotic functions will help to develop and explore strategies in the near future to identify novel compounds that focus not only on the anti-apoptotic domain, but also on the mitotic domain of Bcl-xL for cancer treatment.

3.5 Materials and methods

Cell culture, cDNA constructs, lentivirus preparations and cell analysis. Human BJ cell lines were obtained from the American Type Culture Collection at population doubling of 22 and grown at 37°C under 5% CO_2 in Eagle's minimum essential medium (EMEM) supplemented with 10% heat-inactivated fetal bovine serum (FBS), 100 U/ml penicillin and 100 μg/ml streptomycin, respectively. Cell numbers were counted by standard hemocytometer in duplicate. All cDNA constructs were generated and subcloned in pLenti6.2 Blast DEST vector (Invitrogen Corporation, Carlsbad, CA) as described previously (10-12). All vectors were sequenced in both orientations.

Lentiviruses were produced in 293FT cells, also obtained from Invitrogen. Transduced BJ cells with lentiviruses were grown under blasticidin (7 μg/ml) selection. Titrations of the lentivirus were performed and determined according to the manufacturer's protocol. MOI ratio of 1:1 was used during the infection.

The kinetics of cell cycle phase distribution were monitored by BD-LSRII Fortessa cytometer with BD FacsDiva (v6) software (Becton, Dickinson & Company, San Jose, CA), phospho-H3(Ser10) labeling and PI staining. In senescence-associated β-galactosidase assays, cells were fixed in 3% formaldehyde buffered with phosphote-buffered saline (PBS) for 2-3 min, then washed with PBS. They were incubated in a staining solution containing 20 mM citrate-phosphate, pH 6.0, 150 mM NaCl, 5 mM potassium ferricyanide, 5 mM potassium ferrocyanide, 2 mM $MgCl_2$ and 200 μM chromogenic substrate 5-bromo-4-chloro-3-indoyl β-D-galactopyranoside in a humidified chamber at 37°C for 24h in the dark (9). The cells were then washed and visualized by phase contrast microscopy. Cell death was monitored by standard Hoechst 33342- and PI-staining with visualization by fluorescence microscopy. IL-6 secretion was measured using Human IL-6 ELISA Ready-Set-Go reagent set, according to the manufacturer's instructions (eBioscience Inc, SanDiego, CA).

Protein extraction and immunoblotting. To prepare total protein, cells were extracted with lysis buffer containing 20 mM Hepes- KOH, pH 7.4, 120 mM NaCl, 1% Triton X-100, 2 mM phenylmethylsulfonyl fluoride, a cocktail of protease inhibitors (Complete™, Roche Applied Science, Laval QC) and a cocktail of phosphatase inhibitors (PhosStop™,

Roche Applied Science). The antibodies (Abs) in this study were Bcl-xL (54H6) rabbit monoclonal Ab (mAb), Ki-67(8D5) mouse mAb, p21Waf1/Cip1(12D1) rabbit mAb, p16INK4A rabbit polyclonal Ab (pAb), p53(1C12) mouse mAb and phospho-Histone H3(Ser10) Alexa 488 rabbit pAb obtained from Cell Signaling Technology Inc. (Beverly, MA). Phospho-histone H3(Ser10) rabbit pAb, and phospho-histone H2A.X (Ser139) (JBW301) mouse mAb were purchased from EMD Millipore Corporation (Temecula, CA), β-actin (AC-15) mouse mAb was from Abcam Inc. (Cambridge, MA). The production and controls of phospho-Bcl-xL(S62) and phospho-Bcl-xL(S49) rabbit pAb specificities have been well documented, with competitive phosphorylated and unphosphorylated peptides and small interfering RNAs, by Western blotting and immunofluorescence staining (10-12). Peroxidase-labeled secondary Ab were detected by enhanced chemiluminescence with reagent set from GE Healthcare Life Science (Mississauga, ON) or SuperSignal WestPico chemiluminescence substrates from Thermo Scientific (Rockford, IL).

FISH analysis, IF microscopy and cytogenetic analysis. For FISH analysis, BJ cells were seeded and grown directly on coverslips, then hybridized with fluorophobe-labeled chromosome enumeration 6p11.1-q11 alpha satellite DNA FISH probe employing manufacturer's protocol and reagents (Abbott Molecular, Abbott Park, IL). For IF microscopy, BJ cells seeded and grown on coverslips, were fixed in methanol at -20°C for 30 min, then immersed rapidly in ice-cold acetone for a few seconds. The slides were allowed to dry at room temperature and rehydrated in PBS. Nonspecific binding sites were blocked in PBS containing 5% FBS (blocking solution); then, the slides were incubated sequentially with specific primary Ab (10 μg/ml in blocking solution) and specific labeled secondary Ab (10 μg/ml in blocking solution; Alexa-594 Fluor goat anti-mouse or goat anti-rabbit from Invitrogen Corp.), followed by 4′,6-diamidino-2-phenylindole (DAPI) staining, also in blocking solution.

For dual FISH/IF-labeling, FISH was performed prior to IF staining. Images were generated with a Nikon microsystem mounted on a Nikon Eclipse E600 microscope with a photometric Cool-Snap HQ2 camera and Nikon NIS-Elements software 9 (v 3.8AR) and with a Zeiss Axio Observer Z1 automated microscope and Axiovision software (v4.8.2). Images were analysed by Image J software (v1.49), a Java-based processing

program developed by the National Institutes of Health (USA). Metaphase preparation, G-banding techniques and cytogenetic analysis were performed according to standard cytogenetic procedures. Clonal chromosomal abnormalities were reported according to the recommendations of the International System for Human Cytogenetic Nomenclature (2013). Statistical analyses (student's t test) were conducted with Prism GraphPad software (v 5.0d**).**

3.6 Disclosure of conflicts of interest

The authors declare that they have no potential conflicts of interest

3.7 Acknowledgements

This work was funded by Grant MOP-97913 from the Canadian Institutes of Health Research and Grant 328207 from the Natural Sciences and Engineering Research Council of Canada to R.B, and a grant from the Cancer Research Network of Fonds de recherche du Québec- Santé to J.H. P.S.B. received scholarships from the Faculté des études supérieures (Université de Montréal, Canada) and the Fondation de l'Institut du cancer de Montréal (Canada). The authors thank Guillaume Chouinard (CRCHUM, Canada) for valuable help with image analysis and Sylvie Lavallée (Quebec Leukemia Cell Bank, Hôpital Maisonneuve-Rosemont, Canada) for karyotype preparation. This manuscript was edited by Ovid Da Silva.

Table 1 Chromosomal aberrations in control BJ cells and BJ cells expressing Bcl-xL (wt) and Bcl-xL phosphorylation mutants at various cell population doublings

Cell population doubling	Karyotypes
BJ control (PD 43.3)	46,XY[22]
BJ control (PD 70.1)	46,XY[10]
pLenti (PD 53.7)	46,XY[22]
Bcl-xL wt (PD 52.0)	46,XY[22]
Bcl-xL S49A (PD 42.4)	46,XY[18]
Bcl-xL S49A (PD 53.6)	46,XY[20]
Bcl-xL S62A (PD 39.2)	46,XY,t(6;7)(q21;q32)[3]/46, XY[17]
Bcl-xL S62A (PD 55.3)	46,XY,add(16)p13.1[9]/48,XY,+2mar[2]/46,XY[10]
Bcl-xL S49/62A (PD 39.0)	46,XY[22]
Bcl-xL S49/62A (PD 52.1)	46,XY[7]
Bcl-xL S49D (PD 37.1)	46,XY,add(16)q2?2)[4]/46,XY[12]
Bcl-xL S49D (PD 54.1)	46,XY,i(18)(q10)[3]/46,XY[18]
Bcl-xL S62D (PD 40.1)	46,XY[22]
Bcl-xL S62D (PD 52.5)	46,XY,t(4:5)(p16:q15)[9]/47,XY,+7[3]/46,XY[5]
Bcl-xL S49/62D (PD 50.1)	46,XY[12]

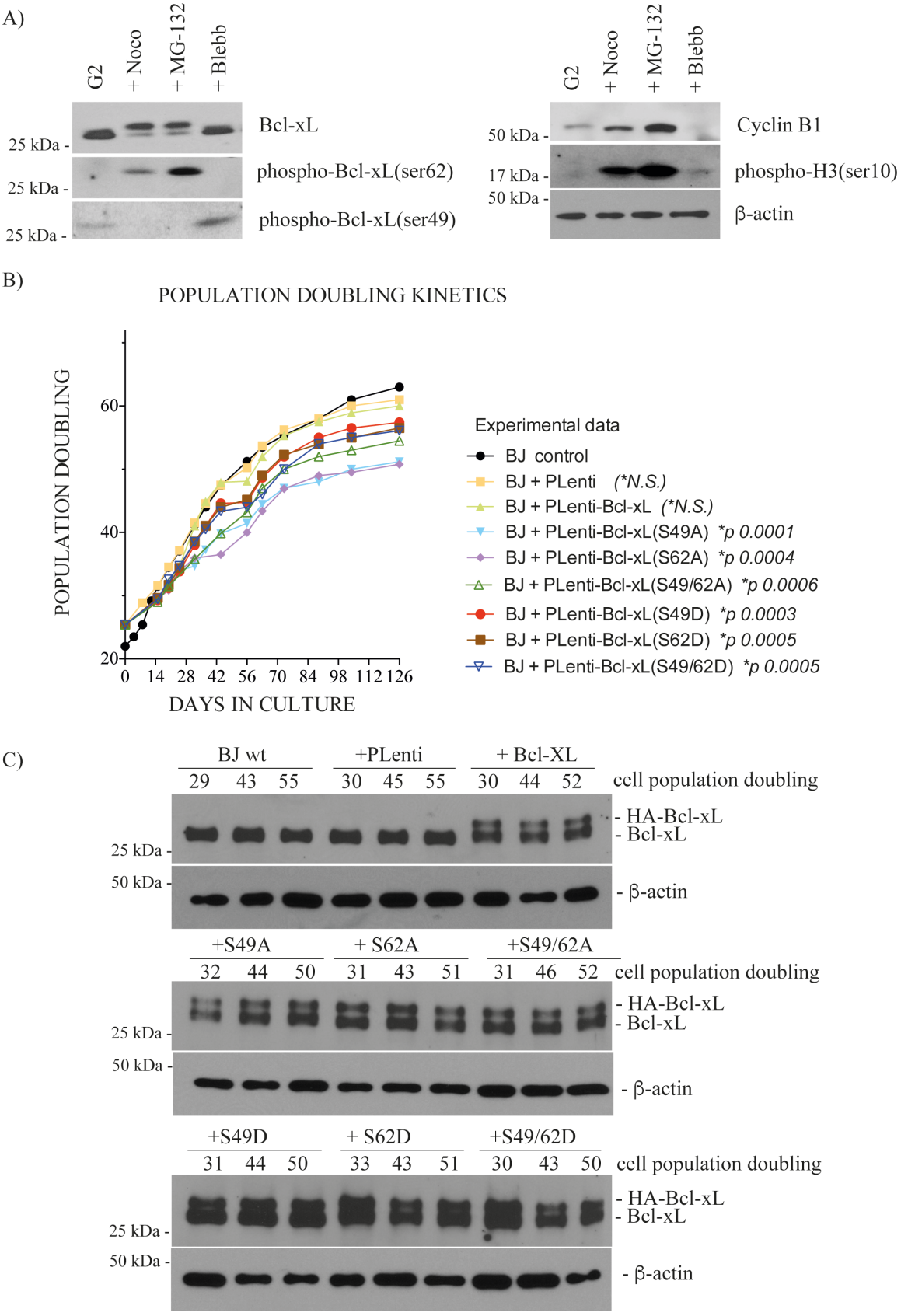
A)
G2
+ Noco
+ MG-132
+ Blebb
25 kDa -
Bcl-xL
25 kDa -
phospho-Bcl-xL(ser62)
25 kDa -
phospho-Bcl-xL(ser49)
50 kDa -
Cyclin B1
17 kDa -
phospho-H3(ser10)
50 kDa -
β-actin
B)
POPULATION DOUBLING KINETICS
POPULATION DOUBLING
60
40
20
0 14 28 42 56 70 84 98 112 126
DAYS IN CULTURE
Experimental data
BJ control
BJ + PLenti (*N.S.)
BJ + PLenti-Bcl-xL (*N.S.)
BJ + PLenti-Bcl-xL(S49A) *p 0.0001
BJ + PLenti-Bcl-xL(S62A) *p 0.0004
BJ + PLenti-Bcl-xL(S49/62A) *p 0.0006
BJ + PLenti-Bcl-xL(S49D) *p 0.0003
BJ + PLenti-Bcl-xL(S62D) *p 0.0005
BJ + PLenti-Bcl-xL(S49/62D) *p 0.0005
C)
BJ wt
29 43 55
+PLenti
30 45 55
+ Bcl-XL
30 44 52
cell population doubling
- HA-Bcl-xL
- Bcl-xL
25 kDa -
50 kDa -
- β-actin
+S49A
32 44 50
+ S62A
31 43 51
+S49/62A
31 46 52
cell population doubling
- HA-Bcl-xL
- Bcl-xL
25 kDa -
50 kDa -
- β-actin
+S49D
31 44 50
+ S62D
33 43 51
+S49/62D
30 43 50
cell population doubling
- HA-Bcl-xL
- Bcl-xL
25 kDa -
50 kDa -
- β-actin

Figure 1 Effect of Bcl-xL and Bcl-xL phosphorylation mutant expression on cell population doubling of BJ cells. (**A**) Kinetics of Bcl-xL, phospho-Bcl-xL(S49), phospho-Bcl-xL(S62), cyclinB1 and phospho-H3(S10) expression in control BJ cells at different steps of mitosis; β-actin expression is shown as control. SDS-PAGE was run on 9-18% gradient gels. (**B**) Population doubling kinetics of control BJ cells and BJ cells expressing empty lentivirus vector or lentivirus vectors encoding HA-Bcl-xL(wt), (S49A), (S49D), (S62A), (S62D) or dual (S49/62A) and (S49/62D) phosphorylation mutants. **(C)** Expression kinetics of endogenous Bcl-xL, HA-Bcl-xL(wt) and various phosphorylation mutants at various cell population doublings; β-actin expression is shown as control. SDS-PAGE was run on 9-18% gradient gels.

A)

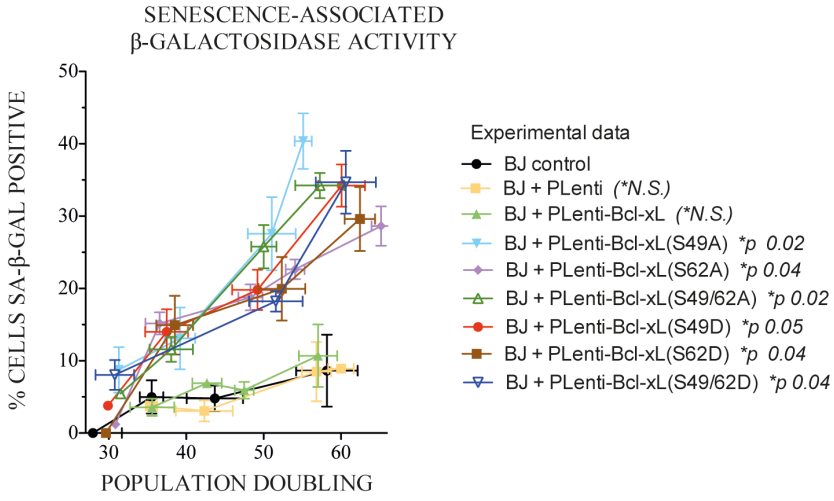
SENESCENCE-ASSOCIATED
β-GALACTOSIDASE ACTIVITY
% CELLS SA-β-GAL POSITIVE
POPULATION DOUBLING
Experimental data
BJ control
BJ + PLenti (*N.S.)
BJ + PLenti-Bcl-xL (*N.S.)
BJ + PLenti-Bcl-xL(S49A) *p 0.02
BJ + PLenti-Bcl-xL(S62A) *p 0.04
BJ + PLenti-Bcl-xL(S49/62A) *p 0.02
BJ + PLenti-Bcl-xL(S49D) *p 0.05
BJ + PLenti-Bcl-xL(S62D) *p 0.04
BJ + PLenti-Bcl-xL(S49/62D) *p 0.04

B)

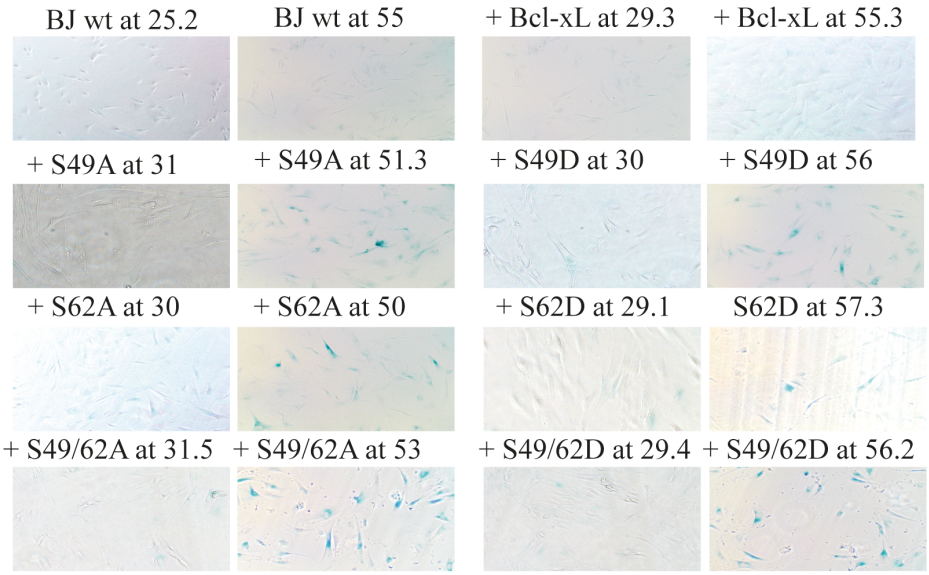
BJ wt at 25.2
BJ wt at 55
+ Bcl-xL at 29.3
+ Bcl-xL at 55.3
+ S49A at 31
+ S49A at 51.3
+ S49D at 30
+ S49D at 56
+ S62A at 30
+ S62A at 50
+ S62D at 29.1
S62D at 57.3
+ S49/62A at 31.5
+ S49/62A at 53
+ S49/62D at 29.4
+ S49/62D at 56.2

C)

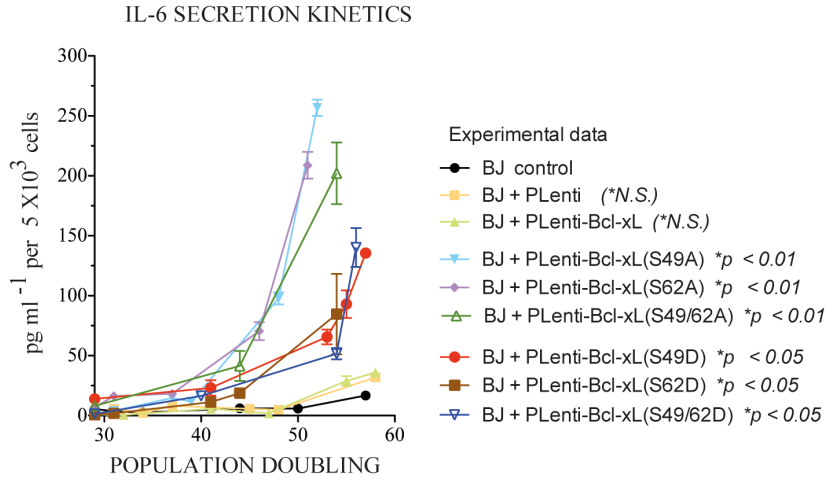
IL-6 SECRETION KINETICS
pg ml-1 per 5 X10^3 cells
POPULATION DOUBLING
Experimental data
BJ control
BJ + PLenti (*N.S.)
BJ + PLenti-Bcl-xL (*N.S.)
BJ + PLenti-Bcl-xL(S49A) *p < 0.01
BJ + PLenti-Bcl-xL(S62A) *p < 0.01
BJ + PLenti-Bcl-xL(S49/62A) *p < 0.01
BJ + PLenti-Bcl-xL(S49D) *p < 0.05
BJ + PLenti-Bcl-xL(S62D) *p < 0.05
BJ + PLenti-Bcl-xL(S49/62D) *p < 0.05

Figure 2 Effect of Bcl-xL and Bcl-xL phosphorylation mutant expression on outbreak of senescence in BJ cells. (**A**) Kinetics of senescence-associated β-galactosidase activity in control BJ cells and BJ cells expressing empty lentivirus vector or lentivirus vectors encoding HA-Bcl-xL(wt), (S49A), (S49D), (S62A), (S62D) or dual (S49/62A) and (S49/62D) phosphorylation mutants at various cell population doublings. The data from 3 independent experiments**. (B)** Typical micrographs of senescence-associated β-galactosidase activity in various cell populations. (**C**) Kinetics of IL-6 secretion from control BJ cells and BJ cells expressing empty lentivirus vector or lentivirus vectors encoding HA-Bcl-xL(wt), (S49A), (S49D), (S62A), (S62D) or dual (S49/62A) and (S49/62D) phosphorylation mutants at various cell population doublings (*n*: 4)**.**

A)

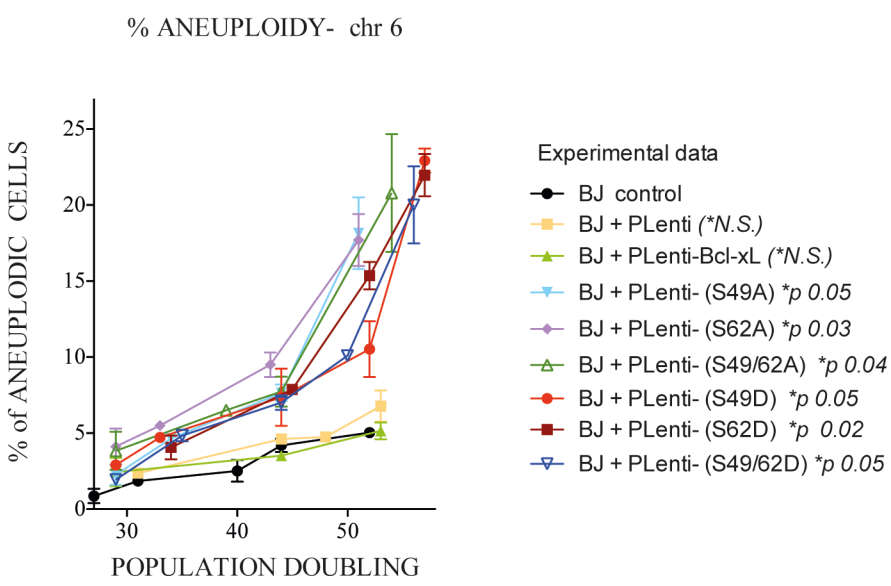
% ANEUPLOIDY- chr 6
% of ANEUPLODIC CELLS
25
20
15
10
5
0
30
40
50
POPULATION DOUBLING
Experimental data
BJ control
BJ + PLenti (*N.S.)
BJ + PLenti-Bcl-xL (*N.S.)
BJ + PLenti- (S49A) *p 0.05
BJ + PLenti- (S62A) *p 0.03
BJ + PLenti- (S49/62A) *p 0.04
BJ + PLenti- (S49D) *p 0.05
BJ + PLenti- (S62D) *p 0.02
BJ + PLenti- (S49/62D) *p 0.05

B)

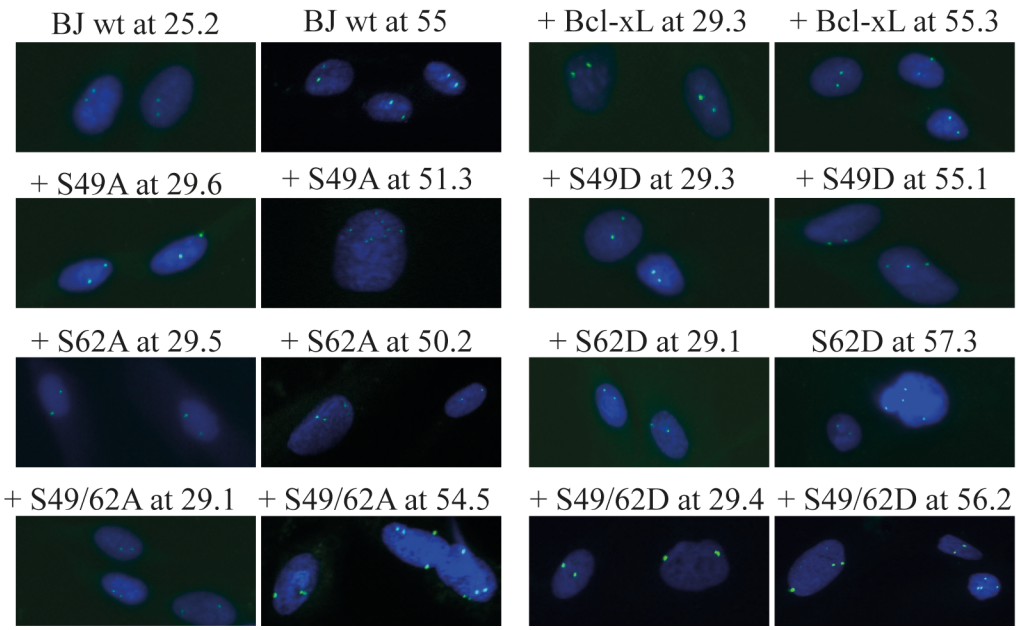
BJ wt at 25.2
BJ wt at 55
+ Bcl-xL at 29.3
+ Bcl-xL at 55.3
+ S49A at 29.6
+ S49A at 51.3
+ S49D at 29.3
+ S49D at 55.1
+ S62A at 29.5
+ S62A at 50.2
+ S62D at 29.1
S62D at 57.3
+ S49/62A at 29.1
+ S49/62A at 54.5
+ S49/62D at 29.4
+ S49/62D at 56.2

Figure 3 Effect of Bcl-xL and Bcl-xL phosphorylation mutant expression on chromosome stability and aneuploidy in BJ cells. (**A**) % of aneuploid kinetics in interphasic control BJ cells and BJ cells expressing empty lentivirus vector or lentivirus vectors encoding HA-Bcl-xL(wt), (S49A), (S49D), (S62A), (S62D) or dual (S49/62A) and (S49/62D) phosphorylation mutants at various cell population doublings. Total number of cells analysed: 2,639 (wt), 1,718 (S49A), 2,168 (S49D), 2,914 (S62A), 2,096 (S62D), 2,194 (S49/62A) and 2,333 (S49/62D)**.** Micrographs from 3 to 5 independent experiments. **(B)** Typical micrographs of FISH-labeling with a fluorophobe-labeled 6p11.1-q11 alpha satellite DNA probe. G-banding karyotypes are liste in Table 1.

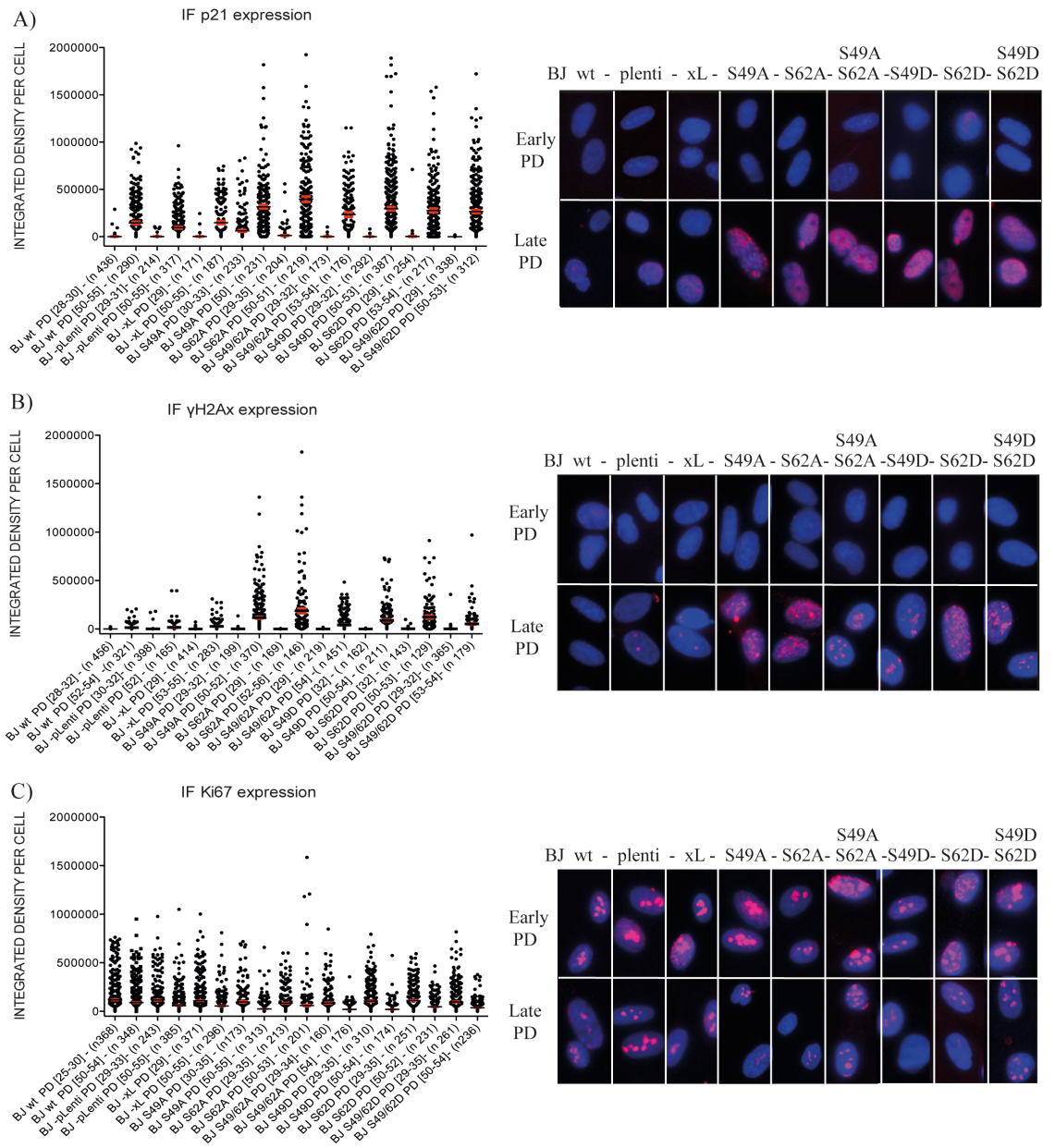

* E, early population doubling (29 to 32); M, middle population doubling (40 to 45); L, late population doubling (50 to 55).

Figure 4 Effect of Bcl-xL and Bcl-xL phosphorylation mutant expression on senescence-associated biomarkers in BJ cells. IF-revealed expression level of **(A)** p21Waf1/Cip1, **(B)** γH2A.X, and **(C)** Ki-67 in early *versus* late population doubling of control BJ cells and BJ cells expressing empty lentivirus vector or lentivirus vectors encoding Bcl-xL(wt) and various Bcl-xL phosphorylation mutants. Left panels, X axis*:* The BJ cell population is indicated with population doubling range (DP [range]) and the numbers of individual cells analysed and represented in the histographs (*n*). Data were collected from a multitude of independent micrographs. Right panels*:* Typical micrographs showing all cell populations at early (29 to 32) and late (50 to 55) population doubling. (**D**) Expression kinetics of Bcl-xL, HA-Bcl-xL (and phosphorylation mutants), p53 and p21Waf1/Cip1 in the control BJ cell population and BJ cells expressing empty lentivirus vector or lentivirus vectors encoding Bcl-xL(wt) and the various Bcl-xL phosphorylation mutants at early (29 to 32), middle (40 to 45) and late (50 to 55) population doublings, revealed by Western blotting; β-actin expression is shown as control. SDS-PAGE was run on 9-18% gradient gels.

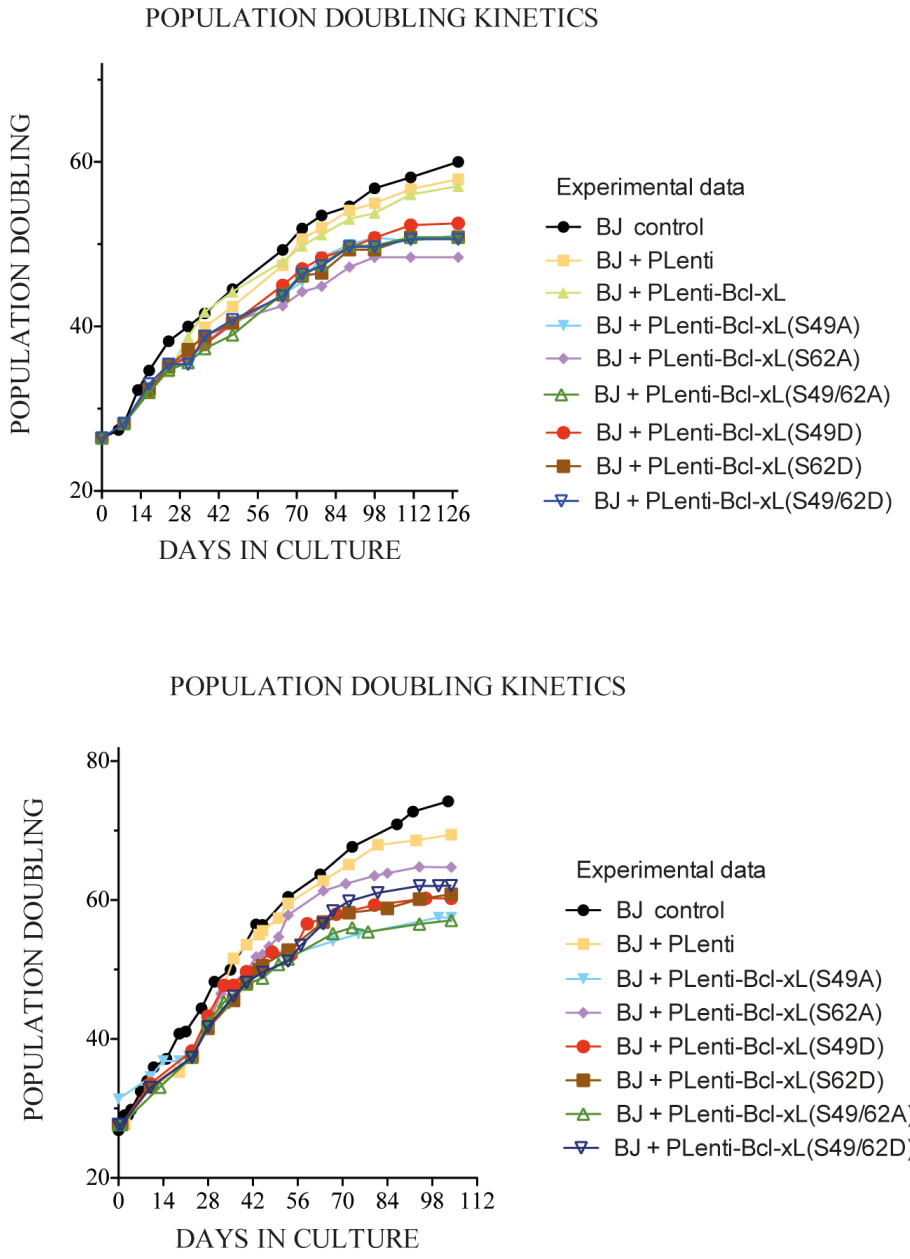

Figure S-1 Kinetics of cell population doubling of control BJ cells and BJ cells expressing empty lentivirus vector or lentivirus vectors encoding HA-Bcl-xL(wt), (S49A), (S49D), (S62A), (S62D) or dual (S49/62A) and (S49/62D) phosphorylation mutants. Two independents experiments are reported.

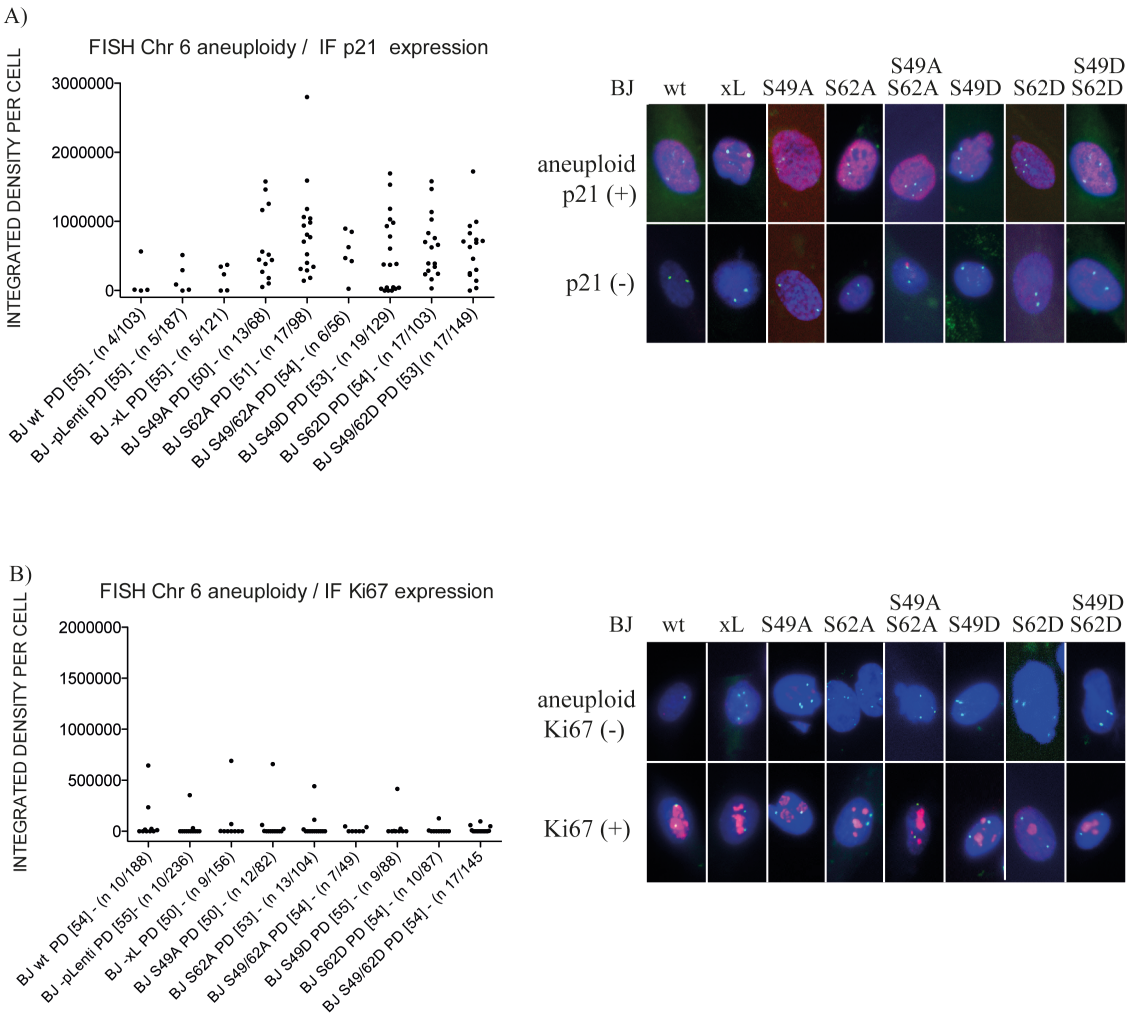

Figure S-2 Correlation between aneuploidy and senescence-associated biomarkers in control BJ cells and BJ cells expressing Bcl-xL(wt) and Bcl-xL phosphorylation mutants. IF-revealed expression of **(A)** p21Waf1/Cip1 and **(B)** Ki-67 in late population doubling of control BJ cells and BJ cells expressing Bcl-xL(wt) or various Bcl-xL phosphorylation mutants harbouring aneuploidy on chromosome 6. Left panels X axis: The BJ cell population is indicated with population doubling number (DP [range]) and numbers of individual aneuploid cells detected over total number of cells observed (n). Right panels: Typical micrographs of aneuploid cells (upper panels). Controls are shown in lower panels.

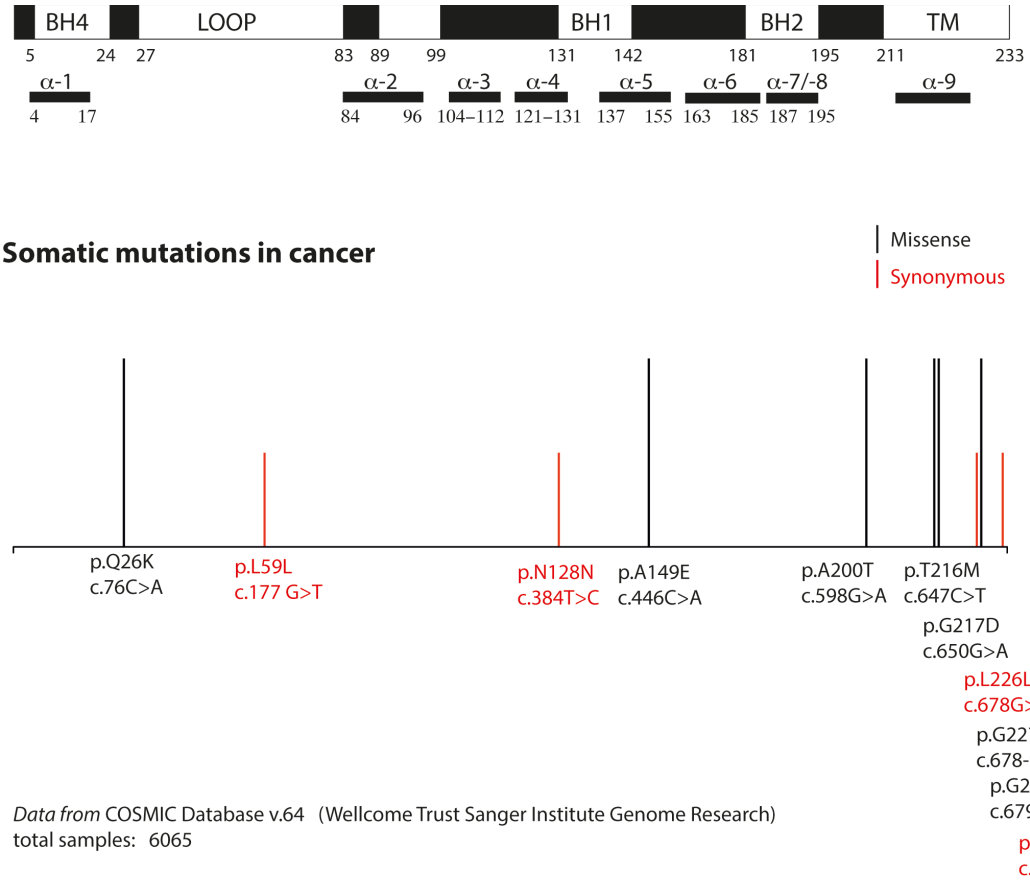

Figure S-3 Bcl-xL somatic mutations found in human tumors and short genetic variations.

3.8 Bibliography

1. Boise LH, Gonzalez-Garcia M, Postema CE, Ding L, Lindsten T, Turka LA, et al. Bcl-x, a bcl-2-related gene that functions as a dominant regulator of apoptotic cell death. Cell. 1993;74:597-608.
2. Reed JC. Bcl-2 and the regulation of programmed cell death. J Cell Biol. 1994;124:1-6.
3. Berman SB, Chen YB, Qi B, McCaffery JM, Rucker EB, 3rd, Goebbels S, et al. Bcl-x L increases mitochondrial fission, fusion, and biomass in neurons. J Cell Biol. 2009;184:707-19.
4. Li H, Alavian KN, Lazrove E, Mehta N, Jones A, Zhang P, et al. A Bcl-xL-Drp1 complex regulates synaptic vesicle membrane dynamics during endocytosis. Nat Cell Biol. 2013;15:773-85.
5. Borner C. Diminished cell proliferation associated with the death-protective activity of Bcl-2. J Biol Chem. 1996;271:12695-8.
6. Huang DCS, Oreilly LA, Strasser A, Cory S. The anti-apoptosis function of Bcl-2 can be genetically separated from its inhibitory effect on cell cycle entry. EMBO J. 1997;16:4628-38.
7. Fujise K, Zhang D, Liu J, Yeh ET. Regulation of apoptosis and cell cycle progression by Mcl1. Differential role of proliferating cell nuclear antigen. J Biol Chem. 2000;275:39458-65.
8. Janumyan YM, Sansam CG, Chattopadhyay A, Cheng N, Soucie EL, Penn LZ, et al. Bcl-xL/Bcl-2 coordinately regulates apoptosis, cell cycle arrest and cell cycle entry. EMBO J. 2003;22:5459-70.
9. Schmitt E, Beauchemin M, Bertrand R. Nuclear co-localization and interaction between Bcl-xL and Cdk1(cdc2) during G2/M cell cycle checkpoint. Oncogene. 2007;26:5851-65.
10. Wang J, Beauchemin M, Bertrand R. Bcl-xL phosphorylation at Ser49 by polo kinase 3 during cell cycle progression and checkpoints. Cell Signal. 2011;23:2030-38.
11. Wang J, Beauchemin M, Bertrand R. Phospho-Bcl-xL(ser62) plays a key role at DNA damage-induced G2 checkpoint. Cell Cycle. 2012;11:2159-69.
12. Wang J, Beauchemin M, Bertrand R. Phospho-Bcl-xL(Ser62) influences spindle assembly and chromosome segregation during mitosis. Cell Cycle. 2014;13:1313-26.
13. Fang W, Mueller DL, Pennell CA, Rivard JJ, Li YS, Hardy RR, et al. Frequent aberrant immunoglobulin gene rearrangements in pro-B cells revealed by a Bcl-X(L) transgene. Immunity. 1996;4:291-9.
14. Saintigny Y, Dumay A, Lambert S, Lopez BS. A novel role for the Bcl-2 protein family: specific suppression of the RAD51 recombination pathway. EMBO J. 2001;20:2596-607.
15. Wiese C, Pierce AJ, Gauny SS, Jasin M, Kronenberg A. Gene conversion is strongly induced in human cells by double-strand breaks and is modulated by the expression of Bcl-x(L). Cancer Res. 2002;62:1279-83.
16. Dumay A, Laulier C, Bertrand P, Saintigny Y, Lebrun F, Vayssiere JL, et al. Bax and Bid, two proapoptotic Bcl-2 family members, inhibit homologous recombination, independently of apoptosis regulation. Oncogene. 2006;25:3196-205.
17. Wang Q, Gao F, May WS, Zhang Y, Flagg T, Deng X. Bcl-2 negatively regulates DNA double-strand-break repair through a nonhomologous end-joining pathway. Mol Cell. 2008;29:488-98.

18. Poruchynsky MS, Wang EE, Rudin CM, Blagosklonny MV, Fojo T. Bcl-X(L) is phosphorylated in malignant cells following microtubule disruption. Cancer Res. 1998;58:3331-8.
19. Fan M, Goodwin M, Vu T, Brantley-Finley C, Gaarde WA, Chambers TC. Vinblastine-induced phosphorylation of Bcl-2 and Bcl-XL is mediated by JNK and occurs in parallel with inactivation of the Raf-1/MEK/ERK cascade. J Biol Chem. 2000;275:29980-5.
20. Basu A, Haldar S. Identification of a novel Bcl-xL phosphorylation site regulating the sensitivity of taxol- or 2-methoxyestradiol-induced apoptosis. FEBS Lett. 2003;538:41-7.
21. Chang BS, Minn AJ, Muchmore SW, Fesik SW, Thompson CB. Identification of a novel regulatory domain in Bcl-X(L) and Bcl-2. EMBO J. 1997;16:968-77.
22. Burri SH, Kim CN, Fang GF, Chang BS, Perkins C, Harris W, et al. 'Loop' domain deletional mutant of Bcl-xL is as effective as p29Bcl-xL in inhibiting radiation-induced cytosolic accumulation of cytochrome C (cyt c), caspase-3 activity, and apoptosis. International journal of radiation oncology, biology, physics. 1999;43:423-30.
23. Muchmore SW, Sattler M, Liang H, Meadows RP, Harlan JE, Yoon HS, et al. X-ray and NMR structure of human Bcl-xL, an inhibitor of programmed cell death. Nature. 1996;381:335-41.
24. Sattler M, Liang H, Nettesheim D, Meadows RP, Harlan JE, Eberstadt M, et al. Structure of Bcl-x(L)-Bak peptide complex: recognition between regulators of apoptosis. Science. 1997;275:983-6.
25. Diaz JL, Oltersdorf T, Horne W, McConnell M, Wilson G, Weeks S, et al. A common binding site mediates heterodimerization and homodimerization of Bcl-2 family members. J Biol Chem. 1997;272:11350-5.
26. Sedlak TW, Oltvai ZN, Yang E, Wang K, Boise LH, Thompson CB, et al. Multiple Bcl-2 family members demonstrate selective dimerizations with Bax. Proc Natl Acad Sci USA. 1995;92:7834-8.
27. Cheng EH-YA, Wei MC, Weiler S, Flavell RA, Mak TW, Lindsten T, et al. Bcl-2, bcl-x(l) sequester BH3 domain-only molecules preventing bax- and bak-mediated mitochondrial apoptosis. Mol Cell. 2001;8:705-11.
28. Letai A, Bassik M, Walensky L, Sorcinelli M, Weiler S, Korsmeyer S. Distinct BH3 domains either sensitize or activate mitochondrial apoptosis, serving as prototype cancer therapeutics. Cancer cell. 2002;2:183-92.
29. Morales CP, Holt SE, Ouellette M, Kaur KJ, Yan Y, Wilson KS, et al. Absence of cancer-associated changes in human fibroblasts immortalized with telomerase. Nat Genet. 1999;21:115-8.
30. Dimri GP, Lee X, Basile G, Acosta M, Scott G, Roskelly C, et al. A biomarker that identifies senescent human cells in culture and in aging skin in vitro. Proc Natl Acad Sci (USA). 1995;92:9363-7.
31. Rodier F, Coppe JP, Patil CK, Hoeijmakers WA, Munoz DP, Raza SR, et al. Persistent DNA damage signalling triggers senescence-associated inflammatory cytokine secretion. Nat Cell Biol. 2009;11:973-9.
32. Rodier F, Munoz DP, Teachenor R, Chu V, Le O, Bhaumik D, et al. DNA-SCARS: distinct nuclear structures that sustain damage-induced senescence growth arrest and inflammatory cytokine secretion. J Cell Sci. 2011;124:68-81.
33. Wong H, Riabowol K. Differential CDK-inhibitor gene expression in aging human diploid fibroblasts. Experimental gerontology. 1996;31:311-25.

34. Campisi J. Cellular senescence as a tumor-suppressor mechanism. Trends Cell Biol. 2001;11:S27-31.
35. Krajewska M, Moss SF, Krajewski S, Song K, Holt PR, Reed JC. Elevated expression of Bcl-X and reduced Bak in primary colorectal adenocarcinomas. Cancer Res. 1996;56:2422-7.
36. Watanabe J, Kushihata F, Honda K, Sugita A, Tateishi N, Mominoki K, et al. Prognostic significance of Bcl-xL in human hepatocellular carcinoma. Surgery. 2004;135:604-12.
37. Sharma J, Srinivasan R, Majumdar S, Mir S, Radotra BD, Wig JD. Bcl-XL protein levels determine apoptotic index in pancreatic carcinoma. Pancreas. 2005;30:337-42.
38. Williams J, Lucas PC, Griffith KA, Choi M, Fogoros S, Hu YY, et al. Expression of Bcl-xL in ovarian carcinoma is associated with chemoresistance and recurrent disease. Gynecologic oncology. 2005;96:287-95.
39. Karczmarek-Borowska B, Filip A, Wojcierowski J, Smolen A, Korobowicz E, Korszen-Pilecka I, et al. Estimation of prognostic value of Bcl-xL gene expression in non-small cell lung cancer. Lung cancer (Amsterdam, Netherlands). 2006;51:61-9.
40. Jin-Song Y, Zhao-Xia W, Cheng-Yu L, Xiao-Di L, Ming S, Yuan-Yuan G, et al. Prognostic significance of Bcl-xL gene expression in human colorectal cancer. Acta histochemica. 2011;113:810-4.
41. Mallick S, Agarwal J, Kannan S, Pawar S, Kane S, Teni T. Bcl-xL protein: predictor of complete tumor response in patients with oral cancer treated with curative radiotherapy. Head & neck. 2013;35:1448-53.
42. Juin P, Geneste O, Gautier F, Depil S, Campone M. Decoding and unlocking the BCL-2 dependency of cancer cells. Nat Rev Cancer. 2013;13:455-65.
43. Zitouni S, Nabais C, Jana SC, Guerrero A, Bettencourt-Dias M. Polo-like kinases: structural variations lead to multiple functions. Nat Rev Mol Cell Biol. 2014;15:433-52.
44. Helmke C, Becker S, Strebhardt K. The role of Plk3 in oncogenesis. Oncogene. 2016;35:135-47.
45. Kumar S, Kim J. PLK-1 targeted inhibitors and their potential against tumorigenesis. BioMed research international. 2015;2015:705745.
46. Liu X. Targeting Polo-like kinases: A promising therapeutic approach for cancer treatment. Translational oncology. 2015;8:185-95.
47. Talati C, Griffiths EA, Wetzler M, Wang ES. Polo-like kinase inhibitors in hematologic malignancies. Critical reviews in oncology/hematology. 2016;98:200-10.
48. Baker DJ, Jeganathan KB, Cameron JD, Thompson M, Juneja S, Kopecka A, et al. BubR1 insufficiency causes early onset of aging-associated phenotypes and infertility in mice. Nat Genet. 2004;36:744-9.
49. Baker DJ, Perez-Terzic C, Jin F, Pitel KS, Niederlander NJ, Jeganathan K, et al. Opposing roles for p16Ink4a and p19Arf in senescence and ageing caused by BubR1 insufficiency. Nat Cell Biol. 2008;10:825-36.
50. Schliekelman M, Cowley DO, O'Quinn R, Oliver TG, Lu L, Salmon ED, et al. Impaired Bub1 function in vivo compromises tension-dependent checkpoint function leading to aneuploidy and tumorigenesis. Cancer Res. 2009;69:45-54.
51. Glotzer M. The molecular requirements for cytokinesis. Science. 2005;307:1735-9.
52. Degterev A, Lugovskoy A, Cardone M, Mulley B, Wagner G, Mitchison T, et al. Identification of small-molecule inhibitors of interaction between the BH3 domain and Bcl-xL. Nat Cell Biol. 2001;3:173-82.

53. Qian J, Voorbach MJ, Huth JR, Coen ML, Zhang H, Ng SC, et al. Discovery of novel inhibitors of Bcl-xL using multiple high-throughput screening platforms. Anal Biochem. 2004;328:131-8.
54. Oltersdorf T, Elmore SW, Shoemaker AR, Armstrong RC, Augeri DJ, Belli BA, et al. An inhibitor of Bcl-2 family proteins induces regression of solid tumours. Nature. 2005;435:677-81.
55. Yamaguchi R, Janssen E, Perkins G, Ellisman M, Kitada S, Reed JC. Efficient elimination of cancer cells by deoxyglucose-ABT-263/737 combination therapy. PLoS One. 2011;6:e24102.
56. Souers AJ, Leverson JD, Boghaert ER, Ackler SL, Catron ND, Chen J, et al. ABT-199, a potent and selective BCL-2 inhibitor, achieves antitumor activity while sparing platelets. Nature medicine. 2013;19:202-8.
57. Tao ZF, Hasvold L, Wang L, Wang X, Petros AM, Park CH, et al. Discovery of a potent and selective Bcl-XL inhibitor with in vivo activity. ACS medicinal chemistry letters. 2014;5:1088-93.

4 Expression of human Bcl-xL (Ser49) and (Ser62) mutants in *Caenorhabditis elegans* causes germline defects and aneuploidy

Baruah PS[1,2], Beauchemin M[1,2], Parker JA[1,3], Bertrand R[1,2,4]

[1]Centre de recherche, Centre hospitalier de l'Université de Montréal (CRCHUM), [2]Institut du cancer de Montréal, [3]Département de neurosciences and [4]Département de médecine, Université de Montréal, Montréal (Québec) Canada

Running title: Bcl-xL expression in *C. elegans*

Corresponding author: Richard Bertrand, CRCHUM, 900 rue St-Denis (Room R10.424), Montréal (Québec) Canada H2X 0A9.
Telephone: +1-514-890-8000 Extension 26615
Fax: +1-514-412-7938

4.1 Summary

An interesting feature of Bcl-xL protein is the presence of an unstructured loop domain between α1 and α2 helices, a domain not essential for its anti-apoptotic function and absent in CED-9 protein. Within this domain, Bcl-xL undergoes dynamic phosphorylation and de-phosphorylation at Ser49 and Ser62 during G2 and mitosis in human cells. Studies have revealed that when these residues are mutated, cells harbour mitotic defects, including chromosome mis-attachment, lagging, bridging and mis-segregation with, ultimately, chromosome instability and aneuploidy. We undertook experiments in *Caenorhabditis elegans* to understand the importance of Bcl-xL (Ser49) and (Ser62) *in-vivo*. Transgenic worms carrying single-site S49A, S62A, S49D, S62D and dual site S49/62A mutants were generated and their effects were analyzed in germlines of young adult worms. Worms expressing Bcl-xL variants showed decreased egg-laying and hatching, variations in the length of their mitotic regions and transition zones, appearance of chromosomal abnormalities at their diplotene stages, and increased germline apoptosis. Some of these transgenic strains, particularly the Ser to Ala variants, also showed slight modulations of lifespan compared to their controls. Our *in vivo* observations confirmed the importance of Ser49 and Ser62 within the loop domain of Bcl-xL in maintaining chromosome stability.

4.2 Introduction

Core components of the cell death machinery, identified by genetic and biochemical studies, are well-conserved across eukaryotes, from nematodes to mammals. First identified in *Caenorhabditis elegans* (*C. elegans*), *ced-9* is required to protect healthy cells from apoptosis[1]. Initially reported at t(14;18) chromosomal translocation in follicular lymphomas[2], human *BCL2* gene, was latter ascertained to be an ortholog of *ced-9*, whose expression plays a key role in controlling cell death[3]. *BCL2* is the founding member of a large family of genes and proteins, now referred to as the Bcl-2 family[4,5]. Transient expression of human Bcl-2 in *ced-9* loss-of-function *C. elegans,* reduces cell death during nematode development and interacts with the cell death machinery of the worms, revealing the highly-conserved structure and function of these proteins among various species[6,7]. Indeed, anti-apoptotic proteins, e.g., mammalian Bcl-2, Bcl-xL [8] and *C. elegans* CED-9 share structural homology in terms of their Bcl-2 homology (BH) domains that control their apoptosis-regulating functions[9,10]. However, Bcl-2 and Bcl-xL proteins contain an additional domain, an unstructured loop domain between α1 and α2 helices, a protein domain that is not essential for their anti-apoptotic functions and absent in CED-9 protein[11-15].

Studies have revealed that 2 serine residues within the unstructured loop domain of human Bcl-xL, Ser49 and Ser62, are subjected to cell cycle-dependent, dynamic phosphorylation when cells are subjected to various stresses, but also during normal cell cycle progression[16-22]. Bcl-xL undergoes cell cycle-dependent phosphorylation on Ser49, and accumulates in centrosomes in G2 phase, particularly during DNA single- and double-strand break-mediated G2 arrest[20]. Bcl-xL(Ser49) is rapidly dephosphorylated in early mitotic phases and is re-phosphorylated during telophase/cytokinesis by Polo kinase 3 (Plk3).

Phospho-Bcl-xL(S49) is found in conjunction with microtubule-associated dynein motor proteins and in mid-zone bodies during telephase/cytokinesis[20]. Bcl-xL is also phosphorylated at Ser62 by Plk1 and mitogen-activated protein kinase 9/c-jun N-terminal kinase 2 (Mapk9/Jnk2) during normal cell cycle progression at G2 and after DNA damage[21]. At G2, phospho-Bcl-xL(Ser62) accumulates in nucleolar structures including nucleoli and Cajal bodies and co-localizes with cyclin-dependent kinase 1 (Cdk1)[21].

During mitosis, Bcl-xL(Ser62) is strongly phosphorylated by Plk1 and Mapk14/stress-activated protein kinase p38α in prophase, prometaphase, metaphase and the anaphase boundary, while it is dephosphorylated in telophase and cytokinesis[22]. At mitosis, phospho-Bcl-xL(Ser62) localizes in centrosomes with γ-tubulin, and in the mitotic cytosol with some spindle-assembly checkpoint (SAC) signalling proteins, including Plk1 and the Mad2-, BubR1-, Bub3- and Cdc20-bound complexes[22].

In normal human fibroblasts or human tumor cells, expression of the phosphorylation mutants Bcl-xL(S49A) or (S49D), Bcl-xL(S62A) or (S62D), or dual Bcl-xL(S49/62A) or (S49/62D) has no significant effect on the apoptosis rate, but leads to mitotic defects associated with chromosome mis-attachement, lagging, bridging, mis-segregation, cytokinesis failure and aneuploidy (submitted manuscripts and [22]). These findings conferred novel functions to the protein linked with the unstructured loop domain of Bcl-xL. In the present study, to better characterize this function *in vivo*, we hypothesize that, although CED-9 lacks Bcl-xL's loop domain, introduction of Bcl-xL(Ser49) and (Ser62) mutants in *C. elegans* has dominant effects and can cause proliferating germline cell defects as well as aneuploidy.

4.3 Results

Expression of human Bcl-xL variants in *C. elegans*. Several strains of transgenic worms containing human Bcl-xL wild-type (wt) and single-site (S49A, S49D, S62A, S62D) or dual-site (S49/62A) mutants were generated (Table 1). First, 2 strains for each Bcl-xL variant were used, and N2 (wt) worms served as controls. Transgenes were confirmed by polymerase chain reaction (PCR) assays of genomic DNA (Fig. 1A), and all PCR products were sequenced for validation (data not shown). mRNA levels were then evaluated by quantitative reverse-transcriptase (q-RT)-PCR using *pmp-3* expression as referencence gene[23], and all transgenic worms expressed similar levels of *BCL-XL* variant mRNAs (Fig. 1B). *Ced-9* mRNA levels were monitored in parallel in these experiments (Fig. 1C). Overall, *BCL-XL* mRNA expression was found slightly lower compared to *ced-9* mRNA expression, with *BCL-XL* / *ced-9* ratios ranging from 0.56 to 0.88 (Fig. 1D).

Mutations within the loop domain of Bcl-xL affect *C. elegans* progeny fecundity. N2 (wt) hermaphrodites under laboratory conditions released embryos from the uterus during their development, and these eggs were easily counted. To determine whether the expression of Bcl-xL (wt) and mutants in *C. elegans* affects their egg-laying capacity, eggs were counted and compared among various transgenic strains. Synchronized L4 hermaphrodite transgenic larvae were plated individually, and eggs laid were counted over a 3-day period once they have reached adulthood (about 12 h after plating).

The transgenic strains expressing Bcl-xL (wt) showed no significant difference in egg-laying potency (Fig. 2A) and in percentage (%) of eggs that hatched (Fig. 2B) compared to N2 (wt) worms. The number of eggs laid by transgenic worms expressing Bcl-xL mutants was decreased significantly compared to Bcl-xL (wt)-expressing worms and N2 (wt) worms (Fig. 2A). When these eggs were followed, the % that hatched was significantly affected across all the mutants with a few exceptions (Bcl-xL (S62D) variant strain 311) that may reflect strain and/or animal variations. In addition, preliminary and simple chromatin staining of germlines revealed increased numbers of aberrant cells harboring condensed chromatin and/or fragmented chromatin and/or doublet cells as well as global spatial disorganization of germline alignment in the transgenic strains expressing the Bcl-xL Ser to Ala mutants, supporting these hypothesis (Supplemental Fig. S1A). Our preliminary observations were then analyzed in more detail.

Mutations within the loop domain of Bcl-xL causes germ cell aberrations in the gonads. To determine if Bcl-xL mutations at Ser49 and Ser62 affect the process of mitosis, we analyzed the germline in the transgenic worms. The *C. elegans* germline contains an anatomically-restricted mitotic cell population that persists throughout life and is thought to be self-renewing[24]. The mitotic region (MR) in the gonads showed reduced lengths in all Bcl-xL variants compared to Bcl-xL (wt)-expressing worms or N2 control worms (Fig. 3A) with the exception of Bcl-xL (S62D) variant (COP299 strain). In contrast, the transition zones (TZ) in the gonads presented no overall difference in all Bcl-xL variants compared to Bcl-xL (wt)-expressing worms or N2 control worms (Fig. 3B). Representative micrographs are reported in Figure 3C.

Mutations within the loop domain of Bcl-xL cause germ line aneuploidy. Chromosome mis-alignment, lagging or bridging, mis-segregation and cytokinesis failure

are major defects that could occur during mitosis and confer chromosome instability as well as aneuploidy[25,26]. Cells will respond in various ways including cell cycle checkpoint activation, cell cycle arrest, premature senescence or cell death and, in mammal cells, they could also enter into an immortalization or tumorigenesis path, depending on particular cellular and environmental contexts[27-29]. To evaluate the effect of the various Bcl-xL variants on chromosome stability, chromosomes were analyzed at the diplotene stage in control and transgenic worms. In N2 control and in Bcl-xL (wt) worms, 6 pairs of chromosomes were clearly visible in the diplotene stage at the end of the gonads. However, various Bcl-xL mutants, with the exception of Bcl-xL (S62D) variant, underwent aneuploidy and/or chromosome fragmentation compared to N2 control and Bcl-xL (wt) strains (Fig. 4).

Mutations within the loop domain of Bcl-xL cause increased apoptosis in the gonads. Finally, to assess apoptosis in germlines, we took advantage of a CED-1:GFP strain[30] by crossing it with our transgenic worms. CED-1, expressed in sheath cells, is a phagocytic receptor that initiates pathways for degrading engulfed apoptotic cells and is thus a good indicator apoptotic bodies[31]. With the exception of the Bcl-xL (S62D) variant, worms expressing Bcl-xL mutants showed significantly increased apoptotic bodies compared to those expressing Bcl-xL (wt) and the N2 (wt) worms (Fig. 5).

Longevity changes due to the expression of Bcl-xL mutants The *C. elegans* N2 strain has an average lifespan of around 2-3 weeks at 20°C[32]. N2 and Bcl-xL (wt) worms showed no significant differences in their lifespan (Fig. 6). Strains expressing Ser to Asp variants also presented no significant differences compared to N2 controls. In contrast, overall lifespan was significantly increased in strains expressing Ser to Ala variants (Fig. 6). This increase might be due to aneuploidy, DNA stand-breaks and apoptosis in the germline serving as nurse cell for the worms. However, the gene expression changes that may contribute to the increased lifespan of these mutants, have yet to be analyzed.

Reversion of the phenotypes Finally, to confirm that the phenotypes observed were due to the expression of Bcl-xL variants in transgenic *C. elegans,* a serie of RNA interference experiments were conducted. Silencing *BCL-XL* mRNA variant expression in the transgenic worms reversed most phenotypes, including effects on germline fecundity,

egg-laying and egg-hatching potency, mitotic region length, germline aneuploidy and apoptotic corpse appearance in the gonads (Supplemental Fig 2 A-G).

4.4 Conclusion and discussion

The loop domain between α1 and α2 helices of Bcl-xL in higher organisms may be due to gain-of-function domain through evolution. In most studies, the loop domain is not necessary for the Bcl-xL's anti-apoptotic activity in mammallian cells[11-15,20-22]. However, mutations within Bcl-xL (Ser49) and (Ser62) residues lead to chromosome instability and aneuploidy in human cells (submitted manuscripts and[22]). *C. elegans* CED-9, the only anti-apoptotic ortholog of the Bcl-2 family, does not contain the Bcl-xL loop domain. A search for sequence homology in the *National Center for Biotechnology Information* (NCBI) and *WormBase* failed to identify other putative proteins possibly containing a similar domain in *C. elegans*. The presence, or absence, of a similar conserved function within *C. elegans* protein remains to be discovered. However, PLK-1 is well conserved in *C. elegans* and involved in multiple process of mitosis, including spindle formation, kinetochore-microtubule attachments, sister chromatid separation and cytokinesis[33,34]. PLK-1 is shown to be involved in nuclear envelope breakdown in the oocyte during meiosis and in mixing maternal and paternal genomes after fertilization. Partial inactivation of PLK-1 caused failure of alignment of chromosomes at metaphase during mitosis and the nuclear membrane remains intact[35]. In contrast, PLK-3 mutations caused delay in chromosome condensation at diakinesis indicating that PLK-3 does not play a major role in meiosis[36]. PLK-1 and PLK-2 are proposed to function together *in vivo,* with PLK-1 contributing more than PLK-2 to net PLK activity[37]. In this study, Bcl-xL phosphorylation in *C. elegans* was not determined*;* however the presence of conserved PLK-1 and PLK-3 activities in *C. elegans* raises a probability of similar phosphorylation at Ser62 and Ser49 alike human cells.

Although the CED-9 protein lacks the Bcl-xL functional loop domain, we tested whether or not human Bcl-xL (Ser49) and (Ser62) variant expression in *C. elegans* exhibits dominant effects on mitotic behaviors, as observed previously in human cells. The proliferative properties of germlines of adult young worms[38], as well as the short and reproducible lifespan of *C. elegans* is well-characterized[39]. Expression of mammalian

proteins is prevalent in *C. elegans* and *viceversa* is prevalent. Expression of human Bcl-2 itself partially prevents apoptosis in *C. elegans*[7,40], whereas CED-9 expression in monkey fibroblast COS cells and embryonic drosophila Schneider's L2 cells reveals co-localization of the 2 proteins, suggesting similar functions[41].

In the present study, we observed that human Bcl-xL (Ser49) and (Ser62) variant expression in *C. elegans* interfered with germline fertility, effects that correlated with MR length variations, the appearance of chromosomal aberrations and increase apoptosis with the exception of Bcl-xL (S62D) variants. Most likely, reduced fecundity resulted from cell division errors in germlines (and embryos), resulting in chromosome aberrations, aneuploidy and augmented apoptosis. MR length variations were seen as being decreased in individual worms and strains bearing Bcl-xL variants. Perhaps defects in mitosis and elevated apoptosis could account for shortened length. All experiments were performed on proliferative germline in the gonads. In the near future, time-lapse imaging on embryos could further document mitotic behaviours and chromosome stability/instability in dividing embryos.

Lifespan modulation also has been observed in Ser to Ala variants, a possible consequence of aneuploidy, DNA damage and increased apoptosis of germlines. Indeed, repeated ultra-violet electromagnetic radiation exposure has been shown to severely reduce lifespan in *C. elegans*[42], whereas mutations in the nucleotide excision repair proteins ERCC-1 and XPF-1 extend lifespan in *daf-2* worms. Fecundity also decreased in worms expressing mutant ERCC-1, XPF-1 and XPG-1 compared to wt proteins[43]. In the long-term, it would be interesting to monitor gene expression profiles in various strains to identify genes whose expression could be altered as well.

The exact mechanisms by which Bcl-xL exerts its function on chromosome stability are unknown, but Ser49 and Ser62 are 2 essential residues associated with this activity in human cells. Previous studies have revealed the presence of phospho-Bcl-xL(Ser49) and (Ser62) in centrosomes with γ-tubulin during G2 and mitosis, respectively[20,22]. In addition, phospho-Bcl-xL(Ser62) interacts in mitotic cytosol with some SAC signaling proteins during prometaphase/metaphase, including the Mad2-, BubR1-, Bub3- and Cdc20-bound complexes[22], while phospho-Bcl-xL(Ser49) is found in mid-zone bodies during telephase/cytokinesis[20]. In *C. elegans*, most of these key players

in the SAC signaling pathway are functionally and structurally conserved, including MAD1, MAD2, MAD3/BubR1, BUB1, BUB3 and FZY-1/Cdc20[44]. Proliferating germlines have functional SAC[45], but SAC function in *C. elegans* embryos is unclear due to their lack of apparent mitotic arrest phenotype[46]. SPDL-1, a *C. elegans* homolog of kinetochore-specific dynein recruiter protein[47] that senses the microtubule attachment status of kinetochore and functions upstream of MAD1MDF-1, is part of the kinetochore receptor of the MAD1MDF-1–MAD2MDF-2 complex that regulate APC/C activity[47,48]. Whether or not, and how, human Bcl-xL interplays with these *C. elegans* components remains to be elucidated.

Bcl-xL expression in human cancers is often associated with poor prognosis and chemotherapy resistance[49-51]. Current efforts are being made to develop and test new drugs targeting the conventional BH1-, BH2-, BH3-forming hydrophobic pocket domain of Bcl-2 anti-apoptotic members including Bcl-xL[52-57]. Future perspectives should also focus on the loop domain of Bcl-xL and Bcl-2 for therapeutic evaluation. These *in vivo* transgenic strains will be an important tool to screen and evaluate the effects of future putative new compounds targeting this function.

4.5 Materials and methods

Worm-handling. Worms were manipulated according to standard methods and maintained at 15°C in nematode growth media (NGM) plates seeded with OP50 *Escherichai coli* (*E. coli*), unless otherwise indicated for specific assays.

***C. elegans* genetic manipulations and molecular assays.** Human influenza hemagglutinin (HA)-tagged Bcl-xL (wt) and single-site (S49A, S49D, S62A, S62D) or dual-site (S49/62A, S49/62D) mutant cDNAs containing the *ced-9* promoter and 3'UTR sequences were generated with the MultiSite Gateway™ recombinational cloning system (Thermo Fisher Scientific , Waltham MA), and inserted into the final destination plasmid pCFJ150-pDESTttTi5605[R4-R3] obtained from Addgene (Cambridge, MA). The strain EG4322 (ttTi5605 II; *unc-119(ced9)* III) was studied, and transgenic worms were generated by Knudra Trangenics (Murray, UT) with the mos1-mediated single copy insertion (MosSCI) method[58]. Transgenic worm insertions were tested by PCR with primers, 5'-ATGGGCCGCATCTTTTAC-3' and 5'-TCATTTCCGACTGAAGAG-3'.

All insertions were validated by DNA sequencing. Quantitative reverse transcriptase PCR (qRT-PCR) was performed on the transgenic worms with *pmp-3* as a control of constitutive gene expression[23]. The oligonucleotide primers for *pmp-3* were 5'-GTTCCCGTGTTCATCACTCAT-3' and 5'-ACACCGTCGAGATGTAGA-3'. The oligonucleotide primers for *BCL-XL* (wt) and mutants were 5'-GGTAAACTGGGGTCGCATTG-3' and 5'-GTTCTCCTGGATCCAAGGCT-3', and for *ced-9* were 5'-ACGGTTGGAAATGCACAGAC-3' and 5'-TGTTCCCAGTTGTTGCG-3'. To monitor apoptotic body formation, transgenic worms expressing CED-1:GFP in sheath cells (strain HR1459 (bcls39[lim7:ced-1:GFP;lim-15(+)]V), generously provided by Dr. Jean-Claude Labbé (Institut de recherche en immunologie et cancer, Montréal QC), were crossed with transgenic male worms expressing Bcl-xL (wt) and mutants. Homozygous progeny were screened and processed for assays. For the RNA interference (RNAi) assays, *BCL-XL* open reading frame (ORF) cDNA was cloned into the vector L4440-gateway (Addgene) and transformed into the HT115 competent bacteria, generously donated by Dr. Jean Claude Labbé. The transformed bacteria colonies were selected and PCR sequenced. The worms were grown in plates containing IPTG (1 mM) and HT115 containing L4440-*BCL-XL* vector. The transgenic worms were grown up to 5 generations prior to perform experiments to achieve high penetrance of *BCL-XL* silencing. Empty L4440 vector was used as negative control in the RNAi assays. All experiments were performed in parallel wild type control N2 worms.

Progeny count. Adult worms were collected and washed with M9 buffer to remove bacterial contamination. Worm pellets were treated with freshly-prepared 0.5 ml NaOH(5N) mixed with 1 ml commercial bleach for 10 min. Samples were briefly vortexed at 2-min interval, then centrifuged for 30 s at 1,300g to pellet the released eggs. The pelleted eggs were washed with sterile H_2O, volume reduced to 100 μl and then plated in fresh NGM. When larvae reached the L4 stage, they were placed individually in fresh NGM plates. Progeny count was started 12 h latter, once they reached the young adult stage. Eggs layed were counted for the first 3 days of adulthood, and hatched eggs were counted every 8 h. Worms were transferred into fresh NGM plates every day.

Gonad staining, MR and TZ measurements, and germ cell count. Young adult worms (12 h from the L4 larvae stage) were washed with M9 buffer and placed on glass slides.

Worms were fixed with 100% cold methanol (-20°C) for 30 s and washed with M9 buffer. Gonads were stained with DAPI at a concentration of 1.0 ng/ml for 3 min and washed with phosphate buffered saline (PBS) prior to microscopy. MR/TZ or TZ/pachytene boundaries were well marked under the microscope. Germ cell numbers in the gonad were also determined by first marking MR/TZ or TZ/pachytene with the microscope, and then counting nuclei through germline width. Images were generated with a Zeiss Axio Observer Z1 automated microscope equipped with Axiovision software (v4.8.2).

Lifespan assay. Lifespan assays were peformed at 20°C. Briefly, 45 to 50 L4 hermaphrodite transgenic larvae, and N2 (wt) larvae were placed in 400 μM 5'flurodeoxyuridine-NGM plates in triplicate, for 6 days. Day 1 was defined as the day when the worms reached adulthood. Worms were scored every 1 to 3 days. On the 6th day, they were transferred to fresh NGM plates. Strains were considered to have lost viability if they exhibited arrested development or died.

4.6 Disclosure of conflicts of interest

The authors declare that they have no potential conflicts of interest.

4.7 Acknowledgements

This work was supported by the Canadian Institutes of Health Research (Grant MOP-97913) and the Natural Sciences and Engineering Research Council of Canada (Grant 328207) to RB. PSB received scholarships from the Faculté des études supérieures (Université de Montréal, Canada) and the Fondation de l'Institut du cancer de Montréal (Canada). The authors thank Dr. Jean-Claude Labbé (Institut de recherche en immunologie et cancer, Montréal QC) for generously providing strain HR1459 (bcls39[lim7:ced-1:GFP;lim-15(+)]V), and for very helpful discussions. They also thank Mr. Guillaume Chouinard (CRCHUM, Canada) for valuable help with image analysis. This manuscript was edited by Ovid Da Silva.

Table 1 Vector design and transgenic strains

Vector design	Transgenic strains
unc-119 ced-9 promoter / HA-Bcl-xL wt / 3'UTR	COP287, COP297,COP672,COP689
unc-119 ced-9 promoter / HA-Bcl-xL(S49A) / 3'UTR	COP285, COP286,COP322
unc-119 ced-9 promoter / HA-Bcl-xL(S62A) / 3'UTR	COP355, COP690,COP691
unc-119 ced-9 promoter / HA-Bcl-xL(S49D) / 3'UTR	COP288, COP298,COP310
unc-119 ced-9 promoter / HA-Bcl-xL(S62D) / 3'UTR	COP289,COP290,COP295, COP299,COP311
unc-119 ced-9 promoter / HA-Bcl-xL(S49/62A) / 3'UTR	COP291,COP293,COP300, COP301,COP312
unc-119 ced-9 promoter / HA-Bcl-xL(S49/62D) / 3'UTR	- none -

A)

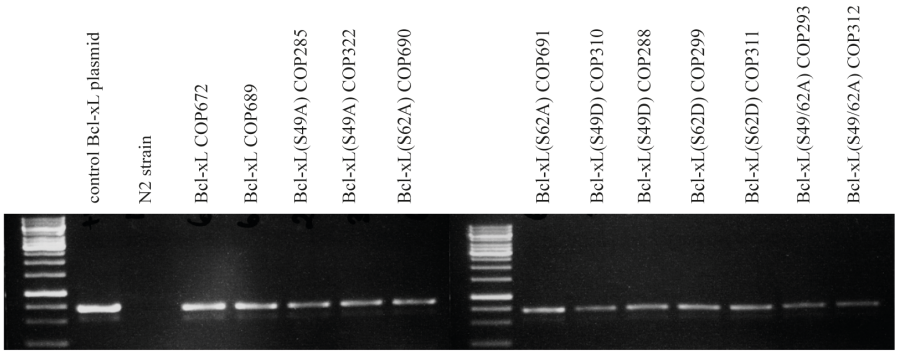
control Bcl-xL plasmid
N2 strain
Bcl-xL COP672
Bcl-xL COP689
Bcl-xL(S49A) COP285
Bcl-xL(S49A) COP322
Bcl-xL(S62A) COP690
Bcl-xL(S62A) COP691
Bcl-xL(S49D) COP310
Bcl-xL(S49D) COP288
Bcl-xL(S62D) COP299
Bcl-xL(S62D) COP311
Bcl-xL(S49/62A) COP293
Bcl-xL(S49/62A) COP312

B)

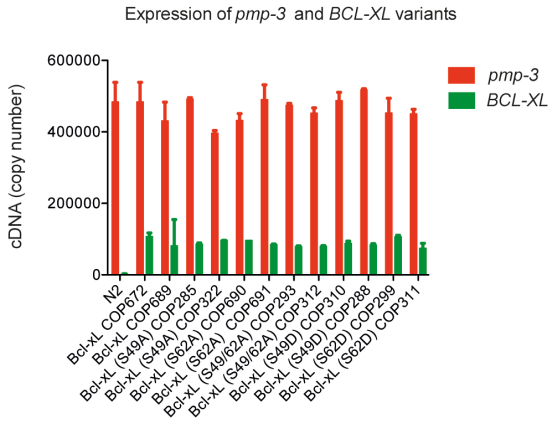
Expression of pmp-3 and BCL-XL variants
cDNA (copy number)
600000
400000
200000
0
pmp-3
BCL-XL
N2
Bcl-xL COP672
Bcl-xL COP689
Bcl-xL (S49A) COP285
Bcl-xL (S49A) COP322
Bcl-xL (S62A) COP690
Bcl-xL (S62A) COP691
Bcl-xL (S49/62A) COP293
Bcl-xL (S49/62A) COP312
Bcl-xL (S49D) COP310
Bcl-xL (S49D) COP288
Bcl-xL (S62D) COP299
Bcl-xL (S62D) COP311

C)

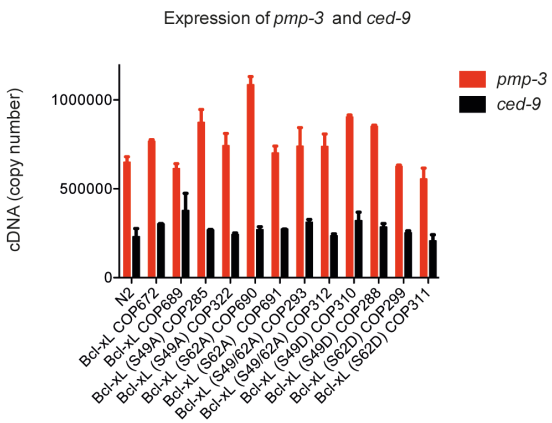
Expression of pmp-3 and ced-9
cDNA (copy number)
1000000
500000
0
pmp-3
ced-9
N2
Bcl-xL COP672
Bcl-xL COP689
Bcl-xL (S49A) COP285
Bcl-xL (S49A) COP322
Bcl-xL (S62A) COP690
Bcl-xL (S62A) COP691
Bcl-xL (S49/62A) COP293
Bcl-xL (S49/62A) COP312
Bcl-xL (S49D) COP310
Bcl-xL (S49D) COP288
Bcl-xL (S62D) COP299
Bcl-xL (S62D) COP311

D)

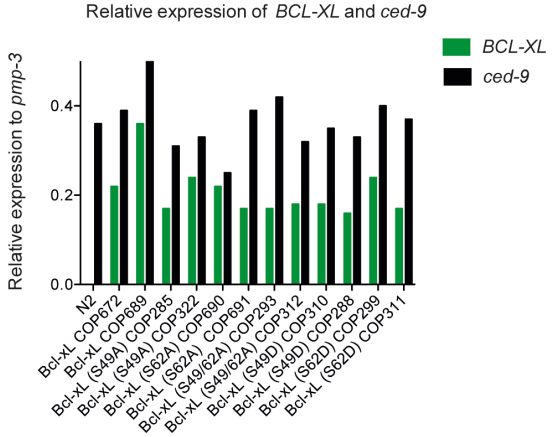
Relative expression of BCL-XL and ced-9
Relative expression to pmp-3
0.4
0.2
0.0
BCL-XL
ced-9
N2
Bcl-xL COP672
Bcl-xL COP689
Bcl-xL (S49A) COP285
Bcl-xL (S49A) COP322
Bcl-xL (S62A) COP690
Bcl-xL (S62A) COP691
Bcl-xL (S49/62A) COP293
Bcl-xL (S49/62A) COP312
Bcl-xL (S49D) COP310
Bcl-xL (S49D) COP288
Bcl-xL (S62D) COP299
Bcl-xL (S62D) COP311

Figure 1 Expression of Bcl-xL (wt) and Bcl-xL variants in transgenic worms. **A**) Ethidium bromide-stained PCR products obtained by genomic DNA amplification reactions. mRNA expression levels assessed by qRT-PCR of **B)** *BCL-XL* and *pmp-3,* **C)** *ced-9* and *pmp-3* and **D)** relative expression of *BCL-XL* and *ced-9* in the transgenic worms. Results from 2 independent determinations. Bars are means ± variations.

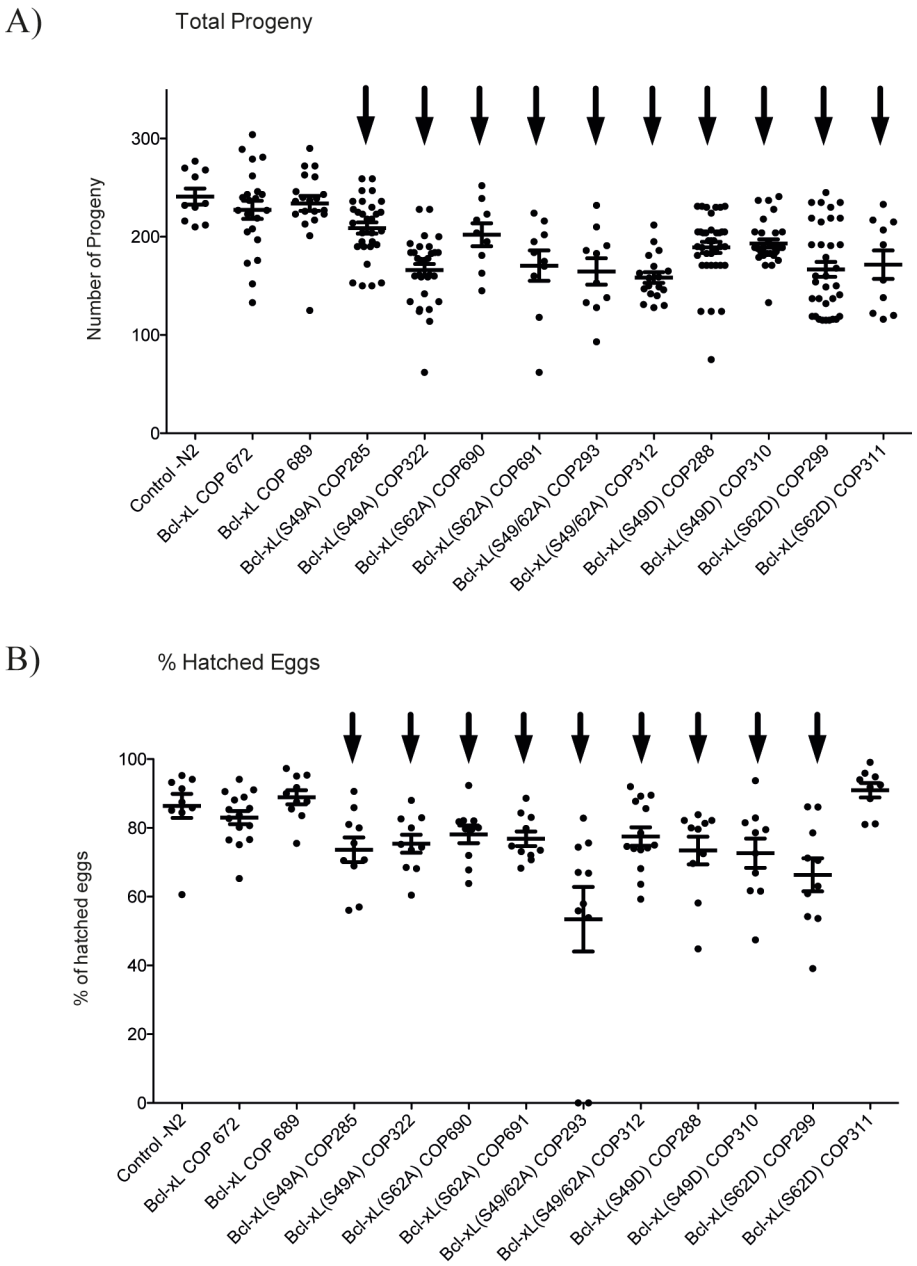

Figure 2 Effects of Bcl-xL (wt) and Bcl-xL variants on *C. elegans* progeny fecundity**.** Number of **A)** total viable progeny, and **B)** percentages of eggs hatched in various transgenic strains and control worms. Each point show in the graphs represents data obtained from a single worm. Bars are means ± s.d. Arrows on top indicate statistical significance with $p<0.05$ when compared to N2 control.

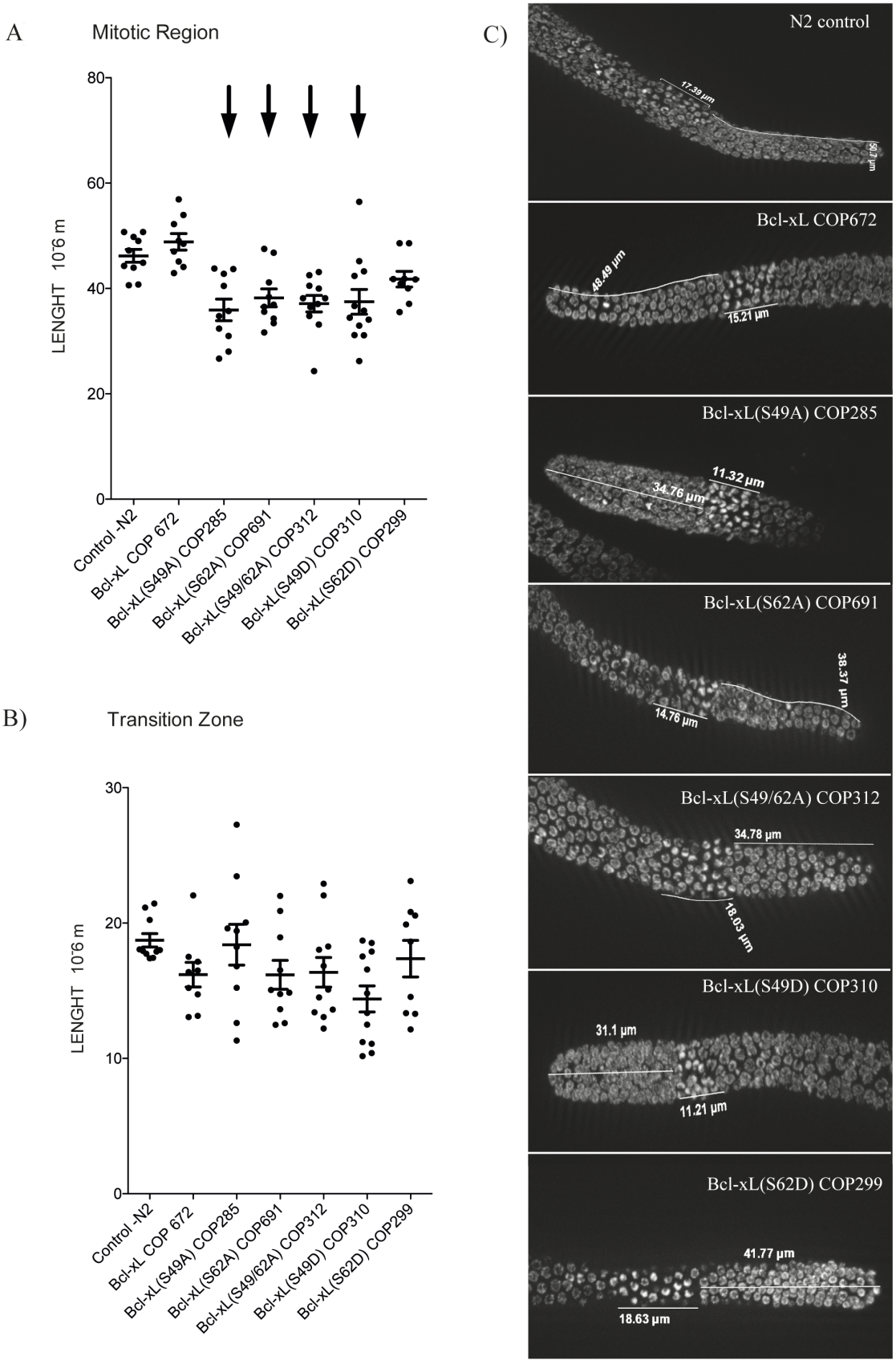
A
Mitotic Region
LENGHT 10^6 m
80
60
40
20
0
Control -N2
Bcl-xL COP 672
Bcl-xL(S49A) COP285
Bcl-xL(S62A) COP691
Bcl-xL(S49/62A) COP312
Bcl-xL(S49D) COP310
Bcl-xL(S62D) COP299
B)
Transition Zone
LENGHT 10^6 m
30
20
10
0
Control -N2
Bcl-xL COP 672
Bcl-xL(S49A) COP285
Bcl-xL(S62A) COP691
Bcl-xL(S49/62A) COP312
Bcl-xL(S49D) COP310
Bcl-xL(S62D) COP299
C)
N2 control
17.39 µm
50.7 µm
Bcl-xL COP672
48.49 µm
15.21 µm
Bcl-xL(S49A) COP285
11.32 µm
34.76 µm
Bcl-xL(S62A) COP691
38.37 µm
14.76 µm
Bcl-xL(S49/62A) COP312
34.78 µm
18.03 µm
Bcl-xL(S49D) COP310
31.1 µm
11.21 µm
Bcl-xL(S62D) COP299
41.77 µm
18.63 µm

Figure 3 Effects of Bcl-xL (wt) and Bcl-xL variants on mitotic region and transition zone length in *C. elegans* gonads. Length (μm) of **A)** mitotic regions and **B)** transition zones of the gonads. Each point in the graphs represents data obtained from a single worm; both MR and TZ were determined from the same worms. Bars are means ± s.d. Arrows on top indicate statistical significance with $p<0.05$ when compared to N2 control **C)** low-maginification images of DAPI-stained cells.

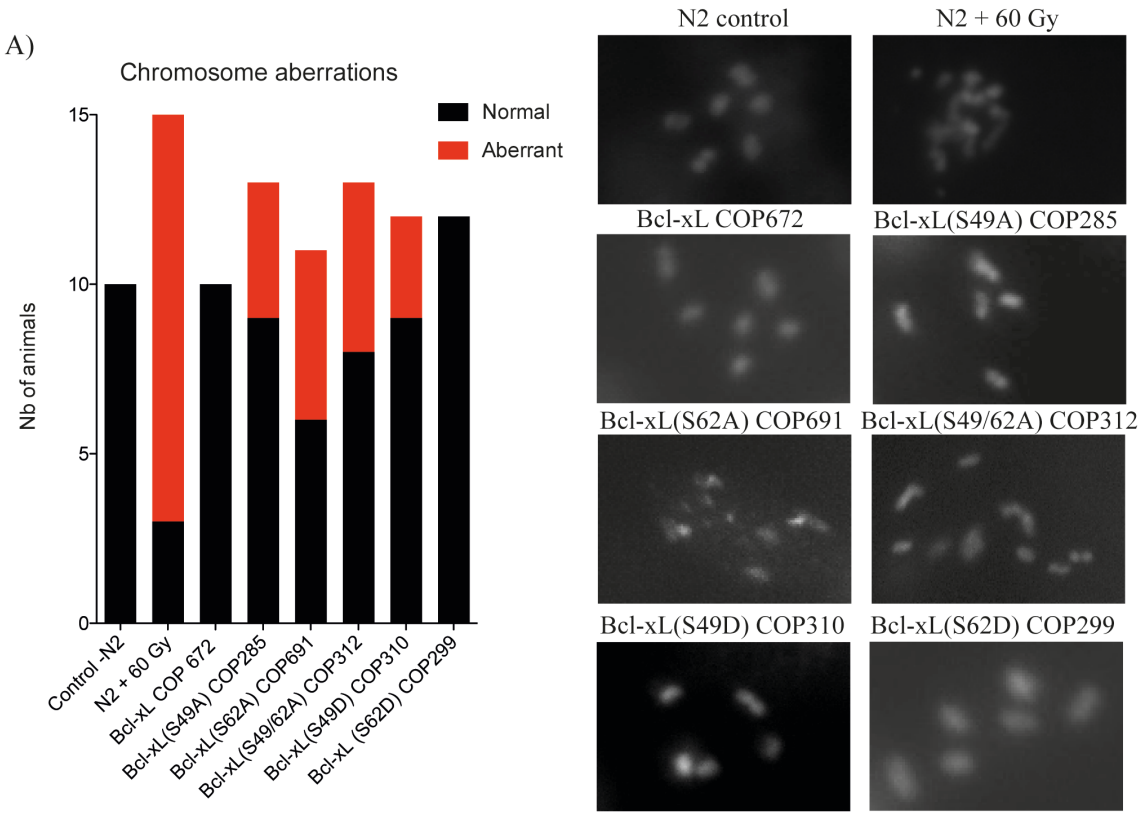

Figure 4 Effects of Bcl-xL (wt) and Bcl-xL variants on *C. elegans* chromosome stability and aneuploidy. The graph on left shows the number of cells with normal (black) and abnormal genotype (red). Right panels: images of DAPI-stained structures observed at the diplotene stages at the end of the gonads. N2 animals subjected to radiation were used as reference controls.

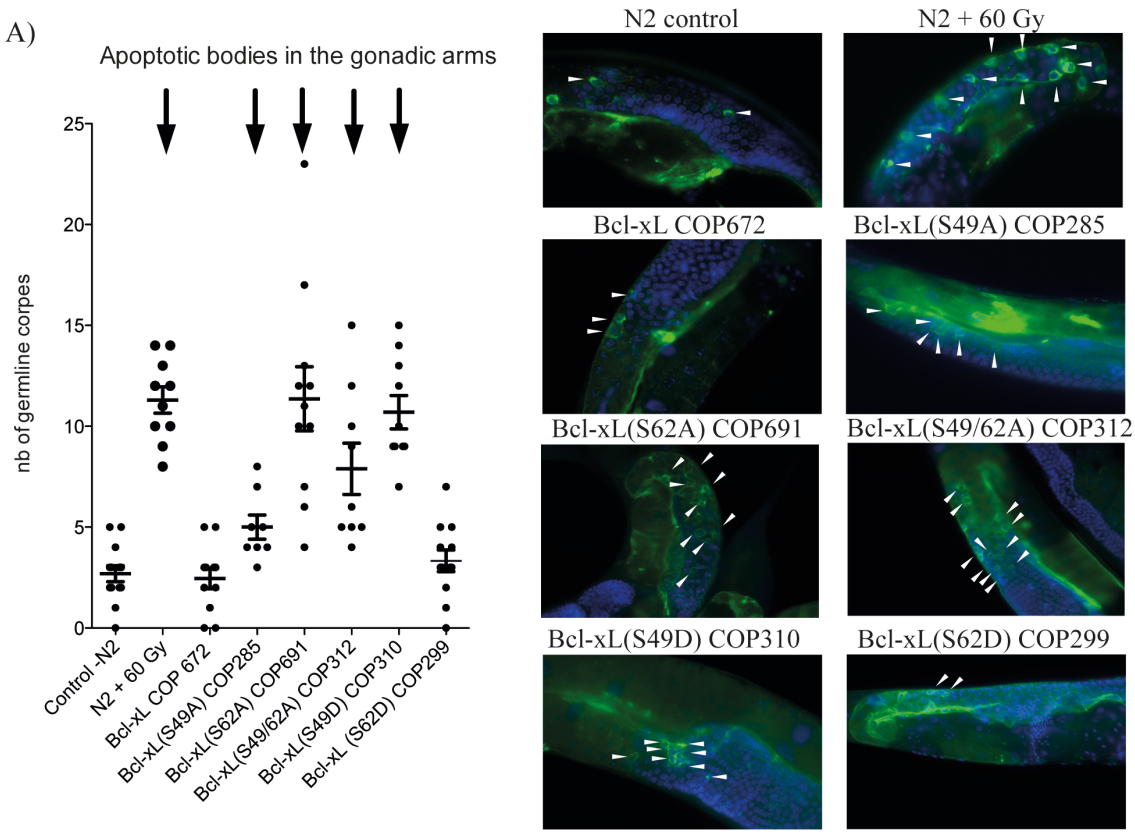

Figure 5 Effects of Bcl-xL (wt) and Bcl-xL variants on germline apoptosis. Left graph: Number of cells showing apoptotic corpses. Left panel, each point in the graphs represents data obtained from a single worm. Bars are means ± s.d. Arrows on top indicate statistical significance with $p<0.05$. Right panels: Typical low-magnification images of CED1:GFP expression in various transgenic strains and control worms. N2 animals subjected to radiation were used as reference controls.

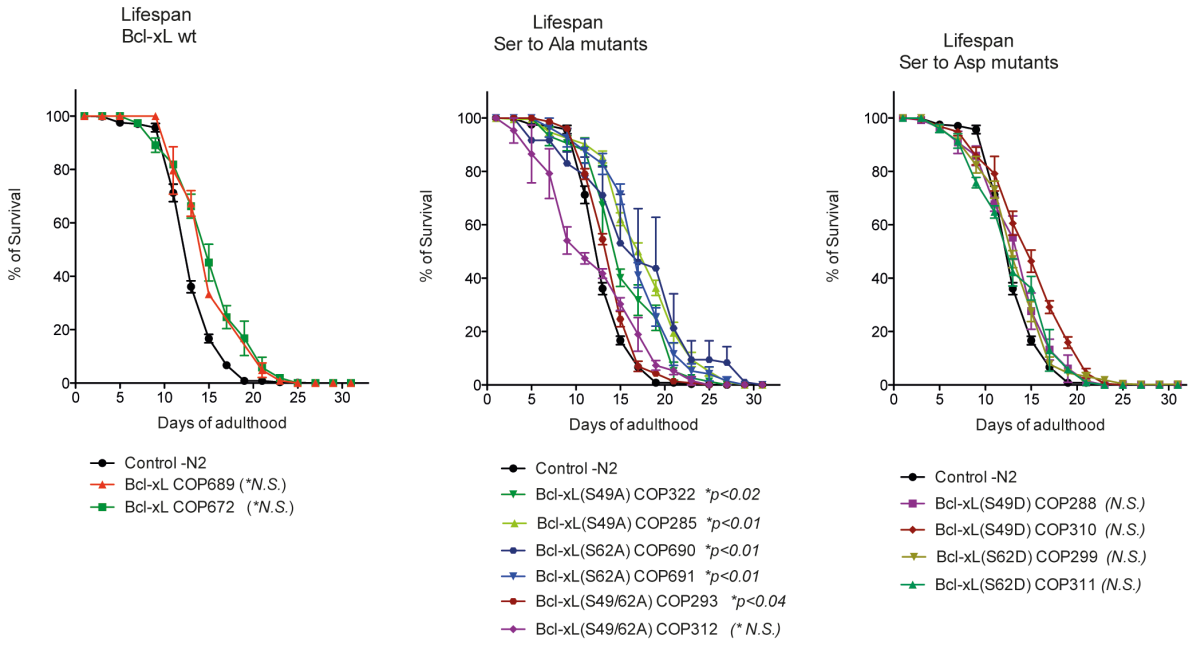

Figure 6 Effects of Bcl-xL (wt) and Bcl-xL variants on *C. elegans* lifespan. Lifespan kinetics of Bcl-xL(wt)-expressing worms (left graph), Bcl-xL (Ser to Ala) variants (middle graph) and Bcl-xL (Ser to Asp) variants (right graph). Data obtained from 2 independent triplicate experiments (n=6). Bars are means ± s.d. Statistical significance is indicated below the graphs.

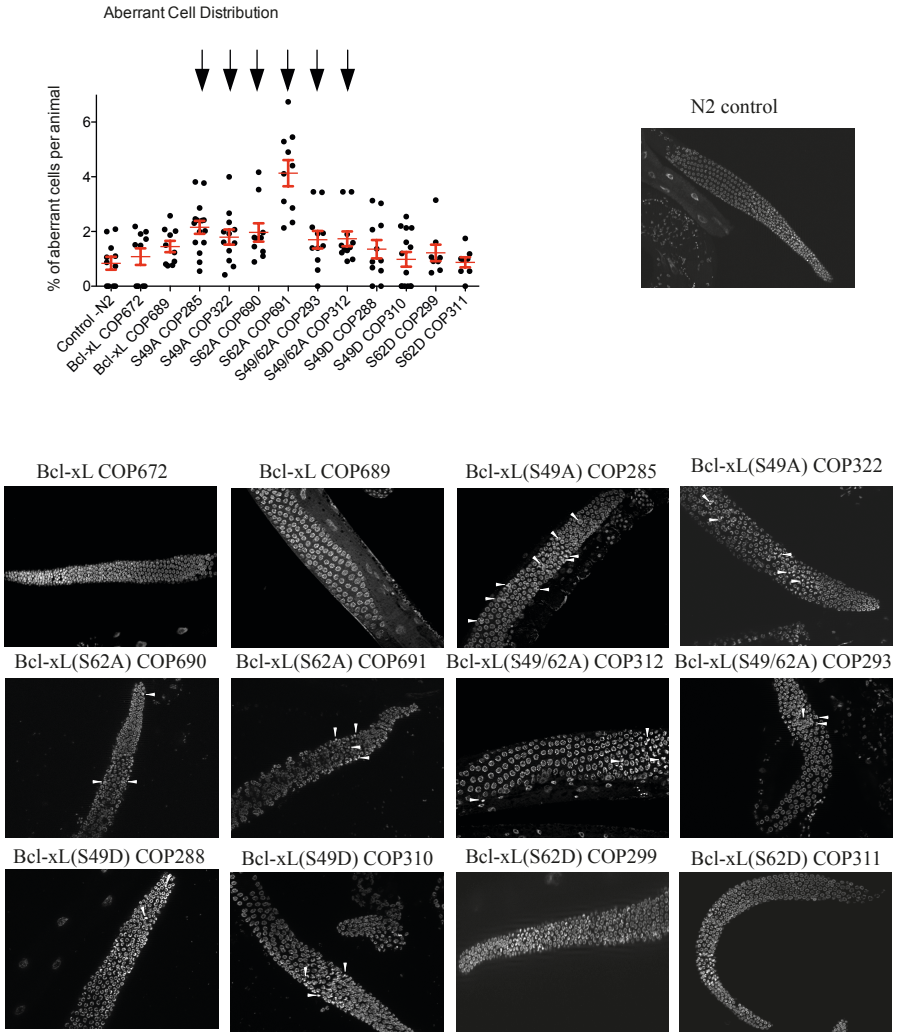

Supplemental Figure S1 Effects of Bcl-xL (wt) and Bcl-xL variants on the gonads. Graph showing the percentage of aberrant cells per worms and images of DAPI-stained germlines of various trangenic strains and control worms. Each point in graph represent data obtained from a single worm. Bars are means ± s.d. Arrows on top indicate statistical significance with $p<0.05$ when compared to N2 control.

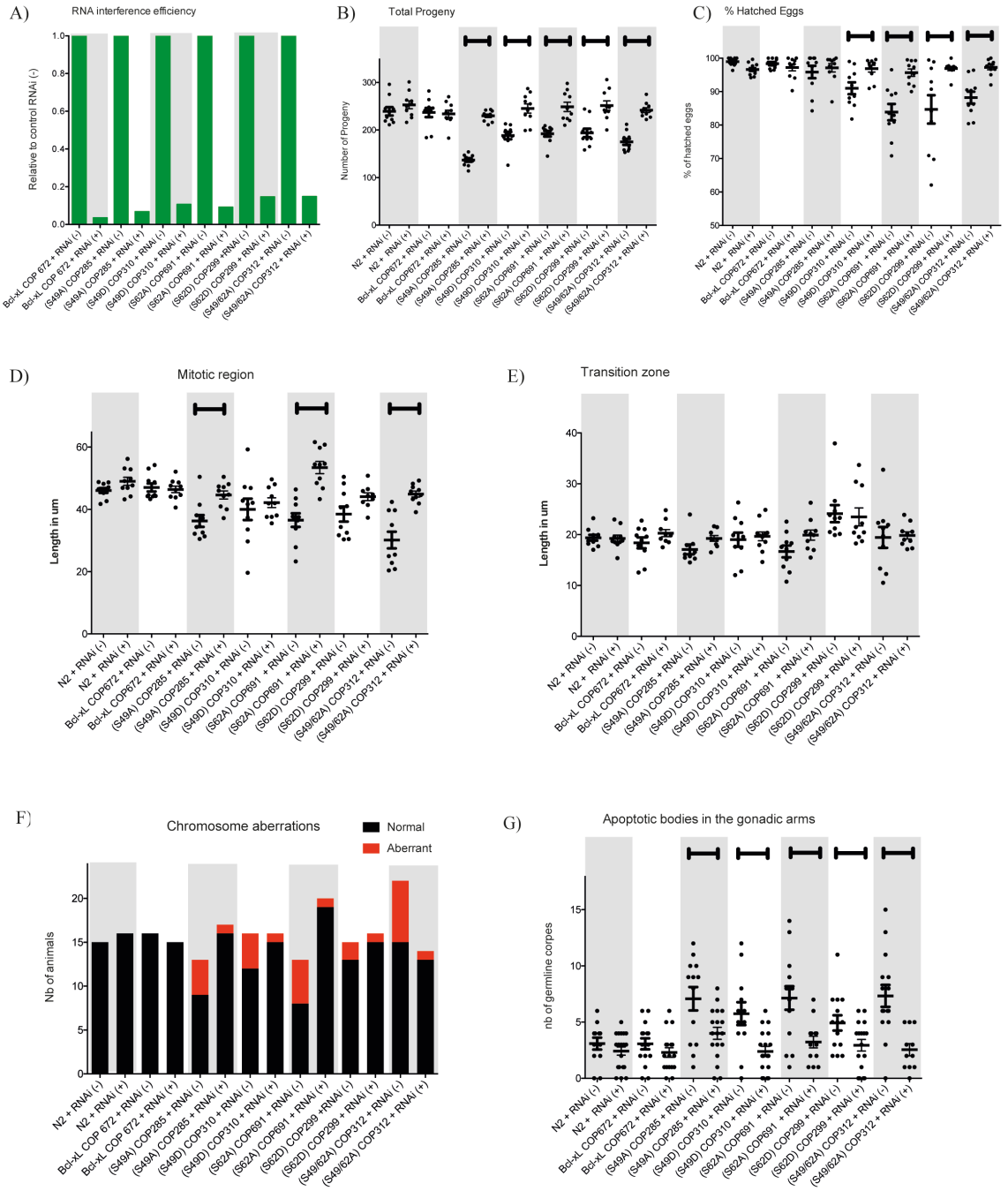

Supplemental Figure S2 Effects of silencing the expression of *BCL-XL* variants in various transgenic strains and control worms. **A)** RNAi efficiency, **B)** total viable progeny and **C)** percentages of eggs hatched, **D)** mitotic regions and **E)** transition zones, **F)** chromosome stability and aneuploidy, **G)** germline apoptosis of the gonads. Each point in graph (B-G) represent data obtained from single worm. Bars are means ± s.d. Brackets on top indicate statistical significance with $p<0.05$ between worms subjected to control RNAi (-) and *BCL-XL* RNAi (+).

4.8 Bibliography

1. Hengartner, M.O., Ellis, R.E. & Horvitz, H.R. Caenorhabditis elegans gene ced-9 protects cells from programmed cell death. *Nature* **356**, 494-496 (1992).
2. Tsujimoto, Y., Cossman, J., Jaffe, E. & Croce, C.M. Involvement of the bcl-2 gene in human follicular lymphoma. *Science* **228**, 1440-1443 (1985).
3. Bissonnette, R.P., Echeverri, F., Mahboubi, A. & Green, D.R. Apoptotic cell death induced by c-myc is inhibited by bcl-2. *Nature* **359**, 552-554 (1992).
4. Reed, J.C. Bcl-2 and the regulation of programmed cell death. *J Cell Biol* **124**, 1-6 (1994).
5. Adams, J.M. & Cory, S. Bcl-2-regulated apoptosis: mechanism and therapeutic potential. *Curr Opin Immunol* **19**: 488-496 (2007).
6. Vaux, D.L., Haecker, G. & Strasser, A. An evolutionary perspective on apoptosis. *Cell* **76**, 777-779 (1994).
7. Hengartner, M.O. & Horvitz, H.R. C. elegans cell survival gene ced-9 encodes a functional homolog of the mammalian proto-oncogene bcl-2. *Cell* **76**, 665-676 (1994).
8. Boise, L.H.*, et al.* Bcl-x, a bcl-2-related gene that functions as a dominant regulator of apoptotic cell death. *Cell* **74**, 597-608 (1993).
9. Petros, A.M., Olejniczak, E.T. & Fesik, S.W. Structural biology of the Bcl-2 family of proteins. *Biochim Biophys Acta* **1644**, 83-94 (2004).
10. Czabotar, P.E., Lessene, G., Strasser, A. & Adams, J.M. Control of apoptosis by the BCL-2 protein family: implications for physiology and therapy. *Nat Rev Mol Cell Biol* **15**, 49-63 (2014).
11. Muchmore, S.W.*, et al.* X-ray and NMR structure of human Bcl-xL, an inhibitor of programmed cell death. *Nature* **381**, 335-341 (1996).
12. Chang, B.S., Minn, A.J., Muchmore, S.W., Fesik, S.W. & Thompson, C.B. Identification of a novel regulatory domain in Bcl-X(L) and Bcl-2. *EMBO J* **16**, 968-977 (1997).
13. Burri, S.H.*, et al.* 'Loop' domain deletional mutant of Bcl-xL is as effective as p29Bcl-xL in inhibiting radiation-induced cytosolic accumulation of cytochrome c (cyt c), caspase-3 activity, and apoptosis. *Int J Radiat Oncol Biol Phys* **43**, 423-430 (1999).
14. Charbonneau, J. & Gauthier, E. Protection of hybridoma cells against apoptosis by a loop domain-deficient Bcl-xL protein. *Cytotechnology* **37**, 41-47 (2001).
15. Schmitt, E., Beauchemin, M. & Bertrand, R. Nuclear co-localization and interaction between Bcl-xL and Cdk1(cdc2) during G2/M cell cycle checkpoint. *Oncogene* **26**, 5851-5865 (2007).
16. Kharbanda, S.*, et al.* Translocation of SAPK/JNK to mitochondria and interaction with Bcl-x(L) in response to DNA damage. *J Biol Chem* **275**, 322-327 (2000).
17. Fan, M.*, et al.* Vinblastine-induced phosphorylation of Bcl-2 and Bcl-XL is mediated by JNK and occurs in parallel with inactivation of the Raf-1/MEK/ERK cascade. *J Biol Chem* **275**, 29980-29985 (2000).
18. Basu, A. & Haldar, S. Identification of a novel Bcl-xL phosphorylation site regulating the sensitivity of taxol- or 2-methoxyestradiol-induced apoptosis. *FEBS Lett* **538**, 41-47 (2003).

19. Terrano, D.T., Upreti, M. & Chambers, T.C. Cyclin-dependent kinase 1-mediated Bcl-xL/Bcl-2 phosphorylation acts as a functional link coupling mitotic arrest and apoptosis. *Mol Cell Biol* **30**, 640-656 (2010).
20. Wang, J., Beauchemin, M. & Bertrand, R. Bcl-xL phosphorylation at Ser49 by polo kinase 3 during cell cycle progression and checkpoints. *Cell Signal* **23**, 2030-2038 (2011).
21. Wang, J., Beauchemin, M. & Bertrand, R. Phospho-Bcl-xL(ser62) plays a key role at DNA damage-induced G2 checkpoint. *Cell Cycle* **11**, 2159-2169 (2012).
22. Wang, J., Beauchemin, M. & Bertrand, R. Phospho-Bcl-xL(Ser62) influences spindle assembly and chromosome segregation during mitosis. *Cell Cycle* **13**, 1313-1326 (2014).
23. Hoogewijs, D., Houthoofd, K., Matthijssens, F., Vandesompele, J. & Vanfleteren, J.R. Selection and validation of a set of reliable reference genes for quantitative sod gene expression analysis in C. elegans. *BMC Mol Biol* **9**, 9 (2008).
24. Crittenden, S.L., Leonhard, K.A., Byrd, D.T. & Kimble, J. Cellular analyses of the mitotic region in the Caenorhabditis elegans adult germ line. *Mol Biol Cell* **17**, 3051-3061 (2006).
25. Thompson, S.L., Bakhoum, S.F. & Compton, D.A. Mechanisms of chromosomal instability. *Curr Biol* **20**, R285-295 (2010).
26. Musacchio, A. Spindle assembly checkpoint: the third decade. *Philos Trans R Soc Lond B Biol Sci* **366**, 3595-3604 (2011).
27. Holland, A.J. & Cleveland, D.W. Boveri revisited: chromosomal instability, aneuploidy and tumorigenesis. *Nat Rev Mol Cell Biol* **10**, 478-487 (2009).
28. Fang, X. & Zhang, P. Aneuploidy and tumorigenesis. *Semin Cell Dev Biol* **22**, 595-601 (2011).
29. Hanahan, D. & Weinberg, R.A. Hallmarks of cancer: the next generation. *Cell* **144**, 642-674 (2011).
30. Lu, N., Yu, X., He, X. & Zhou, Z. Detecting apoptotic cells and monitoring their clearance in the nematode Caenorhabditis elegans. *Methods Mol Biol* **559**, 357-370 (2009).
31. Yu, X., Lu, N. & Zhou, Z. Phagocytic receptor CED-1 initiates a signaling pathway for degrading engulfed apoptotic cells. *PLoS Biol* **6**, e61 (2008).
32. Gems, D. & Riddle, D.L. Defining wild-type life span in Caenorhabditis elegans. *The journals of gerontology. Series A, Biological sciences and medical sciences* **55**, B215-219 (2000).
33. Petronczki, M., Lenart, P. & Peters, J.M. Polo on the Rise-from Mitotic Entry to Cytokinesis with Plk1. *Dev Cell* **14**, 646-659 (2008).
34. Archambault, V. & Glover, D.M. Polo-like kinases: conservation and divergence in their functions and regulation. *Nat Rev Mol Cell Biol* **10**, 265-275 (2009).
35. Rahman, M.M*., et al.* Caenorhabditis elegans polo-like kinase PLK-1 is required for merging parental genomes into a single nucleus. *Mol Biol Cell* **26**, 4718-4735 (2015).
36. Harper, N.C*., et al.* Pairing centers recruit a Polo-like kinase to orchestrate meiotic chromosome dynamics in C. elegans. *Dev Cell* **21**, 934-947 (2011).

37. Nishi, Y., Rogers, E., Robertson, S.M. & Lin, R. Polo kinases regulate C. elegans embryonic polarity via binding to DYRK2-primed MEX-5 and MEX-6. *Development* **135**, 687-697 (2008).
38. Gumienny, T.L., Lambie, E., Hartwieg, E., Horvitz, H.R. & Hengartner, M.O. Genetic control of programmed cell death in the Caenorhabditis elegans hermaphrodite germline. *Development* **126**, 1011-1022 (1999).
39. Finch, C.E. & Ruvkun, G. The genetics of aging. *Annu Rev Genomics Hum Genet* **2**, 435-462 (2001).
40. Vaux, D.L., Weissman, I.L. & Kim, S.K. Prevention of programmed cell death in Caenorhabditis elegans by human bcl-2. *Science* **258**, 1955-1957 (1992).
41. Hisahara, S.*, et al.* Caenorhabditis elegans anti-apoptotic gene ced-9 prevents ced-3-induced cell death in Drosophila cells. *J Cell Sci* **111 (Pt 6)**, 667-673 (1998).
42. Boyd, W.A.*, et al.* Nucleotide excision repair genes are expressed at low levels and are not detectably inducible in Caenorhabditis elegans somatic tissues, but their function is required for normal adult life after UVC exposure. *Mutat Res* **683**, 57-67 (2010).
43. Denver, D.R., Feinberg, S., Steding, C., Durbin, M. & Lynch, M. The relative roles of three DNA repair pathways in preventing Caenorhabditis elegans mutation accumulation. *Genetics* **174**, 57-65 (2006).
44. Lawrence, K.S., Chau, T. & Engebrecht, J. DNA damage response and spindle assembly checkpoint function throughout the cell cycle to ensure genomic integrity. *PLoS Genet* **11**, e1005150 (2015).
45. Kitagawa, R. Key players in chromosome segregation in Caenorhabditis elegans. *Front Biosci* **14**, 1529-1557 (2009).
46. Strome, S. & Wood, W.B. Generation of asymmetry and segregation of germ-line granules in early C. elegans embryos. *Cell* **35**, 15-25 (1983).
47. Yamamoto, T.G., Watanabe, S., Essex, A. & Kitagawa, R. SPDL-1 functions as a kinetochore receptor for MDF-1 in Caenorhabditis elegans. *J Cell Biol* **183**, 187-194 (2008).
48. Tarailo, M., Kitagawa, R. & Rose, A.M. Suppressors of spindle checkpoint defect (such) mutants identify new mdf-1/MAD1 interactors in Caenorhabditis elegans. *Genetics* **175**, 1665-1679 (2007).
49. Karczmarek-Borowska, B.*, et al.* Estimation of prognostic value of Bcl-xL gene expression in non-small cell lung cancer. *Lung Cancer* **51**, 61-69 (2006).
50. Mallick, S.*, et al.* Bcl-xL protein: predictor of complete tumor response in patients with oral cancer treated with curative radiotherapy. *Head & neck* **35**, 1448-1453 (2013).
51. Watanabe, J.*, et al.* Prognostic significance of Bcl-xL in human hepatocellular carcinoma. *Surgery* **135**, 604-612 (2004).
52. Degterev, A.*, et al.* Identification of small-molecule inhibitors of interaction between the BH3 domain and Bcl-xL. *Nat Cell Biol* **3**, 173-182 (2001).
53. Oltersdorf, T.*, et al.* An inhibitor of Bcl-2 family proteins induces regression of solid tumours. *Nature* **435**, 677-681 (2005).
54. Qian, J.*, et al.* Discovery of novel inhibitors of Bcl-xL using multiple high-throughput screening platforms. *Anal Biochem* **328**, 131-138 (2004).

55. Yamaguchi, R., *et al.* Efficient elimination of cancer cells by deoxyglucose-ABT-263/737 combination therapy. *PLoS One* **6**, e24102 (2011).
56. Souers, A.J., *et al.* ABT-199, a potent and selective BCL-2 inhibitor, achieves antitumor activity while sparing platelets. *Nat Med* **19**, 202-208 (2013).
57. Tao, Z.F., *et al.* Discovery of a potent and selective Bcl-XL inhibitor with in vivo activity. *ACS medicinal chemistry letters* **5**, 1088-1093 (2014).
58. Frokjaer-Jensen, C., *et al.* Single-copy insertion of transgenes in Caenorhabditis elegans. *Nat Genet* **40**, 1375-1383 (2008).

5.0 Discussion and perspectives

5.1 Interplay of Bcl-xL in the cell cycle

In addition to their functions on apoptosis, the anti-apoptotic proteins Bcl-2, Bcl-xL and Mcl-1 also have effects on cell cycle progression. Studies have shown that Bcl-2, Bcl-xL and Mcl-1 can delay the progression of cell cycle in presence of DNA damage or cellular stress [53,64, 101-103, 515,516]. Bcl-2 and Bcl-xL elevate p27 during G_0 arrest and inhibit G_1 Cdks during cell cycle re-entry, thus delaying progression to S phase[515,517]. Mutation at the conserved tyrosine 28 (Y28) residue in the BH4 domain of Bcl-2 and Y22 in Bcl-xL eliminated their ability to delay S-phase entry without affecting their ability to inhibit apoptosis[516]. Bcl-2 has been shown to be present in a complex with nucleolin, Cdc2 kinase and PP1 phosphatase at the onset of mitosis[111]. Previous work in the laboratory revealed functions of Bcl-xL during the G2 checkpoint and mitosis[53,101-103]. Studies indicate that the anti-apoptotic role of these proteins can be separated from their function in cell cycle. However one study argue that these two activities cannot be altered independently[65].

Both Bcl-2 and Bcl-xL contain a loop domain between their BH3 and BH4 domains. In one study, the loop domain of Bcl-2 was reported to be necessary for the anti-apoptotic effects of Bcl-2 against paclitaxel-induced apoptosis in HL-60 cells[518]. In contrast, most works indicated that the loop domain is not essential for the anti-apoptotic function of either Bcl-2 or Bcl-xL[53,95,98,101-103]. The exact mechanism by which the Bcl-xL loop domain acts during mitosis has not yet been elucidated. Our lab has determined that Bcl-xL undergoes phosphorylation and dephosphorylation in its loop domain at Ser49 and Ser62 during the course of mitosis and has identified the kinases involved in these phosphorylation processes[101-103]. Bcl-xL (Ser49) and (Ser62) mutants expressed in HeLa cells display insignificant defects in MT-kinetochores attachment, chromosome segregation and cytokinesis completion[101-103]. Because these observations were made in tumor cells, our primary goal was to evaluate the importance of Bcl-xL (Ser49) and (Ser62) in promoting chromosome stability in normal cells and *in vivo*.

Normal BJ foreskin fibroblasts were investigated in our first study. These cells are well-described and can be followed by population doubling to determine their age. The cells are also suitable for various analyses, including staining and immunofluorescence

assays, or to ascertain aneuploidy. They also have the main advantage over HeLa or other cancer cell lines as they have a very stable diploid genome. Fibroblasts are well-characterized as they appear to accumulate senescence and genomic stress after a certain number of population doublings.

BJ fibroblasts were infected by pLenti6/V5-DEST gateway vector (Invitrogen) for the lentiviral expression of Bcl-xL and various mutants. This system provides stable expression of the proteins of interest, and infected cells are selected for blasticidin resistance. The disadvantage of this exogeneous system of expression is its non-similarity with the endogenous gene expression environment, the lentiviral expression system been susceptible to insertion and position effects. However by selecting a mixed population of infected cells rather than individual clones, position effects are attenuated. Furthermore, by calculating the lentiviral titre used to infect the cells, HA-Bcl-xL and mutant expression levels were comparable to those of the endogenous proteins.

The exogenous expression of Bcl-xL phospho-refractile mutations with serine to alanine (S49A, S62A, S49/62A) showed significantly decreased kinetics of population doubling in BJ fibroblasts compared to the controls and cells expressing Bcl-xL (wt). Mutants with serine to aspartate (S49D, S62D, S49/62D) substitution also presented significantly reduced kinetics of cell population doubling. The decrease kinetics of population doubling in cells expressing mutants correlated with the occurrence of cellular senescence, which may be due to the hindrance of normal mitosis and chromosome instability mediated by Bcl-xL mutation at Ser49 and Ser62, suggesting that phosphorylation and dephosphorylation at Ser49 and Ser62 during mitosis play a role in maintaining the proliferative properties of the BJ cells.

5.2 Expression of Bcl-xL (Ser49) and (Ser62) mutants leads to cellular senescence in BJ fibroblasts: association with the p53-p21 pathway

In this study, we observed a decrease in the kinetics of population doubling in BJ fibroblasts expressing Bcl-xL mutants at Ser49 and/or Ser62 compared to the controls. The kinetics of cellular senescence in these mutant cell lines were observed by performing standard SA-β-gal assay. SA-β-gal is a manifestation of residual lysosomal activity at a suboptimal pH, which becomes detectable due to the increased lysosomal

content in senescent cells[519]. SA-β-gal activity is expressed from *GLB1*, the gene encoding lysosomal β-galactosidade, the activity of which is typically measured at acidic pH 4.5. SA-β-gal induction during senescence is due to at least in part to increased expression of lysosomal β-gal protein but SA-β-gal is not required for senescence[520]. Western blotting revealed p53 and p21 activation at the protein level in cells expressing Bcl-xL mutants compared to the controls. p53 pathway activation depicts presence of cellular stress such as DNA strand-breaks. Increased p53 expression leads to heightened protein levels of the Cdk inhibitor p21. This elevation of p21 usually results in cell cycle arrest at G1 in the interphase, but significant arrest can also occur at G2/M transition[521-522].

Proliferating cells continuously experience endogenous or exogenous stress and their response can range from complete recovery from these stresses to cellular senescence, cell death and, in rare situation, to immortalization or tumorigenesis[334]. Cellular senescence represents permanent cell cycle arrest. Fibroblasts or other cell types, when they undergo senescence, show a broad G1 or G2 DNA content. In general, fibroblasts are more resistant to apoptosis and incur senescence in the face of cellular stress. This may be ascribed to their inherent function as a component of the tissue repair machinery during injury.

Cellular senescence is generally associated with elevated p53 levels. P53 is a transcription factor that imparts its tumor suppressive and anti-proliferative effects through the induction of key downstream regulatory factors. As a sequence specific transcription factor, p53 regulates gene expression by directly binding to a p53-responsive element (p53-RE) in the target genes as a tetramer. p53 induces genes, such as p21, to halt cell cycle progression, or genes such as Puma, Noxa and Pidd that trigger apoptosis. Most tumor-associated p53 mutations have been shown to interfere with p53's transcriptional activity, emphasizing its importance as a target of gene regulation in tumor suppression. The most frequently- mutated p53 residues are those that bind directly to DNA[523]. Microarray data show increasing numbers of p53 target genes. The Cki p21, which induces G1/S cell cycle arrest is an immediate and direct target of p53. p53 can also induce 14-3-3σ expression, which has been suggested to halt the cell cycle at G2/M phase[524]. Additionally, p53 has been reported to induce at least 16 genes involved in

PCD[525]. p53 stimulates the BH3-only proteins Puma and Noxa as well as Bax[526-529]. It also induces p53Aip1, p53Dinp1, Pidd and Apaf-1, among others[530,531], which is not surprising as p53 is under tight regulation by various proteins. The regulation of p53 function and transcriptional activity requires multiple layers of signaling and post-translational controls. Mdm2 (HDM2 in human), an E3 ubiquitin ligase that constantly mediates p53 shuttle from the nucleus to the cytoplasm and to the 26S proteosome for degradation[532], is a major regulator of p53. Temporal control of Mdm2 is critically important for the proper function of p53. Upon genotoxic stresses, rapid phosphorylation of p53 at Ser15 by Atm, a serine/threonine protein kinase, and at Ser20 by the checkpoint kinase Chk2 results in p53 dissociation from Mdm2[533]. This results in p53 stabilization and activation of its downstream processes. In the absence of Atm, Atr substitutes the function of Atm through Chk1-induced p53 phosphorylation at Ser15 of p53[386]. ATM also phosphorylates Mdm2 at Ser395, which attenuates the capability of Mdm2 in exporting nuclear p53 to cytoplasm for subsequent p53 degradation, causing p53 nuclear accumulation[534,535]. p53 was also identified as the first non-histone substrate of HATs (histone acetyltransferases)[536] and HDACs (histone deacetylases)[537]. In response to DNA damage, CBP/p300 acetylates p53 on 6 C-terminal lysine (K) residues (K370, K372, K373, K381, K382, and K386), the same target sites of Mdm2-mediated ubiquitination, and hence leads to enhanced stability and DNA binding activity of p53[538]. In addition, acetylation of p53 on K320 by Pcaf preferentially directs p53 to activate target genes involved in cell cycle arrest[539], whereas acetylation of p53 on K120 by Tip60/hMof promotes p53-mediated cell death[540].

Another protein Mdmx is found to directly inhibit p53-mediated transcriptional activity[541]. Mdmx and Mdm2 are also recruited to the promoters of p53-responsive genes and form complexes with p53, which in turn inhibit various p53-target genes[542,543]. Mdmx does not have a ubiquitin ligase activity towards p53 despite having intrinsic ubiquitin ligase activity. Interestingly, although p53 level is elevated in the absence of Mdm2, it is still vitiated in *Mdm2* null mice cells, which indicates the presence of Mdm2-independent pathways for p53 degradation *in vivo*[544]. Indeed, the E3 ubiquitin ligases, Cop1[545], Pirh2[346] and Arf-BP1[346] have been found to contribute to the control of p53 levels *in vitro*. Upon genotoxic insults, p53 is stabilized through post-translational

modifications. Its phosphorylation is classically regarded as the first crucial step in its stabilization. p53 can be phosphorylated by a broad range of kinases, including Atm, Atr, DNA-Pk and Chk1 and Chk2. Ser15 and Ser20 phosphorylation mediated by DNA damage, are generally thought to stabilize p53 by inhibiting its interaction with Mdm2[546,547].

Tumor suppressor homeodomain-interacting protein kinase-2 (HipK2) is a crucial regulator of p53 apoptotic function by phosphorylation of its N-terminal Ser46 residue that facilitates Lys382 acetylation at the C-terminus. HipK2 is activated by numerous genotoxic agents and can be deregulated in tumors by several mechanisms[548]. Chromatin immunoprecipitation (ChIP) assays have confirmed the specific DNA-binding sequence of p53 that contains two inverted pentameric sequences with the 5'-RRR(A/T)I(A/T)GYYY-3' pattern[549]. Gene transactivation requires p53 interaction with the promoter regions of p53 target genes[550]. DNA binding is thought to occur via the conserved central core domain of the protein, whereas the C-terminal region is believed to act as a negative modulator that allows sequence-specific DNA binding. Various post-translational modifications alter the C-terminal region, and thus affect the ability of p53 to bind DNA[551].

Expression of oncogenic Ras promotes acute senescence-like G1 arrest in primary human or rodent cells containing wild-type p53 through Mapk pathways. Ras utilizes Mapk signal transduction pathways, including Raf-1, Mek1/2 and Erk1/2 to promote cell cycle arrest in primary cells but abolished in cells lacking p53[552]. Oncogenic Ras initially forces uncontrolled proliferation, and only later do cells arrest. The fact that oncogenic Ras uses the Mapk signal-transduction pathways to promote both arrest and forced mitogenesis reinforces the view that normal cells counter malignant transformation by actively responding to hyperproliferative signals; in this case, by sensing excessive Mek/Mapk activity and activating senescence[552]. In contrast the ability of Ras to activate PI(3)K promotes membrane ruffling perhaps through Rac and Rho[553] and may also suppress apoptosis through activation of Akt/Pkb[554]. Although p53 and p16 play fundamental roles in Ras-induced arrest, neither have essential roles in differentiation. Cell-cycle arrest induced by Ras and Mek1/2 is accompanied by accumulation of p53, p21, p16, and SA-β-gal activity[552].

The *P21* gene, localized on chromosome 6p21.2, generates a polypeptide of 164 amino acids (p21)[555] or a smaller protein of 132 amino acids (p21B) attributed to the use of alternative promoters[556]. The *P21* promoter contains 2 highly conserved p53-response elements (p53-RE). Moreover, two p53 homologues, p63 and p73 transactivate *P21* and *P21B* mRNAs through binding to the p53-REs[557]. Brca1 has been shown to function as a p53 coactivator, activating the *P21* promoter by recruiting p300/CreBP which, in turn, acetylates and stabilizes p53[558]. *P21* is also activated in p53-independent manner. Various stimuli and stress signals, including Ngf, butyrate, phorbol myristate acetate and Tgf-β are known to regulate p21 expression at Sp1 and Sp3 binding sites in the proximal *P21* promoter[559].

p21 was first identified as an overexpressed marker in senescent cells and later found to be capable of inducing premature senescence in both normal and tumor cells in a p53-dependent and -independent manner. Studies shows that p21 is upregulated during oncogenic Ras-induced cellular senescence and inhibits Ras-induced transformation[342,560].

p21 is accumulated in normal human fibroblasts arrested in G_0 when the conditions for cell cycle entry are not optimal and maintains cells in G_0. It inhibits cell cycle progression primarily by curbing Cdk2 activity. p21 also associates with and inactivates E2f, leading to cell cycle arrest and cellular senescence[561].

The ability of p21 to promote cell cycle arrest may depend on its ability to mediate p53-dependent gene repression, as p21 is both necessary and sufficient for p53-dependent repression of genes regulating cell cycle repression, including Cdc25c, Cdc2, Chek1, Ccnb1, Tert and survivin[562,563]. Cdc2, Chek1 and Tert are repressed by p21, via its inhibition of Cdk2 and phosphorylation of pRb[563,564]. p21 also activates gene transcription by de-repressing p300-CreBP, and p300-CreBP, in turn, cooperates with multiple factors to promote the transcriptional induction of *CDKN1A* as a positive feedback loop[565]. In diploid, non-immortalized, non-transformed cells, oncogenic Ras activates *CDKN1A* transcription through both p53-dependent and p53-independent mechanisms. The p53-independent transactivation of *CDKN1A gene* by activated Ras requires the transcription factor E2f1[566]. Oncogenic Ras and Raf, however induce p21-dependent senescence and other genetic mutations are necessary to bypass oncogene-induced senescence, which acts as a barrier to tumorigenesis[567]. However, p21 can also exhibit oncogenic activities

and has been shown to be overexpressed in various human cancers including prostate, cervical, breast and squamous cell carcinomas. In many cases, p21 upregulation correlates positively with tumor grade, invasiveness and aggressiveness and is a poor prognostic indicator[568].

5.3 Expression of Bcl-xL (Ser49) and (Ser62) mutants leads to cellular senescence in BJ fibroblasts: association with various markers

Elevated p53 levels are indicative of DNA damage. This was confirmed by immunofluorescence assay, which showed increased γ-H2A.X-associated nuclear foci in cells expressing the Bcl-xL mutants. γ-H2A.X, often considered, as a marker associated to replicative and premature senescence, is a key factor in the repair process of DNA double strand-breaks. It is recruited to DNA strand breaks, and is implicated in recruiting other DNA repair proteins[569]. In human, H2A.X constitutes ≈10% of the H2A protein. γ-H2A.X differs from H2A because it is phosphorylated on Ser139 in response to DNA strand breaks. In mammalian cells, Atm is one of the major protein kinase that phosphorylates γ-H2A.X[570,571]. However, γ-H2A.X levels are low in the S-phase, even when Atm is inhibited, implying that other protein kinases could be responsible for its phosphorylation[572]. γ-H2A.X interacts with Brca1 through the C-terminal BRCT or FHA domain. Nbs1 associates with γ-H2A.X through FHA and BRCT domains and is needed for the recruitment of MRE complexes which form around DNA strand break-sites[569]. 53BP1 and Mdc1 contain a BRCT domain and co-localize with γ-H2A.X. When DNA strand-breaks are repaired, γ-H2A.X is dephosphorylated by protein phosphatase 2A (PP2A)[573]. The effect of PP2A on γ-H2A.X expression level is independent of Atm, Atr or DNA-Pk activity[573].

In this study, Ki-67 served as a marker of proliferating cells. Cells expressing Bcl-xL mutants showed markedly decreased Ki-67 expression as they progressed in population doubling experiments. Human Ki-67 expression is strictly associated with cell proliferation. Ki-67 is present during all active phases of the cell cycle (G1, S, G2 and mitosis) with peak during the S-phase, but is absent from resting cells (G0), making it an excellent marker for cell proliferation[574]. Ki-67 protein was originally defined by the Ki-67 antibody, which was generated by immunizing mice with nuclei of the Hodgkin

lymphoma cell line L428. The name Ki-67 is derived from the city of origin (Kiel) and the original clone number in a 96-well plate[575].

BJ fibroblasts harboring Bcl-xL mutants showed augmented Il-6 secretion compared to that of control and Bcl-xL (wt)-expressing cells. Increased Il-6 indicates the onset of a senescence-associated secretory phenotype (SASP). In DNA damage- and oncogenic stress-induced senescence, SASP with Il-6 secretion has been observed in mouse and human fibroblasts and epithelial cells[356]. The exact consequence of SASP is yet unknown, but it is believed to impact neighboring cells. Il-6 is a multifunctional cytokine that regulates cell proliferation, survival, and differentiation, enhancing cellular function in multiple cell lineages[576,577]. Il-6 and its soluble form Il-6Rα are secreted abundantly in tissues with inflammation, aging and tumor infiltration. Il-6 acts on cell as a dimer by binding to specific Il-6 receptors (Il-6R). Upon interaction of Il-6R with Il-6Rα, it activates Jak kinases that will galvanize downstream transduction pathways.

Normal human fibroblastic TIG3 cells have a senescent phenotype after about 55 population doublings, and display constitutive IL-6 and IL-6R expression, while younger cells at population doubling 33 do not express either of them[578]. TIG3 cells, which lack p53 expression, show no sign of senescence under the same conditions, and proliferate normally in the presence of Il-6/Il-6R[578]. RelA, a component of NFκB transcription factor, is required for SASP[579]. However, IL-6 has been also shown to have anti-senescence activity by itself[580]. Indeed, in HCT116 colon cancer cells, secreted IL-6 and activated STAT3 are required for proliferation response[581]. More studies are clearly required to understand the role of SASP.

In this study, no increase in the cell death rate was observed in the course of the experiments. The major cell phenotype was premature senescence. The interplay between apoptosis and senescence is not well-understood. Obviously, a cell must not undergo apoptosis to enter senescence. Often, fibroblast senescence has been linked with apoptosis resistance through mechanisms that are not well-understood. Senescent human fibroblasts are more resistant to oxidative stress-induced apoptosis compared to non-senescent cells. This has been associated with high level expression of anti-apoptotic proteins, including Bcl-2[582], survivin[583], c-myb[584], major vault protein[585] and low Bax expression[586]. Senescent human diploid fibroblasts are shown to be associated with

globally increased repressive histone modification (H4K20Me3), but enriched in association with *BAX*; in contrast, although the active histone modification (H4K16Ac) is globally decreased in senescent human diploid fibroblasts, it is enriched at locus in association with *BCL-2*, consistent with a high Bcl-2 to Bax protein ratio in senescent human diploid fibroblasts[586]. Compared to *BCL-2* locus, the epigenetic modification at *BCL-X* locus remains to be studied. Nevertheless, one can argue the possibility of similar epigenetic modifications at the *BCL-X* locus during senescence alike *BCL-2*. Moreover, expressing the anti-apoptotic protein Bcl-xL in our study, certainly contribute to apoptosis resistance in the BJ cells in a similar fashion.

Although not investigated in our study, others have reported that chromatin modifications are needed to modulate gene expression that induce and support the establishment of a senescence-like state[588]. Methylation and acetylation of lysine residues on the tail of nucleosome core histones have a pivotal role in the regulation of gene expression[589]. The N-terminal region of histone proteins is subjected to various post-translational modifications, including acetylation, methylation, sumoylation and phosphorylation, which constitute the so-called histone code[590]. In general, histone acetylation enhances gene transcription, while histone methylation determines transcriptional repression or activation, depending on the particular lysine residue that is methylated. Histone acetylation and deacetylation are balanced by the activities of HATs and HDACs[589]. HAT activity is lowered in senescent fibroblasts[586]. Reduced H4K16 acetylation is strongly correlated with cellular senescence[591]. Mof, an HAT, is responsible for the acetylation of H4K16[592] and its expression is reduced in senescent cells[592]. Sirt1, an HDAC, has been reported to deacetylate H4K16[593] and increased Sirt1 expression is observed in senescent cells[586].

The methytransferase Suv4-20h1/2 is active in senescent cells and mediates histone H4 lysine 20 tri-methylation (H4K20Me3), a modification associated with transcriptional repression[594]. Interestingly, ChIP analysis revealed that the *BCL2* gene was significantly enriched in acetylated H4K16, while *BAX* gene was enriched with methylated H4K20Me3[586] in senescent cells. This shows how epigenetic mechanisms play role in the regulation of apoptosis-related gene expression, that, in turn, support the establishment of senescence. Other histone modification relevant to cellular senescence include

H3K27Me3 and H3K9Me3, that are catalyzed by Suv39H1/2 and Ezh1/2[595].

Cellular senescence is associated with profound chromatin changes. The most dramatic is the formation of senescence-associated heterochromatin foci (SAHF), visually seen with discrete DAPI-dense regions. SAHF present highly compacted heterochromatin that stains with H3K9Me3, Hp1 proteins, and macroH2A[380]. SAHF have been proposed to enforce and maintain senescence by suppressing the transcription of proliferative E2f-target genes[379]. Indeed the promoters of these genes are stably repressed in senescent cells[379].

H3K9Me3 seems to serve as a specific binding site for the chromodomain heterochromatin proteins Hp1[343,596-599], which in turn recruits DNA methyltransferase Dnmt3a and Dnmt3b[600,601]. H3K9 methytransferase-deficient *Suv39h1/2* double knock-out cells show that Hp1 proteins and Dnmt3b fail to concentrate at heterochromatin foci[602,603]. H3K9 trimethylation clusters may provide a proper environment to recruit DNA methyltransferases coupled with CpG dinucleotide methylation. These CpG dinucleotides are not evenly distributed across the genome, but are concentrated either within short CpG-rich sequences, called CpG islands, in or near approximately 40% of gene promoters, or within repetitive sequences, including large centromeric/pericentromeric repeats and retro-transposon elements, to ensure silencing of these elements. Global DNA methylation changes have been observed in human fibroblasts undergoing hydrogen peroxide-induced premature senescence[604], due to progressive loss of Dnmt1 methyltransferase activity[605,606]. Demethylation of pericentric satellite II and III DNA has been reported in senescent human fibroblasts[607]. Demethylation of genomic DNA may allow transcription of repetitive DNA sequences. Increased transcription of human pericentromeric satellite DNA has been reported in senescent fibroblasts and correlated with demethylation of the locus[608].

5.4 Ser49 and Ser62 of the Bcl-xL loop domain contributes to the maintenance of chromosome stability in BJ cells

Two experimental approaches were undertaken in BJ cells to monitor chromosome instability. First, fluorescent *in situ* hybridization (FISH) assays were performed with a fluorescent-labeled chromosome 6 subcentromeric enumerization DNA probe. This assay

has the advantage of detecting aneuploidy in interphasic cells, whether they are proliferating, non-proliferating or senescent. BJ cells expressing Bcl-xL phospho-mutants showed significantly increased chromosome instability that correlates with senescence output. Interestingly, the majority of cells harboring aneuploidy according to this assay also disclosed enhanced p21 and reduced Ki-67 expression. The occurrence of aneuploidy in these cells is concordant with our previous work on cancer cells[101-103] revealing that sequential phosphorylation and dephosphorylation of Bcl-xL (Ser49) and (Ser62) during mitosis are key events that prevent mitotic defects associated with MT-kinetochore attachment, chromosome segregation and cytokinesis failure. Giemsa-banding assay was performed at various population doublings of control BJ fibroblasts or cells expressing Bcl-xL phospho-mutants. Some of the BJ fibroblast cells expressing Bcl-xL phospho-mutants revealed various random chromosomal structural rearrangement, including deletion, translocation or addition of chromosomal materials. This assay was performed on metaphase cells indicating that although the occurrence of senescence seems to be the main phenotype, some cells that harbor aneuploidy still have a proliferating potency. These findings were in agreement with the immunofluorescence studies where very few cells harboring chromosome 6 aneuploidy where negative for p21 and positive for Ki-67. It suggests a mosaic of responses where a few cells can escape senescence for at least a few cell cycles. This important observation will be addressed in the future as it may have consequence, at least in theory, for immortalization or cancer development in an eventual scenario where other mutations leading to oncogene activation and tumour suppressor gene inactivation occur in the same cells. Our observations are similar to those of others (reviewed in section 1.6.1) who suggested that modulation of the expression of SAC components could lead to aneuploidy and senescence.

5.5 Expression of Bcl-xL (Ser49) and (Ser62) mutants affects germline development in *C. elegans*

C. elegans is a model well-suited to study the consequences of DNA damage and repair deficiency with respect to tissue decline and aging. Replicative declines can be caused by accumulation of stochastic DNA damage that blocks replication and induces

cell cycle checkpoints[609]. DNA damage can contribute to trans-generational functional decline that can include growth and developmental arrest of germ cells, embryos, larvae and adult animals with reduction of viability observed after ultraviolet irradiation of *C. elegans*[610-612]. Accumulation of DNA damage can contribute to diminished growth and fecundity. When mutated, different genes have been found to increase the lifespan of *C. elegans*. The mammalian homologue of insulin and insulin-like growth factor 1 (IGF-1) signaling pathway *daf-2,* when mutated, can extend *C. elegans* lifespan up to three-fold[613-615]. During *C. elegans* larval development, the PI3K pathway, composed of the insulin/IGF-1 receptor tyrosine kinase (InsR) DAF-2, the PI3K AGE-1 and the 3-phosphoinositide-dependent protein kinase PDK-1, controls the redundant activities of AKT-1 and AKT-2 on the forkhead transcription factor DAF-16[616,617]. Phosphorylation of DAF-16 by AKT-1/AKT-2 prevents the translocation of DAF-16 into the nucleus and the subsequent induction of genes required for lifespan[618] and stress response[619]. Whereas AKT-1 dampens the transcriptional activity of the p53 family member CEP-1, AKT-2 functions independently or downstream of CEP-1. AKT-1 transmits an anti-apoptotic signal by negatively regulating the p53-like transcription factor CEP-1[620]. Interestingly components of the worm PI3K pathway upstream of *akt-1* (Daf-2, Age-1) opposes its anti-apoptotic function. DAF-2 and PDK-1 selectively engage AKT-2, DAF-16/FOXO and the RAS/MAPK pathway to promote apoptosis of damaged germ cells[621]. The *C. elegans* p53 gene, *cep-1*, is not a DAF-16/FOXO target gene. Instead, it is postulated that DAF-16/FOXO induces the same response in cells as if they were under genotoxic stress, enabling p53 to stimulate apoptosis[622]. *daf-2* mutation can stimulate apoptosis in *gld-1* germlines and in wt germline cells undergoing apoptosis. Therefore, *daf-2* mutations appear to trigger a general increase in germline cell death[623]. Furthermore, loss-of-function of the nucleotide excision repair protein ERCC-1/XPF can extend the lifespan in *daf-2* mutants via increased germline apoptosis[624]. The effect of CEP-1 (ortholog of mammalian p53) on longevity in worms is controversial[623,625-627]. Physiological apoptosis is part of *C. elegans* development wherein a fixed number of oogenic germ cells die during the development wherein a fixed number of oogenic germ cells die during development of the worm and are proposed to serve as nurse cells for maturing oocytes[482].

In our study, although CED-9 protein, which corresponds to Bcl-2 and Bcl-xL orthologs in *C. elegans*, lacks the functional loop domain, it is possible that the loop domain function is conserved within an another protein in *C. elegans*. We therefore hypothesized that the expression of Bcl-xL and its mutants will undergo gain-of-function and have dominant effects on mitotic behaviors and in the development of the worms. The Bcl-xL cDNAs coding for the wt and mutant proteins (S49A, S62A, S49/62A, S49D, S62D, S49/62D) were constructed under control of the *ced-9* promoter and common *C. elegans* 3'-UTR region to achieve physiological expression compared to its endogenous homolog *ced-9*. Transgenic worms with Bcl-xL (wt) and its variants were derived according to the MosSCI technique[514]. For unknown reasons, despite several attempts, no transgenic worms expressing the S49/62D mutant were obtained. All transgenic worms were homozygous for Bcl-xL (wt) and its mutants, and the insertions were tested by PCR and sequenced. N2 (wt) strain was used as controls for the assays.

qRT-PCR assays showed similar expression of Bcl-xL (wt) and its mutants in the transgenic worms. *pmp3* and *ced-9* were used as control reference gene in qRT-PCR assays[628]. Only young adults (12 h post-synchronized L4 stage) were studied. In our experiments, we examined and calculated the number of eggs laid by transgenic worms expressing Bcl-xL (wt) and its mutants, and found significantly fewer number of eggs laid in the Bcl-xL mutants transgenic worms compared to N2 controls and worms with Bcl-xL (wt). When these eggs were monitored post-10 h, again, a decreased number of them hatched into L1 larvae across most of mutants compared to N2 controls and Bcl-xL (wt) transgenic worms. This was probably due to the introduction of Bcl-xL loop domain mutants into the *C. elegans* system where it might interfere with the normal progression of mitosis and presumably evokes chromosome instability. This impairment may be enough to stall mitosis and activate cell cycle checkpoints.

5.6 Expression of Bcl-xL (Ser62) and (Ser49) mutants lead to chromosomal instability and cellular apoptosis in *C. elegans*

The gonad arm provides an excellent location to study effects on the cell cycle. Germ cells progress from mitosis into meiosis as they pass through the gonadic arm. In each region, underlying specific control regulates this progression and maintains chromosome

stability. *C. elegans* has emerged as an excellent model for molecular studies of mitosis and meiosis, enabling investigators to combine the power of molecular genetics, cytology and live analysis. *C. elegans* bears holokinetochores, and kinetochores of other eukaryotes share conserved properties structurally and functionally. Gonad dissection followed by DAPI staining disclosed the presence of aberrant cells in the gonads of young adult hermaphrodite transgenic worms expressing Bcl-xL mutants. The mitotic regions appeared shorter in most mutants (except the S62D variants) than in N2 controls and worms that express Bcl-xL (wt), with no significant difference in the transition zone length. It could suggests defects in the progression of mitotic germline cells to the meiotic phase, or/and increased apoptosis.

The occurrence of aneuploidy was tested in *C. elegans,* which comprises 6 chromosomes that are very visible under microscope in oocytes at their diakinesis stage of meiosis. When we looked at the gonadic arm with DAPI staining, oocytes in diakinesis stage appeared to be aneuploidic in worms expressing Bcl-xL mutants, except for S62D mutants. Also, DAPI staining in the mitotic zone of the gonads showed the presence of cells that appeared to be larger in size than surrounding cells. We suspect that these cells might be aneuploidic too, but they are difficult to visualize for aneuploidy as the chromatin is dispersed.

Transgenic worms were then crossed with strain HR1459 (*bcls39*[*lim7*:*ced-1*:GFP;*lim-15*(+)]V) to express CED-1:GFP in the sheath cells of the gonad. It is a sensitive method to visualize germ cell apoptosis, CED-1:GFP highlightening the somatic sheath cell cluster around each apoptotic germ cell during engulfment[629]. CED-1 is a phagocytic receptor that initiates pathway for degrading engulfed apoptotic cells[630]. Increased CED-1:GFP expression was seen in all mutants with the exception of S62D mutants. Furthermore, DAPI staining of the gonadic arm revealed a disorganized pattern of germ cells in worms containing the Bcl-xL mutants. The exact reason of this phenotype is not well understood. One putative reason could be due to cell apoptosis due to chromosome instability. Germ cells that undergo apoptosis lose their attachment to neighboring cells in the gonads and are cellularized for engulfment by sheath cells[631]. Overall, the Bcl-xL mutations, except S62D variants, probably lead to errors in chromosome segregation that result in aneuploidy. Apoptosis was not seen in the

intestinal cells (data not shown), in agreement with the literature showing their resistance to apoptosis[632].

How Bcl-xL interacts with the *C. elegans* machinery to maintain chromosome stability is unknown. In *C. elegans* the attachment of sister chromosomes to microtubules can be achieved by proper chromosomal organization, which relies on orchestrated spatio-temporal functions of conserved protein complexes such as the cohesin, condensin, and chromosomal passenger complexes during mitosis and meiosis. The structure of SAC components and their safeguard function are also well-conserved in *C. elegans*. Kinetochore assembly in *C. elegans* depends on 2 conserved proteins, the holocentric proteins HCP-3/CeCENP-A and its associating protein, HCP-4/CeCENP-C[633]. HCP-3/CeCENP-A with chromatin creates the foundation for kinetochore assembly, whereas HCP-4/CeCENP-C serves as a linker between HCP-3/CeCENP-A chromatin and the highly ordered outer kinetochore complex. Depletion of HCP-3/CeCENP-A causes misassembly of functional kinetochores, leading to complete to loss of kinetochore-microtubule attachment. Kinetochore localization of HCP-4/CeCENP-C depends on HCP-3/CeCENP-A and is required for the localization of all kinetochore proteins, except HCP-3/CeCENP-A[634,635]. During interphase, KNL2 protein and HCP-3/CeNP-A are in physical proximity on the chromatin[636]. KNL-2 depletion causes similar chromosome condensation defects as those observed in cells depleted of HCP-3/CeCENP-A. These results suggest that KNL-2 is important in chromosome condensation and kinetochore assembly by physically and functionally interacting with HCP-3/CeCENP-A[636]. KNL-3 lies downstream of HCP-3/CeCENP-A and HCP-4/CeCENP-C and is upstream of KNL-1 in a linear-assembly hierarchy, and HCP-4/CeCENP-C connects the KMN network to HCP-3/CeCENP-A chromatin by interacting with KNL-3[637].

Conserved chromosomal passenger complexes are crucial for accurate chromosome segregation by correcting aberrant microtubule-kinetochore attachment[307]. *C. elegans* chromosomal passenger complex is composed of AIR-2 and three non-enzymatic proteins, BIR-1/Survivin, ICP-1/INCENP, and CSC-1/BIR-1[638]. CSC-1/ BIR-1 depletion causes a defect in mitotic chromosome segregation identical to AIR-2 depletion[639]. AIR-2 activity regulates NDC-80 microtubule-binding status, which, in turn, regulates the chromosomal passenger complex–dependent elimination of incorrect kinetochore-

microtubule attachment[167]. Whether or not, and how, human Bcl-xL interplays with these *C. elegans* components remains to be elucidated.

DNA damage and chromosomal instability lead to apoptosis in *C. elegans*. The *C. elegans* DNA damage response mutants *mrt-2*, *hus-1*, and *clk-2(mn159)* display 8- to 15-fold increases in the frequency of spontaneous mutation in their germlines[640]. Checkpoint proteins such as 9-1-1 complexes or ATL-1, can either initiate apoptosis in meiotic germ cells at the pachytene stage or cell cycle arrest in the mitotic germ cells[487,641]. Somatic cells are refractory to cellular responses to DNA damage[484]. Deficiency for the *C. elegans* HUS-1 or MRT-2 results in defective responses to both ionizing radiation (IR)-induced apoptosis and cell cycle arrest in germ cells[486,642]. Mutation of CLK-2 can confer additional defect in the S-phase DNA-replication checkpoint and has been show to act downstream of ATL-1 which interacts with DNA strand-breaks[487]. In *C. elegant*, HUS-1 mediates an apoptotic response to DNA damage and acts cell-autonomously to control mitotic checkpoints. After DNA damage, it is delocalized in the nucleus to distinct foci that are likely sites of double strand-breaks. RAD-51 is required for efficient repair of DNA damage either downstream or independent of HUS-1[642]. Deletion of *hus-1* also shows meoitic non-disjunction and/or chromosome loss. Chromosome abnormalities are also documented in mouse *HUS-1*$^{-/-}$ cells[643]. Hus-1 is required to prevent telomere shortening during genomic replication. Compared to mammalian cells, *C. elegans* does not undergo cell cycle arrest at loss-of-*cep-1* in response to DNA damage, suggesting that induction of apoptosis might have been the original role of p53 family members along evolution. CEP-1 function is essential for HUS-1-mediated apoptosis. Induction of EGL-1 requires also HUS-1 and CEP-1. HUS-1 and CEP-1 likely functions in a common pathway to activate the apoptotic pathway in *C. elegans*.

5.7 Expression of Bcl-xL (Ser62) and (Ser49) mutants affects *C. elegans* lifespan

Finally, when we measured the lifespan of transgenic worms, we did not see any significant differences between the N2 controls and worms expressing Bcl-xL (wt) and the Ser to Asp mutants. In comparison, worms expressing the Ser to Ala variants showed an increase in lifespan. This could be due to the increase of apoptotic cells monitored in the germ cells that serve as nurse cell in those worms. However, the exact pathway for

this phenotype has yet to be examined and requires further work. In future, RNA sequencing could help to identify the variations of gene expression in worms expressing the Bcl-xL mutants that perhaps contribute to the longevity of these transgenic worms. Similarly, variations of gene expression could help explain the discrepancy with the Ser49D variants.

5.8 Future perspectives

Our study documented the importance of two residues in the Bcl-xL loop domain for the maintenance of chromosome stability in two experimental models. These results and those reported previously by the laboratory, bring us to various future avenues to understand the interaction of the Bcl-xL loop domain with various cellular components during mitosis and to gain better insights into the molecular mechanisms behind the observed phenotypes.

5.8.1 Bcl-xL (Ser62) and MCC complexes for SAC activation and SAC resolution

Previously, our laboratory reported that phospho-Bcl-xL(Ser62) binds to MCC complexes at early step of mitosis, during prophase, metaphase and the metaphase-anaphase boundary. MCC complex consists of Mad2, BubR1, Bub3 along with Cdc20-bound complexes. In contrast, this association does not appear when Ser62 is mutated to Ala. It suggests the potential role of phospho-Bcl-xL(Ser62) at checkpoint scrutiny before the onset of anaphase. To analyse the orderly interaction of phospho-Bcl-xL(Ser62) with MCC and its consequence on SAC activation/resolution, reconstitution in a cell-free system[644] will be deployed.

Briefly, kinetochore-mediated SAC signalling is reconstructed by adding sequentially, one by one, purified components of the SAC to isolated chromosomes with unattached kinetochores and then, the resulting effects on the ubiquitin-ligase activity of APC/C are measured with purified cyclin B1, as substrate[644]. By incorporating sequentially recombinant Bcl-xL (wt), phospho-Bcl-xL(Ser62) or Bcl-xL(S62A) or Bcl-xL(S62D) (but also Bcl-xL(S49A) or Bcl-xL(S49D) as additional controls) to the system, we will determine the molecular interactions between Bcl-xL and its phosphorylation mutants to the described Cdc20- Mad2- BubR1- Bub3 -bound complexes, and their

effects on APC^{cdc20} ubiquitin-ligase activity. Chromosomes with unattached kinetochores will be obtained from colcemid-arrested HeLa mitotic cells (16 h treatment) expressing GFP-H2B collected by mitotic shake-off and then, subjected to hypotonic conditions. Lysates will be purified by 2 successive sucrose step gradient (30%-40%-50%-60% layers) to obtain highly purified chromosomes[644]. The presence of GFP-H2B will facilitate detection of the chromosomes during the purification procedure and will allow us to visualize the quality of the preparations under a microscope. APC/C is obtained by immunoprecipitation using a peptide-derived Cdc27 antibody linked to protein A/G sepharose beads. Incubation of the purified chromosomes with various SAC components at equimolar concentration, alone and in various combinations, in the presence or absence of Bcl-xL (wt), or phospho-Bcl-xL(Ser62) or Bcl-xL(S62A) or Bcl-xL(S62D) or Bcl-xL(S49A) or Bcl-xL(S49D), and APC/C beads will be tested. The APC/C-unbound complexes remaining in the soluble fraction, will contain Cdc20- Mad2- BubR1- Bub3 -bound complexes in association or not, with various Bcl-xL forms. These protein complexes will be resolved by Superose 6 gel filtration chromatography, and proteins in each column fraction analyzed by SDS-PAGE and western blotting. Complex formation will be analysed by gel filtration chromatography and the resulting effects on the APC/C ubiquitin ligase activity analysed with cyclin B1 as a substrate.

By adding Bcl-xL (wt), phospho-Bcl-xL(Ser62) and mutants to the system, we will carefully define their interaction and their effects on SAC activation and resolution. If phospho-Bcl-xL(Ser62) leads to SAC activation or resolution, it will be visible with decreasing or increasing *in vitro* APC/C ubiquitin ligase activity on cyclin B1 ubiquitination. If this hypothesis is true it will open new doors to understand how Bcl-xL influence SAC functions. By comprehending the molecular interaction, it would be possible to design simple screening assays and develop new inhibitors of this activity. The Bcl-xL loop domain will unveil the importance of an anti-apoptotic protein working hand-in-hand in controlling the segregation of mitotic chromosome and, in turn, deciding the fate of cells.

In addition, to further elucidate the role of Bcl-xL during the progression of mitosis, Bcl-xL expression can be targeted at a specific step of mitosis progression taking advantage of the specific APC/C activity at the metaphase-anaphase boundary, and that

of our Bcl-xL cDNA constructs that are resistant to specific siRNA[103]. Indeed, APC/C is an ubiquitin ligase that regulates metaphase to anaphase transition by targeting specific substrates[645]. The APC/C co-activators, Cdc20 and Cdh1, function as specific adaptor proteins to recruit specific substrates to APC/C by their capacity to recognize 2 conserved degron motifs present in APC/C substrates; the 9 residue destruction box or D box[646] and the K-E-N (Lys-Glu-Asn) signal, also called the KEN box[647]. The D box is engaged by Cdc20 and one of the core APC/C subunit, Apc10[648] at the metaphase to anaphase step of mitosis. Both Cdc20 and Apc10 contribute to D-box-dependent recognition and processive ubiquitylation step[648] of D box-containing proteins including securin and cyclin B1 promoting the metaphase-to-anaphase transition[645]. The D-box peptide NVPKKRHALDDVSNFHNK [648] can be fused to the N-terminal of Bcl-xL wt and mutant variant constructs and expressed in BJ fibroblast using lentiviral expression system. In association with specific siRNAs that target endogenous Bcl-xL expression without affecting the expression of our constructs[103], we will be able to modulate Bcl-xL expression specifically at the metaphase to anaphase transition. The D-box henceforth will be recognized at the metaphase-anaphase boundary by APC/C – Cdc20 complexes, that will target D box-containing Bcl-xL protein for degradation. This will reveal the importance of Bcl-xL at the metaphase-anaphase boundary by manipulating its expression level at this specific step of mitosis.

5.8.2 Bcl-xL (Ser49) and (Ser62) and its interaction with cytoplasmic dynein

Our laboratory has also shown that phospho-Bcl-xL (Ser49) is found in centrosomes during G2 and phospho-Bcl-xL(Ser62) is also encountered at centrosomes with γ-tubulin and along the microtubule spindle with dynein proteins during prophase, metaphase and the metaphase-anaphase boundary. Dynein proteins are required for the attachment and migration of centrosomes along the nuclear envelope during interphase and to maintain the attachment of centrosomes to mitotic spindle poles[649]. To understand the role of phospho-Bcl-xL(Ser49) and phospho-Bcl-xL(Ser62) at these locations, we can use *Drosophila menalogaster*, which provides exceptional cytology to analyze dynein proteins in mitosis in both embryos and somatic cells[649].

Transgenic *Drosophila menalogaster* for Bcl-xL and its mutants can be created with

the phage ϕC31 integrase system which catalyzes recombination between two non-identical recognition sites, attP and attB[650,651]. ϕC31-mediated recombination generates stable integrants that cannot be excised or further exchanged[652]. Interaction between Bcl-xL(wt) and variants with the dynein heavy chain Dhc64C will be studied in the syncytial embryo. Immunoprecipitation and immunofluorescence assays will be used to see the effect of Bcl-xL (wt) and mutants on mictrotubule elongation, formation and assembly during mitosis, from centrosome to cytoplasm. Dhc64C inhibition can be achieved with ciliobrevin-D, a cell permeable, reversible and specific blocker of cytoplasmic dynein. It can disrupt spindle pole focusing and kinetochore microtubule attachment[653]. Inhibiting Dhc64C will shed light on whether Bcl-xL uses dynein during mitotic progression to change its location from centrosomes to spindle. Live cell imaging on embryos will help to dissect Bcl-xL interaction with dynein motor proteins.

5.8.3 Bcl-xL (Ser49) and membrane remodelling and trafficking

Phospho-Bcl-xL(Ser49) is located at mid-zone bodies during telophase and cytokinesis[101], a location where dynamin and dynamin-related proteins have been shown to play essential roles in membrane remodelling for cytokinesis[654]. Membrane vesicle trafficking and vesicle fusion to existing membrane regulate the addition of new membranes along the ingressing cleavage furrow at the mid-zone[654,655]. The process involved a complex molecular machinery, including Syntaxins, Rab, Dynamin and Dynamin-like family GTPases, Kinesin, Dynein motor proteins, and subunits of the ESCRT complex[654,655]. Similar membrane fusion occurs in synaptic endocytosis of hippocampal neurons, where Dynamin-1 (Dyn-1) and the Dynamin-like GTPase (Drp-1) co-localizes with Bcl-xL. Bcl-xL binds to and activates the GTPase activity of Drp1, which in turn, enhances the rate of membrane remodeling and recycling[75,656].

We suggest from these lines of evidence that Bcl-xL(Ser49) could interact with Dyn-1 and Drp-1 at the mid-zone bodies to enhance membrane fusion and facilitate cytokinesis. To observe this, first, direct interaction between phospho-Bcl-xL(S49) and mutants with Drp1 and Dyn1 at mid-zone bodies will be monitored in cells by immunofluorescence microscopy. In parallel, co-immunoprecipitation and reversed co-immunoprecipitation studies of phospho-Bcl-xL(S49) and mutants with Drp1 and Dyn1

will be performed from cells highly enriched at telophase and cytokinesis. Second, to visualize membrane fusion mechanisms at mid-zone bodies that will provide the necessary membrane for complete abscission of mother cell into two daughters cells, live-cell microscopy will be performed using the cell membrane marker MyrPalm-mCherry[657]. Cells expressing YFP-Bcl-xL (wt) and mutants with CFP-tagged H2B will be infected to express MyrPalm-mCherry to visualize plasma membrane association and addition at mid-zone bodies. These experiments, in addition to permit visualization of plasma membrane at mid-zone bodies until abscission, will allow us to measure the length of mitosis exit from anaphase onset to complete abscission. In parallel, these experiments will monitor the location of YFP-Bcl-xL and its mutants at mid-zone bodies in live-cells. Its is expected that cells expressing the phosphorylation mutant YFP-Bcl-xL(Ser49A) will show defect in plasma membrane assembly with plasma membrane detached from the mid-zone body leading to cytokinesis failure. A variation of these experiments will imply the silencing of Drp1 and Dyn1[75], to further document their roles in association with Bcl-xL in membrane remodeling during cytokinesis. A key control of these experiments will consist of expressing MgcRacGap mutant lacking its C1 domain - a protein interacting domain with phosphoinositide lipids[657]. Indeed, this mutant prevents association of the protein with the plasma membrane, leading to plasma membrane detachment at the mid-zone body and cytokinesis failure[657]. Knowing the molecular interaction involved in the process could help in the design screening assays and develop novel specific inhibitors of the process.

5.8.4 Bcl-xL and mouse embryonic development

Though our lab has so far studied the role of Bcl-xL (Ser62) and (Ser49) *in vitro* and *in vivo* in *C. elegans*. These two residues and the loop domain are well conserved in mouse Bcl-xL. The mouse model will be used to investigate and distinguish the two functions of Bcl-xL, its anti-apoptotic and cell cycle function, during early embryogenesis and organogenesis. To achieve this goal, we can use mice homozygous in the C57BL/6J background expressing H2B-GFP, and CRISP /Cas9 system to create embryos with Bcl-xL (wt) and various mutants. CRISP-Cas9 system is an excellent knock-in system for gene editing[658,659]. In brief, recombinant Bcl-x DNA template

containing Bcl-xL (wt) and Ser49 and Ser62 mutants will be microinjected into the two-cell stage of oocyte. In parallel, to distinguish mitotic function from anti-apoptotic functions, Bcl-xL will be mutated at the conserved NWGR sequence located in its BH1 domain at Trp137 and Arg139 residues. All embryos in this experiment will contain the inherent histone H2B-GFP for better chromatin/chromosome visualization. First, we will isolate two-cell embryo to monitor the kinetic behaviours of early cell division and segmentation during the early cell division *ex vivo*, from morula to blastocyst starting from the 8-16 cell stage to the 64-128 cell stage, by life fluorescence imaging. It will allow us to study the effects of Bcl-xL and its mutants during early embryogenesis. Simultaneously, the anti-apoptotic role of Bcl-xL and its mutants carrying mutation at Trp137 and Arg139, will be monitored for the first time in early cell division of embryo post-fertilization.

In parallel, the CRISPR/Cas-edited blastocytes containing various Bcl-x mutants will be implanted into the uterine walls for gastrulation and organogenesis development. Whole mice histological phenotypes will be analyzed in detail in developing embryos post-implantation, to detect growth disturbances and pathological changes at the microscopic level. The embryos will be properly controlled to validate the DNA sequence of the *BCLX* gene. During development, various tissues will be collected at various intervals post-implantation. First, simple hematoxylin-eosin staining will be undertaken. Further analyses would involved FISH for aneuploidy analysis, TUNEL assay for cell death analysis, SA-β-gal assay for senescence analysis, and immunofluorescence microscopy for Bcl-xL expression in various tissues. Specific bio-markers will characterize sub-cell type population abundance, primarily focusing on the hematopoietic system with flow cytometry. This study will allow us to address the importance of Bcl-xL mitotic function versus its anti-apoptotic function during early development.

5.8.5 Bcl-xL and cell fate

Bcl-xL is very rarely mutated in human tumors, suggesting that putative key mutations within Bcl-xL would be unsuitable for cell proliferation and survival. Indeed, tumor cells are believed to depend on, or are addicted to, anti-apoptotic Bcl-2 family members, including Bcl-xL[660]. This addiction provides a selective advantage to cancer

cells by allowing them to survive cell stress phenotypes and/or cell death signals that directly ensue from oncogenic signaling, tumor suppressor deficiency or anticancer treatments[660]. In normal BJ cells challenged with Bcl-xL (Ser49) and (Ser62) mutants, aneuploidy occurs with outbreak of senescence. What would be the consequences of inhibiting senescence in these cells? Whether the cells will die or undergo an immortalization and/or tumourigenesis path is yet unknown. We could take advantage of the Bcl-xL mutant properties that cause aneuploidy but maintain its anti-apoptotic activity in normal BJ cells. The system will permit the investigation of the interplays between aneuploidy, senescence, apoptosis and immortalization/tumorigenesis. To block senescence in these cells, we will inhibit p53 activity or expression, as well as silencing p21 expression. We will also express oncogene like Ha-Ras or c-Myc and evaluate if any combinations could lead to an immortalization and tumorigenesis path. Similarly,t he knock-in *Bclx* mutant mice obtained in the previous section, could be crossed with mice expressing oncogenes like *c-Myc* or *Ha-Ras*, or with mice that lack tumor suppressor genes like *p53* or *p21* to study the potential input of Bcl-xL and its cell cycle function mutants and anti-apoptotic mutants, on immortalization, tumor initiation, development and progression.

6. Summary of major findings

The first appended manuscript reports that Bcl-xL undergoes dynamic phosphorylation and dephosphorylation in normal BJ diploid fibroblasts at Ser62 during prometaphase, metaphase and anaphase boundary. In contrast, the Bcl-xL (Ser49) residue undergoes phosphorylation during telophase and cytokinesis. This phosphorylation/ dephosphorylation process has been previously observed in cancer cells[101-103]. In BJ normal cells, expression of Bcl-xL (Ser49) and (Ser62) mutants lead to chromosomal instability, increased expression of p53 and p21, recruitment of γ-H2A.X at chromatin foci and activation of senescence. Senescence was detected with increased activity of SA-β-Gal staining. They also showed increased secretion of IL-6, a marker of SASP. Immunofluorescence and G-banding reveal the presence of chromosomal structural mutations and aneuploidy. A schematic view of our findings is presented in Figure 22.

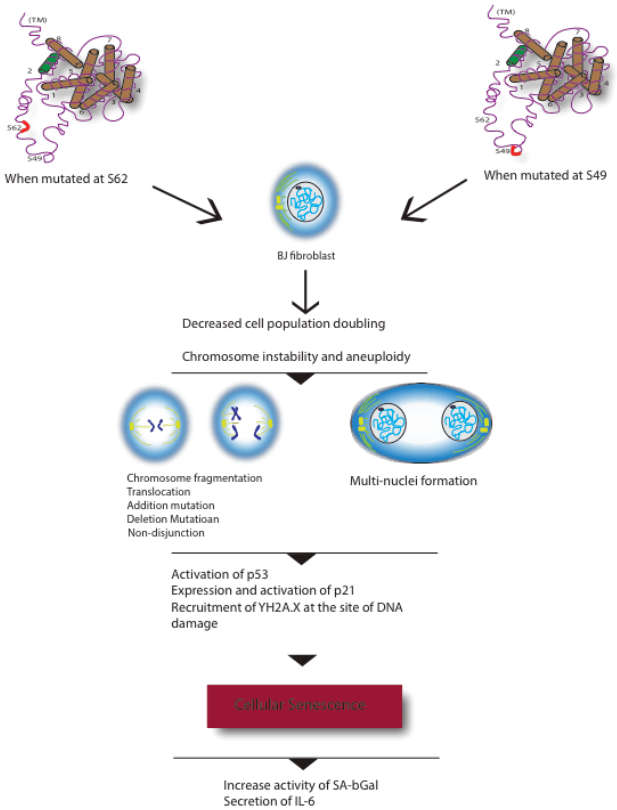

Figure 22. Summary of major finding in normal human BJ fibroblasts.

The second appended manuscript reports that when Bcl-xL (Ser49) and (Ser62) mutants are introduced and expressed in *C. elegans*, they interfere with normal mitosis progression in the germline. These mutations result in chromosome instability and aneuploidy, visualized by abnormal chromosome at diplotene germ cell stage. These effects also trigger apoptosis in the germline. Apoptosis also leads to the spatial disorganization of germ cells, lowered fecundity and variations in the length of mitotic regions and transition zones in the gonads. Germline apoptosis may be the reason for a slight increment of lifespan of these worms. A schematic view of the findings is presented in Figure 23.

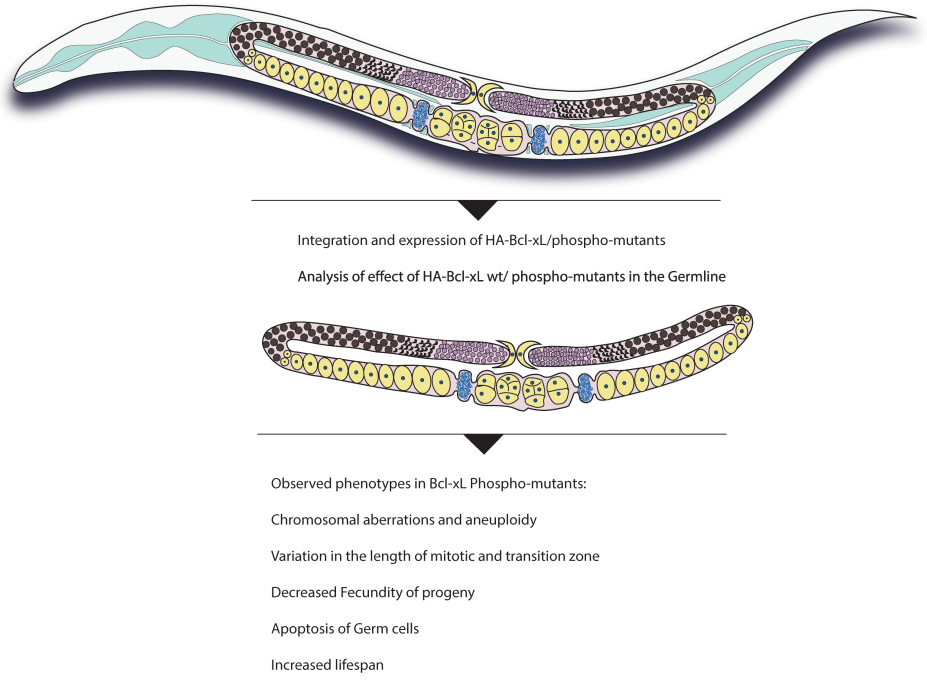

Figure 23: Summary of major finding in *C. elegans*

7. Bibliography

1. Hartwell, L., Weinert, T., Kadyk, L. & Garvik, B. Cell Cycle Checkpoints, Genomic Integrity, and Cancer. *Cold Spring Harbor Symposia on Quantitative Biology* **59**, 259-263 (1994).
2. Hunter, T. & Pines, J. Cyclins and cancer. 2: Cyclin D and CDK inhibitors come of age. *Cell* **79**, 573-582 (1994).
3. Nigg, E.A. Cyclin-dependent protein kinases; key regulators of the eucaryotic cell cycle *Bioessays* **17**, 471-480 (1995).
4. Morgan, D.O. Principles of CDK regulation. *Nature* **374**, 131-134 (1995).
5. Schmitt, C.A. Senescence, apoptosis and therapy--cutting the lifelines of cancer. *Nat Rev Cancer* **3**, 286-295 (2003).
6. Nurse, P. Cyclin dependent Kinases and cell cycle control (Nobel Lecture). *Chembiochem* **3**, 596-603 (2002).
7. Nurse, P. A long twentieth century of the cell cycle and beyond. *Cell* **100**, 71-78 (2000).
8. Kohn, K.W., Jackman, J. & O'Connor, P.M. Cell cycle control and cancer chemotherapy. *J Cell Biochem* **54**, 440-452 (1994).
9. Kastan, M.B., Canman, C.E. & Leonard, C.J. p53, cell cycle control and apoptosis: implications for cancer. *Cancer Metast Rev* **14**, 3-15 (1995).
10. Bharadwaj, R. & Yu, H. The spindle checkpoint, aneuploidy, and cancer. *Oncogene* **23**, 2016-2027 (2004).
11. Abraham, R.T. Cell cycle checkpoint signaling through the ATM and ATR kinases. *Genes Dev* **15**, 2177-2196 (2001).
12. Sancar, A., Lindsey-Boltz, L.A., Unsal-Kaccmaz, K. & Linn, S. Molecular mechanisms of mammalian DNA repair and the DNA damage checkpoints. *Annu Rev Biochem* **73**, 39-85 (2004).
13. Hanahan, D. & Weinberg, R.A. The hallmarks of cancer. *Cell* **100**, 57-70 (2000).
14. Hanahan, D. & Weinberg, R.A. Hallmarks of cancer: the next generation. *Cell* **144**, 642-674 (2011).
15. Hayflick, I. & Moorhead, P.S. The serial cultivation of human diploid cell strains. *Exp Cell Res* **25**, 585-621 (1961).
16. Hayflick, L. The limited in vitro lifetime of human diploid cell strains. *Exp Cell Res* **37**, 614-636 (1965).
17. Harley, C.B., Futcher, A.B. & Greider, C.W. Telomeres shorten during ageing of human fibroblasts. *Nature* **345**, 458-460 (1990).
18. Saretzki, G. Cellular senescence in the development and treatment of cancer. *Curr Pharm Des* **16**, 79-100 (2010).
19. Serrano, M. & Blasco, M.A. Putting the stress on senescence. *Curr Opin Cell Biol* **13**, 748-753 (2001).
20. Campisi, J., Andersen, J.K., Kapahi, P. & Melov, S. Cellular senescence: a link between cancer and age-related degenerative disease? *Semin Cancer Biol* **21**, 354-359 (2011).
21. Campisi, J. Cellular senescence as a tumor-suppressor mechanism. *Trends Cell Biol* **11**, S27-31 (2001).

22. Kerr, J.F., Wyllie, A.H. & Currie, A.R. Apoptosis: a basic biological phenomenon with wide-ranging implications in tissue kinetics. *Br J Cancer* **26**, 239-257 (1972).
23. Kerr, J.F. History of the events leading to the formulation of the apoptosis concept. *Toxicology* **181-182**, 471-474 (2002).
24. Horvitz, H.R. Genetic control of programmed cell death in the nematode Caenorhabditis elegans. *Cancer Res* **59**, 1701S-1706S (1999).
25. Norbury, C.J. & Hickson, I.D. Cellular responses to DNA damage. *Annu Rev Pharmacol Toxicol* **41**, 367-401 (2001).
26. Tan, M.L., Ooi, J.P., Ismail, N., Moad, A.I. & Muhammad, T.S. Programmed cell death pathways and current antitumor targets. *Pharm Res* **26**, 1547-1560 (2009).
27. Martin, S.J. & Green, D.R. Protease activation during apoptosis: death by a thousand cuts?. . *Cell* **82**, 349-352 (1995).
28. Cohen, G.M., *et al*. Formation of large molecular weight fragments of DNA is a key committed step of apoptosis in thymocytes. *J Immunol* **153**, 507-516 (1994).
29. Nishida, K., Yamaguchi, O. & Otsu, K. Crosstalk between autophagy and apoptosis in heart disease. *Circ Res* **103**, 343-351 (2008).
30. Liu, J.J., Lin, M., Yu, J.Y., Liu, B. & Bao, J.K. Targeting apoptotic and autophagic pathways for cancer therapeutics. *Cancer Lett* **300**, 105-114 (2011).
31. Huett, A., Goel, G. & Xavier, R.J. A systems biology viewpoint on autophagy in health and disease. *Current opinion in gastroenterology* **26**, 302-309 (2010).
32. Chen, S., *et al*. Autophagy is a therapeutic target in anticancer drug resistance. *Biochim Biophys Acta* **1806**, 220-229 (2010).
33. Li, Z.Y., Yang, Y., Ming, M. & Liu, B. Mitochondrial ROS generation for regulation of autophagic pathways in cancer. *Biochem Biophys Res Commun* **414**, 5-8 (2011).
34. McCall, K. Genetic control of necrosis - another type of programmed cell death. *Curr Opin Cell Biol* **22**, 882-888 (2010).
35. Leist, M. & Jaattela, M. Four deaths and a funeral: from caspases to alternative mechanisms. *Nat Rev Mol Cell Biol* **2**, 589-598 (2001).
36. Wu, W., Liu, P. & Li, J. Necroptosis: an emerging form of programmed cell death. *Crit Rev Oncol Hematol* **82**, 249-258 (2012).
37. Bialik, S., Zalckvar, E., Ber, Y., Rubinstein, A.D. & Kimchi, A. Systems biology analysis of programmed cell death. *Trends Biochem Sci*. **35**, 556-564 (2010).
38. Evan, G.I., Brown, L., Whyte, M. & Harrington, E. Apoptosis and the cell cycle. *Curr Opin Cell Biol* **7**, 825-834 (1995).
39. Lundberg, A.S. & Weinberg, R.A. Control of the cell cycle and apoptosis. *Eur J Cancer* **35**, 531-539 (1999).
40. Reed, J.C. Dysregulation of apoptosis in cancer. *J Clin Oncol* **17**, 2941-2953 (1999).
41. Evan, G.I. & Vousden, K.H. Proliferation, cell cycle and apoptosis in cancer. *Nature* **411**, 342-348 (2001).
42. Hakem, R. & Mak, T.W. Animal models of tumor-suppressor genes. *Annu Rev Genet* **35**, 209-241 (2001).
43. Wang, J. Ph.D. Thesis, Université de Montréal (2011).

44. Tsujimoto, Y. & Croce, C.M. Analysis of the structure, transcripts, and protein products of bcl-2, the gene involved in human follicular lymphoma. *Proc Natl Acad Sci USA* **83**, 5214-5218 (1986).
45. Tsujimoto, Y., Cossman, J., Jaffe, E. & Croce, C.M. Involvement of the bcl-2 gene in human follicular lymphoma. *Science* **228**, 1440-1443 (1985).
46. Adams, J.M. & Cory, S. Life-or-death decisions by the Bcl-2 protein family. *Trends Biochem Sci* **26**, 61-66 (2001).
47. Cory, S., Huang, D.C. & Adams, J.M. The Bcl-2 family: roles in cell survival and oncogenesis. *Oncogene* **22**, 8590-8607 (2003).
48. Reed, J.C. Bcl-2-family proteins and hematologic malignancies: history and future prospects. *Blood* **111**, 3322-3330 (2008).
49. Krajewski, S., *et al*. Reduced expression of proapoptotic gene BAX is associated with poor response rates to combination chemotherapy and shorter survival in women with metastatic breast adenocarcinoma. *Cancer Res* **55**, 4471-4478 (1995).
50. Brousset, P., *et al*. Frequent expression of the cell death-inducing gene Bax in Reed-Sternberg cells of Hodgkin's disease. *Blood* **87**, 2470-2475 (1996).
51. Yip, K.W., *et al*. Prognostic significance of the Epstein-Barr virus, p53, Bcl-2, and survivin in nasopharyngeal cancer. *Clin Cancer Res* **12**, 5726-5732 (2006).
52. Krajewska, M., *et al*. Expression of bcl-2 family member bid in normal and malignant tissues. *Neoplasia* **4**, 129-140 (2002).
53. Schmitt, E., Beauchemin, M. & Bertrand, R. Nuclear co-localization and interaction between Bcl-xL and Cdk1(cdc2) during G2/M cell cycle checkpoint. *Oncogene* **26**, 5851-5865 (2007).
54. Borner, C. Diminished cell proliferation associated with the death-protective activity of Bcl-2. *J Biol Chem* **271**, 12695-12698 (1996).
55. Brady, H.J.M., Gil-Gómez, G., Kirberg, J. & Berns, A.J.M. Bax-a perturbs T cell development and affects cell cycle entry of T cells. *EMBO J* **15**, 6991-7001 (1996).
56. Vairo, G., Innes, K.M. & Adams, J.M. Bcl-2 has a cell cycle inhibitory function separable from its enhancement of cell survival. *Oncogene* **13**, 1511-1519 (1996).
57. Mazel, S., Burtrum, D. & Petrie, H.T. Regulation of cell division cycle progression by Bcl-2 expression: a potential mechanism for inhibition of programmed cell death. *J Exp Med* **183**, 2219-2226 (1996).
58. O'Reilly, L.A., Huang, D.C.S. & Strasser, A. The death inhibitor Bcl-2 and its homologues influence control of cell cycle. *EMBO J* **15**, 6979-6990 (1996).
59. Chao, D.T., *et al*. Bcl-XL and Bcl-2 repress a common pathway of cell death. *J Exp Med* **182**, 821-828 (1995).
60. Linette, G.P., Li, Y., Roth, K. & Korsmeyer, S.J. Cross talk between cell death and cell cycle progression: Bcl-2 regulates Nfat-mediated activation. *Proc Natl Acad Sci USA* **93**, 9545-9552 (1996).
61. Huang, D.C.S., Oreilly, L.A., Strasser, A. & Cory, S. The anti-apoptosis function of Bcl-2 can be genetically separated from its inhibitory effect on cell cycle entry. *EMBO J* **16**, 4628-4638 (1997).
62. Knowlton, K., *et al*. Bcl-2 slows in vitro breast cancer growth despite its antiapoptotic effect. *J Surg Res* **76**, 22-26 (1998).

63. Gillardon, F., Moll, I., Meyer, M. & Michaelidis, T.M. Alterations in cell death and cell cycle progression in the UV-irradiated epidermis of Bcl-2-deficient mice. *Cell Death Differ* **6**, 55-60 (1999).
64. Fujise, K., Zhang, D., Liu, J. & Yeh, E.T. Regulation of apoptosis and cell cycle progression by Mcl1. Differential role of proliferating cell nuclear antigen. *J Biol Chem* **275**, 39458-39465 (2000).
65. Janumyan, Y.M.*, et al*. Bcl-xL/Bcl-2 coordinately regulates apoptosis, cell cycle arrest and cell cycle entry. *EMBO J* **22**, 5459-5470 (2003).
66. Jamil, S.*, et al*. A proteolytic fragment of Mcl-1 exhibits nuclear localization and regulates cell growth via interaction with Cdk1. *Biochem J* **387**, 659-667 (2005).
67. Zinkel, S.S.*, et al*. A role for proapoptotic BID in the DNA-damage response. *Cell* **122**, 579-591 (2005).
68. Jamil, S., Mojtabavi, S., Hojabrpour, P., Cheah, S. & Duronio, V. An essential role for MCL-1 in ATR-mediated CHK1 phosphorylation. *Mol Biol Cell* **19**, 3212-3220 (2008).
69. Janumyan, Y.*, et al*. G0 function of Bcl-2 and Bcl-xL requires Bax, Bak, and p27 phosphorylation by Mirk, revealing a novel role of Bax and Bak in quiescence regulation. *J Biol Chem* **283**, 34108-34120 (2008).
70. Komatsu, K.*, et al*. Human homologue of S. pombe Rad9 interacts with Bcl-2/Bcl-x L and promotes apoptosis. *Nat Cell Biol* **2**, 1-6 (2000).
71. Saintigny, Y., Dumay, A., Lambert, S. & Lopez, B.S. A novel role for the Bcl-2 protein family: specific suppression of the RAD51 recombination pathway. *EMBO J* **20**, 2596-2607 (2001).
72. Wiese, C., Pierce, A.J., Gauny, S.S., Jasin, M. & Kronenberg, A. Gene conversion is strongly induced in human cells by double-strand breaks and is modulated by the expression of Bcl-x(L). *Cancer Res* **62**, 1279-1283 (2002).
73. Youn, C.K.*, et al*. Bcl-2 expression suppresses mismatch repair activity through inhibition of E2F transcriptional activity. *Nat Cell Biol* **7**, 137-147 (2005).
74. Berman, S.B.*, et al*. Bcl-x L increases mitochondrial fission, fusion, and biomass in neurons. *J Cell Biol* **184**, 707-719 (2009).
75. Li, H.*, et al*. A Bcl-xL-Drp1 complex regulates synaptic vesicle membrane dynamics during endocytosis. *Nat Cell Biol* **15**, 773-785 (2013).
76. Schmitt, E., Paquet, C., Bergeron, S. & Bertrand, R. Interface between apoptosis and cell cycle regulation: implications for tumor proliferation and therapy. in *Recent Research Developments in Cancer*, Vol. 4 (ed. Pandalai, S.G.) 453-477 (Transworld Research Network, Trivandrum, 2002).
77. Hardwick, J.M. & Soane, L. Multiple functions of BCL-2 family proteins. *Cold Spring Harb Perspect Biol* **5**(2013).
78. Petros, A.M., Olejniczak, E.T. & Fesik, S.W. Structural biology of the Bcl-2 family of proteins. *Biochim Biophys Acta* **1644**, 83-94 (2004).
79. Czabotar, P.E., Lessene, G., Strasser, A. & Adams, J.M. Control of apoptosis by the BCL-2 protein family: implications for physiology and therapy. *Nat Rev Mol Cell Biol* **15**, 49-63 (2014).
80. Muchmore, S.W.*, et al*. X-ray and NMR structure of human Bcl-xL, an inhibitor of programmed cell death. *Nature* **381**, 335-341 (1996).

81. Yin, X.M., Oltval, Z.N. & Korsmeyer, S.J. BH1 and BH2 domains of Bcl-2 are required for inhibition of apoptosis and heterodimerization with Bax. *Nature* **369**, 321-323 (1994).
82. Sedlak, T.W., *et al*. Multiple Bcl-2 family members demonstrate selective dimerizations with Bax. *Proc Natl Acad Sci USA* **92**, 7834-7838 (1995).
83. Yang, E., *et al*. Bad, a heterodimeric partner for Bcl-xL and Bcl-2, displaces Bax and promotes cell death. *Cell* **80**, 285-291 (1995).
84. Chittenden, T. BH3 domains: intracellular death-ligands critical for initiating apoptosis. *Cancer Cell* **2**, 165-166 (2002).
85. Chittenden, T., *et al*. A conserved domain in Bak, distinct from BH1 and BH2, mediates cell death and protein binding functions. *EMBO J* **14**, 5589-5596 (1995).
86. Boyd, J.M., *et al*. Bik, a novel death-inducing protein shares a distinct sequence motif with Bcl-2 family proteins and interacts with viral and cellular survival-promoting proteins. *Oncogene* **11**, 1921-1928 (1995).
87. Sattler, M., *et al*. Structure of Bcl-x(L)-Bak peptide complex: recognition between regulators of apoptosis. *Science* **275**, 983-986 (1997).
88. Liu, X., Dai, S., Zhu, Y., Marrack, P. & Kappler, J.W. The structure of a Bcl-xL/Bim fragment complex: implications for Bim function. *Immunity* **19**, 341-352 (2003).
89. Czabotar, P.E., *et al*. Structural insights into the degradation of Mcl-1 induced by BH3 domains. *Proc Natl Acad Sci USA* **27**, 27 (2007).
90. Lee, E.F., *et al*. Conformational changes in Bcl-2 pro-survival proteins determine their capacity to bind ligands. *J Biol Chem* **284**, 30508-30517 (2009).
91. Smits, C., Czabotar, P.E., Hinds, M.G. & Day, C.L. Structural plasticity underpins promiscuous binding of the prosurvival protein A1. *Structure* **16**, 818-829 (2008).
92. Adams, J.M. & Cory, S. The Bcl-2 protein family: arbiters of cell survival. *Science* **281**, 1322-1326 (1998).
93. Green, D.R. Apoptosis - Death deceiver. *Nature* **396**, 629-630 (1998).
94. Parker, M.W. & Pattus, F. Rendering a membrane protein soluble in water: a common packing motif in bacterial protein toxins. *Trends Biochem Sci* **18**, 391-395 (1993).
95. Chang, B.S., Minn, A.J., Muchmore, S.W., Fesik, S.W. & Thompson, C.B. Identification of a novel regulatory domain in Bcl-X(L) and Bcl-2. *EMBO J* **16**, 968-977 (1997).
96. Charbonneau, J. & Gauthier, E. Protection of hybridoma cells against apoptosis by a loop domain-deficient Bcl-xL protein. *Cytotechnology* **37**, 41-47 (2001).
97. Ito, T., Deng, X.M., Carr, B. & May, W.S. Bcl-2 phosphorylation required for anti-apoptosis function. *J Biol Chem* **272**, 11671-11673 (1997).
98. Burri, S.H., *et al*. 'Loop' domain deletional mutant of Bcl-xL is as effective as p29Bcl-xL in inhibiting radiation-induced cytosolic accumulation of cytochrome C (cyt c), caspase-3 activity, and apoptosis. *Int J Radiat Oncol Biol Phys* **43**, 423-430 (1999).
99. Cheng, E.H., *et al*. Conversion of Bcl-2 to a Bax-like death effector by caspases. *Science* **278**, 1966-1968 (1997).

100. Fujita, N., Nagahashi, A., Nagashima, K., Rokudai, S. & Tsuruo, T. Acceleration of apoptotic cell death after the cleavage of Bcl-xL protein by caspase-3-like proteases. *Oncogene* **17**, 1295-1304 (1998).
101. Wang, J., Beauchemin, M. & Bertrand, R. Bcl-xL phosphorylation at Ser49 by polo kinase 3 during cell cycle progression and checkpoints. *Cell Signal* **23**, 2030-2038 (2011).
102. Wang, J., Beauchemin, M. & Bertrand, R. Phospho-Bcl-xL(ser62) plays a key role at DNA damage-induced G2 checkpoint. *Cell Cycle* **11**, 2159-2169 (2012).
103. Wang, J., Beauchemin, M. & Bertrand, R. Phospho-Bcl-xL(Ser62) influences spindle assembly and chromosome segregation during mitosis. *Cell Cycle* **13**, 1313-1326 (2014).
104. Poruchynsky, M.S., Wang, E.E., Rudin, C.M., Blagosklonny, M.V. & Fojo, T. Bcl-X(L) is phosphorylated in malignant cells following microtubule disruption. *Cancer Res* **58**, 3331-3338 (1998).
105. Fan, M.*, et al*. Vinblastine-induced phosphorylation of Bcl-2 and Bcl-XL is mediated by JNK and occurs in parallel with inactivation of the Raf-1/MEK/ERK cascade. *J Biol Chem* **275**, 29980-29985 (2000).
106. Basu, A. & Haldar, S. Identification of a novel Bcl-xL phosphorylation site regulating the sensitivity of taxol- or 2-methoxyestradiol-induced apoptosis. *FEBS Lett* **538**, 41-47 (2003).
107. Du, L., Lyle, C.S. & Chambers, T.C. Characterization of vinblastine-induced Bcl-xL and Bcl-2 phosphorylation: evidence for a novel protein kinase and a coordinated phosphorylation/dephosphorylation cycle associated with apoptosis induction. *Oncogene* **24**, 107-117 (2005).
108. Tamura, Y.*, et al*. Polo-like kinase 1 phosphorylates and regulates Bcl-x(L) during pironetin-induced apoptosis. *Oncogene* **28**, 107-116 (2009).
109. Terrano, D.T., Upreti, M. & Chambers, T.C. Cyclin-dependent kinase 1-mediated Bcl-xL/Bcl-2 phosphorylation acts as a functional link coupling mitotic arrest and apoptosis. *Mol Cell Biol* **30**, 640-656 (2010).
110. Upreti, M.*, et al*. Identification of the major phosphorylation site in Bcl-xL induced by microtubule inhibitors and analysis of its functional significance. *J Biol Chem* **283**, 35517-35525 (2008).
111. Barboule, N., Truchet, I. & Valette, A. Localization of phosphorylated forms of Bcl-2 in mitosis: co-localization with Ki-67 and nucleolin in nuclear structures and on mitotic chromosomes. *Cell Cycle* **4**, 590-596 (2005).
112. Kozopas, K.M., Yang, T., Buchan, H.L., Zhou, P. & Craig, R.W. Mcl-1, a gene expressed in programmed myeloid cell differentiation, has sequence similarity to Bcl-2. *Proc Natl Acad Sci USA* **90**, 3516-3520 (1993).
113. Craig, R.W. Mcl1 provides a window on the role of the Bcl2 family in cell proliferation, differentiation and tumorigenesis. *Leukemia* **16**, 444-454 (2002).
114. Fang, G.F.*, et al*. Loop domain is necessary for taxol-induced mobility shift and phosphorylation of Bcl-2 as well as for inhibiting taxol-induced cytosolic accumulation of cytochrome c and apoptosis. *Cancer Res* **58**, 3202-3208 (1998).
115. Johnson, A.L., Bridgham, J.T. & Jensen, T. Bcl-x(Long) protein expression and phosphorylation in granulosa cells. *Endocrinology* **140**, 4521-4529 (1999).

116. Fan, M., Du, C., Stone, A.A., Gilbert, K.M. & Chambers, T.C. Modulation of mitogen-activated protein kinases and phosphorylation of Bcl-2 by vinblastine represent persistent forms of normal fluctuations at G2-M. *Cancer Res* **60**, 6403-6407 (2000).
117. Malumbres, M. & Barbacid, M. Cell cycle, CDKs and cancer: a changing paradigm. *Nat Rev Cancer* **9**, 153-166 (2009).
118. Nurse, P., Thuriaux, P. & Nasmyth, K. Genetic control of the cell division cycle in the fission yeast Schizosaccharomyces pombe. *Mol Gen Genetics* **146**, 167-178 (1976).
119. Beach, D., Durkacz, B. & Nurse, P. Functionally homologous cell cycle control genes in budding and fission yeast. *Nature* **300**, 706-709 (1982).
120. Evans, T., Rosenthal, E.T., Youngblom, J., Distel, D. & Hunt, T. Cyclin: a protein specified by maternal mRNA in sea urchin eggs that is destroyed at each cleavage division. *Cell* **33**, 389-396 (1983).
121. Reed, S.I., Ferguson, J. & Groppe, J.C. Preliminary characterization of the transcriptional and translational products of the Saccharomyces cerevisiae cell division cycle gene CDC28. *Mol Cell Biol* **2**, 412-425 (1982).
122. Draetta, G., Brizuela, L., Potashkin, J. & Beach, D. Identification of p34 and p13, human homologs of the cell cycle regulators of fission yeast encoded by cdc2+ and suc1+. *Cell* **50**, 319-325 (1987).
123. Lee, M.G. & Nurse, P. Complementation used to clone a human homologue of the fission yeast cell cycle control gene cdc2. *Nature* **327**, 31-35 (1987).
124. Elledge, S.J. & Spottswood, M.R. A new human p34 protein kinase, CDK2, identified by complementation of a cdc28 mutation in Saccharomyces cerevisiae, is a homolog of Xenopus Eg1. *EMBO J* **10**, 2653-2659 (1991).
125. Paris, J., *et al*. Cloning by differential screening of a Xenopus cDNA coding for a protein highly homologous to cdc2. *Proc Natl Acad Sci U S A* **88**, 1039-1043 (1991).
126. Tsai, L.H., Harlow, E. & Meyerson, M. Isolation of the human cdk2 gene that encodes the cyclin A- and adenovirus E1A-associated p33 kinase. *Nature* **353**, 174-177 (1991).
127. Ninomiya-Tsuji, J., Nomoto, S., Yasuda, H., Reed, S.I. & Matsumoto, K. Cloning of a human cDNA encoding a CDC2-related kinase by complementation of a budding yeast cdc28 mutation. *Proc Natl Acad Sci U S A* **88**, 9006-9010 (1991).
128. Gopinathan, L., Ratnacaram, C.K. & Kaldis, P. Established and novel Cdk/cyclin complexes regulating the cell cycle and development. *Results Probl Cell Differ* **53**, 365-389 (2011).
129. Malumbres, M. & Barbacid, M. Mammalian cyclin-dependent kinases. *Trends Biochem Sci* **30,** 630-640 (2005).
130. Sherr, C.J. & Roberts, J.M. CDK inhibitors: positive and negative regulators of G1-phase progression. *Genes Dev* **13**, 1501-1512 (1999).
131. Malumbres, M. & Barbacid, M. To cycle or not to cycle: a critical decision in cancer. *Nature Rev Cancer* **1**, 222-231 (2001).
132. Cobrinik, D. Pocket proteins and cell cycle control. *Oncogene* **24**, 2796-2809 (2005).

133. Harbour, J.W. & Dean, D.C. Rb function in cell-cycle regulation and apoptosis. *Nat Cell Biol* **2**, E65-E67 (2000).
134. Harbour, J.W., Luo, R.X., Dei Santi, A., Postigo, A.A. & Dean, D.C. Cdk phosphorylation triggers sequential intramolecular interactions that progressively block Rb functions as cells move through G1. *Cell* **98**, 859-869 (1999).
135. Lundberg, A.S. & Weinberg, R.A. Functional inactivation of the retinoblastoma protein requires sequential modification by at least two distinct cyclin-cdk complexes. *Mol Cell Biol* **18**, 753-761 (1998).
136. Hwang, H.C. & Clurman, B.E. Cyclin E in normal and neoplastic cell cycles. *Oncogene* **24**, 2776-2786 (2005).
137. Ray-Gallet, D.*, et al*. HIRA is critical for a nucleosome assembly pathway independent of DNA synthesis. *Mol Cell* **9**, 1091-1100 (2002).
138. Moghadam, S.J., Hanks, A.M. & Keyomarsi, K. Breaking the cycle: An insight into the role of ERalpha in eukaryotic cell cycles. *J Carcinogenesis* **10**, 25 (2011).
139. Pines, J. Cyclins and cyclin-dependent kinases: a biochemical view. *Biochem J* **308 (Pt 3)**, 697-711 (1995).
140. Smits, V.A. & Medema, R.H. Checking out the G(2)/M transition. *Biochim Biophys Acta* **1519**, 1-12 (2001).
141. Lock, R.B. & Ross, W.E. Inhibition of p34cdc2 kinase by etoposide or irradiation as a mechanism of G2 arrest in chinese hamster ovary cells. *Cancer Res* **50**, 3761-3766 (1990).
142. Parker, L.L.*, et al*. Cyclin promotes the tyrosine phosphorylation of p34cdc2 in a Wee1+ dependent manner. *EMBO J* **10**, 1255-1263 (1991).
143. Parker, L.L. & Piwnica-Worms, H. Inactivation of the p34cdc2-cyclin B complex by the human WEE1 tyrosine kinase. *Science* **257**, 1955-1957 (1992).
144. McGowan, C.H. & Russell, P. Cell cycle regulation of human WEE1. *EMBO J* **14**, 2166-2175 (1995).
145. Mueller, P.R., Coleman, T.R., Kumagai, A. & Dunphy, W.G. Myt1: a membrane-associated inhibitory kinase that phosphorylates Cdc2 on both threonine-14 and tyrosine-15. *Science* **270**, 86-90 (1995).
146. Booher, R.N., Holman, P.S. & Fattaey, A. Human Myt1 is a cell cycle-regulated kinase that inhibits Cdc2 but not Cdk2 activity. *J Biol Chem* **272**, 22300-22306 (1997).
147. Furnari, B., Rhind, N. & Russell, P. Cdc25 mitotic inducer targeted by Chk1 DNA damage checkpoint kinase. *Science* **277**, 1495-1497 (1997).
148. Sanchez, Y.*, et al*. Conservation of the Chk1 checkpoint pathway in mammals: linkage of DNA damage to Cdk regulation through Cdc25. *Science* **277**, 1497-1501 (1997).
149. Peng, C.Y.*, et al*. Mitotic and G2 checkpoint control: regulation of 14-3-3 protein binding by phosphorylation of Cdc25C on serine-216. *Science* **277**, 1501-1505 (1997).
150. Zeng, Y.*, et al*. Replication checkpoint requires phosphorylation of the phosphatase Cdc25 by Cds1 or Chk1. *Nature* **395**, 507-510 (1998).
151. Baldin, V., Pelpel, K., Cazales, M., Cans, C. & Ducommun, B. Nuclear localization of Cdc25B1 and serine 146 integrity are required for induction of mitosis. *J Biol Chem* **277**, 35176-35182 (2002).

152. Cazales, M., *et al*. CDC25B phosphorylation by Aurora-A occurs at the G2/M transition and is inhibited by DNA damage. *Cell Cycle* **4**, 1233-1238 (2005).
153. Schmitt, E., *et al*. CHK1 phosphorylates CDC25B during the cell cycle in the absence of DNA damage. *J Cell Sci* **119**, 4269-4275 (2006).
154. Gavet, O. & Pines, J. Activation of cyclin B1-Cdk1 synchronizes events in the nucleus and the cytoplasm at mitosis. *J Cell Biol* **189**, 247-259 (2010).
155. Gavet, O. & Pines, J. Progressive activation of CyclinB1-Cdk1 coordinates entry to mitosis. *Dev Cell* **18**, 533-543 (2010).
156. Belmont, A.S. Mitotic chromosome structure and condensation. *Curr Opin Cell Biol* **18**, 632-638 (2006).
157. Cheeseman, I.M. & Desai, A. Molecular architecture of the kinetochore-microtubule interface. *Nature Rev Mol Cell Biol* **9**, 33-46 (2008).
158. Walczak, C.E., Cai, S. & Khodjakov, A. Mechanisms of chromosome behaviour during mitosis. *Nat Rev Mol Cell Biol* **11**, 91-102 (2010).
159. Nasmyth, K. & Haering, C.H. Cohesin: its roles and mechanisms. *Annu Rev Genet* **43**, 525-558 (2009).
160. Musacchio, A. & Salmon, E.D. The spindle-assembly checkpoint in space and time. *Nature Rev Mol Cell Biol* **8**, 379-393 (2007).
161. Holland, A.J. & Cleveland, D.W. Boveri revisited: chromosomal instability, aneuploidy and tumorigenesis. *Nat Rev Mol Cell Biol* **10**, 478-487 (2009).
162. Lara-Gonzales, P., Westhorpe, F.G. & Taylor, S.S. The spindle-assembly checkpoint. *Curr Biol* **22**, R966-980 (2012).
163. Pollard, T.D. Mechanics of cytokinesis in eukaryotes. *Curr Opin Cell Biol* **22**, 50-56 (2010).
164. Gordon, D.J., Resio, B. & Pellman, D. Causes and consequences of aneuploidy in cancer. *Nat Rev Genet* **13**, 189-203 (2012).
165. Ricke, R.M. & van Deursen, J.M. Aneuploidy in health, disease, and aging. *J Cell Biol* **201**, 11-21 (2013).
166. McAinsh, A.D. & Meraldi, P. The CCAN complex: linking centromere specification to control of kinetochore-microtubule dynamics. *Semin Cell Dev Biol* **22**, 946-952 (2011).
167. Cheeseman, I.M., Chappie, J.S., Wilson-Kubalek, E.M. & Desai, A. The conserved KMN network constitutes the core microtubule-binding site of the kinetochore. *Cell* **127**, 983-997 (2006).
168. Santaguida, S. & Musacchio, A. The life and miracles of kinetochores. *EMBO J* **28**, 2511-2531 (2009).
169. Ciferri, C., *et al*. Architecture of the human ndc80-hec1 complex, a critical constituent of the outer kinetochore. *J Biol Chem* **280**, 29088-29095 (2005).
170. Ciferri, C., Musacchio, A. & Petrovic, A. The Ndc80 complex: hub of kinetochore activity. *FEBS Lett* **581**, 2862-2869 (2007).
171. Wei, R.R., *et al*. Structure of a central component of the yeast kinetochore: the Spc24p/Spc25p globular domain. *Structure* **14**, 1003-1009 (2006).
172. Wei, R.R., Sorger, P.K. & Harrison, S.C. Molecular organization of the Ndc80 complex, an essential kinetochore component. *Proc Natl Acad Sci U S A* **102**, 5363-5367 (2005).

173. Ciferri, C., *et al*. Implications for kinetochore-microtubule attachment from the structure of an engineered Ndc80 complex. *Cell* **133**, 427-439 (2008).
174. Wei, R.R., Al-Bassam, J. & Harrison, S.C. The Ndc80/HEC1 complex is a contact point for kinetochore-microtubule attachment. *Nat Struct Mol Biol* **14**, 54-59 (2007).
175. Petrovic, A., *et al*. The MIS12 complex is a protein interaction hub for outer kinetochore assembly. *J Cell Biol* **190**, 835-852 (2010).
176. Bock, L.J., *et al*. Cnn1 inhibits the interactions between the KMN complexes of the yeast kinetochore. *Nat Cell Biol* **14**, 614-624 (2012).
177. Alushin, G.M., *et al*. The Ndc80 kinetochore complex forms oligomeric arrays along microtubules. *Nature* **467**, 805-810 (2010).
178. Przewloka, M.R., *et al*. The kinetochore and the centromere: a working long distance relationship. *Annu Rev Genet* **43,** 439-465 (2009).
179. Screpanti, E., *et al*. Direct binding of Cenp-C to the Mis12 complex joins the inner and outer kinetochore. *Curr Biol* **21**, 391-398 (2011).
180. Kops, G.J. & Shah, J.V. Connecting up and clearing out: how kinetochore attachment silences the spindle assembly checkpoint. *Chromosoma* **121**, 509-525 (2012).
181. Foley, E.A. & Kapoor, T.M. Microtubule attachment and spindle assembly checkpoint signalling at the kinetochore. *Nat Rev Mol Cell Biol* **14**, 25-37 (2013).
182. Hoyt, M.A., Totis, L. & Roberts, B.T. S. cerevisiae genes required for cell cycle arrest in response to loss of microtubule function. *Cell* **66**, 507-517 (1991).
183. Li, R. & Murray, A.W. Feedback control of mitosis in budding yeast. *Cell* **66**, 519-531 (1991).
184. Weiss, E. & Winey, M. The Saccharomyces cerevisiae spindle pole body duplication gene MPS1 is part of a mitotic checkpoint. *J Cell Biol* **132**, 111-123 (1996).
185. Musacchio, A. Spindle assembly checkpoint: the third decade. *Philos Trans R Soc Lond B Biol Sci* **366**, 3595-3604 (2011).
186. Taylor, S.S., Scott, M.I. & Holland, A.J. The spindle checkpoint: a quality control mechanism which ensures accurate chromosome segregation. *Chromosome Res* **12**, 599-616 (2004).
187. Fang, G., Yu, H. & Kirschner, M.W. Direct binding of CDC20 protein family members activates the anaphase-promoting complex in mitosis and G1. *Mol Cell* **2**, 163-171 (1998).
188. Kramer, E.R., Gieffers, C., Holzl, G., Hengstschlager, M. & Peters, J.M. Activation of the human anaphase-promoting complex by proteins of the CDC20/Fizzy family. *Curr Biol* **8**, 1207-1210 (1998).
189. Peters, J.M. The anaphase promoting complex/cyclosome: a machine designed to destroy. *Nat Rev Mol Cell Biol* **7**, 644-656 (2006).
190. Sudakin, V., Chan, G.K. & Yen, T.J. Checkpoint inhibition of the APC/C in HeLa cells is mediated by a complex of BUBR1, BUB3, CDC20, and MAD2. *J Cell Biol* **154**, 925-936 (2001).
191. Fang, G., Yu, H. & Kirschner, M.W. The checkpoint protein MAD2 and the mitotic regulator CDC20 form a ternary complex with the anaphase-promoting complex to control anaphase initiation. *Genes Dev* **12**, 1871-1883 (1998).

192. Wassmann, K., Liberal, V. & Benezra, R. Mad2 phosphorylation regulates its association with Mad1 and the APC/C. *EMBO J* **22**, 797-806 (2003).
193. Tang, Z., Bharadwaj, R., Li, B. & Yu, H. Mad2-independent inhibition of APCCdc20 by the mitotic checkpoint protein BubR1. *Dev Cell* **1**, 227-237 (2001).
194. Shannon, K.B., Canman, J.C. & Salmon, E.D. Mad2 and BubR1 function in a single checkpoint pathway that responds to a loss of tension. *Mol Biol Cell* **13**, 3706-3719 (2002).
195. Hardwick, K.G., Johnston, R.C., Smith, D.L. & Murray, A.W. MAD3 encodes a novel component of the spindle checkpoint which interacts with Bub3p, Cdc20p, and Mad2p. *J Cell Biol* **148**, 871-882 (2000).
196. Poddar, A., Stukenberg, P.T. & Burke, D.J. Two complexes of spindle checkpoint proteins containing Cdc20 and Mad2 assemble during mitosis independently of the kinetochore in Saccharomyces cerevisiae. *Eukaryot Cell* **4**, 867-878 (2005).
197. Kallio, M.J., McCleland, M.L., Stukenberg, P.T. & Gorbsky, G.J. Inhibition of aurora B kinase blocks chromosome segregation, overrides the spindle checkpoint, and perturbs microtubule dynamics in mitosis. *Curr Biol* **12**, 900-905 (2002).
198. Skinner, J.J., Wood, S., Shorter, J., Englander, S.W. & Black, B.E. The Mad2 partial unfolding model: regulating mitosis through Mad2 conformational switching. *J Cell Biol* **183**, 761-768 (2008).
199. Luo, X. & Yu, H. Protein metamorphosis: the two-state behavior of Mad2. *Structure* **16**, 1616-1625 (2008).
200. Heinrich, S., Windecker, H., Hustedt, N. & Hauf, S. Mph1 kinetochore localization is crucial and upstream in the hierarchy of spindle assembly checkpoint protein recruitment to kinetochores. *J Cell Sci* **125**, 4720-4727 (2012).
201. Howell, B.J.*, et al*. Spindle checkpoint protein dynamics at kinetochores in living cells. *Curr Biol* **14**, 953-964 (2004).
202. Gillett, E.S., Espelin, C.W. & Sorger, P.K. Spindle checkpoint proteins and chromosome-microtubule attachment in budding yeast. *J Cell Biol* **164**, 535-546 (2004).
203. Sharp-Baker, H. & Chen, R.H. Spindle checkpoint protein Bub1 is required for kinetochore localization of Mad1, Mad2, Bub3, and CENP-E, independently of its kinase activity. *J Cell Biol* **153**, 1239-1250 (2001).
204. Kiyomitsu, T., Obuse, C. & Yanagida, M. Human Blinkin/AF15q14 is required for chromosome alignment and the mitotic checkpoint through direct interaction with Bub1 and BubR1. *Dev Cell* **13**, 663-676 (2007).
205. Kiyomitsu, T., Murakami, H. & Yanagida, M. Protein interaction domain mapping of human kinetochore protein Blinkin reveals a consensus motif for binding of spindle assembly checkpoint proteins Bub1 and BubR1. *Mol Cell Biol* **31**, 998-1011 (2011).
206. London, N., Ceto, S., Ranish, J.A. & Biggins, S. Phosphoregulation of Spc105 by Mps1 and PP1 regulates Bub1 localization to kinetochores. *Curr Biol* **22**, 900-906 (2012).
207. Shepperd, L.A.*, et al*. Phosphodependent recruitment of Bub1 and Bub3 to Spc7/KNL1 by Mph1 kinase maintains the spindle checkpoint. *Curr Biol* **22**, 891-899 (2012).

208. Yamagishi, Y., Yang, C.H., Tanno, Y. & Watanabe, Y. MPS1/Mph1 phosphorylates the kinetochore protein KNL1/Spc7 to recruit SAC components. *Nat Cell Biol* **14,** 746-752 (2012).
209. Campbell, L. & Hardwick, K.G. Analysis of Bub3 spindle checkpoint function in Xenopus egg extracts. *J Cell Sci* **116**, 617-628 (2003).
210. Suijkerbuijk, S.J., *et al*. The vertebrate mitotic checkpoint protein BUBR1 is an unusual pseudokinase. *Dev Cell* **22**, 1321-1329 (2012).
211. Primorac, I., *et al*. Bub3 reads phosphorylated MELT repeats to promote spindle assembly checkpoint signaling. *eLife* **2**, e01030 (2013).
212. Johnson, V.L., Scott, M.I., Holt, S.V., Hussein, D. & Taylor, S.S. Bub1 is required for kinetochore localization of BubR1, Cenp-E, Cenp-F and Mad2, and chromosome congression. *J Cell Sci* **117**, 1577-1589 (2004).
213. Kadura, S., He, X., Vanoosthuyse, V., Hardwick, K.G. & Sazer, S. The A78V mutation in the Mad3-like domain of Schizosaccharomyces pombe Bub1p perturbs nuclear accumulation and kinetochore targeting of Bub1p, Bub3p, and Mad3p and spindle assembly checkpoint function. *Mol Biol Cell* **16**, 385-395 (2005).
214. Millband, D.N. & Hardwick, K.G. Fission yeast Mad3p is required for Mad2p to inhibit the anaphase-promoting complex and localizes to kinetochores in a Bub1p-, Bub3p-, and Mph1p-dependent manner. *Mol Cell Biol* **22**, 2728-2742 (2002).
215. Howell, B.J., Hoffman, D.B., Fang, G., Murray, A.W. & Salmon, E.D. Visualization of Mad2 dynamics at kinetochores, along spindle fibers, and at spindle poles in living cells. *J Cell Biol* **150**, 1233-1250 (2000).
216. Jablonski, S.A., Chan, G.K., Cooke, C.A., Earnshaw, W.C. & Yen, T.J. The hBUB1 and hBUBR1 kinases sequentially assemble onto kinetochores during prophase with hBUBR1 concentrating at the kinetochore plates in mitosis. *Chromosoma* **107**, 386-396 (1998).
217. Shimogawa, M.M., Wargacki, M.M., Muller, E.G. & Davis, T.N. Laterally attached kinetochores recruit the checkpoint protein Bub1, but satisfy the spindle checkpoint. *Cell Cycle* **9**, 3619-3628 (2010).
218. Brady, D.M. & Hardwick, K.G. Complex formation between Mad1p, Bub1p and Bub3p is crucial for spindle checkpoint function. *Curr Biol* **10**, 675-678 (2000).
219. Vleugel, M., Hoogendoorn, E., Snel, B. & Kops, G.J. Evolution and function of the mitotic checkpoint. *Dev Cell* **23**, 239-250 (2012).
220. Kops, G.J., *et al*. ZW10 links mitotic checkpoint signaling to the structural kinetochore. *J Cell Biol* **169**, 49-60 (2005).
221. Varma, D., *et al*. Spindle assembly checkpoint proteins are positioned close to core microtubule attachment sites at kinetochores. *J Cell Biol* **202**, 735-746 (2013).
222. Kasuboski, J.M., *et al*. Zwint-1 is a novel Aurora B substrate required for the assembly of a dynein-binding platform on kinetochores. *Mol Biol Cell* **22**, 3318-3330 (2011).
223. Shah, J.V., *et al*. Dynamics of centromere and kinetochore proteins; implications for checkpoint signaling and silencing. *Curr Biol* **14**, 942-952 (2004).
224. Luo, X., *et al*. The Mad2 spindle checkpoint protein has two distinct natively folded states. *Nat Struct Mol Biol* **11**, 338-345 (2004).

225. Luo, X., *et al*. Structure of the Mad2 spindle assembly checkpoint protein and its interaction with Cdc20. *Nat Struct Biol* **7**, 224-229 (2000).
226. Sironi, L., *et al*. Crystal structure of the tetrameric Mad1-Mad2 core complex: implications of a 'safety belt' binding mechanism for the spindle checkpoint. *EMBO J* **21**, 2496-2506 (2002).
227. De Antoni, A., *et al*. The Mad1/Mad2 complex as a template for Mad2 activation in the spindle assembly checkpoint. *Curr Biol* **15**, 214-225 (2005).
228. Nasmyth, K. How do so few control so many? *Cell* **120**, 739-746 (2005).
229. Hewitt, L., *et al*. Sustained Mps1 activity is required in mitosis to recruit O-Mad2 to the Mad1-C-Mad2 core complex. *J Cell Biol* **190**, 25-34.
230. Yang, M., *et al*. p31comet blocks Mad2 activation through structural mimicry. *Cell* **131**, 744-755 (2007).
231. Chao, W.C., Kulkarni, K., Zhang, Z., Kong, E.H. & Barford, D. Structure of the mitotic checkpoint complex. *Nature* **484**, 208-213 (2012).
232. Lara-Gonzalez, P., Westhorpe, F.G. & Taylor, S.S. The spindle assembly checkpoint. *Current biology* **22**, R966-980 (2012).
233. Magidson, V., *et al*. The Spatial Arrangement of Chromosomes during Prometaphase Facilitates Spindle Assembly. *Cell* **146**, 555-567 (2011).
234. Pinsky, B.A., Kung, C., Shokat, K.M. & Biggins, S. The Ipl1-Aurora protein kinase activates the spindle checkpoint by creating unattached kinetochores. *Nat Cell Biol* **8**, 78-83 (2006).
235. Lampson, M.A., Renduchitala, K., Khodjakov, A. & Kapoor, T.M. Correcting improper chromosome-spindle attachments during cell division. *Nat Cell Biol* **6**, 232-237 (2004).
236. Lampson, M.A. & Cheeseman, I.M. Sensing centromere tension: Aurora B and the regulation of kinetochore function. *Trends Cell Biol* **21**, 133-140 (2011).
237. Liu, D. & Lampson, M.A. Regulation of kinetochore-microtubule attachments by Aurora B kinase. *Biochem Soc Trans* **37**, 976-980 (2009).
238. Welburn, J.P., *et al*. Aurora B phosphorylates spatially distinct targets to differentially regulate the kinetochore-microtubule interface. *Mol Cell* **38**, 383-392 (2010).
239. Cai, S., O'Connell, C.B., Khodjakov, A. & Walczak, C.E. Chromosome congression in the absence of kinetochore fibres. *Nat Cell Biol* **11**, 832-838 (2009).
240. Uchida, K.S., *et al*. Kinetochore stretching inactivates the spindle assembly checkpoint. *J Cell Biol* **184**, 383-390 (2009).
241. Salimian, K.J., *et al*. Feedback control in sensing chromosome biorientation by the Aurora B kinase. *Curr Biol* **21**, 1158-1165 (2011).
242. Suijkerbuijk, S.J., Vleugel, M., Teixeira, A. & Kops, G.J. Integration of kinase and phosphatase activities by BUBR1 ensures formation of stable kinetochore-microtubule attachments. *Dev Cell* **23**, 745-755 (2012).
243. Cleveland, D.W., Mao, Y. & Sullivan, K.F. Centromeres and kinetochores: from epigenetics to mitotic checkpoint signaling. *Cell* **112**, 407-421 (2003).
244. Maiato, H., DeLuca, J., Salmon, E.D. & Earnshaw, W.C. The dynamic kinetochore-microtubule interface. *J Cell Sci* **117**, 5461-5477 (2004).

245. Hwang, L.H., *et al*. Budding yeast Cdc20: a target of the spindle checkpoint. *Science* **279**, 1041-1044 (1998).
246. Kim, S.H., Lin, D.P., Matsumoto, S., Kitazono, A. & Matsumoto, T. Fission yeast Slp1: an effector of the Mad2-dependent spindle checkpoint. *Science* **279**, 1045-1047 (1998).
247. Chen, R.H., Waters, J.C., Salmon, E.D. & Murray, A.W. Association of spindle assembly checkpoint component XMAD2 with unattached kinetochores. *Science* **274**, 242-246 (1996).
248. Ditchfield, C., *et al*. Aurora B couples chromosome alignment with anaphase by targeting BubR1, Mad2, and Cenp-E to kinetochores. *J Cell Biol* **161**, 267-280 (2003).
249. Howell, B.J., *et al*. Cytoplasmic dynein/dynactin drives kinetochore protein transport to the spindle poles and has a role in mitotic spindle checkpoint inactivation. *J Cell Biol* **155**, 1159-1172 (2001).
250. Famulski, J.K., Vos, L.J., Rattner, J.B. & Chan, G.K. Dynein/Dynactin-mediated transport of kinetochore components off kinetochores and onto spindle poles induced by nordihydroguaiaretic acid. *PLoS One* **6**, e16494 (2011).
251. Gassmann, R., *et al*. Removal of Spindly from microtubule-attached kinetochores controls spindle checkpoint silencing in human cells. *Genes Dev* **24**, 957-971 (2010).
252. Skoufias, D.A., Andreassen, P.R., Lacroix, F.B., Wilson, L. & Margolis, R.L. Mammalian mad2 and bub1/bubR1 recognize distinct spindle-attachment and kinetochore-tension checkpoints. *Proc Natl Acad Sci U S A* **98**, 4492-4497 (2001).
253. Lesage, B., Qian, J. & Bollen, M. Spindle checkpoint silencing: PP1 tips the balance. *Curr Biol* **21**, R898-903 (2011).
254. Hardwick, K.G. & Shah, J.V. Spindle checkpoint silencing: ensuring rapid and concerted anaphase onset. *F1000 Biol Rep* **2**, 55 (2010).
255. Mapelli, M., Massimiliano, L., Santaguida, S. & Musacchio, A. The Mad2 conformational dimer: structure and implications for the spindle assembly checkpoint. *Cell* **131**, 730-743 (2007).
256. Teichner, A., *et al*. p31comet Promotes disassembly of the mitotic checkpoint complex in an ATP-dependent process. *Proc Natl Acad Sci U S A* **108**, 3187-3192 (2011).
257. Nilsson, J., Yekezare, M., Minshull, J. & Pines, J. The APC/C maintains the spindle assembly checkpoint by targeting Cdc20 for destruction. *Nat Cell Biol* **10**, 1411-1420 (2008).
258. Westhorpe, F.G., Tighe, A., Lara-Gonzalez, P. & Taylor, S.S. p31comet-mediated extraction of Mad2 from the MCC promotes efficient mitotic exit. *J Cell Sci* **124**, 3905-3916 (2011).
259. Visconti, R., Palazzo, L. & Grieco, D. Requirement for proteolysis in spindle assembly checkpoint silencing. *Cell Cycle* **9**, 564-569 (2010).
260. Varetti, G., *et al*. Homeostatic control of mitotic arrest *Mol Cell*. **44**, 710-720. (2011).
261. Reddy, S.K., Rape, M., Margansky, W.A. & Kirschner, M.W. Ubiquitination by the anaphase-promoting complex drives spindle checkpoint inactivation. *Nature* **446**, 921-925 (2007).

262. Foster, S.A. & Morgan, D.O. The APC/C subunit Mnd2/Apc15 promotes Cdc20 autoubiquitination and spindle assembly checkpoint inactivation. *Mol Cell* **47**, 921-932 (2012).
263. Mansfeld, J., Collin, P., Collins, M.O., Choudhary, J.S. & Pines, J. APC15 drives the turnover of MCC-CDC20 to make the spindle assembly checkpoint responsive to kinetochore attachment. *Nat Cell Biol* **13**, 1234-1243 (2011).
264. Brito, D.A. & Rieder, C.L. Mitotic checkpoint slippage in humans occurs via cyclin B destruction in the presence of an active checkpoint. *Curr Biol* **16**, 1194-1200 (2006).
265. Gascoigne, K.E. & Cheeseman, I.M. Kinetochore assembly: if you build it, they will come. *Curr Opin Cell Biol*. **23**, 102-108 (2011)
266. Clute, P. & Pines, J. Temporal and spatial control of cyclin B1 destruction in metaphase. *Nat Cell Biol* **1**, 82-87 (1999).
267. Oliveira, R.A., Hamilton, R.S., Pauli, A., Davis, I. & Nasmyth, K. Cohesin cleavage and Cdk inhibition trigger formation of daughter nuclei. *Nat Cell Biol* **12**, 185-192 (2010).
268. Musacchio, A. Cell cycle: deconstructing tension. *Curr Biol* **20**, R634-637 (2010).
269. Vazquez-Novelle, M.D. & Petronczki, M. Relocation of the chromosomal passenger complex prevents mitotic checkpoint engagement at anaphase. *Curr Biol* **20**, 1402-1407.
270. Palframan, W.J., Meehl, J.B., Jaspersen, S.L., Winey, M. & Murray, A.W. Anaphase Inactivation of the Spindle Checkpoint. *Science* **314(5787)**, 680-684 (2006).
271. Mirchenko, L. & Uhlmann, F. Sli15(INCENP) dephosphorylation prevents mitotic checkpoint reengagement due to loss of tension at anaphase onset. *Curr Biol* **20**, 1396-1401 (2010).
272. D'Angiolella, V., Mari, C., Nocera, D., Rametti, L. & Grieco, D. The spindle checkpoint requires cyclin-dependent kinase activity. *Genes Dev* **17**, 2520-2525 (2003).
273. Parry, D.H., Hickson, G.R. & O'Farrell, P.H. Cyclin B destruction triggers changes in kinetochore behavior essential for successful anaphase. *Curr Biol* **13**, 647-653 (2003).
274. Normand, G. & King, R.W. Understanding cytokinesis failure. *Adv Exp Med Biol* **676**, 27-55 (2010).
275. Rappaport, R. Cytokinesis in animal cells. *Int Rev Cytol* **31**, 169-213 (1971).
276. Canman, J.C., *et al*. Determining the position of the cell division plane. *Nature* **424**, 1074-1078 (2003).
277. Hiramoto, Y. Analysis of cleavage stimulus by means of micromanipulation of sea urchin eggs. *Exp Cell Res* **68**, 291-298 (1971).
278. Danowski, B.A. Fibroblast contractility and actin organization are stimulated by microtubule inhibitors. *J Cell Sci* **93 (Pt 2)**, 255-266 (1989).
279. Ren, X.D., Kiosses, W.B. & Schwartz, M.A. Regulation of the small GTP-binding protein Rho by cell adhesion and the cytoskeleton. *EMBO J* **18**, 578-585 (1999).
280. Pletjushkina, O.J., *et al*. Induction of cortical oscillations in spreading cells by depolymerization of microtubules. *Cell Motil Cytoskeleton* **48**, 235-244 (2001).

281. Canman, J.C. & Bement, W.M. Microtubules suppress actomyosin-based cortical flow in Xenopus oocytes. *J Cell Sci* **110 (Pt 16)**, 1907-1917 (1997).
282. Werner, M., Munro, E. & Glotzer, M. Astral signals spatially bias cortical myosin recruitment to break symmetry and promote cytokinesis. *Curr Biol* **17**, 1286-1297 (2007).
283. Yonemura, S., Hirao-Minakuchi, K. & Nishimura, Y. Rho localization in cells and tissues. *Exp Cell Res* **295**, 300-314 (2004).
284. Yuce, O., Piekny, A. & Glotzer, M. An ECT2-centralspindlin complex regulates the localization and function of RhoA. *J Cell Biol* **170**, 571-582 (2005).
285. Nishimura, Y. & Yonemura, S. Centralspindlin regulates ECT2 and RhoA accumulation at the equatorial cortex during cytokinesis. *J Cell Sci* **119**, 104-114 (2006).
286. Yoshizaki, H., *et al*. Activity of Rho-family GTPases during cell division as visualized with FRET-based probes. *J Cell Biol* **162**, 223-232 (2003).
287. Bement, W.M., Benink, H.A. & von Dassow, G. A microtubule-dependent zone of active RhoA during cleavage plane specification. *J Cell Biol* **170**, 91-101 (2005).
288. Kamijo, K., *et al*. Dissecting the role of Rho-mediated signaling in contractile ring formation. *Mol Biol Cell* **17**, 43-55 (2006).
289. Somers, W.G. & Saint, R. A RhoGEF and Rho family GTPase-activating protein complex links the contractile ring to cortical microtubules at the onset of cytokinesis. *Dev Cell* **4**, 29-39 (2003).
290. Mishima, M., Kaitna, S. & Glotzer, M. Central spindle assembly and cytokinesis require a kinesin-like protein/RhoGAP complex with microtubule bundling activity. *Dev Cell* **2**, 41-54 (2002).
291. Birkenfeld, J., *et al*. GEF-H1 modulates localized RhoA activation during cytokinesis under the control of mitotic kinases. *Dev Cell* **12**, 699-712 (2007).
292. Wu, D., Asiedu, M., Adelstein, R.S. & Wei, Q. A novel guanine nucleotide exchange factor MyoGEF is required for cytokinesis. *Cell Cycle* **5**, 1234-1239 (2006).
293. Wolf, A., *et al*. The armadillo protein p0071 regulates Rho signalling during cytokinesis. *Nat Cell Biol* **8**, 1432-1440 (2006).
294. Kitzing, T.M., *et al*. Positive feedback between Dia1, LARG, and RhoA regulates cell morphology and invasion. *Genes Dev* **21**, 1478-1483 (2007).
295. Yamakita, Y., Yamashiro, S. & Matsumura, F. In vivo phosphorylation of regulatory light chain of myosin II during mitosis of cultured cells. *J Cell Biol* **124**, 129-137 (1994).
296. Satterwhite, L.L., *et al*. Phosphorylation of myosin-II regulatory light chain by cyclin-p34cdc2: a mechanism for the timing of cytokinesis. *J Cell Biol* **118**, 595-605 (1992).
297. Straight, A.F., *et al*. Dissecting temporal and spatial control of cytokinesis with a myosin II Inhibitor. *Science* **299**, 1743-1747 (2003).
298. Margolis, R.L. & Andreassen, P.R. The telophase disc: its possible role in mammalian cell cleavage. *Bioessays* **15**, 201-207 (1993).
299. Mollinari, C., *et al*. PRC1 is a microtubule binding and bundling protein essential to maintain the mitotic spindle midzone. *J Cell Biol* **157**, 1175-1186 (2002).

300. Gruneberg, U., *et al*. KIF14 and citron kinase act together to promote efficient cytokinesis. *J Cell Biol* **172**, 363-372 (2006).
301. Neef, R., *et al*. Choice of Plk1 docking partners during mitosis and cytokinesis is controlled by the activation state of Cdk1. *Nat Cell Biol* **9**, 436-444 (2007).
302. Burkard, M.E., *et al*. Chemical genetics reveals the requirement for Polo-like kinase 1 activity in positioning RhoA and triggering cytokinesis in human cells. *Proc Natl Acad Sci U S A* **104**, 4383-4388 (2007).
303. Petronczki, M., Glotzer, M., Kraut, N. & Peters, J.M. Polo-like kinase 1 triggers the initiation of cytokinesis in human cells by promoting recruitment of the RhoGEF Ect2 to the central spindle. *Dev Cell* **12**, 713-725 (2007).
304. Brennan, I.M., Peters, U., Kapoor, T.M. & Straight, A.F. Polo-like kinase controls vertebrate spindle elongation and cytokinesis. *PLoS One* **2**, e409 (2007).
305. Neef, R., *et al*. Phosphorylation of mitotic kinesin-like protein 2 by polo-like kinase 1 is required for cytokinesis. *J Cell Biol* **162**, 863-875 (2003).
306. Lowery, D.M., *et al*. Proteomic screen defines the Polo-box domain interactome and identifies Rock2 as a Plk1 substrate. *EMBO J* **26**, 2262-2273 (2007).
307. Ruchaud, S., Carmena, M. & Earnshaw, W.C. Chromosomal passengers: conducting cell division. *Nat Rev Mol Cell Biol* **8**, 798-812 (2007).
308. Cooke, C.A., Heck, M.M. & Earnshaw, W.C. The inner centromere protein (INCENP) antigens: movement from inner centromere to midbody during mitosis. *J. Cell. Biol.* **105**, 2053-2067 (1987).
309. Earnshaw, W.C. & Cooke, C.A. Analysis of the distribution of the INCENPs throughout mitosis reveals the existence of a pathway of structural changes in the chromosomes during metaphase and early events in cleavage furrow formation. *J Cell Sci* **98 (Pt 4)**, 443-461 (1991).
310. Adams, R.R., *et al*. Human INCENP colocalizes with the Aurora-B/AIRK2 kinase on chromosomes and is overexpressed in tumour cells. *Chromosoma* **110**, 65-74 (2001).
311. Minoshima, Y., *et al*. Phosphorylation by aurora B converts MgcRacGAP to a RhoGAP during cytokinesis. *Dev Cell* **4**, 549-560 (2003).
312. Ban, R., Irino, Y., Fukami, K. & Tanaka, H. Human mitotic spindle-associated protein PRC1 inhibits MgcRacGAP activity toward Cdc42 during the metaphase. *J Biol Chem* **279**, 16394-16402 (2004).
313. Toure, A., *et al*. Phosphoregulation of MgcRacGAP in mitosis involves Aurora B and Cdk1 protein kinases and the PP2A phosphatase. *FEBS Lett* **582**, 1182-1188 (2008).
314. Yasui, Y., *et al*. Protein kinases required for segregation of vimentin filaments in mitotic process. *Oncogene* **20**, 2868-2876 (2001).
315. Goto, H., *et al*. Aurora-B regulates the cleavage furrow-specific vimentin phosphorylation in the cytokinetic process. *J Biol Chem* **278**, 8526-8530 (2003).
316. Yokoyama, T., Goto, H., Izawa, I., Mizutani, H. & Inagaki, M. Aurora-B and Rho-kinase/ROCK, the two cleavage furrow kinases, independently regulate the progression of cytokinesis: possible existence of a novel cleavage furrow kinase phosphorylates ezrin/radixin/moesin (ERM). *Genes Cells* **10**, 127-137 (2005).

317. Zeitlin, S.G., Shelby, R.D. & Sullivan, K.F. CENP-A is phosphorylated by Aurora B kinase and plays an unexpected role in completion of cytokinesis. *J Cell Biol* **155**, 1147-1157 (2001).
318. Gromley, A.*, et al*. Centriolin anchoring of exocyst and SNARE complexes at the midbody is required for secretory-vesicle-mediated abscission. *Cell* **123**, 75-87 (2005).
319. Schweitzer, J.K., Burke, E.E., Goodson, H.V. & D'Souza-Schorey, C. Endocytosis resumes during late mitosis and is required for cytokinesis. *J Biol Chem* **280**, 41628-41635 (2005).
320. Chavrier, P. & Goud, B. The role of ARF and Rab GTPases in membrane transport. *Curr Opin Cell Biol* **11**, 466-475 (1999).
321. Fielding, A.B.*, et al*. Rab11-FIP3 and FIP4 interact with Arf6 and the exocyst to control membrane traffic in cytokinesis. *EMBO J* **24**, 3389-3399 (2005).
322. Yu, X., Prekeris, R. & Gould, G.W. Role of endosomal Rab GTPases in cytokinesis. *Eur J Cell Biol* **86**, 25-35 (2007).
323. Damke, H., Baba, T., Warnock, D.E. & Schmid, S.L. Induction of mutant dynamin specifically blocks endocytic coated vesicle formation. *J Cell Biol* **127**, 915-934 (1994).
324. Herskovits, J.S., Burgess, C.C., Obar, R.A. & Vallee, R.B. Effects of mutant rat dynamin on endocytosis. *J Cell Biol* **122**, 565-578 (1993).
325. van der Bliek, A.M. & Meyerowitz, E.M. Dynamin-like protein encoded by the Drosophila shibire gene associated with vesicular traffic. *Nature* **351**, 411-414 (1991).
326. van der Bliek, A.M.*, et al*. Mutations in human dynamin block an intermediate stage in coated vesicle formation. *J Cell Biol* **122**, 553-563 (1993).
327. Salazar, M.A.*, et al*. Tuba, a novel protein containing bin/amphiphysin/Rvs and Dbl homology domains, links dynamin to regulation of the actin cytoskeleton. *J Biol Chem* **278**, 49031-49043 (2003).
328. Hussain, N.K.*, et al*. Endocytic protein intersectin-l regulates actin assembly via Cdc42 and N-WASP. *Nat Cell Biol* **3**, 927-932 (2001).
329. Morita, E.*, et al*. Human ESCRT and ALIX proteins interact with proteins of the midbody and function in cytokinesis. *EMBO J* **26**, 4215-4227 (2007).
330. Cabezas, A., Bache, K.G., Brech, A. & Stenmark, H. Alix regulates cortical actin and the spatial distribution of endosomes. *J Cell Sci* **118**, 2625-2635 (2005).
331. Rodier, F. & Campisi, J. Four faces of cellular senescence. *J Cell Biol* **192**, 547-556 (2011).
332. Munoz-Espin, D. & Serrano, M. Cellular senescence: from physiology to pathology. *Nat Rev Mol Cell Biol* **15**, 482-496 (2014).
333. Schmitt, C.A. Senescence, apoptosis and therapy: cutting the lifelines of cancer. *Nat Rev Cancer* **3**, 286-295 (2003).
334. Campisi, J. & d'Adda di Fagagna, F. Cellular senescence: when bad things happen to good cells. *Nat Rev Mol Cell Biol* **8**, 729-740 (2007).
335. d'Adda di Fagagna, F. Living on a break: cellular senescence as a DNA-damage response. *Nat Rev Cancer* **8**, 512-522 (2008).
336. Takai, H., Smogorzewska, A. & de Lange, T. DNA damage foci at dysfunctional telomeres. *Curr Biol* **13**, 1549-1556 (2003).

337. Collado, M. & Serrano, M. The power and the promise of oncogene-induced senescence markers. *Nat Rev Cancer* **6**, 472-476 (2006).
338. Stein, G.H., Drullinger, L.F., Soulard, A. & Dulic, V. Differential roles for cyclin-dependent kinase inhibitors p21 and p16 in the mechanisms of senescence and differentiation in human fibroblasts. *Mol Cell Biol* **19**, 2109-2117 (1999).
339. Kim, W.Y. & Sharpless, N.E. The regulation of INK4/ARF in cancer and aging. *Cell* **127**, 265-275 (2006).
340. Fumagalli, M.*, et al*. Telomeric DNA damage is irreparable and causes persistent DNA-damage-response activation. *Nat Cell Biol* **14**, 355-365 (2012).
341. Schwarze, S.R., Shi, Y., Fu, V.X., Watson, P.A. & Jarrard, D.F. Role of cyclin-dependent kinase inhibitors in the growth arrest at senescence in human prostate epithelial and uroepithelial cells. *Oncogene* **20**, 8184-8192 (2001).
342. Serrano, M., Lin, A., W., McCurrach, M.E., Beach, D. & Lowe, S.W. Oncogenic ras provokes premature cell senescence associated with accumulation of p53 and p16INK4a. *Cell* **88**, 593-602 (1997).
343. Bartkova, J.*, et al*. Oncogene-induced senescence is part of the tumorigenesis barrier imposed by DNA damage checkpoints. *Nature* **444**, 633-637 (2006).
344. Di Micco, R.*, et al*. Oncogene-induced senescence is a DNA damage response triggered by DNA hyper-replication. *Nature* **444**, 638-642 (2006).
345. Mallette, F.A., Gaumont-Leclerc, M.F. & Ferbeyre, G. The DNA damage signaling pathway is a critical mediator of oncogene-induced senescence. *Genes Dev* **21**, 43-48 (2007).
346. Leng, R.P.*, et al*. Pirh2, a p53-induced ubiquitin-protein ligase, promotes p53 degradation. *Cell* **112**, 779-791 (2003).
347. Levine, A.J. & Oren, M. The first 30 years of p53: growing ever more complex. *Nat Rev Cancer* **9**, 749-758 (2009).
348. Vousden, K.H. & Lane, D.P. p53 in health and disease. *Nat Rev Mol Cell Biol* **8**, 275-283 (2007).
349. Pearson, M.*, et al*. PML regulates p53 acetylation and premature senescence induced by oncogenic Ras. *Nature* **406**, 207-210 (2000).
350. Kortlever, R.M., Higgins, P.J. & Bernards, R. Plasminogen activator inhibitor-1 is a critical downstream target of p53 in the induction of replicative senescence. *Nat Cell Biol* **8**, 877-884 (2006).
351. Dimri, G.P.*, et al*. A biomarker that identifies senescent human cells in culture and in aging skin in vitro. *Proc Natl Acad Sci (USA)* **92**, 9363-9367 (1995).
352. Halazonetis, T.D., Gorgoulis, V.G. & Bartek, J. An oncogene-induced DNA damage model for cancer development. *Science* **319**, 1352-1355 (2008).
353. Coppe, J.P.*, et al*. Senescence-associated secretory phenotypes reveal cell-nonautonomous functions of oncogenic RAS and the p53 tumor suppressor. *PLoS Biol* **6**, 2853-2868 (2008).
354. Kuilman, T. & Peeper, D.S. Senescence-messaging secretome: SMS-ing cellular stress. *Nat Rev Cancer* **9**, 81-94 (2009).
355. Campisi, J. Senescent cells, tumor suppression, and organismal aging: good citizens, bad neighbors. *Cell* **120**, 513-522 (2005).
356. Kuilman, T.*, et al*. Oncogene-induced senescence relayed by an interleukin-dependent inflammatory network. *Cell* **133**, 1019-1031 (2008).

357. Rodier, F., *et al*. Persistent DNA damage signalling triggers senescence-associated inflammatory cytokine secretion. *Nat Cell Biol* **11**, 973-979 (2009).
358. Garfinkel, S., Brown, S., Wessendorf, J.H. & Maciag, T. Post-transcriptional regulation of interleukin 1 alpha in various strains of young and senescent human umbilical vein endothelial cells. *Proc Natl Acad Sci U S A* **91**, 1559-1563 (1994).
359. Kumar, S., Millis, A.J. & Baglioni, C. Expression of interleukin 1-inducible genes and production of interleukin 1 by aging human fibroblasts. *Proc Natl Acad Sci U S A* **89**, 4683-4687 (1992).
360. Mantovani, A., Locati, M., Vecchi, A., Sozzani, S. & Allavena, P. Decoy receptors: a strategy to regulate inflammatory cytokines and chemokines. *Trends Immunol* **22**, 328-336 (2001).
361. Coppe, J.P., Desprez, P.Y., Krtolica, A. & Campisi, J. The senescence-associated secretory phenotype: the dark side of tumor suppression. *Annual review of pathology* **5**, 99-118 (2010).
362. Wang, S., Moerman, E.J., Jones, R.A., Thweatt, R. & Goldstein, S. Characterization of IGFBP-3, PAI-1 and SPARC mRNA expression in senescent fibroblasts. *Mech Ageing Dev* **92**, 121-132 (1996).
363. Grillari, J., Hohenwarter, O., Grabherr, R.M. & Katinger, H. Subtractive hybridization of mRNA from early passage and senescent endothelial cells. *Exp Gerontol* **35**, 187-197 (2000).
364. Lopez-Bermejo, A., *et al*. Characterization of insulin-like growth factor-binding protein-related proteins (IGFBP-rPs) 1, 2, and 3 in human prostate epithelial cells: potential roles for IGFBP-rP1 and 2 in senescence of the prostatic epithelium. *Endocrinology* **141**, 4072-4080 (2000).
365. Orjalo, A.V., Bhaumik, D., Gengler, B.K., Scott, G.K. & Campisi, J. Cell surface-bound IL-1alpha is an upstream regulator of the senescence-associated IL-6/IL-8 cytokine network. *Proc Natl Acad Sci U S A* **106**, 17031-17036 (2009).
366. Bhaumik, D., *et al*. MicroRNAs miR-146a/b negatively modulate the senescence-associated inflammatory mediators IL-6 and IL-8. *Aging (Albany NY)* **1**, 402-411 (2009).
367. Hoare, M. & Narita, M. Transmitting senescence to the cell neighbourhood. *Nat Cell Biol* **15**, 887-889 (2013).
368. Krtolica, A., Parrinello, S., Lockett, S., Desprez, P.Y. & Campisi, J. Senescent fibroblasts promote epithelial cell growth and tumorigenesis: a link between cancer and aging. *Proc Natl Acad Sci U S A* **98**, 12072-12077 (2001).
369. Hubackova, S., Krejcikova, K., Bartek, J. & Hodny, Z. IL1- and TGFbeta-Nox4 signaling, oxidative stress and DNA damage response are shared features of replicative, oncogene-induced, and drug-induced paracrine 'bystander senescence'. *Aging (Albany NY)* **4**, 932-951 (2012).
370. Yoshimoto, S., *et al*. Obesity-induced gut microbial metabolite promotes liver cancer through senescence secretome. *Nature* **499**, 97-101 (2013).
371. Xue, W., *et al*. Senescence and tumour clearance is triggered by p53 restoration in murine liver carcinomas. *Nature* **445**, 656-660 (2007).
372. Acosta, J.C., *et al*. A complex secretory program orchestrated by the inflammasome controls paracrine senescence. *Nat Cell Biol* **15**, 978-990 (2013).

373. Krizhanovsky, V., *et al*. Senescence of activated stellate cells limits liver fibrosis. *Cell* **134**, 657-667 (2008).
374. Jun, J.I. & Lau, L.F. Cellular senescence controls fibrosis in wound healing. *Aging (Albany NY)* **2**, 627-631 (2010).
375. Jun, J.I. & Lau, L.F. The matricellular protein CCN1 induces fibroblast senescence and restricts fibrosis in cutaneous wound healing. *Nat Cell Biol* **12**, 676-685 (2010).
376. Sparmann, A. & Bar-Sagi, D. Ras-induced interleukin-8 expression plays a critical role in tumor growth and angiogenesis. *Cancer Cell* **6**, 447-458 (2004).
377. Liu, D. & Hornsby, P.J. Senescent human fibroblasts increase the early growth of xenograft tumors via matrix metalloproteinase secretion. *Cancer Res* **67**, 3117-3126 (2007).
378. Hornebeck, W. & Maquart, F.X. Proteolyzed matrix as a template for the regulation of tumor progression. *Biomed Pharmacother* **57**, 223-230 (2003).
379. Narita, M., *et al*. Rb-mediated heterochromatin formation and silencing of E2F target genes during cellular senescence. *Cell* **113**, 703-716 (2003).
380. Zhang, R., Chen, W. & Adams, P.D. Molecular dissection of formation of senescent associated heterochromatin foci. *Mol Cell Biol* **27**, 2343-2358 (2007).
381. Kosar, M., *et al*. Senescence-associated heterochromatin foci are dispensable for cellular senescence, occur in a cell type- and insult-dependent manner and follow expression of p16(ink4a). *Cell Cycle* **10**, 457-468 (2011).
382. Ye, X., *et al*. Definition of pRB- and p53-dependent and -independent steps in HIRA/ASF1a-mediated formation of senescence-associated heterochromatin foci. *Mol Cell Biol* **27**, 2452-2465 (2007).
383. Narita, M., *et al*. A novel role for high-mobility group a proteins in cellular senescence and heterochromatin formation. *Cell* **126**, 503-514 (2006).
384. Zhang, R., *et al*. Formation of MacroH2A-containing senescence-associated heterochromatin foci and senescence driven by ASF1a and HIRA. *Dev Cell* **8**, 19-30 (2005).
385. Rogakou, E.P., Boon, C., Redon, C. & Bonner, W.M. Megabase chromatin domains involved in DNA double-strand breaks in vivo. *J Cell Biol* **146**, 905-916 (1999).
386. Herbig, U., Jobling, W.A., Chen, B.P., Chen, D.J. & Sedrivy, J.M. Telomere shortening triggers senescence of human cells through a pathway involving ATM, p53, and p21(Cip1), but not p16(INK4a). *Mol Cell* **14**, 501-513 (2004).
387. Chin, L., *et al*. p53 deficiency rescues the adverse effects of telomere loss and cooperates with telomere dysfunction to accelerate carcinogenesis. *Cell* **97**, 527-538 (1999).
388. Vaziri, H. & Benchimol, S. From telomere loss to p53 induction and activation of a DNA-damage pathway at senescence: the telomere loss/DNA damage model of cell aging. *Exp Gerontol* **31**, 295-301 (1996).
389. Schultz, L.B., Chehab, N.H., Malikzay, A. & Halazonetis, T.D. p53 binding protein 1 (53BP1) is an early participant in the cellular response to DNA double-strand breaks. *J Cell Biol* **151**, 1381-1390 (2000).
390. Braig, M., *et al*. Oncogene-induced senescence as an initial barrier in lymphoma development. *Nature* **436**, 660-665 (2005).

391. Michaloglou, C., *et al*. BRAFE600-associated senescence-like cell cycle arrest of human naevi. *Nature* **436**, 720-724 (2005).
392. Lazzerini Denchi, E., Attwooll, C., Pasini, D. & Helin, K. Deregulated E2F activity induces hyperplasia and senescence-like features in the mouse pituitary gland. *Mol Cell Biol* **25**, 2660-2672 (2005).
393. Ricke, R.M., van Ree, J.H. & van Deursen, J.M. Whole chromosome instability and cancer: a complex relationship. *Trends Genet* **24**, 457-466 (2008).
394. Baker, D.J., *et al*. BubR1 insufficiency causes early onset of aging-associated phenotypes and infertility in mice. *Nat Genet* **36**, 744-749 (2004).
395. Faggioli, F., Vijg, J. & Montagna, C. Chromosomal aneuploidy in the aging brain. *Mech Ageing Dev* **132**, 429-436 (2011).
396. Kops, G.J., Weaver, B.A. & Cleveland, D.W. On the road to cancer: aneuploidy and the mitotic checkpoint. *Nat Rev Cancer* **5**, 773-785 (2005).
397. Baker, D.J., *et al*. Opposing roles for p16Ink4a and p19Arf in senescence and ageing caused by BubR1 insufficiency. *Nat Cell Biol* **10**, 825-836 (2008).
398. Baker, D.J., *et al*. Increased expression of BubR1 protects against aneuploidy and cancer and extends healthy lifespan. *Nat Cell Biol* **15**, 96-102 (2013).
399. Bernard, P., Hardwick, K. & Javerzat, J.P. Fission yeast bub1 is a mitotic centromere protein essential for the spindle checkpoint and the preservation of correct ploidy through mitosis. *J Cell Biol* **143**, 1775-1787 (1998).
400. Warren, C.D., *et al*. Distinct chromosome segregation roles for spindle checkpoint proteins. *Mol Biol Cell* **13**, 3029-3041 (2002).
401. Vanoosthuyse, V., Valsdottir, R., Javerzat, J.P. & Hardwick, K.G. Kinetochore targeting of fission yeast Mad and Bub proteins is essential for spindle checkpoint function but not for all chromosome segregation roles of Bub1p. *Mol Cell Biol* **24**, 9786-9801 (2004).
402. Kalitsis, P., Earle, E., Fowler, K.J. & Choo, K.H. Bub3 gene disruption in mice reveals essential mitotic spindle checkpoint function during early embryogenesis. *Genes Dev* **14**, 2277-2282 (2000).
403. Babu, J.R., *et al*. Rae1 is an essential mitotic checkpoint regulator that cooperates with Bub3 to prevent chromosome missegregation. *J Cell Biol* **160**, 341-353 (2003).
404. Wang, Q., *et al*. BUBR1 deficiency results in abnormal megakaryopoiesis. *Blood* **103**, 1278-1285 (2004).
405. Michel, L.S., *et al*. MAD2 haplo-insufficiency causes premature anaphase and chromosome instability in mammalian cells. *Nature* **409**, 355-359 (2001).
406. Schliekelman, M., *et al*. Impaired Bub1 function in vivo compromises tension-dependent checkpoint function leading to aneuploidy and tumorigenesis. *Cancer Res* **69**, 45-54 (2009).
407. Habu, T., Kim, S.H., Weinstein, J. & Matsumoto, T. Identification of a MAD2-binding protein, CMT2, and its role in mitosis. *EMBO J* **21**, 6419-6428 (2002).
408. Shah, J.V. & Cleveland, D.W. Waiting for anaphase: Mad2 and the spindle assembly checkpoint. *Cell* **103**, 997-1000 (2000).
409. Larsen, N.A. & Harrison, S.C. Crystal structure of the spindle assembly checkpoint protein Bub3. *J Mol Biol* **344**, 885-892 (2004).

410. Baker, D.J., *et al*. Early aging-associated phenotypes in Bub3/Rae1 haploinsufficient mice. *J Cell Biol* **172**, 529-540 (2006).
411. Lentini, L., Barra, V., Schillaci, T. & Di Leonardo, A. MAD2 depletion triggers premature cellular senescence in human primary fibroblasts by activating a p53 pathway preventing aneuploid cells propagation. *J Cell Physiol* **227**, 3324-3332 (2012).
412. Schvartzman, J.M., Duijf, P.H., Sotillo, R., Coker, C. & Benezra, R. Mad2 is a critical mediator of the chromosome instability observed upon Rb and p53 pathway inhibition. *Cancer Cell* **19**, 701-714 (2011).
413. Mukherjee, M., *et al*. Separase loss of function cooperates with the loss of p53 in the initiation and progression of T- and B-cell lymphoma, leukemia and aneuploidy in mice. *PLoS One* **6**, e22167 (2011).
414. Pati, D., *et al*. Hormone-induced chromosomal instability in p53-null mammary epithelium. *Cancer Res* **64**, 5608-5616 (2004).
415. Zhang, N. & Pati, D. Handcuff for sisters: a new model for sister chromatid cohesion. *Cell Cycle* **8**, 399-402 (2009).
416. van Ree, J.H., Jeganathan, K.B., Malureanu, L. & van Deursen, J.M. Overexpression of the E2 ubiquitin-conjugating enzyme UbcH10 causes chromosome missegregation and tumor formation. *J Cell Biol* **188**, 83-100 (2010).
417. Drechsel, D.N., Hyman, A.A., Hall, A. & Glotzer, M. A requirement for Rho and Cdc42 during cytokinesis in Xenopus embryos. *Curr Biol* **7**, 12-23 (1997).
418. Jantsch-Plunger, V., *et al*. CYK-4: A Rho family gtpase activating protein (GAP) required for central spindle formation and cytokinesis. *J Cell Biol* **149**, 1391-1404 (2000).
419. Kudryavtsev, B.N., Kudryavtseva, M.V., Sakuta, G.A. & Stein, G.I. Human hepatocyte polyploidization kinetics in the course of life cycle. *Virchows Arch B Cell Pathol Incl Mol Pathol* **64**, 387-393 (1993).
420. Yu, Y.Y., *et al*. The association of calmodulin with central spindle regulates the initiation of cytokinesis in HeLa cells. *Int J Biochem Cell Biol* **36**, 1562-1572 (2004).
421. Kosako, H., *et al*. Rho-kinase/ROCK is involved in cytokinesis through the phosphorylation of myosin light chain and not ezrin/radixin/moesin proteins at the cleavage furrow. *Oncogene* **19**, 6059-6064 (2000).
422. Mundt, K.E., Golsteyn, R.M., Lane, H.A. & Nigg, E.A. On the regulation and function of human polo-like kinase 1 (PLK1): effects of overexpression on cell cycle progression. *Biochem Biophys Res Commun* **239**, 377-385 (1997).
423. Meraldi, P., Honda, R. & Nigg, E.A. Aurora-A overexpression reveals tetraploidization as a major route to centrosome amplification in p53-/- cells. *EMBO J* **21**, 483-492 (2002).
424. Neef, R., Klein, U.R., Kopajtich, R. & Barr, F.A. Cooperation between mitotic kinesins controls the late stages of cytokinesis. *Curr Biol* **16**, 301-307 (2006).
425. Holland, A.J. & Cleveland, D.W. Losing balance: the origin and impact of aneuploidy in cancer. *EMBO Rep* **13**, 501-514 (2012).

426. Janssen, A., van der Burg, M., Szuhai, K., Kops, G.J. & Medema, R.H. Chromosome segregation errors as a cause of DNA damage and structural chromosome aberrations. *Science* **333**, 1895-1898 (2011).
427. Giunta, S. & Jackson, S.P. Give me a break, but not in mitosis: the mitotic DNA damage response marks DNA double-strand breaks with early signaling events. *Cell Cycle* **10**, 1215-1221 (2011).
428. Rieder, C.L. & Cole, R.W. Entry into mitosis in vertebrate somatic cells is guarded by a chromosome damage checkpoint that reverses the cell cycle when triggered during early but not late prophase. *J Cell Biol* **142**, 1013-1022 (1998).
429. Rieder, C.L. Mitosis in vertebrates: the G2/M and M/A transitions and their associated checkpoints. *Chromosome Res* **19**, 291-306 (2011).
430. Giunta, S., Belotserkovskaya, R. & Jackson, S.P. DNA damage signaling in response to double-strand breaks during mitosis. *J Cell Biol* **190**, 197-207 (2010).
431. Zhang, W., Peng, G., Lin, S.Y. & Zhang, P. DNA damage response is suppressed by the high cyclin-dependent kinase 1 activity in mitotic mammalian cells. *J Biol Chem* **286**, 35899-35905 (2011).
432. Quignon, F.*, et al*. Sustained mitotic block elicits DNA breaks: one-step alteration of ploidy and chromosome integrity in mammalian cells. *Oncogene* **26**, 165-172 (2007).
433. Shen, K., Wang, Y., Brooks, S.C., Raz, A. & Wang, Y.A. ATM is activated by mitotic stress and suppresses centrosome amplification in primary but not in tumor cells. *J Cell Biochem* **99**, 1267-1274 (2006).
434. Brenner, S. The genetics of behaviour. *Br Med Bull* **29**, 269-271 (1973).
435. Byerly, L., Cassada, R.C. & Russell, R.L. The life cycle of the nematode Caenorhabditis elegans. I. Wild-type growth and reproduction. *Dev Biol* **51**, 23-33 (1976).
436. Sulston, J.E., Schierenberg, E., White, J.G. & Thomson, J.N. The embryonic cell lineage of the nematode Caenorhabditis elegans. *Dev Biol* **100**, 64-119 (1983).
437. Kimble, J. & Hirsh, D. The postembryonic cell lineages of the hermaphrodite and male gonads in Caenorhabditis elegans. *Dev Biol* **70**, 396-417 (1979).
438. Kimble, J.E. & White, J.G. On the control of germ cell development in Caenorhabditis elegans. *Dev Biol* **81**, 208-219 (1981).
439. McCarter, J., Bartlett, B., Dang, T. & Schedl, T. Soma-germ cell interactions in Caenorhabditis elegans: multiple events of hermaphrodite germline development require the somatic sheath and spermathecal lineages. *Dev Biol* **181**, 121-143 (1997).
440. Rose, K.L.*, et al*. The POU gene ceh-18 promotes gonadal sheath cell differentiation and function required for meiotic maturation and ovulation in Caenorhabditis elegans. *Dev Biol* **192**, 59-77 (1997).
441. Hall, D.H.*, et al*. Ultrastructural features of the adult hermaphrodite gonad of Caenorhabditis elegans: relations between the germ line and soma. *Dev Biol* **212**, 101-123 (1999).
442. Newman, A.P. & Sternberg, P.W. Coordinated morphogenesis of epithelia during development of the Caenorhabditis elegans uterine-vulval connection. *Proc Natl Acad Sci U S A* **93**, 9329-9333 (1996).

443. Seydoux, G. & Fire, A. Soma-germline asymmetry in the distributions of embryonic RNAs in Caenorhabditis elegans. *Development* **120**, 2823-2834 (1994).
444. Seydoux, G. & Dunn, M.A. Transcriptionally repressed germ cells lack a subpopulation of phosphorylated RNA polymerase II in early embryos of Caenorhabditis elegans and Drosophila melanogaster. *Development* **124**, 2191-2201 (1997).
445. Seydoux, G.*, et al*. Repression of gene expression in the embryonic germ lineage of C. elegans. *Nature* **382**, 713-716 (1996).
446. Capowski, E.E., Martin, P., Garvin, C. & Strome, S. Identification of grandchildless loci whose products are required for normal germ-line development in the nematode Caenorhabditis elegans. *Genetics* **129**, 1061-1072 (1991).
447. Korf, I., Fan, Y. & Strome, S. The Polycomb group in Caenorhabditis elegans and maternal control of germline development. *Development* **125**, 2469-2478 (1998).
448. Holdeman, R., Nehrt, S. & Strome, S. MES-2, a maternal protein essential for viability of the germline in Caenorhabditis elegans, is homologous to a Drosophila Polycomb group protein. *Development* **125**, 2457-2467 (1998).
449. Strome, S. & Wood, W.B. Immunofluorescence visualization of germ-line-specific cytoplasmic granules in embryos, larvae, and adults of Caenorhabditis elegans. *Proc Natl Acad Sci U S A* **79**, 1558-1562 (1982).
450. Strome, S. & Wood, W.B. Generation of asymmetry and segregation of germ-line granules in early C. elegans embryos. *Cell* **35**, 15-25 (1983).
451. Wolf, N., Priess, J. & Hirsh, D. Segregation of germline granules in early embryos of Caenorhabditis elegans: an electron microscopic analysis. *Journal of embryology and experimental morphology* **73**, 297-306 (1983).
452. Mello, C.C.*, et al*. The PIE-1 protein and germline specification in C. elegans embryos. *Nature* **382**, 710-712 (1996).
453. Guedes, S. & Priess, J.R. The C. elegans MEX-1 protein is present in germline blastomeres and is a P granule component. *Development* **124**, 731-739 (1997).
454. Tabara, H., Hill, R.J., Mello, C.C., Priess, J.R. & Kohara, Y. pos-1 encodes a cytoplasmic zinc-finger protein essential for germline specification in C. elegans. *Development* **126**, 1-11 (1999).
455. Updike, D. & Strome, S. P granule assembly and function in Caenorhabditis elegans germ cells. *J Androl* **31**, 53-60 (2010).
456. Kuwabara, P.E., Lee, M.H., Schedl, T. & Jefferis, G.S. A C. elegans patched gene, ptc-1, functions in germ-line cytokinesis. *Genes Dev* **14**, 1933-1944 (2000).
457. Siegfried, K.R. & Kimble, J. POP-1 controls axis formation during early gonadogenesis in C. elegans. *Development* **129**, 443-453 (2002).
458. Kidd, A.R., 3rd, Miskowski, J.A., Siegfried, K.R., Sawa, H. & Kimble, J. A beta-catenin identified by functional rather than sequence criteria and its role in Wnt/MAPK signaling. *Cell* **121**, 761-772 (2005).
459. Lam, N., Chesney, M.A. & Kimble, J. Wnt signaling and CEH-22/tinman/Nkx2.5 specify a stem cell niche in C. elegans. *Curr Biol* **16**, 287-295 (2006).
460. Kopan, R. & Ilagan, M.X. The canonical Notch signaling pathway: unfolding the activation mechanism. *Cell* **137**, 216-233 (2009).

461. Crittenden, S.L., Troemel, E.R., Evans, T.C. & Kimble, J. GLP-1 is localized to the mitotic region of the C. elegans germ line. *Development* **120**, 2901-2911 (1994).
462. Henderson, S.T., Gao, D., Lambie, E.J. & Kimble, J. lag-2 may encode a signaling ligand for the GLP-1 and LIN-12 receptors of C. elegans. *Development* **120**, 2913-2924 (1994).
463. Nadarajan, S., Govindan, J.A., McGovern, M., Hubbard, E.J. & Greenstein, D. MSP and GLP-1/Notch signaling coordinately regulate actomyosin-dependent cytoplasmic streaming and oocyte growth in C. elegans. *Development* **136**, 2223-2234 (2009).
464. Petcherski, A.G. & Kimble, J. LAG-3 is a putative transcriptional activator in the C. elegans Notch pathway. *Nature* **405**, 364-368 (2000).
465. Doyle, T.G., Wen, C. & Greenwald, I. SEL-8, a nuclear protein required for LIN-12 and GLP-1 signaling in Caenorhabditis elegans. *Proc Natl Acad Sci U S A* **97**, 7877-7881 (2000).
466. Kimble, J. & Seidel, H. C. elegans germline stem cells and their niche. in *StemBook* (: 2013 Judith Kimble and Hannah Seidel., Cambridge MA, 2008).
467. Austin, J. & Kimble, J. glp-1 is required in the germ line for regulation of the decision between mitosis and meiosis in C. elegans. *Cell* **51**, 589-599 (1987).
468. Berry, L.W., Westlund, B. & Schedl, T. Germ-line tumor formation caused by activation of glp-1, a Caenorhabditis elegans member of the Notch family of receptors. *Development* **124**, 925-936 (1997).
469. Zhang, B*., et al*. A conserved RNA-binding protein that regulates sexual fates in the C. elegans hermaphrodite germ line. *Nature* **390**, 477-484 (1997).
470. Wickens, M., Bernstein, D.S., Kimble, J. & Parker, R. A PUF family portrait: 3'UTR regulation as a way of life. *Trends Genet* **18**, 150-157 (2002).
471. Crittenden, S.L.*, et al*. A conserved RNA-binding protein controls germline stem cells in Caenorhabditis elegans. *Nature* **417**, 660-663 (2002).
472. Jones, A.R. & Schedl, T. Mutations in gld-1, a female germ cell-specific tumor suppressor gene in Caenorhabditis elegans, affect a conserved domain also found in Src-associated protein Sam68. *Genes Dev* **9**, 1491-1504 (1995).
473. Marin, V.A. & Evans, T.C. Translational repression of a C. elegans Notch mRNA by the STAR/KH domain protein GLD-1. *Development* **130**, 2623-2632 (2003).
474. Hansen, D., Hubbard, E.J. & Schedl, T. Multi-pathway control of the proliferation versus meiotic development decision in the Caenorhabditis elegans germline. *Dev Biol* **268**, 342-357 (2004).
475. Eckmann, C.R., Crittenden, S.L., Suh, N. & Kimble, J. GLD-3 and control of the mitosis/meiosis decision in the germline of Caenorhabditis elegans. *Genetics* **168**, 147-160 (2004).
476. Nousch, M., Yeroslaviz, A., Habermann, B. & Eckmann, C.R. The cytoplasmic poly(A) polymerases GLD-2 and GLD-4 promote general gene expression via distinct mechanisms. *Nucleic Acids Res* **42**, 11622-11633 (2014).
477. Kuersten, S. & Goodwin, E.B. The power of the 3' UTR: translational control and development. *Nature reviews. Genetics* **4**, 626-637 (2003).

478. Qiao, L., *et al*. Enhancers of glp-1, a gene required for cell-signaling in Caenorhabditis elegans, define a set of genes required for germline development. *Genetics* **141**, 551-569 (1995).
479. Maine, E.M. & Kimble, J. Suppressors of glp-1, a gene required for cell communication during development in Caenorhabditis elegans, define a set of interacting genes. *Genetics* **135**, 1011-1022 (1993).
480. Sulston, J.E. & Horvitz, H.R. Abnormal cell lineages in mutants of the nematode Caenorhabditis elegans. *Dev Biol* **82**, 41-55 (1981).
481. Ellis, R.E., Jacobson, D.M. & Horvitz, H.R. Genes required for the engulfment of cell corpses during programmed cell death in Caenorhabditis elegans. *Genetics* **129**, 79-94 (1991).
482. Gumienny, T.L., Lambie, E., Hartwieg, E., Horvitz, H.R. & Hengartner, M.O. Genetic control of programmed cell death in the Caenorhabditis elegans hermaphrodite germline. *Development* **126**, 1011-1022 (1999).
483. Hodgkin, J., Horvitz, H.R. & Brenner, S. Nondisjunction mutants of the nematode Caenorhabditis elegans. *Genetics* **91**, 67-94 (1979).
484. Gartner, A., Milstein, S., Ahmed, S., Hodgkin, J. & Hengartner, M.O. A conserved checkpoint pathway mediates DNA damage--induced apoptosis and cell cycle arrest in C. elegans. *Mol Cell* **5**, 435-443 (2000).
485. Hartman, P.S. & Herman, R.K. Radiation-sensitive mutants of Caenorhabditis elegans. *Genetics* **102**, 159-178 (1982).
486. Ahmed, S. & Hodgkin, J. MRT-2 checkpoint protein is required for germline immortality and telomere replication in C. elegans. *Nature* **403**, 159-164 (2000).
487. Garcia-Muse, T. & Boulton, S.J. Distinct modes of ATR activation after replication stress and DNA double-strand breaks in Caenorhabditis elegans. *EMBO J* **24**, 4345-4355 (2005).
488. Kalogeropoulos, N., Christoforou, C., Green, A.J., Gill, S. & Ashcroft, N.R. chk-1 is an essential gene and is required for an S-M checkpoint during early embryogenesis. *Cell Cycle* **3**, 1196-1200 (2004).
489. Stergiou, L., Doukoumetzidis, K., Sendoel, A. & Hengartner, M.O. The nucleotide excision repair pathway is required for UV-C-induced apoptosis in Caenorhabditis elegans. *Cell Death Differ* **14**, 1129-1138 (2007).
490. MacQueen, A.J. & Villeneuve, A.M. Nuclear reorganization and homologous chromosome pairing during meiotic prophase require C. elegans chk-2. *Genes Dev* **15**, 1674-1687 (2001).
491. Bailly, A.P., *et al*. The Caenorhabditis elegans homolog of Gen1/Yen1 resolvases links DNA damage signaling to DNA double-strand break repair. *PLoS Genet* **6**, e1001025 (2010).
492. Boulton, S.J., *et al*. Combined functional genomic maps of the C. elegans DNA damage response. *Science* **295**, 127-131 (2002).
493. Boerckel, J., Walker, D. & Ahmed, S. The Caenorhabditis elegans Rad17 homolog HPR-17 is required for telomere replication. *Genetics* **176**, 703-709 (2007).
494. Derry, W.B., Putzke, A.P. & Rothman, J.H. Caenorhabditis elegans p53: role in apoptosis, meiosis, and stress resistance. *Science* **294**, 591-595 (2001).

495. Schumacher, B., Hofmann, K., Boulton, S. & Gartner, A. The C. elegans homolog of the p53 tumor suppressor is required for DNA damage-induced apoptosis. *Curr Biol* **11**, 1722-1727 (2001).
496. Schumacher, B., *et al*. C. elegans ced-13 can promote apoptosis and is induced in response to DNA damage. *Cell Death Differ* **12**, 153-161 (2005).
497. Conradt, B. & Horvitz, H.R. The c. elegans protein Egl-1 is required for programmed cell death and interacts with the Bcl-2-like protein Ced-9. *Cell* **93**, 519-529 (1998).
498. Ellis, H.M. & Horvitz, H.R. Genetic control of programmed cell death in the nematode C. elegans. *Cell* **44**, 817-829 (1986).
499. Hengartner, M.O., Ellis, R.E. & Horvitz, H.R. Caenorhabditis elegans gene ced-9 protects cells from programmed cell death. *Nature* **356**, 494-496 (1992).
500. Spector, M.S., Desnoyers, S., Hoeppner, D.J. & Hengartner, M.O. Interaction between the C-Elegans cell death regulators Ced-9 and Ced-4. *Nature* **385**, 653-656 (1997).
501. Chinnaiyan, A.M., O'Rourke, K., Lane, B.R. & Dixit, V.M. Interaction of CED-4 with CED-3 and CED-9: a molecular framework for cell death. *Science* **275**, 1122-1126 (1997).
502. Yan, N., *et al*. Structural, biochemical, and functional analyses of CED-9 recognition by the proapoptotic proteins EGL-1 and CED-4. *Mol Cell* **15**, 999-1006 (2004).
503. Chen, F., *et al*. Translocation of C. elegans CED-4 to nuclear membranes during programmed cell death. *Science* **287**, 1485-1489 (2000).
504. Yuan, J. & Horvitz, H.R. The Caenorhabditis elegans cell death gene ced-4 encodes a novel protein and is expressed during the period of extensive programmed cell death. *Development* **116**, 309-320 (1992).
505. Alnemri, E.S., *et al*. Human ICE/CED-3 protease nomenclature. *Cell* **87**, 171 (1996).
506. Xue, D., Shaham, S. & Horvitz, H.R. The Caenorhabditis elegans cell-death protein CED-3 is a cysteine protease with substrate specificities similar to those of the human CPP32 protease. *Genes Dev* **10**, 1073-1083 (1996).
507. Jagasia, R., Grote, P., Westermann, B. & Conradt, B. DRP-1-mediated mitochondrial fragmentation during EGL-1-induced cell death in C. elegans. *Nature* **433**, 754-760 (2005).
508. Labrousse, A.M., Zappaterra, M.D., Rube, D.A. & van der Bliek, A.M. C. elegans dynamin-related protein DRP-1 controls severing of the mitochondrial outer membrane. *Mol Cell* **4**, 815-826 (1999).
509. Schumacher, B., *et al*. C. elegans ced-13 can promote apoptosis and is induced in response to DNA damage. *Cell Death Differ* **17**, 17 (2004).
510. Nehme, R. & Conradt, B. egl-1: a key activator of apoptotic cell death in C. elegans. *Oncogene* **27 Suppl 1**, S30-40 (2008).
511. Chung, S., Gumienny, T.L., Hengartner, M.O. & Driscoll, M. A common set of engulfment genes mediates removal of both apoptotic and necrotic cell corpses in C. elegans. *Nat Cell Biol* **2**, 931-937 (2000).
512. Reddien, P.W. & Horvitz, H.R. The engulfment process of programmed cell death in caenorhabditis elegans. *Annu Rev Cell Dev Biol* **20**, 193-221 (2004).

513. Morales, C.P., *et al*. Absence of cancer-associated changes in human fibroblasts immortalized with telomerase. *Nat Genet* **21**, 115-118 (1999).
514. Frokjaer-Jensen, C., *et al*. Single-copy insertion of transgenes in Caenorhabditis elegans. *Nat Genet* **40**, 1375-1383 (2008).
515. Greider, C., Chattopadhyay, A., Parkhurst, C. & Yang, E. BCL-x(L) and BCL2 delay Myc-induced cell cycle entry through elevation of p27 and inhibition of G1 cyclin-dependent kinases. *Oncogene* **21**, 7765-7775 (2002).
516. Huang, D.C., O'Reilly, L.A., Strasser, A. & Cory, S. The anti-apoptosis function of Bcl-2 can be genetically separated from its inhibitory effect on cell cycle entry. *EMBO J* **16**, 4628-4638 (1997).
517. Vairo, G., *et al*. Bcl-2 retards cell cycle entry through p27(Kip1), pRB relative p130, and altered E2F regulation. *Mol Cell Biol* **20**, 4745-4753 (2000).
518. Fang, G., *et al*. "Loop" domain is necessary for taxol-induced mobility shift and phosphorylation of Bcl-2 as well as for inhibiting taxol-induced cytosolic accumulation of cytochrome c and apoptosis. *Cancer Res* **58**, 3202-3208 (1998).
519. Kurz, D.J., Decary, S., Hong, Y. & Erusalimsky, J.D. Senescence-associated (beta)-galactosidase reflects an increase in lysosomal mass during replicative ageing of human endothelial cells. *J Cell Sci* **113 (Pt 20)**, 3613-3622 (2000).
520. Lee, B.Y., *et al*. Senescence-associated beta-galactosidase is lysosomal beta-galactosidase. *Aging cell* **5**, 187-195 (2006).
521. Agarwal, M.L., Agarwal, A., Taylor, W.R. & Stark, G.R. P53 Controls Both the G(2)/M and the G(1) Cell Cycle Checkpoints and Mediates Reversible Growth Arrest In Human Fibroblasts. *Proc Natl Acad Sci USA* **92**, 8493-8497 (1995).
522. Gartel, A.L. & Tyner, A.L. The role of the cyclin-dependent kinase inhibitor p21 in apoptosis. *Mol Cancer Ther* **1**, 639-649 (2002).
523. Hussain, S.P. & Harris, C.C. Molecular epidemiology and carcinogenesis: endogenous and exogenous carcinogens. *Mutat Res* **462**, 311-322 (2000).
524. Hermeking, H., *et al*. 14-3-3 sigma is a p53-regulated inhibitor of G2/M progression. *Mol Cell* **1**, 3-11 (1997).
525. Vousden, K.H. & Lu, X. Live or let die: the cell's response to p53. *Nat Rev Cancer* **2**, 594-604 (2002).
526. Nakano, K. & Vousden, K.H. Puma, a novel proapoptotic gene, is induced by p53. *Mol Cell* **7**, 683-694 (2001).
527. Miyashita, T., *et al*. Overexpression of the Bcl-2 protein increases the half-life of p21(Bax). *J Biol Chem* **270**, 26049-26052 (1995).
528. Oda, E., *et al*. Noxa, a BH3-only member of the bcl-2 family and candidate mediator of p53-induced apoptosis. *Science* **288**, 1053-1058 (2000).
529. Yu, J., Zhang, L., Hwang, P.M., Kinzler, K.W. & Vogelstein, B. Puma induces the rapid apoptosis of colorectal cancer cells. *Mol Cell* **7**, 673-682 (2001).
530. Okamura, S., *et al*. p53DINP1, a p53-inducible gene, regulates p53-dependent apoptosis. *Mol Cell* **8**, 85-94 (2001).
531. Moroni, M.C., *et al*. Apaf-1 is a transcriptional target for E2F and p53. *Nat Cell Biol* **3**, 552-558 (2001).
532. Honda, R., Tanaka, H. & Yasuda, H. Oncoprotein MDM2 is a ubiquitin ligase E3 for tumor suppressor p53. *FEBS Lett* **420**, 25-27 (1997).

533. Lavin, M.F. & Gueven, N. The complexity of p53 stabilization and activation. *Cell Death Differ* **13**, 941-950 (2006).
534. Khosravi, R., *et al*. Rapid ATM-dependent phosphorylation of MDM2 precedes p53 accumulation in response to DNA damage. *Proc Natl Acad Sci U S A* **96**, 14973-14977 (1999).
535. Maya, R., *et al*. ATM-dependent phosphorylation of Mdm2 on serine 395: role in p53 activation by DNA damage. *Genes Dev* **15**, 1067-1077 (2001).
536. Gu, W. & Roeder, R.G. Activation of p53 sequence-specific DNA binding by acetylation of the p53 C-terminal domain. *Cell* **90**, 595-606 (1997).
537. Luo, J., Su, F., Chen, D., Shiloh, A. & Gu, W. Deacetylation of p53 modulates its effect on cell growth and apoptosis. *Nature* **408**, 377-381 (2000).
538. Dai, C. & Gu, W. p53 post-translational modification: deregulated in tumorigenesis. *Trends Mol Med* **16**, 528-536 (2010).
539. Knights, C.D., *et al*. Distinct p53 acetylation cassettes differentially influence gene-expression patterns and cell fate. *J Cell Biol* **173**, 533-544 (2006).
540. Sykes, S.M., *et al*. Acetylation of the p53 DNA-binding domain regulates apoptosis induction. *Mol Cell* **24**, 841-851 (2006).
541. Marine, J.C. & Jochemsen, A.G. Mdmx as an essential regulator of p53 activity. *Biochem Biophys Res Commun* **331**, 750-760 (2005).
542. Minsky, N. & Oren, M. The RING domain of Mdm2 mediates histone ubiquitylation and transcriptional repression. *Mol Cell* **16**, 631-639 (2004).
543. Ohkubo, S., Tanaka, T., Taya, Y., Kitazato, K. & Prives, C. Excess HDM2 impacts cell cycle and apoptosis and has a selective effect on p53-dependent transcription. *J Biol Chem* **281**, 16943-16950 (2006).
544. Ringshausen, I., O'Shea, C.C., Finch, A.J., Swigart, L.B. & Evan, G.I. Mdm2 is critically and continuously required to suppress lethal p53 activity in vivo. *Cancer Cell* **10**, 501-514 (2006).
545. Dornan, D., *et al*. The ubiquitin ligase COP1 is a critical negative regulator of p53. *Nature* **429**, 86-92 (2004).
546. Appella, E. & Anderson, C.W. Post-translational modifications and activation of p53 by genotoxic stresses. *Eur J Biochem* **268**, 2764-2772 (2001).
547. Shieh, S.Y., Ikeda, M., Taya, Y. & Prives, C. DNA damage-induced phosphorylation of p53 alleviates inhibition by MDM2. *Cell* **91**, 325-334 (1997).
548. Puca, R., Nardinocchi, L., Givol, D. & D'Orazi, G. Regulation of p53 activity by HIPK2: molecular mechanisms and therapeutical implications in human cancer cells. *Oncogene* **29**, 4378-4387 (2010).
549. Wei, C.L., *et al*. A global map of p53 transcription-factor binding sites in the human genome. *Cell* **124**, 207-219 (2006).
550. Kruse, J.P. & Gu, W. Modes of p53 regulation. *Cell* **137**, 609-622 (2009).
551. Hupp, T.R., Meek, D.W., Midgley, C.A. & Lane, D.P. Regulation of the specific DNA binding function of p53. *Cell* **71**, 875-886 (1992).
552. Lin, A.W., *et al*. Premature senescence involving p53 and p16 is activated in response to constitutive MEK/MAPK mitogenic signaling. *Genes Dev* **12**, 3008-3019 (1998).
553. Van Aelst, L. & D'Souza-Schorey, C. Rho GTPases and signaling networks. *Genes Dev* **11**, 2295-2322 (1997).

554. Downward, J. Ras signalling and apoptosis. *Curr Opin Genet Dev* **8**, 49-54 (1998).
555. el-Deiry, W.S., *et al*. WAF1, a potential mediator of p53 tumor suppression. *Cell* **75**, 817-825 (1993).
556. Nozell, S. & Chen, X. p21B, a variant of p21(Waf1/Cip1), is induced by the p53 family. *Oncogene* **21**, 1285-1294 (2002).
557. Harms, K., Nozell, S. & Chen, X. The common and distinct target genes of the p53 family transcription factors. *Cell Mol Life Sci* **61**, 822-842 (2004).
558. Chai, Y.L., *et al*. The second BRCT domain of BRCA1 proteins interacts with p53 and stimulates transcription from the p21WAF1/CIP1 promoter. *Oncogene* **18**, 263-268 (1999).
559. Gartel, A.L. & Tyner, A.L. Transcriptional regulation of the p21((WAF1/CIP1)) gene. *Exp Cell Res* **246**, 280-289 (1999).
560. Missero, C., Di Cunto, F., Kiyokawa, H., Koff, A. & Dotto, G.P. The absence of p21Cip1/WAF1 alters keratinocyte growth and differentiation and promotes ras-tumor progression. *Genes Dev* **10**, 3065-3075 (1996).
561. Afshari, C.A., Nichols, M.A., Xiong, Y. & Mudryj, M. A role for a p21-E2F interaction during senescence arrest of normal human fibroblasts. *Cell Growth Differ* **7**, 979-988 (1996).
562. Lohr, K., Moritz, C., Contente, A. & Dobbelstein, M. p21/CDKN1A mediates negative regulation of transcription by p53. *J Biol Chem* **278**, 32507-32516 (2003).
563. Shats, I., *et al*. p53-dependent down-regulation of telomerase is mediated by p21waf1. *J Biol Chem* **279**, 50976-50985 (2004).
564. Gottifredi, V., Karni-Schmidt, O., Shieh, S.S. & Prives, C. p53 down-regulates CHK1 through p21 and the retinoblastoma protein. *Mol Cell Biol* **21**, 1066-1076 (2001).
565. Snowden, A.W., Anderson, L.A., Webster, G.A. & Perkins, N.D. A novel transcriptional repression domain mediates p21(WAF1/CIP1) induction of p300 transactivation. *Mol Cell Biol* **20**, 2676-2686 (2000).
566. Gartel, A.L., Najmabadi, F., Goufman, E. & Tyner, A.L. A role for E2F1 in Ras activation of p21(WAF1/CIP1) transcription. *Oncogene* **19**, 961-964 (2000).
567. Collado, M., Blasco, M.A. & Serrano, M. Cellular senescence in cancer and aging. *Cell* **130**, 223-233 (2007).
568. Roninson, I.B. Oncogenic functions of tumour suppressor p21(Waf1/Cip1/Sdi1): association with cell senescence and tumour-promoting activities of stromal fibroblasts. *Cancer Lett* **179**, 1-14 (2002).
569. Kobayashi, J. Molecular mechanism of the recruitment of NBS1/hMRE11/hRAD50 complex to DNA double-strand breaks: NBS1 binds to gamma-H2AX through FHA/BRCT domain. *J Radiat Res* **45**, 473-478 (2004).
570. Pilch, D.R., *et al*. Characteristics of gamma-H2AX foci at DNA double-strand breaks sites. *Biochem Cell Biol* **81**, 123-129 (2003).
571. Burma, S., Chen, B.P., Murphy, M., Kurimasa, A. & Chen, D.J. ATM phosphorylates histone H2AX in response to DNA double-strand breaks. *J Biol Chem* **276**, 42462-42467 (2001).

572. Huang, X., Traganos, F. & Darzynkiewicz, Z. DNA damage induced by DNA topoisomerase I- and topoisomerase II inhibitors detected by histone H2AX phosphorylation in relation to the cell cycle phase and apoptosis. *Cell Cycle* **2**, 614-619 (2003).
573. Chowdhury, D.*, et al*. gamma-H2AX dephosphorylation by protein phosphatase 2A facilitates DNA double-strand break repair. *Mol Cell* **20**, 801-809 (2005).
574. Scholzen, T. & Gerdes, J. The Ki-67 protein: from the known and the unknown. *J Cell Physiol* **182**, 311-322 (2000).
575. Gerdes, J., Schwab, U., Lemke, H. & Stein, H. Production of a mouse monoclonal antibody reactive with a human nuclear antigen associated with cell proliferation. *Int J Cancer* **31**, 13-20 (1983).
576. Nakajima, K.*, et al*. A central role for Stat3 in IL-6-induced regulation of growth and differentiation in M1 leukemia cells. *EMBO J* **15**, 3651-3658 (1996).
577. Hirano, T., Ishihara, K. & Hibi, M. Roles of STAT3 in mediating the cell growth, differentiation and survival signals relayed through the IL-6 family of cytokine receptors. *Oncogene* **19**, 2548-2556 (2000).
578. Kojima, H., Inoue, T., Kunimoto, H. & Nakajima, K. IL-6-STAT3 signaling and premature senescence. *Jak-stat* **2**, e25763 (2013).
579. Chien, Y.*, et al*. Control of the senescence-associated secretory phenotype by NF-kappaB promotes senescence and enhances chemosensitivity. *Genes Dev* **25**, 2125-2136 (2011).
580. Gilbert, L.A. & Hemann, M.T. DNA damage-mediated induction of a chemoresistant niche. *Cell* **143**, 355-366 (2010).
581. Yun, U.J., Park, S.E., Jo, Y.S., Kim, J. & Shin, D.Y. DNA damage induces the IL-6/STAT3 signaling pathway, which has anti-senescence and growth-promoting functions in human tumors. *Cancer Lett* **323**, 155-160 (2012).
582. Wang, E. Senescent human fibroblasts resist programmed cell death, and failure to suppress bcl2 is involved. *Cancer Res* **55**, 2284-2292 (1995).
583. Al-Khalaf, H.H. & Aboussekhra, A. Survivin expression increases during aging and enhances the resistance of aged human fibroblasts to genotoxic stress. *Age (Dordrecht, Netherlands)* **35**, 549-562 (2013).
584. Lee, Y.H.*, et al*. c-myb has a character of oxidative stress resistance in aged human diploid fibroblasts: regulates SAPK/JNK and Hsp60 pathway consequently. *Biogerontology* **11**, 267-274 (2010).
585. Ryu, S.J.*, et al*. On the role of major vault protein in the resistance of senescent human diploid fibroblasts to apoptosis. *Cell Death Differ* **15**, 1673-1680 (2008).
586. Sanders, Y.Y.*, et al*. Histone modifications in senescence-associated resistance to apoptosis by oxidative stress. *Redox biology* **1**, 8-16 (2013).
587. Fernandez, Y., Espana, L., Manas, S., Fabra, A. & Sierra, A. Bcl-xL promotes metastasis of breast cancer cells by induction of cytokines resistance. *Cell Death Differ* **7**, 350-359 (2000).
588. Dimauro, T. & David, G. Chromatin modifications: the driving force of senescence and aging? *Aging (Albany NY)* **1**, 182-190 (2009).
589. Jenuwein, T. & Allis, C.D. Translating the histone code. *Science* **293**, 1074-1080 (2001).

590. Strahl, B.D. & Allis, C.D. The language of covalent histone modifications. *Nature* **403**, 41-45 (2000).
591. Krishnan, V., *et al*. Histone H4 lysine 16 hypoacetylation is associated with defective DNA repair and premature senescence in Zmpste24-deficient mice. *Proc Natl Acad Sci U S A* **108**, 12325-12330 (2011).
592. Taipale, M., *et al*. hMOF histone acetyltransferase is required for histone H4 lysine 16 acetylation in mammalian cells. *Mol Cell Biol* **25**, 6798-6810 (2005).
593. Hajji, N., *et al*. Opposing effects of hMOF and SIRT1 on H4K16 acetylation and the sensitivity to the topoisomerase II inhibitor etoposide. *Oncogene* **29**, 2192-2204 (2010).
594. Evertts, A.G., *et al*. H4K20 methylation regulates quiescence and chromatin compaction. *Mol Biol Cell* **24**, 3025-3037 (2013).
595. Bannister, A.J. & Kouzarides, T. Regulation of chromatin by histone modifications. *Cell Res* **21**, 381-395 (2011).
596. Lachner, M., O'Carroll, D., Rea, S., Mechtler, K. & Jenuwein, T. Methylation of histone H3 lysine 9 creates a binding site for HP1 proteins. *Nature* **410**, 116-120 (2001).
597. Bannister, A.J., *et al*. Selective recognition of methylated lysine 9 on histone H3 by the HP1 chromo domain. *Nature* **410**, 120-124 (2001).
598. Nielsen, P.R., *et al*. Structure of the HP1 chromodomain bound to histone H3 methylated at lysine 9. *Nature* **416**, 103-107 (2002).
599. Stewart, M.D., Li, J. & Wong, J. Relationship between histone H3 lysine 9 methylation, transcription repression, and heterochromatin protein 1 recruitment. *Mol Cell Biol* **25**, 2525-2538 (2005).
600. Fuks, F., Hurd, P.J., Deplus, R. & Kouzarides, T. The DNA methyltransferases associate with HP1 and the SUV39H1 histone methyltransferase. *Nucleic Acids Res* **31**, 2305-2312 (2003).
601. Bachman, K.E., Rountree, M.R. & Baylin, S.B. Dnmt3a and Dnmt3b are transcriptional repressors that exhibit unique localization properties to heterochromatin. *J Biol Chem* **276**, 32282-32287 (2001).
602. Lehnertz, B., *et al*. Suv39h-mediated histone H3 lysine 9 methylation directs DNA methylation to major satellite repeats at pericentric heterochromatin. *Curr Biol* **13**, 1192-1200 (2003).
603. Peters, A.H., *et al*. Loss of the Suv39h histone methyltransferases impairs mammalian heterochromatin and genome stability. *Cell* **107**, 323-337 (2001).
604. Zhang, W., *et al*. Comparison of global DNA methylation profiles in replicative versus premature senescence. *Life Sci* **83**, 475-480 (2008).
605. Tamminga, J., Kathiria, P., Koturbash, I. & Kovalchuk, O. DNA damage-induced upregulation of miR-709 in the germline downregulates BORIS to counteract aberrant DNA hypomethylation. *Cell Cycle* **7**, 3731-3736 (2008).
606. Chuang, L.S., *et al*. Human DNA-(cytosine-5) methyltransferase-PCNA complex as a target for p21WAF1. *Science* **277**, 1996-2000 (1997).
607. Suzuki, T., Fujii, M. & Ayusawa, D. Demethylation of classical satellite 2 and 3 DNA with chromosomal instability in senescent human fibroblasts. *Exp Gerontol* **37**, 1005-1014 (2002).

608. Enukashvily, N.I., Donev, R., Waisertreiger, I.S. & Podgornaya, O.I. Human chromosome 1 satellite 3 DNA is decondensed, demethylated and transcribed in senescent cells and in A431 epithelial carcinoma cells. *Cytogenetic and genome research* **118**, 42-54 (2007).
609. Lombard, D.B.*, et al*. DNA repair, genome stability, and aging. *Cell* **120**, 497-512 (2005).
610. Astin, J.W., O'Neil, N.J. & Kuwabara, P.E. Nucleotide excision repair and the degradation of RNA pol II by the Caenorhabditis elegans XPA and Rsp5 orthologues, RAD-3 and WWP-1. *DNA Repair (Amst)* **7**, 267-280 (2008).
611. Lans, H.*, et al*. Involvement of global genome repair, transcription coupled repair, and chromatin remodeling in UV DNA damage response changes during development. *PLoS Genet* **6**, e1000941 (2010).
612. Boyd, W.A.*, et al*. Nucleotide excision repair genes are expressed at low levels and are not detectably inducible in Caenorhabditis elegans somatic tissues, but their function is required for normal adult life after UVC exposure. *Mutat Res* **683**, 57-67 (2010).
613. Wadsworth, W.G. & Riddle, D.L. Developmental regulation of energy metabolism in Caenorhabditis elegans. *Dev Biol* **132**, 167-173 (1989).
614. Kenyon, C., Chang, J., Gensch, E., Rudner, A. & Tabtiang, R. A C. elegans mutant that lives twice as long as wild type. *Nature* **366**, 461-464 (1993).
615. Kimura, K.D., Tissenbaum, H.A., Liu, Y. & Ruvkun, G. daf-2, an insulin receptor-like gene that regulates longevity and diapause in Caenorhabditis elegans. *Science* **277**, 942-946 (1997).
616. Paradis, S., Ailion, M., Toker, A., Thomas, J.H. & Ruvkun, G. A PDK1 homolog is necessary and sufficient to transduce AGE-1 PI3 kinase signals that regulate diapause in Caenorhabditis elegans. *Genes Dev* **13**, 1438-1452 (1999).
617. Paradis, S. & Ruvkun, G. Caenorhabditis elegans Akt/PKB transduces insulin receptor-like signals from AGE-1 PI3 kinase to the DAF-16 transcription factor. *Genes Dev* **12**, 2488-2498 (1998).
618. Lin, K., Dorman, J.B., Rodan, A. & Kenyon, C. daf-16: An HNF-3/forkhead family member that can function to double the life-span of Caenorhabditis elegans. *Science* **278**, 1319-1322 (1997).
619. Lithgow, G.J., White, T.M., Melov, S. & Johnson, T.E. Thermotolerance and extended life-span conferred by single-gene mutations and induced by thermal stress. *Proc Natl Acad Sci U S A* **92**, 7540-7544 (1995).
620. Quevedo, C., Kaplan, D.R. & Derry, W.B. AKT-1 regulates DNA-damage-induced germline apoptosis in C. elegans. *Curr Biol* **17**, 286-292 (2007).
621. Perrin, A.J.*, et al*. Noncanonical control of C. elegans germline apoptosis by the insulin/IGF-1 and Ras/MAPK signaling pathways. *Cell Death Differ* **20**, 97-107 (2013).
622. Hesp, K., Smant, G. & Kammenga, J.E. Caenorhabditis elegans DAF-16/FOXO transcription factor and its mammalian homologs associate with age-related disease. *Exp Gerontol* **72**, 1-7 (2015).
623. Pinkston, J.M., Garigan, D., Hansen, M. & Kenyon, C. Mutations that increase the life span of C. elegans inhibit tumor growth. *Science* **313**, 971-975 (2006).

624. Lans, H., *et al*. DNA damage leads to progressive replicative decline but extends the life span of long-lived mutant animals. *Cell Death Differ* **20**, 1709-1718 (2013).
625. Arum, O. & Johnson, T.E. Reduced expression of the Caenorhabditis elegans p53 ortholog cep-1 results in increased longevity. *The journals of gerontology. Series A, Biological sciences and medical sciences* **62**, 951-959 (2007).
626. Ventura, N., *et al*. p53/CEP-1 increases or decreases lifespan, depending on level of mitochondrial bioenergetic stress. *Aging cell* **8**, 380-393 (2009).
627. Feng, Z., Lin, M. & Wu, R. The Regulation of Aging and Longevity: A New and Complex Role of p53. *Genes & cancer* **2**, 443-452 (2011).
628. Zhang, Y., Chen, D., Smith, M.A., Zhang, B. & Pan, X. Selection of Reliable Reference Genes in Caenorhabditis elegans for Analysis of Nanotoxicity. *PLoS One* **7**(2012).
629. Schumacher, B., *et al*. Translational repression of C. elegans p53 by GLD-1 regulates DNA damage-induced apoptosis. *Cell* **120**, 357-368 (2005).
630. Yu, X., Lu, N. & Zhou, Z. Phagocytic receptor CED-1 initiates a signaling pathway for degrading engulfed apoptotic cells. *PLoS Biol* **6**, e61 (2008).
631. Denning, D.P., Hatch, V. & Horvitz, H.R. Programmed elimination of cells by caspase-independent cell extrusion in C. elegans. *Nature* **488**, 226-230 (2012).
632. Sternberg, P.W. & Horvitz, H.R. Postembryonic nongonadal cell lineages of the nematode Panagrellus redivivus: description and comparison with those of Caenorhabditis elegans. *Dev Biol* **93**, 181-205 (1982).
633. Kitagawa, R. Key players in chromosome segregation in Caenorhabditis elegans. *Front Biosci* **14**, 1529-1557 (2009).
634. Oegema, K., Desai, A., Rybina, S., Kirkham, M. & Hyman, A.A. Functional analysis of kinetochore assembly in Caenorhabditis elegans. *J Cell Biol* **153**, 1209-1226 (2001).
635. Desai, A., *et al*. KNL-1 directs assembly of the microtubule-binding interface of the kinetochore in C. elegans. *Genes Dev* **17**, 2421-2435 (2003).
636. Maddox, P.S., Hyndman, F., Monen, J., Oegema, K. & Desai, A. Functional genomics identifies a Myb domain-containing protein family required for assembly of CENP-A chromatin. *J Cell Biol* **176**, 757-763 (2007).
637. Cheeseman, I.M., *et al*. A conserved protein network controls assembly of the outer kinetochore and its ability to sustain tension. *Genes Dev* **18**, 2255-2268 (2004).
638. Romano, A., *et al*. CSC-1: a subunit of the Aurora B kinase complex that binds to the survivin-like protein BIR-1 and the incenp-like protein ICP-1. *J Cell Biol* **161**, 229-236 (2003).
639. Kaitna, S., Pasierbek, P., Jantsch, M., Loidl, J. & Glotzer, M. The aurora B kinase AIR-2 regulates kinetochores during mitosis and is required for separation of homologous Chromosomes during meiosis. *Curr Biol* **12**, 798-812 (2002).
640. Harris, J., *et al*. Mutator phenotype of Caenorhabditis elegans DNA damage checkpoint mutants. *Genetics* **174**, 601-616 (2006).
641. Gartner, A., MacQueen, A.J. & Villeneuve, A.M. Methods for analyzing checkpoint responses in Caenorhabditis elegans. *Methods Mol Biol* **280**, 257-274 (2004).

642. Hofmann, E.R., *et al*. Caenorhabditis elegans HUS-1 is a DNA damage checkpoint protein required for genome stability and EGL-1-mediated apoptosis. *Curr Biol* **12**, 1908-1918 (2002).
643. Weiss, R.S., Enoch, T. & Leder, P. Inactivation of mouse Hus1 results in genomic instability and impaired responses to genotoxic stress. *Genes Dev* **14**, 1886-1898 (2000).
644. Kulukian, A., Han, J.S. & Cleveland, D.W. Unattached kinetochores catalyze production of an anaphase inhibitor that requires a Mad2 template to prime Cdc20 for BubR1 binding. *Dev Cell* **16**, 105-117 (2009).
645. Barford, D. Structure, function and mechanism of the anaphase promoting complex (APC/C). *Q Rev Biophys* **44**, 1-38 (2010).
646. Glotzer, M., Murray, A.W. & Kirschner, M.W. Cyclin is degraded by the ubiquitin pathway. *Nature* **349**, 132-138 (1991).
647. Pfleger, C.M. & Kirschner, M.W. The KEN box: an APC recognition signal distinct from the D box targeted by Cdh1. *Genes Dev* **14**, 655-665 (2000).
648. da Fonseca, P.C., *et al*. Structures of APC/C(Cdh1) with substrates identify Cdh1 and Apc10 as the D-box co-receptor. *Nature* **470**, 274-278 (2011).
649. Robinson, J.T., Wojcik, E.J., Sanders, M.A., McGrail, M. & Hays, T.S. Cytoplasmic dynein is required for the nuclear attachment and migration of centrosomes during mitosis in Drosophila. *J Cell Biol* **146**, 597-608 (1999).
650. Thorpe, H.M. & Smith, M.C. In vitro site-specific integration of bacteriophage DNA catalyzed by a recombinase of the resolvase/invertase family. *Proc Natl Acad Sci U S A* **95**, 5505-5510 (1998).
651. Groth, A.C., Fish, M., Nusse, R. & Calos, M.P. Construction of transgenic Drosophila by using the site-specific integrase from phage phiC31. *Genetics* **166**, 1775-1782 (2004).
652. Thorpe, H.M., Wilson, S.E. & Smith, M.C. Control of directionality in the site-specific recombination system of the Streptomyces phage phiC31. *Mol Microbiol* **38**, 232-241 (2000).
653. Firestone, A.J., *et al*. Small-molecule inhibitors of the AAA+ ATPase motor cytoplasmic dynein. *Nature* **484**, 125-129 (2012).
654. Skop, A.R., Liu, H., Yates, J., 3rd, Meyer, B.J. & Heald, R. Dissection of the mammalian midbody proteome reveals conserved cytokinesis mechanisms. *Science* **305**, 61-66 (2004).
655. Albertson, R., Riggs, B. & Sullivan, W. Membrane traffic: a driving force in cytokinesis. *Trends Cell Biol* **15**, 92-101 (2005).
656. Li, H., *et al*. Bcl-xL induces Drp1-dependent synapse formation in cultured hippocampal neurons. *Proc Natl Acad Sci U S A* **105**, 2169-2174 (2008).
657. Lekomtsev, S., *et al*. Centralspindlin links the mitotic spindle to the plasma membrane during cytokinesis. *Nature* **492**, 276-279 (2012).
658. Barrangou, R., *et al*. Advances in CRISPR-Cas9 genome engineering: lessons learned from RNA interference. *Nucleic Acids Res* **43**, 3407-3419 (2015).
659. Mou, H., Kennedy, Z., Anderson, D.G., Yin, H. & Xue, W. Precision cancer mouse models through genome editing with CRISPR-Cas9. *Genome MeD* **7,** 53 (2015).

660. Juin, P., Geneste, O., Gautier, F., Depil, S. & Campone, M. Decoding and unlocking the BCL-2 dependency of cancer cells. *Nat Rev Cancer* **13**, 455-465 (2013).